Polymetallic, sulphide ore deposits and associated volcanic rocks from, the harsit river area, N. E. Turkey

D. Egin

Polymetallic, Sulphide Ore Deposits and Associated Volcanic Rocks from the Harsit River Area, N.E. Turkey

D.Eğin
(Higher Licence in Geological Engineering,
Hacettepe, Ankara)

A thesis submitted for the degree of

Doctor of Philosophy

in the University of Durham

October 1978

to my parents..

(ANNE VE BABAMA)..

ABSTRACT

The Pontid magmatic arc developed during the late Cretaceous and early Tertiary as a result of the northward subduction of Tethyan ocean-floor beneath "Pontian Land", due to the relative northwards movement of Anatolia.

Two volcanic cycles, both basalt-andesite-dacite-rhyodacite sequences, can be distinguished in the northern Harsit river area. Basic members of the Upper Cretaceous Lower Volcanic Cycle include tholeiitic basalts and andesitic lavas. They are overlain by dacite lavas. Only the waning stage of this cycle, the rhyolites, tuffs and breccias, contain abundant pyroclastics. This stage is closely related to the mineralisation and constitutes the host-rock horizon. The host-rock and its associated mineralisation show spatial association with the regional fault pattern. The early Tertiary, Upper Volcanic Cycle shows evidence of explosive vulcanicity in the basalts of the Upper Basic Series. Dacites and rhyodacites are locally developed and again show spatial association with the faulting.

Both the major and trace element chemistries of the two volcanic cyclesddemonstrate the clear separation into a lower tholeiitic and an upper calc-alkaline cycle. The rocks show similar chemistry to volcanics from island arcs in other areas.

The origin of the tholeiitic magma is ascribed to melting of "dry" amphibolite formed by metamorphism of Tethyan oceanic crust during early subduction. Fractional crystallisation of this magma has led to the development of the Lower Volcanic Cycle.

The calc-alkaline magma is thought to have formed during a later stage in the subduction process when melting of amphibolite was joined by melting of biotite or phlogopite. This produced a relatively "wet" magma which suppressed plagioclase fractionation until a late stage and prevented enrichment of iron in the residual melts. The volatiles

produced in this process may have promoted some melting of lherzolite overlying the subducted slab. A "high-level" fractional crystallisation of the calc-alkaline magma is thought to have yielded the Upper Volcanic Cycle.

Massive, polymetallic mineralisation is associated with the final phase of the Lower Volcanic Cycle. The mineralisation is characterised by a sequence in which a quartz-pyrite and/or sphalerite and chalcopyrite stockwork ore is overlain by massive ore containing galena, sphalerite, chalcopyrite, barite and sulphosalts. This is, in turn, overlain by a horizon in which barite is dominant, succeeded by hematitic and/or manganiferous tuffs and sediments. The ore deposits, in their mode of occurrence, in their mineralogy and morphology bear close resemblance to the Kuroko deposits found in the Miocene, tholeiitic, felsic volcanic rocks of Japan.

The lack of evidence for the derivation of ore fluids from igneous activity during the Tertiary era, and the unmineralised nature of the early differentiates of the Lower Volcanic Cycle restrict the mineralising episode to a short period of the felsic, Upper Cretaceous volcanism. The ore fluids responsible for the ore-bodies are thought to be the metal-rich fluids that separated during the final stage of fractionation and solidification of the tholeiitic silicate magma. The ascending magmatic ore solutions interacted with sea water. This process resulted in the exchange of Co, Ni, Se, Mg, Ca, Na and K, in a decrease in temperature and salinity, and in an increase in the oxidation state and pH relative to the initial composition of the magmatic fluids.

Lithogeochemical analysis and wall-rock alteration patterns in the host-rock and hanging wall may be used in conjunction with detailed stratigraphical and structural analysis to provide directional vectors to determine the proximity of ore bodies.

ACKNOWLEDGEMENTS

I would like to thank the Mineral Research and Exploration Institute of Turkey (M.T.A. Enstitüsü) for the award of a Research Studentship. I also wish to thank Professors G.M.Brown and M.H.P.Bott for the use of facilities in the Department of Geological Sciences, Durham.

I am very grateful to my supervisors, Dr.D.M.Hirst and Mr.R.Phillips for various discussions, advice, interest and encouragement during the course of this research. In particular I would like to thank Dr.D.M.Hirst for critically reading the whole manuscript and to Mr.R.Phillips for reading appropriate chapters of this thesis.

I would like to thank Mr.R.G.Hardy and Dr.J.G.Holland for supervision in X-ray techniques. In addition, I am indebted to Dr.A.Peckett for his instruction in the use of electron microprobe and for allowing the use of his correction programme.

I would like to extend my thanks to the technical staff of the department, especially to Mr.G.Randall and Mr.L.MacGregor for preparing polished sections, disc wafers and thin sections, respectively, Mr.G.Dresser for help in the production of various photographic plates and Mr.R.Lambert for instruction in wet chemical analysis.

Many members of the Department, both past and present, have contributed much through active assistance and discussion. Amongst them, I would especially like to thank Professor G.M.Brown, Dr.F.W.Smith, Dr.R.H.Pinsent, Dr.P.D.Taylor, Dr.C.H.Emeleus and Dr.G.Larwood.

Less directly, help was received through discussions from fellow research students, namely Mr.I.M.Frith (Imperial College), Mr.A.H.Al-Khamees, Miss A.H.Hoey, Mr.J.Robinson and Mr.R.Dogan.

I also wish to thank the members of staff of the Mineral Research and Exploration Institute of Turkey for providing facilities during the fieldwork; Dr.Ö.T.Akinci, Dr.T.Engin, Mr.R.Kutlu, Mr.M.Kayaalp and Mr.E.Acar were

particularly helpful.

Special thanks go to Miss M.S.Kingsnorth, her patience and encouragement during the preparation of this thesis was extremely helpful to me.

Finally, I wish to thank Mrs.C.Rowes for patiently typing the manuscript.

CONTENTS

LIST OF FIGURES

* Figure also located in the attached map pocket.

LIST OF TABLES

LIST OF PLATES

CHAPTER ONE

INTRODUCTION

1.1 Introduction

The eastern Pontid (eastern Black Sea) volcanic and metallogenic province extends east-west along the Black Sea coast of northeast Turkey, from the vicinity of Samsun to the Russian border. It has a length of approximately 600 km and a width of about 75 km (Fig.1.1). In the region some 16,000 Km^2 of volcanic rocks (Fig.1.2) contain approximately 60 massive sulphide deposits (Fig.4.1).

The region is characterised by the rugged topographical feature of the east-west stretching Pontid mountain ranges. The maximum elevation 3937 m occurs at Mount Kacgar. As a result of high relief, the area constitutes a great barrier between the Black Sea and the Anatolian interior, with poorly developed roads only along the major rivers, such as the river Harsit. Mineral exploration in the province is thus hindered by the high-topographical relief, extremely limited accessibility and dense vegetation.

The Pontid range has been well noted for its copper production since medieval times. The known sulphide occurrences are usually indicated by surface outcrops, or found in the immediate vicinity of medieval slags.

The area studied lies within the central part of the eastern Pontids and is located in Tirebolu town, Giresun province (Fig.1.1). The area contains the major geological units as well as massive sulphide deposits.

This study examines the geology, geotectonic setting and the ore deposits of the Pontids as a whole, in the light of the available literature, and considers the geochemistry and the petrology of the volcanic rocks with special reference to the northern Harsit river valley area.

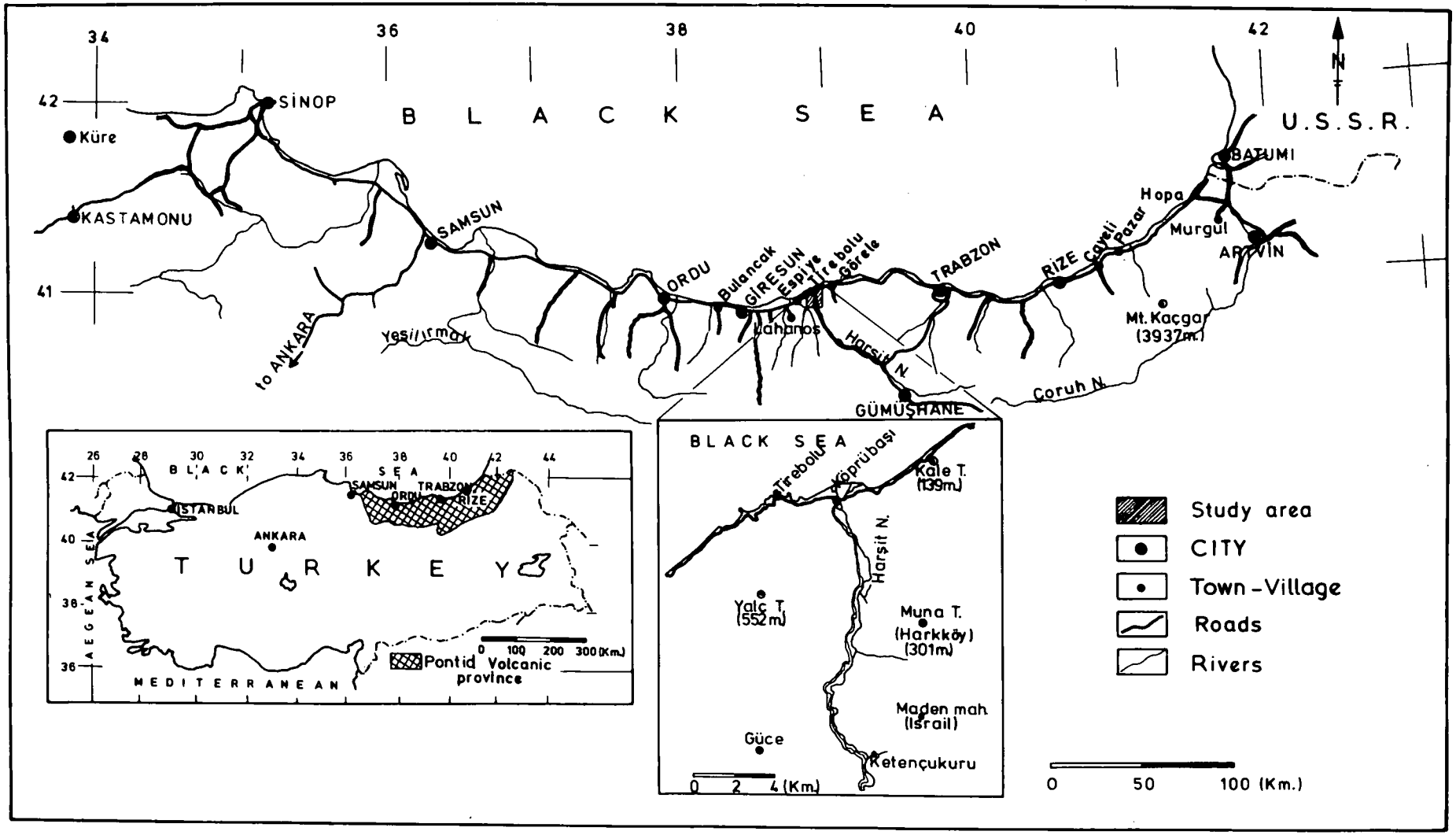

Figure 1.1: The Pontid Volcanic and Metallogenic Province showing the locality of the northern Harsit river area

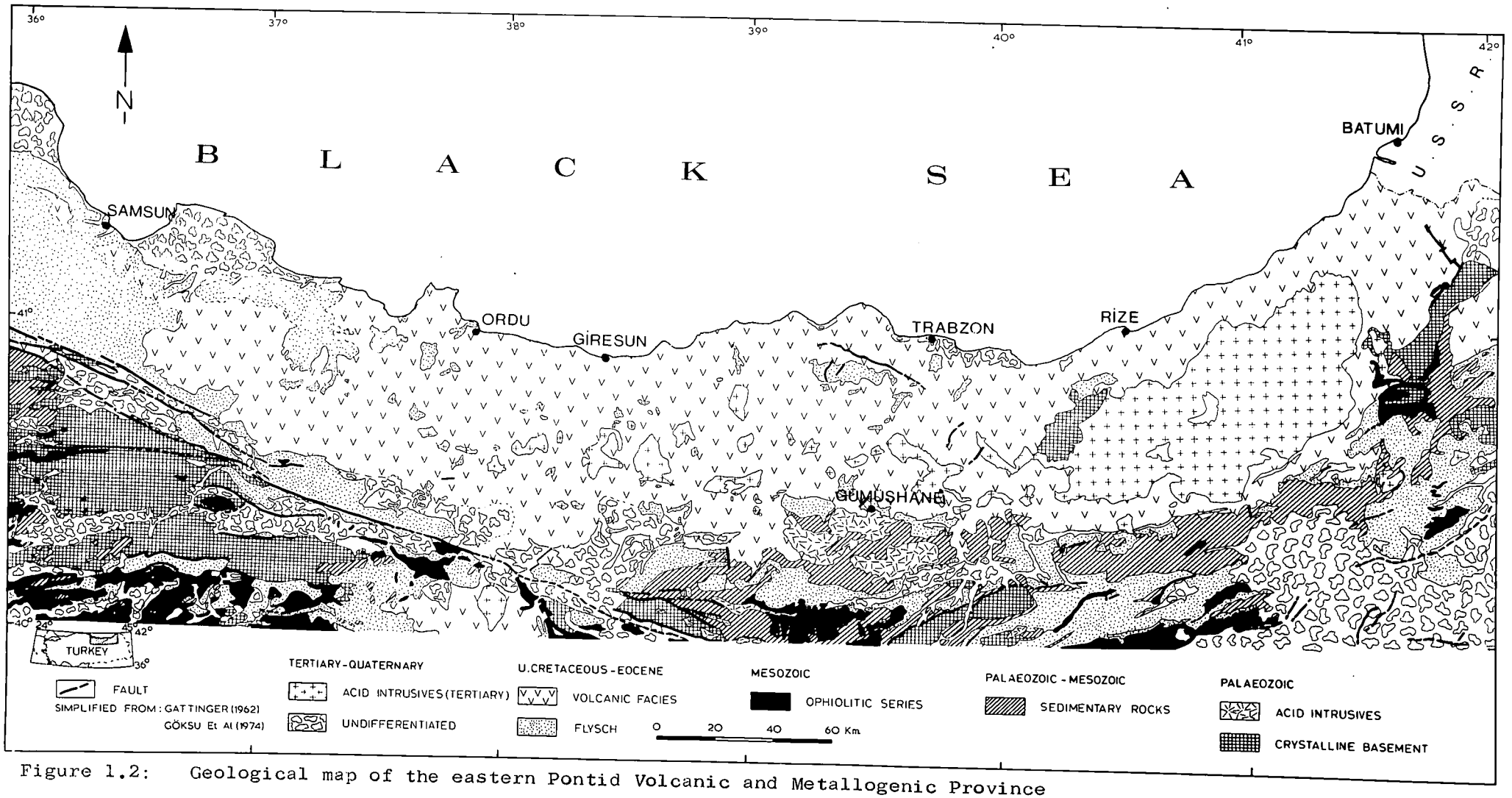

Figure 1.2: Geological map of the eastern Pontid Volcanic and Metallogenic Province

The mode of occurrence, ore mineralogy, texture and the chemistry of the sulphide ore bodies in the study area are investigated. The nature of the ore forming solutions together with some physico-chemical parameters involved during the mineralisation are discussed.

Since all the massive sulphide deposits in the Pontids are conspicuously associated with the end members of the Lower Volcanic Cycle, to test the implication of such association the major and minor element chemistry of the geological units in the vicinity of the ore deposits is studied. To this extent some limitations upon the time and space relationships of the mineralisation is sought. Finally possible exploration targets for concealed ore bodies are proposed.

1.2 Orogenic Belts of Anatolia

Although a large number of published articles, books and unpublished reports are available concerning various aspects of Turkish geology, there is still no overall agreement on the tectonic features and the geological history of the country.

The present day geotectonic setting of Turkey developed mainly as a result of the Alpine orogeny, although prealpine movements (e.g. Caledonian, Hercynian) have also been active in the region.

During the last few decades attempts have been made to divide the region into sub-zones using large-scale linear features, such as faults, as the boundaries. As a first attempt, the orogenic belts of Anatolia were divided into three units connected with the Alpine units of the Balkans. They were, from North to South, the Pontids, the intermediate massifsof Anatolia and the Taurids. (Argant, 1924; Staub, 1928; Seidlitz,1931; Kober, 1931, in Ketin 1966).

Arni (1939) completed a more detailed study of the region using all the available information on Turkish geology and making a comparison with the mountain belts of Iran. According to Arni, Anatolia can be divided

from north to south into the following units:

Pontids (Northern Branch / Southern Branch

Anatolids

Taurids

Iranids

Border folds (Inner folds / Outer folds

Syrian-Arabian blocks

Egeran (1947) attempted to define units on the basis of magmatic intrusions and metallogenic provinces. His work was somewhat more detailed and complicated. However, he produced a classification of ten units which was very similar to that of Arni.

Today the most widely used simple classification is that of Ketin (1966). Ketin bases his classification on the orogenic development of Anatolia. The evolution of Anatolia started with Caledonian and Hercynian movements in the north resulting in the development of the Pontid orogenic belt. The Anatolids subsequently developed at the end of the Cretaceous, and the tectonic development of the country was completed by the Oligocene Taurus system in the south and the Pliocene Border folds in the south-east. Ketin thus concluded that the tectonic-orogenic evolution of Anatolia proceeded gradually from north to south.

Recent speculations based on the concept of global tectonics in the Eastern Mediterranean and Asia Minor, however, show that the past movements of Afro-Arabia in respect to the Eurasian continent, and the subsequent contraction of the Tethyan Ocean, would make the tectonic development of the region far more complicated than the ideas formulated by Ketin (1966), and other previous workers.

It is beyond the scope of this work to go into the geotectonic setting of the country in detail, within which complicated epirogenetic movements,

orogenic events, intrusions, metamorphism and intense vulcanicity are widespread. A brief outline of the major units is however presented below, with special attention being given to the Eastern Pontid Metallogenic-Volcanic belt.

The orogenic mountain ranges of Anatolia trend in an east-west direction, parallel to the present coast lines of the Black Sea and the Mediterranean. These two belts are separated by a median plateau containing the Kirsehir, Menderes, Bitlis and other stable massifs (Ketin, 1966; Ilhan 1974; Brinkmann,1976). In a general way the northern belt, the Pontids, is connected to the Carpathian Mountains through Bulgaria in the west and to Transcaucasia and the western continuation of the Alborz mountains in the east. The Black Sea oceanic crustal segment (Neprochnov, 1959; Rezanov and Chamo 1969) to the north separates the Pontids from the Russian platform. The Dinarids and the Hellenides form the westerly extension of the southern belt, the Taurids. To the east the Rezaiye-Esfandagheh orogenic belt marks the extension of this unit (Takin, 1972). The southern boundary of the Taurids is well defined by the shelf zone of the Arabian shield. This zone contains conformable sedimentation from the Phanerozoic era (Ilhan, 1974). Mediterranean oceanic segments separate the Taurids from the African continent and Aegean plates to the south-west and west respectively (McKenzie, 1972; Papazachos, 1976).

1.3 The geotectonic development of the Pontids

Very little information is available on the early Palaeozoic era of the region. A median massif, the so-called "Pontian Land" occupied the area between the southern Ukranian platform and the inland sea. The latter was a part of Anatolia which formed a large Palaeozoic miogeosyncline (Ilhan, 1971; Brinkmann, 1974). "Pontian Land" was the source for clastic material deposited in the inland Anatolian sea during the middle Palaeozoic. The presence of coral limestone in the northwest (Tokel,1973) and of

graptolite shales in southern Anatolia (Brinkmann,1976) suggest, that a shallow water facies of this sea lay to the north.

During the Carboniferous, Variscan (Hercynian) movements subdivided this geosynclinal sea into northern and southern straits separated by a short-lived geanticline, "the North Anatolian Welt" (Brinkmann,1972, 1976). This uplift was accompanied by granitic intrusions (e.g. the Gumushane granitic batholith) forming the core of the geanticline (Yilmaz,1973).

Derived clastic material from the "Pontian Land" to the north, subsequent Variscan subsidence, and an early Alpine-Kimmerian transgression, mark an unconformity in the Trias, and the development of Tethys. Along the northern margin of Tethys, in Dobregea, the major Caucasus and the Kopet Dagh, a Rhaetian-Triassic unconformity is reported (Dewey et al, 1973). In southern Anatolia, Triassic strata are widespread (Brinkmann, 1976, p.43) suggesting that the early Alpine movements were not equally effective over the whole of Anatolia.

During the Lias and Dogger a deep trough formed, bordered to the north by the "Pontian Land" (Brinkmann,1974; Akinci, 1974; Adamia, 1975; Cagatay, 1977). This area probably had an oceanic crust prior to the movements of Afro-Arabia relative to Eurasia, which resulted in development of this Jurassic gulf (trough) in Tethys.

The general northward drift of the Afro-Arabian continent continued in the late Mesosoic. This led to a narrowing of the Lias-Dogger trough and a marine transgression over the southern margin of the continental "Pontian Land". At this time subduction of the northward dipping oceanic crust and overlying pelagic sediments, beneath "Pontian Land" began. Formation of the extensive tholeiitic, calc-alkaline Upper Cretaceous-Eocene volcanic rocks described by Tugal (1969), Akinci (1974), Peccerillo and Taylor (1976, 1977) and Cagatay (1977) was probably initiated by this middle-upper Cretaceous subduction process. This led to the development of the Pontid

island arc (Adamia,1975; Adamia et al, 1977)which was separated from southern Russia by a marginal sea.

The main succession of Mesozoic ophiolitic rocks along the southern part of the present Pontids (Fig.1.2) has been evaluated in recent years (Ilhan,1964; Brinkmann, 1972; Ilhan, 1974; Ataman et al, 1975). The rocks comprise an upward sequence of ultramafic rocks with subordinate gabbros, basaltic dikes, pillow lavas and minor tuffaceous material and finally radiolarian cherts. The lithology and the stratigraphy of these rocks clearly resembles that of the oceanic crust (c.f. Gass, 1977). A relative absence of contact phenomena between the ophiolites and the country rock (Brinkmann, 1974) indicate that they were tectonically emplaced into their present position as cool and solid masses. Dewey and Bird (1970) have suggested that the ophiolitic rocks of orogenic belts are tectonically emplaced oceanic crust and mantle materials. According to Dixon and Pereira (1974, p.187), their present positions mark the sutures along which plates met and joined. The ophiolitic suture zone to the south of the Pontids, along the well-known North Anatolian Fault, therefore indicates that the intervening Tethyan Ocean has been consumed (Fig.1.2).

A chaotic melange (Bailey and McCallien, 1953), occurs between the Pontid volcanic belt and the main ophiolites. In this Zone clastic materials, probably derived from the erosion of "Pontian Land" together with some ophiolitic masses are encountered frequently. The latter are interpreted as shredded ocean floor and according to Dewey and Bird (1970) this type of association probably indicates the position of a trench.

Palaeomagnetic data, and available pole positions (Van Der Voo, 1968), indicate that Anatolia has essentially travelled as a part of Africa in the late Mesozoic. A recent palaeobiogeographical discovery in the western Pontids shows strong faunal similarities between northern Anatolia and Eurasia (Andrews and Tobien, 1977). On the basis of this evidence,

together with the ophiolitic suture zone, it is suggested that the Pontids are genetically related to the Eurasion Plate, not to the Afro-Arabian or Anatolian plates.

The occurrence of red beds and arkosic sandstone (Tokel, 1973), and a marly limestone series (Kamen-Kaye, 1971) on both sides of the ophiolitic rocks is assumed to indicate the development of an epicontinental sea where the Upper Cretaceous-Eocene transgression had reached its maximum extent. Further emplacement of the disintegrated oceanic crust led to development of some Eocene ophiolites. (Not to be confused with the magmatic age of the series, see Smith, 1973). This implies that closure, or reduction in size, of the ocean took place as late as the early Tertiary.

Adamia et al (1977) suggest that, the Black Sea owes it oceanic character to Paleocene, Black Sea-South Caspian Sea rifting in which initial basaltic spreading took place in the middle Eocene, producing the non-granitic parts of the basin. The necessary heat to produce such a rift system may have been derived from the subducted slab (Toksoz M.N.,M.I.T., pers.comm.) described above.

Towards the end of the Eocene the Pontid belt was subjected to Pyrenean folding (Brinkmann, 1976, p.103). This folding was accompanied by granitic to granodioritic intrusives together with some porphyries. They mark the last magmatic activity in the region.

Since the Oligocene the continuously subsiding Black Sea basin has become the foredeep of the Pontid volcanic belt. Their high mountainous character has been achieved through the vertical movements and isostatic adjustment associated with the rifting in the Black Sea.

1.4. The Stratigraphy of the Eastern Pontids

The stratigraphy of the region has been compiled and has been presented in the Explanatory Text of the Geological Map of Turkey for Samsun and Trabzon Sheets on a 1:500 000 scale (Gattinger et al, 1962 ;

Goksu et al, 1974). Based on more detailed studies in the region, Table 1.1 shows the general stratigraphy, and the comparative terminology of the eastern Pontid region, at different localities from west to east. Description of the formations is as follows.

1.4.1 Basement:

The crystalline basement of the eastern Pontids is believed to be of Palaeozoic age and was affected by the Hercynian orogeny.

The oldest exposed rocks in the region are folded gneisses and sericite-biotite schists. A stratigraphic correlation of the crystalline basement with the neighbouring areas suggests a Cambrian age (Schuiling, 1962). In the western Pontids (Daday massif), the basement is comprised of basal conglomerates of Cambrian age followed by ortho-quartzites and siltstones. The latter contain inarticulate brachiopods indicating a Cambrian to Ordovician age (Demirtasli,1975). A recent correlation between the Proterozoic crystalline basement of the Ukranian Shield and the Pontid region suggests that the gneissic rocks of the eastern Pontids are younger than their southern Russian counterparts (Brinkmann, 1974), although both have similar planes of schistosity. The upper part of the metamorphic series is overlain by fossiliferous Permo-Carboniferous arkose, quartzite and sandy schists. These rocks are interstratified with minor amounts of acidic lavas and tuffs; limestones occur near to the top of the sequence.

Major igneous activity in the region is marked by Palaeozoic granitic and granodioritic instrusions. Available geochronological data on the Gumushane batholith (Fig.1.2) suggests an age of 300 m.y.B.P. (Cogulu,1970, in Akinci, 1974) indicating its emplacement during the Hercynian orogeny.

1.4.2 Lower Basic Series and Base Volcanic Rocks:

These rocks are mainly composed of basic volcanics, in the form of lava flows, sheets, sills and less commonly dykes. They rest on, and

Table 1.1: Comparative stratigraphic sequences from the eastern Pontid volcanic belt (after Egin et al, in print).

	GIRESUN Schutze-Westrum (1961)	BULANCAK Akinci (1974)	LAHANOS Tuğal (1969)	NORTHERN HARŞIT RIVER	ÇAYELI Çağatay (1977)	HOPA-MURGUL Kraëff (1963)
PLEISTOCENE -RECENT	SEA and RIVER TERRACES	SCREE	SEA and RIVER TERRACES	SEA and RIVER TERRACES	ALLUVIUM and TERRACE DEPOSITS	ALLUVIAL DEPOSITS
TERTIARY	YOUNG VOLCANICS and SEDIMENTS	BASALT DYKES	LATE DYKES	---	BASIC INTRUSIVE SERIES	LATE TERTIARY BASALTS and ANDESITES
	GRANITIC INTRUSIVES	QUARTZ MICRODIORITE	GRANITIC INTRUSIONS	GRANITIC INTRUSIONS (In extreme south)	GRANITIC and DIORITIC INTRUSIONS	ALBITE TONALITE, ALBITE GRANITE and GRANODIORITE
	---	---	HYPABYSSAL ROCKS (Quartz-feldspar porphyry)	DACITE-RHYODACITE	---	ALBITE DACITE III
	UPPER BASIC SERIES	---	UPPER BASIC SERIES	UPPER BASIC SERIES ? DOLERITE SHEETS	UPPER BASIC SERIES	SPILITIC SERIES II
MESOZOIC	DACITE II	AGGLOMERATE, SANDSTONE LIMESTONE BIOTITE ANDESITE	UPPER VOLCANICS (Dacite-Rhyodacite lavas)	TUFFACEOUS SEDIMENTARY SERIES	---	ALBITE DACITE II
	DACITIC TUFFS	RHYODACITIC LAVAS and PYROCLASTICS Mineralisation	DACITE TUFFS Mineralisation	DACITIC-RHYOLITIC LAVA, TUFF and BRECCIA. Mineralisation	DACITE SERIES Mineralisation	DACITE I Mineralisation
	DACITE I Mineralisation	PORPHYRITIC DACITE	LOWER VOLCANICS (Dacites)	DACITE LAVAS and QUARTZ PORPHYRY INTRUSIVES		
	LOWER BASIC SERIES and SEDIMENTARY ROCKS	LIMESTONE and TUFFS	MASSIVE LIMESTONES	LIMESTONE	---	---
		LOWER BASIC SERIES	LOWER BASIC SERIES	LOWER BASIC SERIES	LOWER BASIC SERIES	SPILITIC SERIES I
	BASE VOLCANIC SERIES	---	---	---	---	---
PALAEOZOIC	CRYSTALLINE BASEMENT	---	---	---	---	---

intrude into the crystalline basement. In the Cayeli area they consist of tholeiitic basalts, andesites and breccias (De Geoffroy, 1960). Spilites and Spilitic keratophyres, with minor amounts of tuff, represent the series in the Hopa-Murgul region as described by Kraeff (1963). In the west of the Province of Giresun, the spilitic keratophyres and andesites are overlain by the "Inoceramus limestone and tuffite" commonly called the "pelitic limestone and tuffs". The whole sequence is referred to as "the Lower Basic Series" by Akinci, 1974. In the study area they form the lowermost unit and are mainly represented by tholeiitic basalts and andesites.

As yet a definite age cannot be given to this unit, Tugal (1969) suggests Jurassic-Upper Cretaceous, while Peccerillo and Taylor (1975) and the present study support the Upper Cretaceous age. Various reports relate to basic volcanism in the region before the major episode of Upper Cretaceous, subduction initiated volcanism of the Lower Basic Series. They include the "Base volcanic rocks" of Schultze-Westrum (1961) indicated in Table 1.1. There are no geochemical studies available on these early volcanics. They include those related to the Kure ore-deposits of Jurassic age, similar to volcanics associated with Cyprus-type ore deposits (Cagatay, 1977). They most probably result, therefore, from volcanism associated with the oceanic setting of the Lias-Dogger trough. The term Lower Basic Series is therefore used only for those rocks whose formation is associated with the Middle-Upper Cretaceous subduction processes in the region.

1.4.3 Acidic Volcanic Rocks:

These rocks are probably the most closely studied due to their relationship with the major phase of the mineralisation. Their stratigraphy is very complicated. They can be divided into three major units:

c. Dacitic rhyolitic lava tuff and breccias
b. Quartz-feldspar, porphyries
a. Dacitic lava flows, sills and dykes

Similar divisions were suggested previously for these rocks but did not often refer to the presence of the rhyolitic lava, tuff and breccias. It is with these rocks that massive sulphide mineralisation is closely associated..

In the Mürgul area, the mineralisation is confined to the Lower Dacitic Series which is locally called albite-dacite I.. Unaltered greenish and somewhat coarse-textured, albite dacite II forms the upper -unmineralised parts of this series (Kraeft,1963). In the Cayeli area Dacite II is not present, mineralisation occurs in Dacite I and in the overlying pyroclasts and tuffs (Cagatay, 1977). In the vicinity of the well-known Lahanos ore field, the acidic volcanic rocks have been divided into two units and termed "The Lower and Upper Volcanic Series". The former is, "....possibly characterised by either a single composite lava flow containing three different lava units or by three different lava flows" (Tugal, 1969). The latter is mainly composed of alternations of lava flows, pyroclastics and marine sediments. Pyritic sulphide mineralisation often occurs near the contact of the two units but can also be found within the Upper Volcanic Series (Ibid).

Quartz-feldspar porphyries are the intrusive equivalents of the dacitic lavas. Brinkmann (1976) termed these rocks 'dacite' but to distinguish them from the earlier extrusive dacites described above, these intrusive rocks are best called quartz-feldspar porphyry. Quartz-feldspar porphyries of this age occur throughout the region. Their presence has been reported in the Mürgul area, where they are called "Dacite II" (Kraeff,1963). To the south of the Cayeli area they are composed of feldspar and quartz phenocrysts together with some mafic minerals, set in a glassy groundmass. They have been termed "Quartz-feldspar porphyries"

by Cagatay (1977).

The volume of acid volcanic rocks increases from Samsun towards the east. Near Giresun, Trabzon and Artvin, calcareous marine sediments are intercalated with the volcanics (Fig.1.2). They are of Santonian to Campanian age (Tugal,1969; Brinkmann,1976, p.54).

1.4.4 The Upper Volcanic Series:

They consist of the Upper Basic Series and their acid members of the dacitic to rhyodacitic composition.

Widespread basic volcanism is commonly observed along the coastal region, where it overlies the whole of the stratigraphical units described above, and sometimes caps the mineralisation, e.g. in the Cayeli Region. In Gumushane province calc-alkaline basaltic to andesitic lavas and tuffs, associated with some sedimentary rocks, represent this series (Tokel,1973). The same calc-alkaline unit is observed, near Kastomonu province (Peccerillo and Taylor,1976). The rocks can be either lavas associated with agglomerates and tuffs, or intrusive dolerite sheets or dykes.

Terminology is not consistent for the acid members of the unit, they are termed Albite-Dacite III in Hopa-Murgul region by Kraeff (1963). In the Lahanos area biotite-quartz-feldspar porphyry forms a huge dome-shaped instrusive body, often referred to as the "Lahanos Tepe Dasiti" Pollak (1961) or "hypa bysal dacite". It has an intrusive, as well as an extrusive character (Tugal,1969).

Brinkmann (1976) reports the abundance of the Maestrichtian carbonate sedimentation in the region. This may suggest a waning of the submarine vulcanicity in the uppermost Cretaceous in the Pontids (e.g. the Lower Basic Series and the acidic volcanic rocks) prior to the new basaltic-andesitic volcanism which started in the Eocene and formed the so-called 'Upper Volcanic Series".

1.4.5. Tertiary Igneous Intrusives:

A number of granitic plutons occur in the cores of anticlines (Brinkmann,1976). They are probably syntectonic and solidified under a rather thin cover. From their contact relationship with Eocene volcano-sedimentary formations (Tokel 1973) and (Cagatay 1977) suggest that they are younger than Eocene. One radiometric age of 40 m.y. B.P. is available from the 100 km long Tatos batholith near Rize province (Delaloye et al, 1972 in Brinkmann,1976).

These instrusives are commonly recorded in the Pontids. They include the albite-tonalite of the Murgul Mine (Kraeff,1963), the tonalite granite, with a well developed contact aureole zone, in the Lahanos area (Tugal, 1969) and the quartz-microdiorite to the south of the Bulancak mine (Akinci,1974). Intrusive granitic bodies near Harsit and Emeksan villages to the south of Espiye are of similar age.

1.4.6. The Young Basic Unit:

Minor episode of the volcanism is composed of andesites, basalts and olivine basalts in the Murgul mine (Kraeff, 1963), and of andesitic breccia, volcanic conglomerate and some dolerite dykes in the Cayeli Region (Cagatay,1977). Along the Artvin-YusufeliHighway dykes and sills of basalt and dolerite of this age frequently cut the Tertiary granodioritic intrusives (Popovic,1975). The unit is not present in the study area.

1.4.7 Sea and River Terraces and Glacial Deposits:

A few marine Oligocene deposits along the coastal strip of Trabzon, and at Unye for example, show that the southern coast of the ancient Black Sea was almost identical with the present shore line (Brinkmann, 1976). Sea and river terraces, and alluvium deposits, are frequently encountered along the coastal-line. Sea terraces are found at about 200 m. Q.D. They indicate the latest epirogenic movements.

Glacial moraine deposits were formed in the Pleistocene glacial epoch

on the high plateau regions in the south. They extend almost parallel to the coastline. A well-known glacier moraine deposit in the eastern Pontids occurs on Kacgar mountain (Fig.1.1 Messerli, 1967 in Brinkmann 1976).

1.5 Structural Geology of the Eastern Pontids

The southern boundary of the Pontids is well defined by the most seismically active feature in Turkey - the North Anatolian Fault system. Along this fault zone, which is over a 1000 km long, many destructive earthquakes have occurred.

The first structural definition of the Pontids was given by Oswald (1912) who referred to the area as "the Northern Broken Mass". Oswald claimed that during the compressional phase of the Alpine Orogeny the presence of the rigid masses of volcanics led to block uplift and subsidence. This view has been supported in recent years, although the terminology has changed somewhat to include the terms "Horst" and "Graben" (Zankl,1961; Gattinger et al,1962; Kronberg,1970; Goksu et al,1974). None of these reports indicate any formation of major thrusts, nappes or parallel folding of typical Alpine style tectonics in the region.

From the structural viewpoint, as well as the regional geology, a distinction must be made between the Palaeozoic basement and the overlying Mesozoic and Tertiary formations. The latter, as described in the previous section, have been mainly affected by the Alpine movements. The Palaeozoic basement, however, was refolded and the earlier planes of schistosity and the directions of folds were virtually destroyed during the Alpine orogeny. This left very little information on the earlier directions and sense of folding in the unit. Boccaletti et al (1968 p.675), however, indicated that a sharp contrast exists between the fold trends of the metamorphic rocks (basement) and those of the overlying Mesozoic-Tertiary formations. They state that the fold directions of the basement rocks agree closely with those of the southern Russian metamorphic unit, and are essentially

disposed in a NNE-SSW or N-S direction. The overlying Mesozoic-Tertiary units trend WNW-ESE, this trend being attributed to the compressional N-S nature of the Alpine Orogeny, resulting from the relative northward movement of the Anatolian Plate.

Gattinger et al (1962) pointed out that, while the crystalline basement isintensely folded its Mesozoic-Tertiary cover is far less affected by folding. Since the latter largely comprise fine-grained volcanics in the eastern Pontids, the common response to compressional deformation in the region would most likely be faulting. The volcano-sedimentary Mesozoic-Tertiary formations generally strike in a E-W direction and have a gentle regional dip towards the Black Sea (North). This northward dip of the Pontids is augumented by a series of step faults roughly parallel to the coast of the Black Sea, and generally downthrown to the north. According to Kayaalp (pers.comm.) three of these steps, together with their associated fault planes, may be recognised on the Samsun-Trabzon highway, near Trabzon.

A photogeological interpretation of the fault trends by Kronberg (1970) revealed that the eastern Pontids have two dominant trends, 50^{o}-60^{o} and 120^{o}-130^{o}. This agrees well with the trends measured in the study area, in the Cayeli region (Cagatay,1977), and from the Murgul mine (Kraeft,1963), where intersection of these fractures exerts a control on the ore deposition (Snelgrove,1971). Examination of the Black Sea coastline of northeast Turkey (Fig.1.3) suggests that it is also controlled by these two dominant fault trends.

The affects of fault-tectonics on the mineralisation have been studied in the eastern Pontids. Pollak (1968) implied that the mineralisation was mainly influenced by the lineaments, such as faults; the pyritic mineralisation preferring the 50^{o}-60^{o} fracture system, while copper is generally found along the 120^{o}-130^{o} oriented fault set. According to Gumus (1970), the 50^{o} fault trend is related to the main mineralisation phase, while the set at 120^{o} often controls the disposition of a later

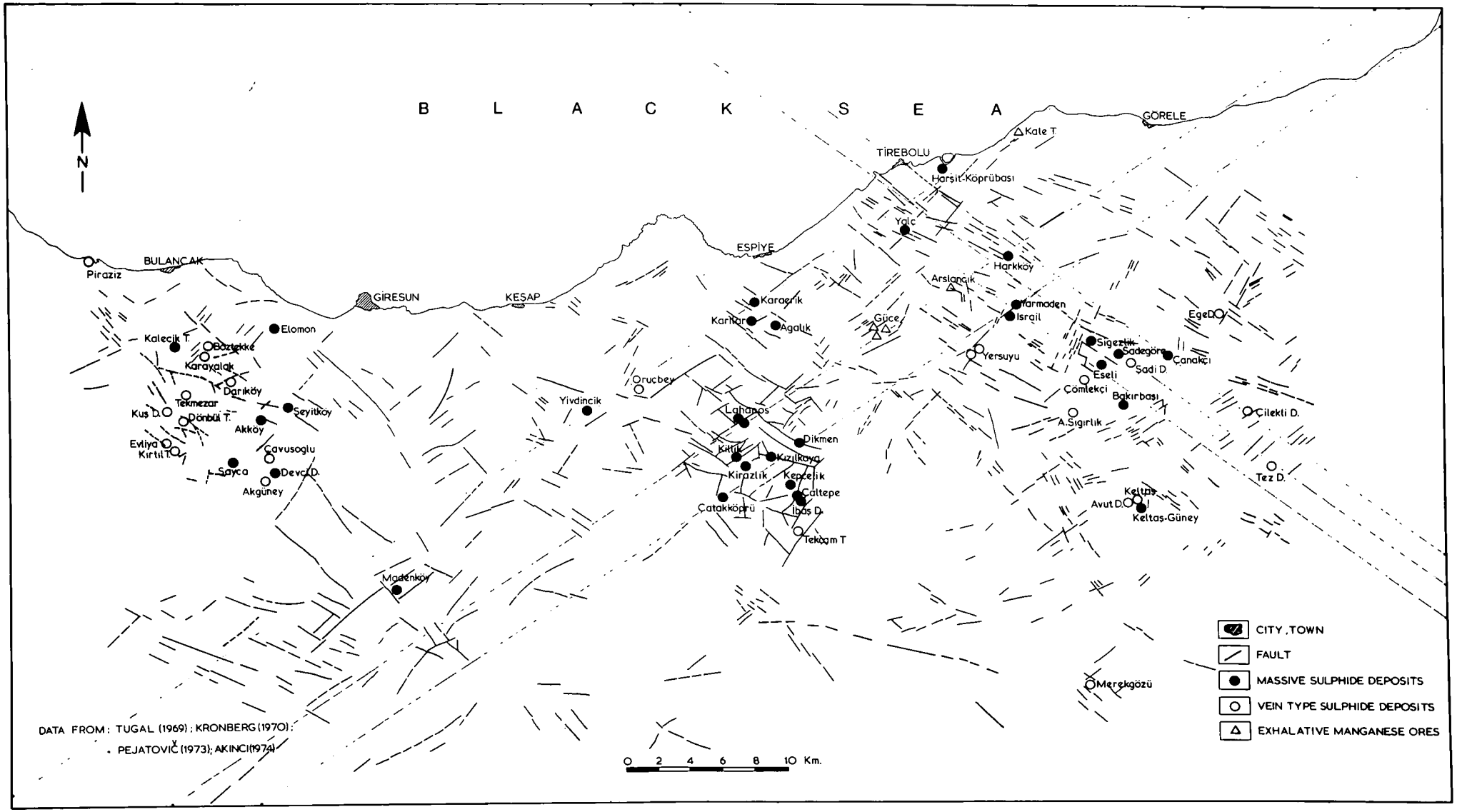

FIGURE 1.3: Distribution of mineral deposits with respect to the regional fault pattern in the central-eastern Pontids

phase of impregnated mineralisation. Akinci (1974) has put forward a contradictory view to that of Gumus. In a detailed study of vein-type mineralisation in the Bulancak area he suggested that "Data obtained from isotherms indicates that the ore-bearing fluids rose along NW-SE trending faults", these are presumably the 120^{o} set.

The presence of dome strucutres, and their close association with the massive-type mineralisation, are commonly reported in the region (Oner and Iwao, 1974, p.33; Cagatay,1977, p.56). Kieft (1955) described a felsitic lava dome near to the Israil mine, and documented its relation to the pyritic massive ore body. Until recently, this association had received scant attention as a control of ore deposition, but it has been re-emphasised in the present study, particularly in the Harkkoy mine, and possibly in the Harsit mine.

There appears to be a good correlation between magmatic activity and the dominant fault patterns of the region. Tugal (1969) suggested that hypabyssal rocks in the Lahanos area trend in a NW-SE direction while Popovic(1975) reported that small intrusions of granodiorite in the eastern Pontids trend NE-SW. To the west of Trabzon intrusions of granitic rocks and rhyolitic and dacitic domes are also disposed along the NE-SW direction (Oner and Iwao,1974). A careful appraisal of the disposition of the major massive sulphide and Mn deposits, deposits of Yarmaden, Israil, Yersuyu, Dikmen, Kizilkaya, Catakkopru and Harkkoy, Aslancik, Guce, Lahanos and finally Koprubasi, Yalc Karaerik, Karilar, Yivdincik, Madenkoy suggests that they too may lie along three parallel NE-SW lineaments (Fig.1.3). This is perhaps not surprising if one accepts a genetic connection between this type of deposit and intrusive rhyolitic and dacite domes, an association which is well documented for the Japanese Kuroko deposits (Horikoshi, 1969; Ishihara,1974).

The brief review given above suggests that the distribution of the

main types of mineralisation is closely associated with the fault pattern. These faults must have provided the channel-ways for the hydrothermal solutions responsible for the mineralisation. Fracture-filling clearly led to the vein type of mineralisation described by Akinci (1974). The same dominant fracture pattern also acted as the feeders for the magmatic activity, including particularly the emplacement of the lava domes. These, in turn, are closely associated in time and space with the formation of the massive sulphide deposits such as those at Harkkoy and Harsit-Koprubasi.

In detail the massive ore-bodies (Harkkoy and Harsit-Koprubasi) are disrupted by normal faults. These faults have similar general strike to the regional patterns described above, but they post-date the mineralisation, and thus have no direct genetic connections. Emplacement of the lava domes and associated mineralisation probably introduced local stresses, which in turn produce faulting. These would tend to be concentric to the lava dome, or would adopt earlier directions by re-activation of previously established fault planes. These features are well illustrated by the Harkkoy and Harsit-Koprubasi deposits where this late fault pattern conforms in a general way with the regional trend, though a slight tendency to concentricity is shown at Harkkoy, (Fig.5.9). The late normal faulting has throws of up to 60 m and, in a general way, the down thrown side is away from the lava dome. This suggests that the faults do indeed result from compensations related to the emplacement of the dome. They cause some difficulty in estimating the lateral and vertical extent of massive ore-bodies, and without detailed drilling, make estimation of the tonnage of a deposit difficult.

The search for blind massive sulphide ore deposits in the eastern Pontids, thus, requires a good structural analysis, including the recognition of the regional fault pattern and major lineaments, the distribution of acid lava domes and definition of the consequent fault patterns. The domes are

genetically associated with the massive, polymetallic mineralisation, while the later faults exert a control on its subsequent disposition. The massive, polymetallic sulphide deposits should also be clearly distinguished from the vein type mineralisation whose disposition is closely associated with the regional fault pattern as described by Pollak (1968) and Akinci (1974).

CHAPTER TWO

FIELD OCCURRENCE AND PETROGRAPHY OF THE COUNTRY ROCKS

2.1 Introduction

The Pontid Volcanic Province is one of the most active mineral exploration regions in Turkey and has tremendous potential. Most of the research undertaken in the region is thus confined to the vicinity of mineralised areas. In regions believed to be away from the mineralisation, there has been little detailed fieldwork and few petrological and geochemical observations. Studies based on mineralised areas, however, always include a discussion of the petrology of the associated volcanics. In general, these observations are inconclusive owing to the extensive hydrothermal alteration and chemical weathering of the volcanics in these areas.

The main purpose of this study is to evaluate the sulphide ore bodies in the northern Harsit river area and to attempt to establish an exploration programme for the Pontids as a whole. To this end, the nature and evolution of the volcanics is of prime importance in finding favourable mineralised horizons. The general characteristics of the volcanic sequence can be established provided that the effects of hydrothermal alteration associated with mineralisation, and chemical weathering, can be distinguished. Minimisation of interference by the first factor may be achieved by concentrating on volcanics in areas away from known mineralisation. Some 200 surface rock samples were collected from volcanics assumed to fall into this category, several unaltered or weakly altered (weathered), representative samples from each stratigraphical horizon being collected. The remaining volcanic rocks, approximately 350 samples, are from mineralised areas.

The 1:25000 scale geological map of the northern Harsit river area

(Fig.2.1) covers approximately 225 km^2. This map is a considerable modification of that produced by Van der Kaaden (1967). In addition to the above, more detailed geological maps have been produced for the Harsit (Fig.5.1) and Harkkoy (Fig 5.9) mine areas. Several visits were made to the surrounding areas in an attempt to establish a lateral correlation with the study area.

The following list gives the English translation of Turkish place names and topographical features which appear on the geological maps:

Inkoy	-	In village
Mahalle	-	Hamlet
Tepe (T.)	-	Hill, peak
Dag, Dagi	-	Mountain
Dere (D)	-	Stream
Nehir (N)	-	River

2.2 Geological Succession

The following units may be recognised in the northern Harsit river area. Their lateral correspondence with other parts of the eastern Pontids has been briefly summarised previously, table 1.1 (p.11).

The units are:

2-Upper Volcanic Cycle
- f - Dacite - rhyodacite
- e - Upper Basic series, dolerites

1-Lower Volcanic Cycle
- d - Sedimentary Series
- c - Dacitic - rhyolitic lava, tuff and breccia
- b - Dacitic rocks, quartz-feldspar porphyry
- a - Lower Basic series and limestone

Close time and space relations and similiarity in lithology between the Lower and Upper Volcanics makes distinction of the two units very difficult in the field. Such distinction is nevertheless very necessary to mineral exploration as the massive sulphide deposits of the northern Harsit river area occur predominantly associated with rocks from the

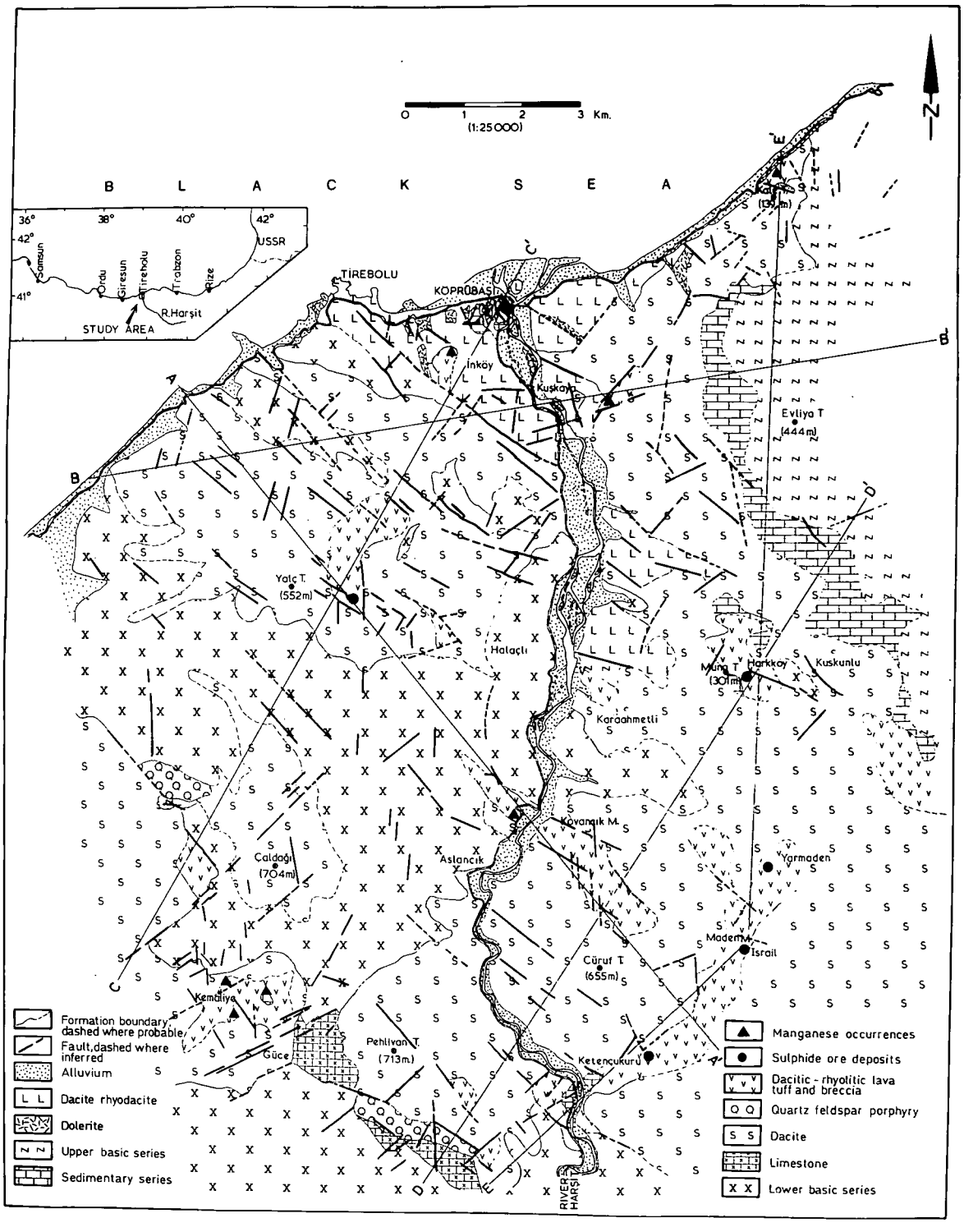

FIGURE 2.1: Geological map of the northern Harsit river area

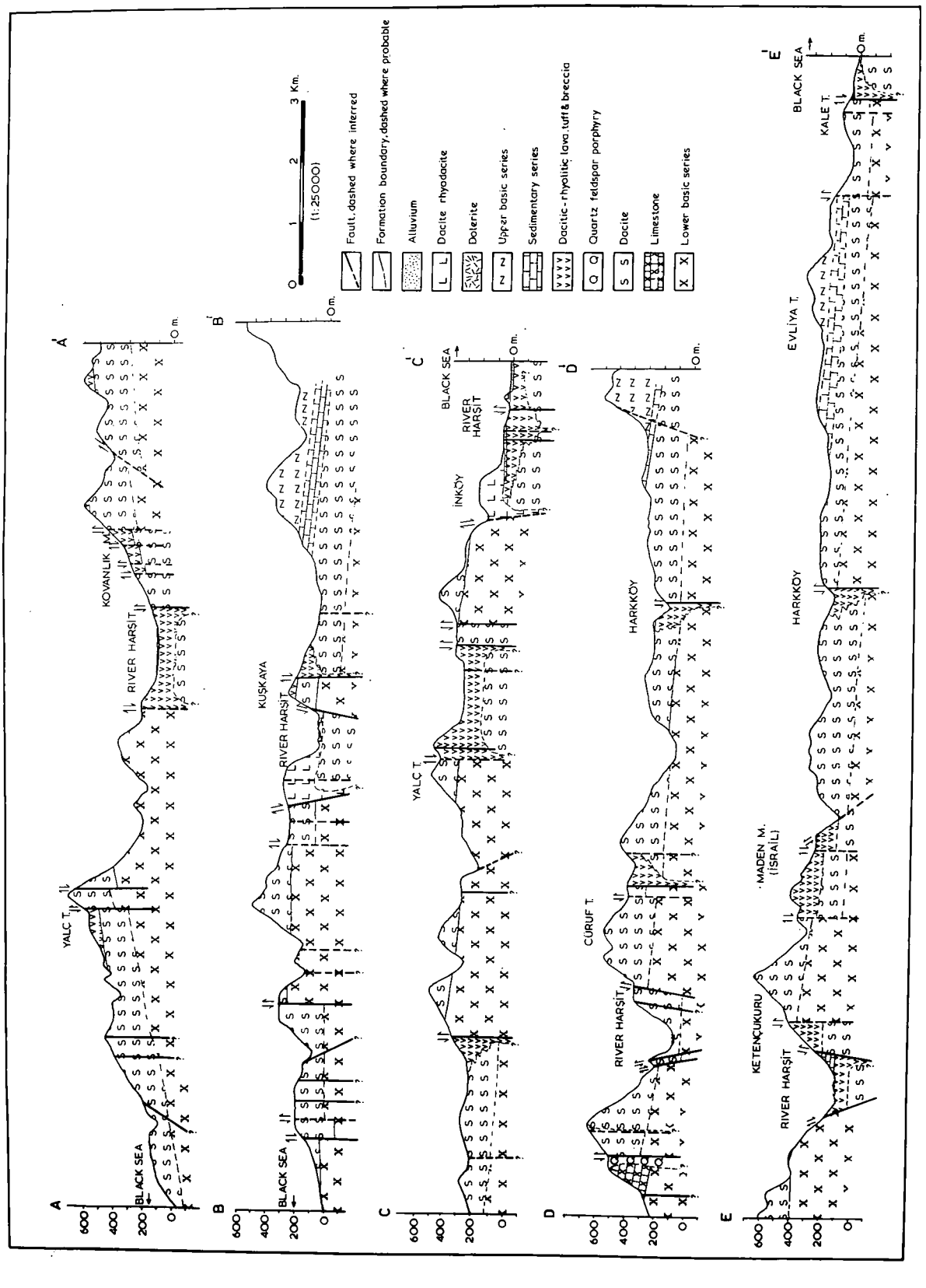

FIGURE 2.2: Geological cross-sections from the northern Harsit river area

felsic end of the Lower Volcanic Cycle. This difficulty is not a unique feature of the eastern Black Sea region as similar volcanic sequences are found associated with volcanogenic mineralisation elsewhere in the world. At Burchans in Newfoundland, Thurlow et al (1975) report the presence of four cycles of calcalkaline volcanism. Of these, only one cycle is associated with polymetallic, massive sulphide ore deposits. In Noranda province, Canada, only one of five successive cycles of volcanism is associated with the ore-deposits (Spence and DeRosen-Spence, 1975). In Japan, the prototype massive, polymetallic sulphide Kuroko ores are again, conspicuously confined to certain horizons of the tholeiitic felsic volcanic suite (Lambert and Sato, 1974; Ishihara and Terashima, 1974).

The distinction between the two major volcanic cycles will be discussed in the sections that follow. The description of each unit is presented in the form:

i) Field occurrence
ii) Petrography

Sample numbers used in the text allow reference to the data contained in Appendix 1.

2.2.1 The Lower Volcanic Cycle

2.2.1a The Lower Basic Series

i. Field Occurrence: This is the oldest exposed unit in the field area and mainly consists of andesitic and basaltic lavas. Intrusive sheets and pyroclastics are not abundant components of this unit. The Lower Basic Series has its major exposure in the southern part of the field area, Fig.2.1. This is principally due to the gentle, regional, northerly dip of the volcanics, towards the Black Sea (Fig.2.2). This unit is occasionally observed near the coast and along the river valleys, due to erosion, or as a result of block faulting of inliers as seen, for example, in the area to the south and north of Yalc Tepe, southwest of

Tirebolu and southwest of Inkoy, Figs. 2.1, 2.2.

The thickness of the lower Basic Series is difficult to estimate but is of the order of a few hundred metres in this area. Maucher (1958) and Zankl (1959) have estimated a thickness of 700 m for Giresun Province, while Akinci (1974) has reported that the series reaches 1000 m in thickness in the Bulancak area.

Intrusive sheets from the unit are well jointed. They are of very limited extent but may be seen 3 km northwest of Caldagi and northwest of Kovancik Mahalle.

Extrusive lavas are the predominant rock type, and although they occasionally exhibit ill-defined pillow structures better examples undoubtedly occur in the surrounding areas (Tugal, 1969; Stojanov, 1975; Koprivica, 1976).

Optical, chemical and normative mineralogical data, presented below, show that the lavas are mainly andesitic, although basalts also occur. Distinction between andesites and basalts in the field was virtually impossible, partly due to the high degree of alteration by weathering. Consequently no attempt was made to map boundaries between these rock-types.

In the Lahanos area, to the southwest, Tugal (1969) reports that the Lower Basic Series is predominantly basaltic in composition. This suggests that the Harsit Lower Basic Series may be higher in the stratigraphic sequence in accordance with the general trend for the eastern Black Sea region as discussed on p.17.

To the east and southeast of Guce village the Lower Basic Series is associated with, and overlain by foraminiferal limestone. Similar intercalations of lenticular marl and limestone in the region between Giresun and Trabzon have yielded a fauna which indicate an Upper Cretaceous age (Oner and Iwao, 1974).

The presence of thin sediment intercalations together with pillow

lava structures, is suggestive of a marine environment and discontinuous volcanism.

Tugal (1969) for the Lahanos area and Akinci (1974) for Bulancak believe that the Lower Basic Series are members of a calc-alkaline suite. The present study has, however, produced evidence which suggests that these lavas are of tholeiitic type in agreement with the conclusions drawn from studies of the Cayeli region by De Geoffroy (1960) and the Gumushane region by Tokel (1973).

ii Petrography: Reasonably fresh rocks of this unit are exposed near to Aslancik village in the Harsit river valley.

In hand specimen the rocks appear massive, dark coloured and vesicular. The vesicles are infilled with chlorite, calcite and chalcedony. Samples 27, 33, 35, 86 (porphyritic) and 242 (aphanitic) are fresh lavas which may reflect the general charactertistics of the Lower Basic Series.

The lavas are mainly porphyritic in texture, the grain size of the phenocrysts rarely exceeding 1 mm. Plagioclase and pyroxene are the major phenocrysts, and these minerals together with minor olivine or quartz, and a small amount of magnetite form the groundmass.

The plagioclase phenocrysts are usually zoned, their optically determined composition varying from An_{54} to An_{76} (Samples 27, 29, 34, 86, 245). Groundmass plagioclases are less Ca rich with the composition of andesine. In zoned plagioclase the original calcic nature is sometimes reflected by alteration to calcite (sample 25).

The pyroxenes are principally augite and hypersthene which occur both as phenocrysts and as constituents of the groundmass. Pigeonite is also commonly present in the groundmass, where it may be identified on the basis of its faint pleochroism, polysynthetic twinning and very small 2V, (samples 31,34, 36, 86 and 242). In some samples orthopyroxene (hypersthene) is rimmed by augite (sample 35). A similar relationship

was observed by Wilkinson (1968) in the central basalts of Japan, and basalts from Korea and the Cascades.

Olivine is not common in the Lower Basic Series. When present, it is confined to the lower stratigraphic horizons. It is often rimmed by pyroxene (hypersthene?) and thus exhibits the typical reaction relationship of the tholeiitic magma series.

2.2.1.b. Dacitic rocks, quartz-feldspar porphyry:

i. Field occurrence: Rocks of dacitic composition conformably overlie the Lower Basic Series. Close spatial association with, and similar chemical characteristics (Chapter 3) to, the Lower Basics, suggest that this unit is the acid member of the Lower Volcanics.

The rocks may be intrusive sheets and dykes or extrusive lava flows. The intrusives are coarse grained and exhibit columnar jointing. They are only of local development, and are well exposed to the south of Pehlivan Tepe and northwest of Caldagi. At the latter locality they exhibit horizontal columnar jointing indicative of either a dyke or plug intrusion. Here the rocks show strong spatial association with a series of northwest trending faults which may have controlled the instrusions. These intrusions may well represent feeders to the dacitic lavas. The name quartz-feldspar porphyry is suggested for these instrusives to reflect their hypabyssal nature.

The extrusives comprise principally dacite lava flows, with limited development of flow breccia at, or near, the base of the sequence. Flow vesicles in the lavas are infilled with quartz, chalcedony, calcite and chlorite.

Distinct columnar jointing, in addition to coarse grain size are the major criteria for distinguishing quartz-felspar porphyry from true extrusive dacites. However, in mineralogy and chemistry the two units are very similar.

ii. Petrography: The dacite lavas are predominantly represented by porphyritic dacite of fine to medium grain size. The phenocrysts vary between 0.08-3 mm in diameter, with an average value of about 1.5 mm. The majority of the lavas contain phenocrysts of quartzfeldspar, and amphibole with minor biotite and opaque minerals.

West of Halacli and Yalc Tepe reasonably fresh dacitic lavas are present. Microscopic examination of these lavas reveals that they mainly consist of corroded and partially resorbed quartz phenocrysts, sometimes surrounded by a silica rim. Their form suggests some disequilibrium between quartz phenocrysts and the liquid phase.

Twinned, zoned plagioclase (An_{20} to An_{50}) forms the other major phenocryst mineral. Variation in the anorthite content is attributed to stratigraphic height in the lava sequence, the plagioclase becoming less Ca-rich with height in the succession.

Hornblende and/or biotite and orthoclase are the additional phenocrysts. However, near to the contact with the Lower Basic Series rare clinopyroxene (augite) phenocrysts are present (samples 42,48).

The observed change in the composition of the mafic phenocrysts from pyroxene to hornblende to biotite, and in average plagioclase composition from andesine to oligoclase to orthoclase, together with the smooth variation diagrams (Figs.3.1and3.3)in respect of stratigraphy may indicate the continuous differentiation of a single magma.

The groundmass of the unit is glassy but may contain tiny crystals of quartz and laths of albitic plagioclase. In general, the groundmass makes up approximately 60% to 70% of the rock. Devitrification of the glass is not common but sample 6 is an example of a dacite having a completely devitrified groundmass. Very small amounts of magnetite and/or hematite, with minor pyrite are the accessory minerals.

The dacite lavas have not been affected by metasomatic additions

unlike the alteration involved near the ore bodies (Chapter 7.3). Heavy rainfall ($\sim$ 2m/year, Cagatay, 1977) acting as a carrier of dissolved oxygen and CO_2, together with various acids and organic products derived from the soil (dense vegetation and forestry), as explained in Holmes (1965), are believed to be the main agents for the alteration and solution of dacite lavas by chemical weathering. Consequently, orthoclase and biotite generally alter to sericite, leaving complete pseudomorphs. The removal of iron during the biotite to sericite transformation results in the formation of hematite and/or iron hydroxides (e.g.goethite). These compounds are also formed by the alteration of hornblende (sample 1). The commonest alteration product of plagioclase is kaolinite with a minor development of carbonate pseudomorphs after calcic plagioclase.

Apart from coarser grain-size, the petrography of the quartz-feldspar porphyry is similar to that of the dacitic lavas.

2.2.1c Dacitic-rhyotitic lava, tuff and breccia:

i. Field occurrence: Reports relating to mineralisation in the Pontids generally indicate that the volcanogenic sulphide mineralisation of the eastern Black Sea region is intimately related to the dacitic series of upper Cretaceous age (Kraeft,1963; Oner and Iwao, 1974; Cagatay, 1977). In general, the series is thick from 400 to 500 m and it is thus necessary to recognise the criteria particularly applicable to the mineralised "host rock" horizons.

A consideration of the host-rock lithology, form of the lavas, and their chemistry allows a subdivision of the acid member of the Lower Volcanics into two distinct horizons. These are the dacitic lavas (2.2.1b) and the dacitic rhyolitic lava, tuff and breccia (2.2.1c). The former always occur at a stratigraphically lower horizon, while the overlying group (2.2.1c) show local disconformities with them. Schultze-Westrum (1961) has shown a similar lithological change in the Giresun area. He states that, dacite 1 (presumably, the dacite lavas of group

2.2.1b) begins with an albite dacite with a glassy groundmass, but upwards grades into an extensively altered, fine grained, ore-bearing dacite.

The difference in the proportion of pyroclastic material between dacite (2.2.1b) and the overlying dacite rhyolitic lava, tuff and breccia is the major field criterion in distinguishing one from the other. Examination of some 70 dacite lavas failed to establish the presence of any pyroclastic component, while the overlying unit (2.2.1c) contains very large amounts of pyroclastic material associated with minor amounts of lava of a very acidic nature. The striking association of sulphide mineralisation with the latter unit (2.2.1c) suggested that the search for volcanogenic massive sulphide mineralisation must be aimed at this unit. Petrological studies confined to the dacite lavas allow some interpretation of the heavily altered "host rock", by extrapolation.

The dacite lavas show some alteration by chemical weathering, as described above, but true hydrothermal alteration is confined to the overlying dacitic-rhyolitic lava, tuff and breccia formations in the proximity of the ore bodies.

The association of dacitic-rhyolitic lava, tuff and breccia with the dominant fault pattern has been described above (p.19). The association is well demonstrated at Koprubasi, near Yalc Tepe to the west and south of Caldagi, in the Ketencukuru valley, near Kovancik M., and in the vicinity of Harkkoy (Fig.2.1). The extent of this association in the northern Harsit river area and its probable extension to the eastern Pontids (p.17) in general, implies a genetic connection. The implication is that the fracture system acted as a channelway for magmatic activity in the formation of this unit.

It is interesting to note that the unit is not evident between the dacite lavas (2.2.1b) and sediments (2.2.1d) to the north and east of

Harkkoy, west of Evliya Tepe.

To the west of Caldagi the unit contains a breccia (rhyolitic?) which includes angular fragments of the Lower Basic Series and of the dacite lavas. This rock is an explosion breccia and points to the presence of volcanic centres associated with the fault zone.

The rocks of unit (2.2.1c) can be divided into two categories; the lavas, and the tuffs and breccia. The Ketencukuru valley provides a good section through the unit. Erosion reveals that in the deepest part of the valley the rocks are of rhyolitic composition and contain a lava flow (sample 142). In the upper part of the valley the nature of the rocks changes gradually from lavas to breccias to tuffs (samples 66, 69, 74, 145) giving a good indication of the true stratigraphy of the unit.

Near the top of the unit, intercalated mudstone lenses appear (Koprubasi Mine, 425, 427 and surface samples 123, 125) together with thin, discontinuous horizons of radiolarian cherts (Koprubasi mine boreholes; H20/28-30 m and H38/32-36 m). The association of these sediments with tuffaceous rocks is indicative of a submarine environment and a paucity of volcanics, probably associated with the waning stage of volcanism.

ii. Petrography: these rocks are found to be the most altered unit in the area, due to close association with the mineralisation.

The lavas (sample 142) exhibit flow textures indicated by the alignment of the C axis of quartz or rarely the (010) cleavage traces of orthoclase and minor, altered biotite (sericite) laths. Phenocrysts are rare, and where present, consist of quartz and/or feldspar and sometimes a few biotite laths. The groundmass may be devitrified and consists of quartz-sericite aggregates with occasional identifiable albite and orthoclase feldspars.

The volcanic breccias contain angular fragments of the lavas of the unit, and ash in small quantities (samples 168, 204, 313, 345). The matrix is usually silicified and/or sericitized and contains

varying amounts of disseminated sulphides. Breccia horizons grade vertically and laterally into well sorted tuffs and tuffaceous sedimentary rocks, and are overlain by reddish, bedded cherts as at the Koprubasi mine, or by hematite and iron hydroxide bearing tuffaceous sedimentary rocks as at the Harkkoy mine.

The very fine grained nature, and extensive metasomatic wall-rock alteration makes it difficult to give an adequate description of these tuffacaeous rocks. Available chemical and wall rock alteration data will be discussed in Chapter 7.3.

2.2.1d The Sedimentary Series

The sedimentary series covers rather small areas, either directly overlying the dacitic series (2.2.1b) or the dacitic-rhyolitic lava, tuff and breccia formations (2.2.1c). In the east of the study area the series overlies the dacite lavas and consists of limestone and marl (samples 122, 126, 251), and sandstone (sample 263). In the Harkkoy and Koprubasi mine areas, the sedimentary rocks, which comprise radiolarian cherts, foraminiferal limestone, marl, mudstone and sandstone together with tuffaceous material, overlie the dacitic-rhyolitic tuffs. The abundance of radiolarian beds and mudstone lenses near to the mineralised areas may be attributed to the discharge of liquids, rich in silica and the constituents of clay minerals, into marine environments. Fossils in the series are all of the Globotruncana species (Akinci, 1974)

Prior to the sedimentation, it is believed that erosion was active. In places the sedimentary series contains ore pebbles (Sawa and Altun, 1977) while small lenses of barytes parallel to bedding planes are seen in the radiolarian cherts at the Koprubasi mine. These are taken to indicate that erosion of the underlying mineralised volcanics was taking place simultaneous with sedimentation.

2.2.2. The Upper Volcanic Cycle:

The Upper Volcanic Cycle consists of basic and acid members. It is the last major volcanism in the north-eastern Black Sea region, covering large areas (Kraeft, 1963; Oner and Iwao, 1974; Sawa and Altun, 1977).

The age attributed to the Upper Volcanics varies between Upper Cretaceous to Eocene (Cagatay, 1977) and Eocene (Gattinger, et.al,1964) The rocks overlie Upper Cretaceous sediments, and thus it is safe to conclude that the volcanism took place in Upper Cretaceous to early Tertiary times.

2.2.2e Upper Basic Series:

i. Field Occurrence: The series includes rocks of basaltic and andesitic composition. Limited data from various parts of the Pontids show that the series is calc-alkaline (Tugal, 1969; Tokel,1973; Akinci, 1974; Peccerillo and Taylor, 1975; Cagatay , 1977) and that both intrusive and extrusive members are present.

The Upper Basic Series occurs in the vicinity of the Harsit mine. The rocks are exposed along the major faults. They are intrusive, described as diorite by Acar (1976), and are included in the category of 'late dykes' by Acar and Ronkovic (1970) and Stojanov (1975).

Detailed study of these rocks indicates that they are dolerite sheets, their chemistry (described in Chapter 3) showing close affinity to that of the Upper Basic Series. Exposures of the dolerites are very poor with outcrop widths seldom exceeding 10 m - 20 m in the vicinity of Tirebolu. Their distribution as indicated on Fig. 2.1 is clearly related to northwest trending faults although the sheets as a whole are confined to the northeast trending coastal lineament extending from the vicinity of Tirebolu to Kale Tepe.

The intrusive dolerites show columnar jointing (sample 188) and on

their lower margin they give way to intrusion breccias, which include abundant angular, dacitic-rhyolitic tuff fragments of 5-10 cm length (Harsit Mine Borehole - H15 - 156 m).

The Upper Basic Series covers large areas extending eastwards from Evliya T. In the immediate vicinity of this hill they are characterised by coarse agglomerates and breccias, with fragments varying in size from a few centimetres to 40-50 cm in diameter. This may indicate the presence of an explosion centre whose significance is discussed in the chemistry of the volcanic rocks (Chapter 3). The lowermost horizons of the series contain limestone-marl xenoliths which presumably originate from the underlying sedimentary series. In the Gorele and Cayeli areas, De Geoffroy (1960) has similarly described both dacitic and limestone zenoliths in the Upper Basic Series. The upper parts of the unit are dominantly lava flows with amygdaloidal cavities which are infilled by chlorite, quartz and calcite. Flows may exhibit columnar jointing or spheroidal alteration(Onion structure) which can resemble pillow structures.

The thickness of the unit varies between 150 m for the intrusives of the area and 500 m for the lavas and the pyroclastics to the south east of Kale Tepe. Akinci (1974), however, reports a thickness of 1000 m in the Bulancak area.

ii. Petrography: Coarse grained intrusive sheets and fine grained porphyritic or aphanitic lavas differ little in their mineralogy, although ophitic or subophitic texture is more common in the intrusives. Both contain abundant zoned and twinned plagioclase and pyroxene phenocrysts with some hornblende and biotite, while quartz or olivine and magnetite and ilmenite occur as groundmass constituents. The plagioclase lies in the composition range An_{50} to An_{70} although universal stage determinations (Tugal,1969) and Microbeam (EPMA) techniques (Akinci, 1974) reveal that the average lies in the andesine range.

The pyroxenes include both clino and orthopyroxenes both as phenocrysts and groundmass constituents. Diopside-augite or augite are the commonest phenocrysts. Hypersthene phenocrysts may be rimmed by clinopyroxene (samples 124, 161).

Olivine is more abundant than in the Lower Basic Series. It is inevitably surrounded by pyroxene (hypersthene?, sample 208) in the reaction relationship. Biotite occurs as lath-shaped fragments together with euhedral hornblende in the andesites of the unit. Quartz is sometimes present as discrete grains in the groundmass (sample 346). The quartz often shows strained extinction. Tugal (1969) reports that xenoliths, including Lower Basic Series lavas, are abundant in his Upper Basic Series "Andesites". Apart from sedimentary xenoliths no igneous xenoliths were noted in the study area although the strained quartz may represent xenocrysts derived from pre-existing lavas or underlying Pontid basement gneissic rocks.

Alteration is fairly widespread. The main results are goethite pseudomorphs after ferro-magnesian minerals, chlorite after olivine, and calcite after pyroxene with clay minerals after plagioclase. Common alteration of pyroxene to calcite may reflect the calcic nature of the pyroxenes (sample 132).

2.2.2.f Dacite-rhyodacitic series

i. Field occurrence: Rocks of this unit are only locally developed in the vicinity of Tirebolu and Koprubasi and extending south-east towards Harkkoy.

Their emplacement seems to be related to the dominant fault pattern of the region, particularly to the northwest trending faults. Their distinct reddish colour, due to the alteration of abundant biotite to iron oxides and hydroxides, and their perfect columnar jointing are the major field criteria used to distinguish these rocks from the dacite lavas of the Lower Volcanic Cycle. The best exposures are along the river Harsit

near Inkoy and Kuskaya.

This unit is difficult to place in the time sequence of the magmatic activity due to its simple nature but complex, though limited, outcrop pattern.

The rocks are underlain by the dolerite sheets of the Upper Basic Series and the author considered that they are the acid members of the Upper Volcanic Cycle. In turn, this explains its disputed place in the stratigraphical column and makes it difficult to accept that it is a single acid volcanic ev ent derived from the assimilation of sialic material, as proposed recently by Stojanov (1975). Furthermore, in the variation diagrams, their continuity with the Upper Basics (Fig.3.3) may confirm that they were probably derived from a common source.

They exhibit perfect columnar jointing approximately at right angles to the contact with underlying rocks. Pyroclastic material is lacking throughout the unit.

ii. Petrography: The dacite-rhyodacites contain abundant quartz, feldspar and biotite phenocrysts in a glassy matrix.

Corroded and rimmed quartz phenocrysts make up almost 5% - 10% of the total phenocrysts. Nearly equal amounts of orthoclase, which is always altered to kaolinite and occasionally to sericite, together with o ligoclase, sometimes pseudomorphed by clay minerals are the other major phenocrysts. Altered biotite is always present both as phenocrysts and groundmass material. The biotite laths show good alignment with flow direction.

The groundmass makes up 60% - 70% of the rock and comprises clay minerals and devitrified glass. This, makes it impossible to recognise any of the original constituents.

Iron, derived from the process of sericitization of ferromagnesian minerals, gives rise to iron hydroxides or oxides (Akinci, 1974). These cause the red colouration of the unit, which may be a diagnostic field

criterion in the area.

2.3 Summary and discussion

In various parts of the Pontids, different stratigraphical columns and sections show that rocks, from the Lower Volcanic Cycle through the Upper Volcanic Cycle, were possibly formed during Upper Cretaceous-early Tertiary times. From the paleogeographical view point, it seems that the land and sea distribution during that particular era was not uniform. According to Brinkmann(1976;p.59) "... in the Pontian geosyncline, during the Upper Cretaceous the water depth increased..... the Campanian-Maestrichtian, marked the greatest expansion of the Cretaceous seas in Turkey." In the Tertiary, the Pontids emerged again and a short interruption in sedimentation occurred during the Palaeogene and lower Eocene. This regression was followed by another transgression in the Lutetian (Middle Eocene , Tokel, 1973).

The microfaunas found in the study area, in the radiolarian cherts and mudstones of the sediments immediately overlying the "host rock" (the Lower Volcanic Cycle) are pelagic or semi-pelagic. They have recently been examined by Dr.A.T.S.Ramsay of Swansea University, who has identified the fauna as Upper Cretaceous (Upper Maestrichtian) and suggested that they indicate water depths in excess of 700 m. However, a limestone (sample 122) from east of Kuskunlu, very near to the contact of the Upper Basic lavas contains the following bioclast;

Crinoidal debris
Coralline algae
Molluscan debris

These faunas are characteristic of a shallow water limestone of Palaeocene or Eocene age (A.T.S.Ramsay, pers.comm.).

Thus pillow lava structures and marine sediments associated with the Lower Volcanic Cycle, together with the above evidence and paleogeographical data, suggest that the volcanism started in a deep marine environment

(Lower Volcanic Cycle) and ended possibly in shallow water - subaerial conditions (Upper Volcanic Cycle). Considering the abundance of columnar jointing in the whole Upper Volcanic lavas, a subaerial environment may be explained by reference to the ideas of McDonald (1968,p.41) "... in Hawaii, the evidence suggests that good columnar jointing was formed only when the underlying surface was saturated with water. The more effective cooling brought about by the water seems to have been the factor that in marginal cases, determined the formation of good columnar jointing."

The major mineralogical difference between the alkali and the tholeiitic (Subalkaline) series is that, the subalkaline rocks are characterised by the reaction relation (Bowen) between olivine and pyroxene (Kuno, 1957, 1959, 1968; McDonald and Katsura, 1964; Wilkinson, 1968). If normative hypersthene and quartz or nepheline in addition to olivine exist, the rocks are consequently called tholeiites or alkali basalts, respectively (Yoder and Tilley, 1962:p.355). As already mentioned in the preceding pages, both Lower and Upper Volcanic Cycles contain normative quartz or olivine and no feldspathoids (Appendix 1). When olivine is present, it is inevitably rimmed by pyroxene. This, in turn, suggests that both series are of subalkaline nature and are represented by normative quartz bearing residua as compared to the undersaturated nature of the residua of the alkalic series. According to Kuno (1968) such a reaction relation (pyroxene-rimmed olivine) accounts for the crystal fractionation of tholeiitic magmas.

Separation between Lower and Upper Basic Series is also in accordance with the pyroxene distribution of the related rocks. As was pointed out in p. 28 , the pyroxenes in the Lower Basic Series are augite and hypersthene as phenocrysts and in additon to these, pigeonite occurs in the groundmass material. On the other hand, the pyroxenes in the Upper Basic Series include augite, diopside and hypersthene both as

phenocrysts and as groundmass constituents. This data, together with the geochemistry of both series (chapter 3) may suggest that the Pontid volcanic rocks are highly compatible with those of the Japanese Pigeonitic (tholeiitic) andhypersthenic (calc-alkaline) series which were defined by Kuno (1959).

The difference between the acid members of the 'two' volcanic cycles are by no means clear. However, distinct columnar jointing and reddish colouration in the field, together with microscopic data (e.g. abundant biotite laths, completely devitrified groundmass) can be used to separate the dacites-rhyodocites of the Upper Volcanic Cycle from the acid members of the Lower Volcanics within which two members have already been described (p.31-32).

CHAPTER THREE

CHEMISTRY OF THE VOLCANIC ROCKS

3.1 Introduction

Distinct differences are apparent between the Lower and Upper Volcanic Cycles both with respect to their field occurrence and to their petrography. These differences should also be reflected in the chemistry of the two cycles and thus unmineralised samples were analysed by X-ray fluorescence for Si, Al, Fe, Mg, Ca, Na, K, Ti, Mn, S, P and for the trace elements Ba, Nb, Zr, Y, Sr, Rb, Zn, Cu, Ni and Cr. Both FeO and H_2O determinations were made on a number of representative samples by wet chemical methods. Where FeO was not determined total iron is expressed as Fe_2O_3.

X-ray fluorescence analysis was performed on pressed powder briquettes using a Phillips PW1212 spectrometer, coupled to a Torrens TE108 automatic sample loader. The instrument is connected to a card punch, for direct data handling on an IBM 360-67 computer.

The following U.S.G.S. international standards were employed to calibrate the major element analysis; BR, W-1, BCR-1, AGV-1, SY-1, GR, T-1, GSP-1, G-2, GA, G-1 and GH.

Trace elements were determined using a series of synthetic Glass Standards prepared by Pilkington Laboratories (Brown et al, 1970). Peak to background ratios were calculated, and referred to calibration curves established for each of the elements sought. Inter-element line-line interferences are relatively common and it was necessary to correct the $ZrK\alpha_1$, $NbK\alpha_1$, and $Y\ K\alpha_1$ readings for $Sr\ K\beta_1$, $Y\ K\beta_1$ and $Nb\ K\beta_1$ interferences respectively (Brown et al,1977). Analysis conditions are described in Appendix 1.

C.I.P.W. norms were calculated using the NORMCAL program (Gill, 1972) of this department. This procedure adopts a fixed oxidation ratio, for the ratio Fe_2O_3/Fe_2O_3+FeO, of 0.27 (Fitton and Gill, 1970). This method

proved inconsistent, presumably owing to factors such as surface weathering. Norms were thus only calculated for those rocks having wet chemically determined FeO and Fe_2O_3 values.

The major and trace element analysis, and available norm calculations are presented in Appendix 1. Due to the extensive alteration, both from weathering and mineralisation, only 108 representative unmineralised rock analyses are used in discussing the chemistry of the volcanics.

The distinction, in the field, between basalts and andesites is impossible. The collective name 'Basic Series' thus includes both basalts and andesites, but where necessary, the two rock types are referred to separately. Three criteria may be used to separate basalts and andesites, firstly a plagioclase composition of An_{50} (Gorshkov,1969), secondly the Colour Index of Thornton and Tutle (1960); the value 30 corresponding to the boundary between the types, and finally silica values less than 55% may be taken to delineate the basaltic field (Taylor,1969; Fitton,197la). Appendix 1 lists basalts and andesites from both the Lower and Upper Volcanic Cycles. No attempt has been made to classify each rock type volumetrically, owing to lack of surface outcrops, and possible biased sample collection. This would tend towards the acid members of the Lower Volcanic Cycle, because of their spatial association with the mineralisation.

3.2 Major Elements

The most obvious chemical variation shown by both Volcanic Cycles is that of silica enrichment, with the resultant formation of basalt.- andesite - dacite - rhyolite associations. The contents of SiO_2, Na_2O and K_2O in the magmas increase and the total Fe, MgO, CaO, TiO2, MnO and P_2O_5 levels decrease with "advancing fractionation" (Miyashiro,1974). Since the silica content increases fairly regularly with advancing fractionation, "Harker-type" variation diagrams can be used to represent the compositional variation. The variation diagrams, for some of the major oxides from both the Lower and Upper

Volcanic Cycles are shown in Figures 3.1 and 3.3.

It is clear from Figure 3.1 that there is a continuous variation in the Lower Volcanic Cycle from basalts towards rhyolites; supporting the smooth changes in the composition of plagioclase, and the decrease in the content of ferromagnesion minerals, through the series. No gap is evident in the silica content of these series. In the Upper Volcanic Cycle, however, a continuum of this kind was neither established in the field, nor during the course of laboratory examination. Figures 3.1 and 3.3 demonstrates the gap between the Upper Basic Series and their related dacites-rhyodacites. The gap obviously must be present for other elements - silica relationship not plotted or shown in Figures 3.1 and 3.3. This gap is also well pronounced petrographically and is reflected in the entire absence of pyroxene and intermediate plagioclase from the dacitic rhyodacitic Upper Volcanic rocks. Taylor (1968) reports a similar gap between the Saipan andesites and dacites.

The smooth variation in the Lower Volcanic Cycle is presumably caused by continuous fractionation from basalt through to rhyolite (Taylor, 1968; Miyashiro, 1974), whereas the compositional gap in the Upper Volcanics may be controlled by high-level extreme fractionation. This is reflected in exponential drops in many major and trace elements, resulting in the extremely fractionated dacites-rhyodacites of the Upper Volcanic Cycle, discussed in 3.4.

The variation in the Al_2O_3 content of the Harsit volcanics is closely comparable with that of volcanics from orogenic areas (Jakes and White, 1972a). Scattering of Al_2O_3 values is strongly controlled by the extent to which the rocks are porphyritic. The Lower Basic Series containing abundant plagioclase phonocrysts (cf.samples 86, 227) are rich in Al_2O_3 (and CaO) contents (compare samples 28, 30, 242 with samples 178, 187) at

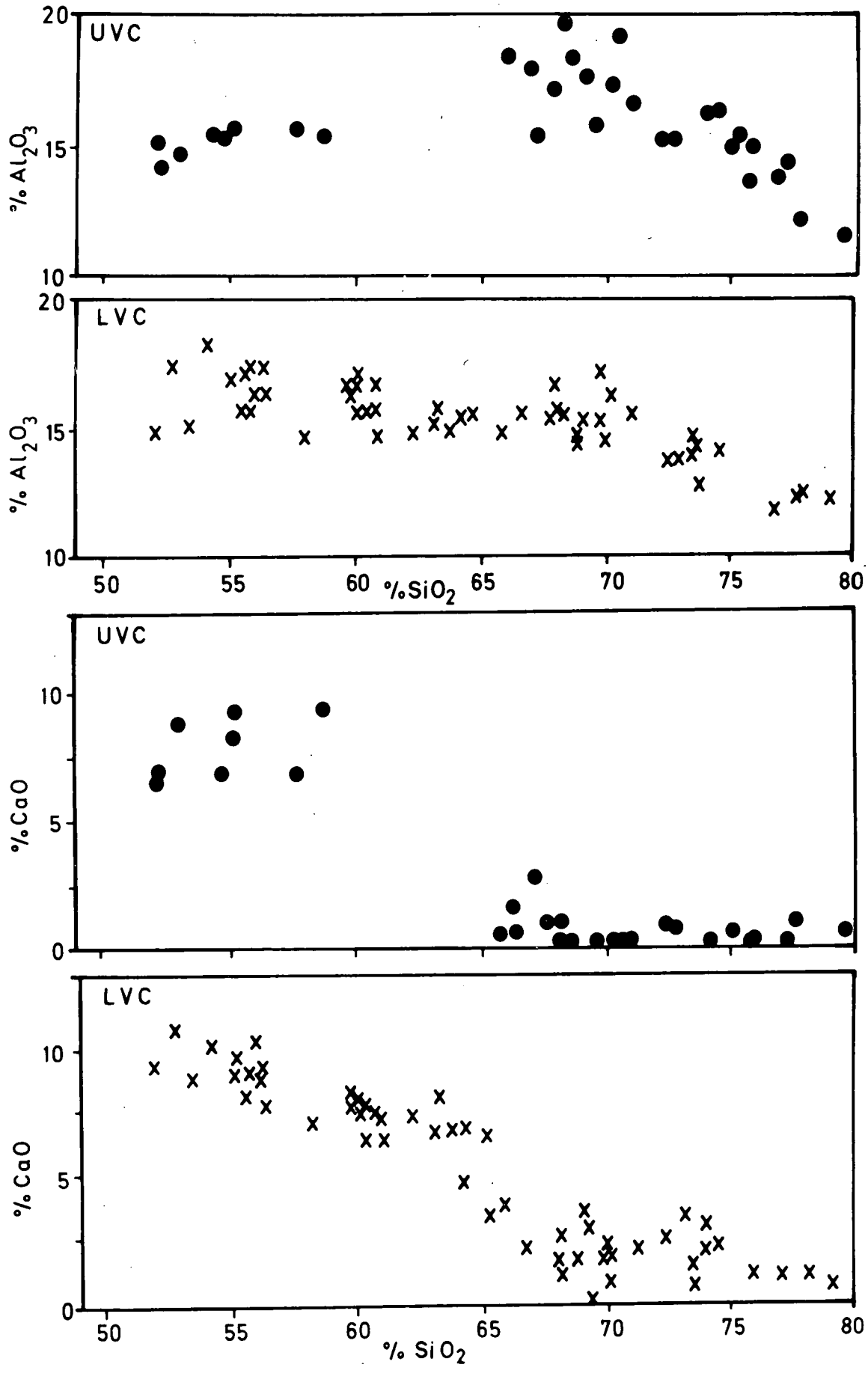

FIGURE 3.1: Al_2O_3 and CaO vs. SiO_2 for basalts, andesites and dacites from the Lower (LVC) and Upper (UVC) Volcanic Cycles.

a given silica value. With increasing silica content, the difference between the Lower and Upper Volcanic Cycles become marked. In the former Al_2O_3 decreases slightly towards the rhyolites, while in the latter, substantially constant Al_2O_3 in the basic rocks is followed by a slight enrichment in the middle stage and a subsequent decrease (Fig.3.1). This effect is probably derived from the different fractionation histories of plagioclase, discussed below.

Extremely Al_2O_3 rich samples from both series, particularly from the dacites-rhyodacites of the Upper Volcanic Cycle, are oversaturated in alumina and give normative corundum. This is believed to result from secondary processes, such as, kaolinisation. The Upper Volcanic Cycle have a higher modal K-feldspar content than the dacites of the Lower Volcanic Cycle and are thus more subject to kaolinitic and/or sericitic alteration.

The differences in the major and trace element levels of each volcanic cycle are summarised in Table 3.1, using the Wilcoxon Rank Sum Test (Wilcoxon and Wilcox, 1964). Table 3.1 shows that there is a significant difference between the total Fe, as Fe_2O_3, contents of the basalts from the Lower and Upper Volcanic Cycles; the Lower Basic Series are characterised by relatively high Fe_2O_3 contents.

Analyses of rocks from the two cycles are plotted in an AFM diagram in Figure 3.2. The distinct difference shown between the Lower and Upper Volcanics is closely compatible to that between the Japanese Pigeonitic and Hypersthenic series (Kuno, 1968a) or between worldwide tholeiitic and calc-alkaline series as demonstrated by Irvine and Baragar (1971,p.528). The Lower Volcanic Cycle is characterised by total Fe enrichment, relative to MgO and K_2O+Na_2O, in the early stages of fractionation while in the Upper Volcanic Cycle, particularly in the basic lavas, there is little or no relative enrichment of Fe. In the latter series both total Fe and MgO

Table 3.1: Comparative chemistry of basalts, andesites and dacites - rhyodacites from the Lower and Upper Volcanic Cycles (after Egin et al, in print)

	BASALTS					ANDESITES					DACITE-RHYODACITE				
	L.B.S.		U.B.S.			L.B.S.		U.B.S.			L.V.C.		U.V.C.		
	Range	Mean	Range	Mean	WRST	Range	Mean	Range	Mean	WRST	Range	Mean	Range	Mean	WRST
SiO_2	51.27-54.18	52.76	52.13-55.12	53.41	-	55.04-70.75	59.77	55.43-58.79	57.30	-	64.11-77.72	70.62	65.96-79.66	71.92	-
Al_2O_3	14.82-18.30	16.16	14.19-15.72	15.20	-	13.27-17.43	15.78	15.52-16.56	15.95	-	11.77-17.21	14.81	11.49-19.86	15.97	0.05
Fe_2O_3*	10.11-11.92	10.63	7.28- 9.58	8.74	0.01	4.74-10.48	7.23	6.14- 8.34	7.02	-	1.37- 3.94	2.59	0.60- 3.66	1.74	0.01
MgO	2.81- 8.34	5.43	5.14- 8.93	7.21	-	0.84- 5.86	2.57	3.40- 5.65	4.31	0.05	0.04- 1.33	0.52	0.04- 0.62	0.28	0.02
CaO	8.91-10.90	9.80	6.61- 8.62	7.38	0.01	4.51-10.48	7.52	6.95- 9.30	8.49	-	0.58- 4.68	2.22	0.00- 2.85	0.60	0.01
Na_2O	1.48- 2.19	1.75	1.63- 4.61	2.99	0.05	1.64- 3.32	2.42	1.29- 3.14	2.44	-	1.46- 3.67	2.62	1.13- 2.84	2.05	0.01
K_2O	0.12- 0.90	0.48	2.18- 3.30	2.84	0.01	0.47- 2.78	1.26	2.03- 3.82	2.79	0.01	1.65- 5.79	3.58	3.94- 9.45	6.59	0.01
TiO_2	0.82- 1.21	0.99	0.76- 0.79	0.84	0.10	0.51- 1.06	0.79	0.86- 1.03	0.93	0.10	0.18- 0.42	0.32	0.14- 0.45	0.29	-
MnO	0.07- 0.31	0.19	0.11- 0.18	0.16	-	0.03- 0.35	0.15	0.10- 0.14	0.12	-	0.01- 0.12	0.06	0.01- 0.06	0.03	0.01
S	0.02- 0.38	0.12	0.06- 0.18	0.10	-	0.02- 0.25	0.07	0.03- 0.14	0.09	-	0.02- 0.16	0.05	0.02- 0.22	0.06	-
P_2O_5	0.11- 0.16	0.14	0.23- 0.36	0.27	0.01	0.09- 0.22	0.16	0.24- 0.30	0.27	0.01	0.03- 0.17	0.10	0.01- 0.09	0.03	0.01
Ba	115-302	205	305-544	398	0.01	266-519	366	481-708	569	0.01	174-796	559	601-1512	1227	0.01
Nb	2	2	2-7	4	0.05	0-5	3	3-5	4	0.10	1-6	4	4-14	11	0.01
Zr	51-69	62	67-113	83	0.05	49-107	83	68-121	105	0.10	81-140	106	90-244	166	0.01
Y	17-21	20	18-25	21	-	20-54	30	18-27	21	-	11-53	21	8-23	18	-
Sr	256-306	280	382-690	515	0.01	145-314	252	570-685	634	0.01	65-280	146	27-335	94	0.01
Rb	5-26	14	46-74	62	0.01	0-93	43	62-93	80	0.05	64-132	99	133-266	195	0.01
Zn	71-310	135	70-82	75	-	0-117	82	54-84	74	-	0-46	30	5-136	23	0.01
Cu	20-122	60	38-262	148	0.05	0-68	15	44-107	69	0.01	0-12	1	0	0	-
Ni	0-23	6	32-117	73	0.01	0-45	7	16-34	25	0.05	0-6	1	0	0	-
Cr	20-137	104	138-232	200	0.01	0-153	22	69-146	111	0.01	0-25	8	0-20	3	0.01

* Total Fe expressed as Fe_2O_3. L.B.S., Lower Basic Series. U.B.S., Upper Basic Series. L.V.C., Lower Volcanic Cycle. U.V.C., Upper Volcanic Cycle. W.R.S.T., Two sided Wilcoxon Rank Sum Test probability levels (Wilcoxon and Wilcox, 1964), only values up to a probability level of 0.10 are included.

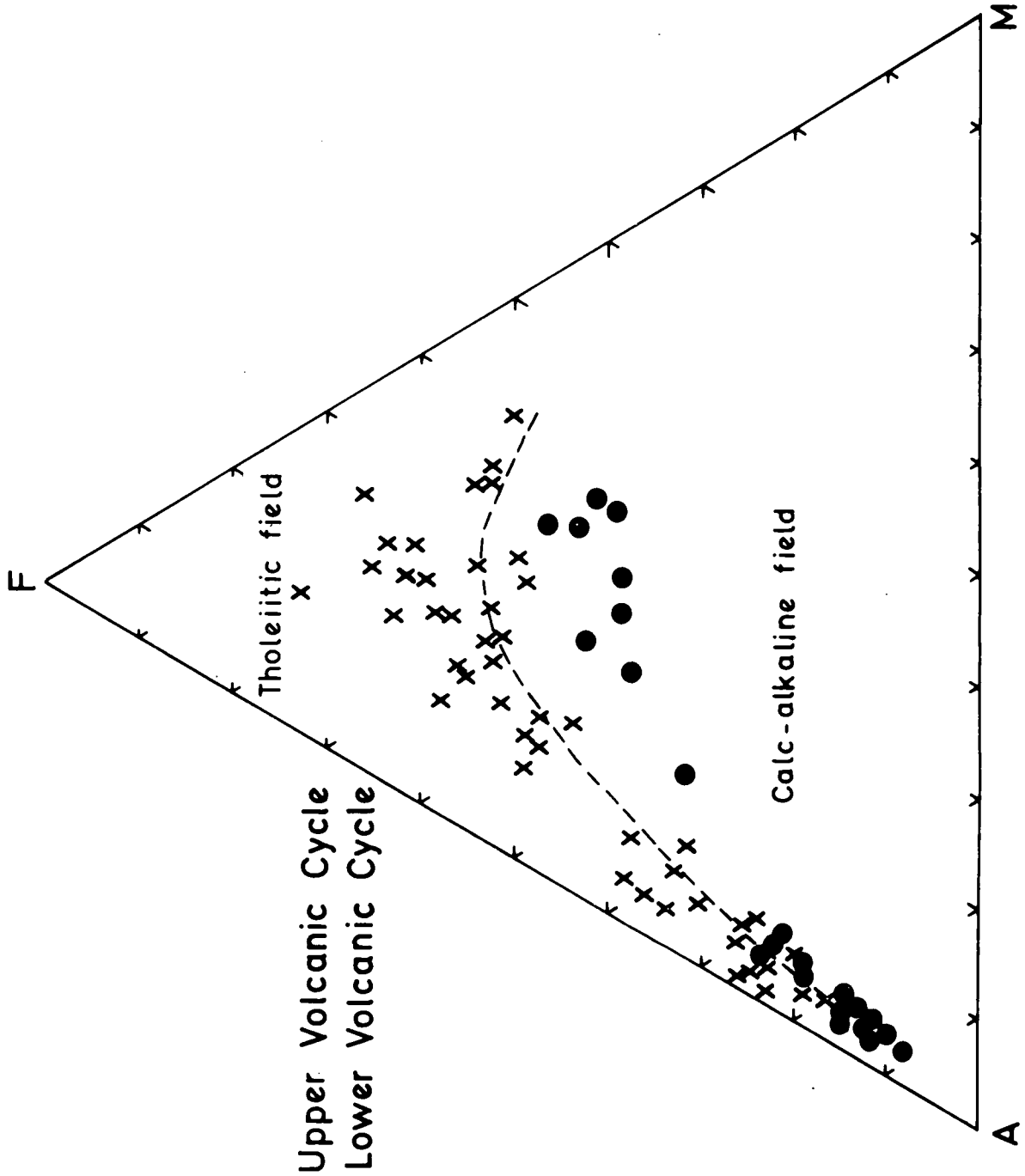

FIGURE 3.2: AFM diagram for rocks of the Lower and Upper Volcanic Cycles. Field boundary after Kuno (1968a).

decrease smoothly with increase in K_2O+Na_2O throughout fractionation resulting in a trend which is roughly perpendicular to the F-M axis. Enrichment of total Fe, relative to MgO, is also clear for the Lower Volcanic Cycle using "the Ferro-Femic Indices". Coats (1968) has devised an index that expresses concisely the degree of encrichment of iron characteristic of various differentiation series. "The Ferro-Femic Indices" of the Lower and Upper Volcanic Cycles are respectively 75 and 64, being closely comparable values to those of tholeiitic and calc-alkaline rocks, respectively.

Numerous studies made previously (Kennedy, 1955; Kuno,1966; Osborn, 1959, 1962) have shown that, under moderate to high pressures of oxygen, differentiation leads to enrichment in alkalies and silica, whereas crystallisation under very low oxygen pressures leads also to iron enrichment. The water content of the initial magmas exerts great control over oxygen pressure (Kuno 1966, 1968b; Yoder, 1969), and is essential to the early formation of magnetite (Osborn, 1959). Thus, depending on the water content of the magma, under conditions of constant or increasing oxygen fugacity, precipitation of magnetite takes place, with a resultant calc-alkaline melt, poor in iron. The observed relative iron-enrichment in the tholeiitic rocks of the Lower Volcanic Cycle thus probably results from the fact that iron was not incorporated into magnetite in the early stages of crystallisation.

The decrease in MgO content, together with Ni and Cr, with increasing silica can be explained largely by their preferential incorporation in early formed olivines and pyroxenses (Burns, 1969/1970). Aphanitic samples of the Lower Basic Series have lower MgO contents than porphyritic samples. It is interesting to note that intrusive dolerites of the Upper Basic Series have MgO values similar to the Lower Basic Series and that both have lower values than the Upper Basic Series lavas.

Basic rocks of the Lower Volcanic Cycle have significantly higher CaO

contents than their counterparts from the Upper Volcanics (Fig.3.1, Table 3.1), presumably reflecting the more basic nature of their plagioclase. There is a continuous decrease in the CaO content of the Lower Volcanics as the silica values increase, while in the Upper Volcanic Cycle, particularly in the basic lavas, a slight increase is followed by a sharp decrease as the rocks become dacitic-rhyodacitic in composition. This pattern of variation, taken together with those for Al_2O_3 and Sr, suggests that pyroxene controlled fractionation in the basalts of the Upper Basic Series, allowing build up of Ca and Sr. Once plagioclase start to fractionate the levels of Ca and Sr in the magma will fall.

An orthodox alkali-silica variation diagram can be used to distinguish the subalkaline rocks (e.g. tholeiitic and calc-alkaline, Wilkinson, 1968) from the alkaline rocks. According to Irvine and Baragar (1971) over 90% of analyses plot satisfactorily in their appropriate fields. The alkali-silica diagram is illustrated in Figure 3.3. The diagram shows some scattering, due to the mobility of K and Na, but despite this most of the Lower Volcanic rocks plot within, or very close to, the trend for well-known tholeiitic rocks (Carmichael et al,1974) or are closely comparable to the field of the Japanese Pigeonitic series (Kuno,1960, 1968a, Sugimura, 1968). The Upper Volcanics are similarly compatible with calc-alkaline rocks from well-known volcanic fields, particularly with those from the Cascades, the Andes (Carmichael et al,1974) and the English Lake District (Fitton, 1971a).

The plot of SiO_2(Wt%) against the molecular proportions ratio Na_2O+K_2O/Al_2O_3 (Sugimura, 1968) shown in Figure 3.4a again reveals a good separation between the Lower and Upper Basic Series. The ratio Na_2O+K_2O/Al_2O_3, expresses the "alkalinity" of a suite and increase in this ratio makes the composition of the feldspar more alkalic (Ibid). This is in accordance with the observed petrography of the respective basic series described in

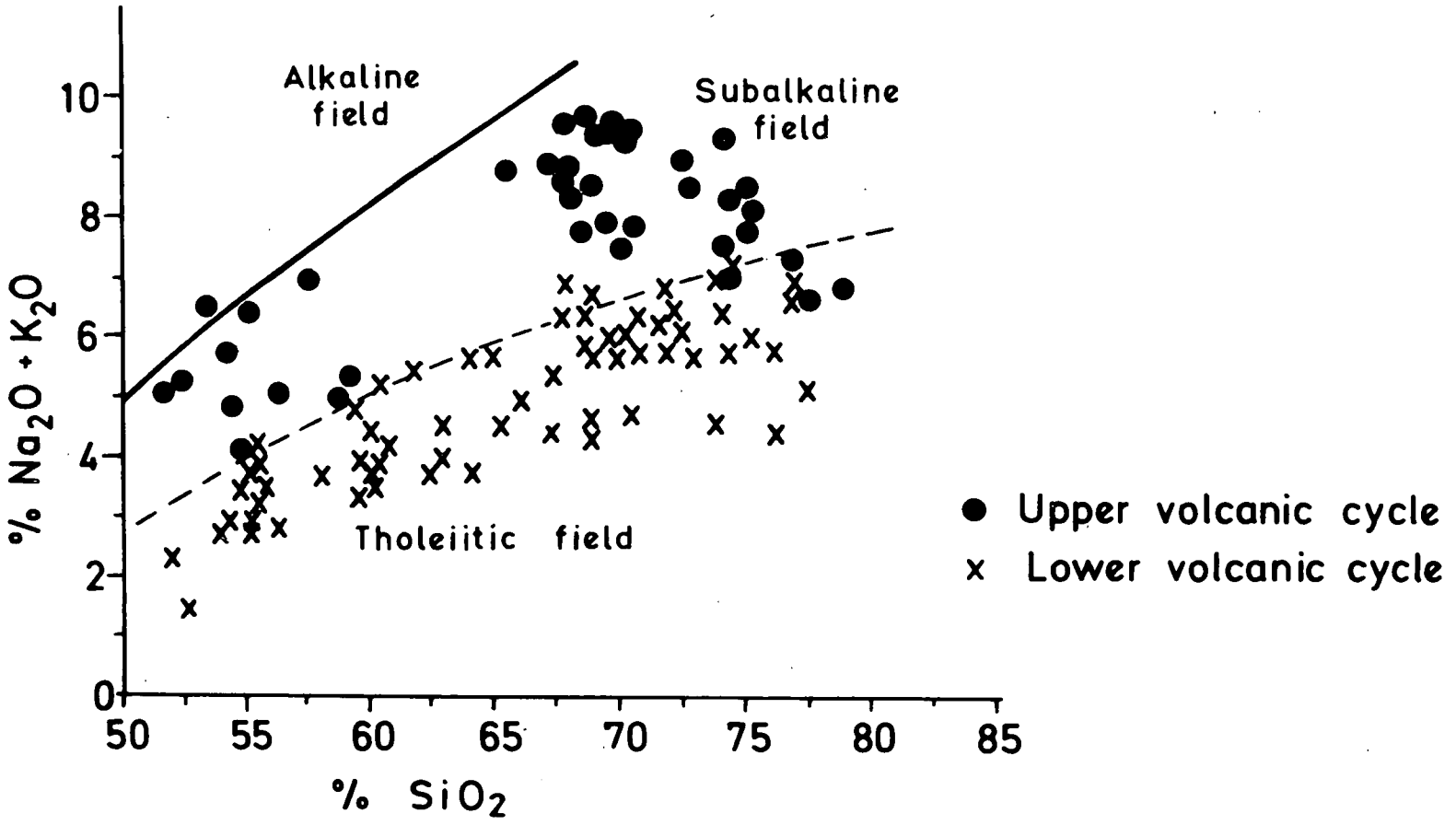

FIGURE 3.3: $K_2O + Na_2O$ vs. SiO_2 for volcanic rocks of the northern Harsit river area. Alkaline-subalkaline field boundary after Irvine and Baragar (1971) subalkaline-tholeiitic boundary after Kuno (1968a)

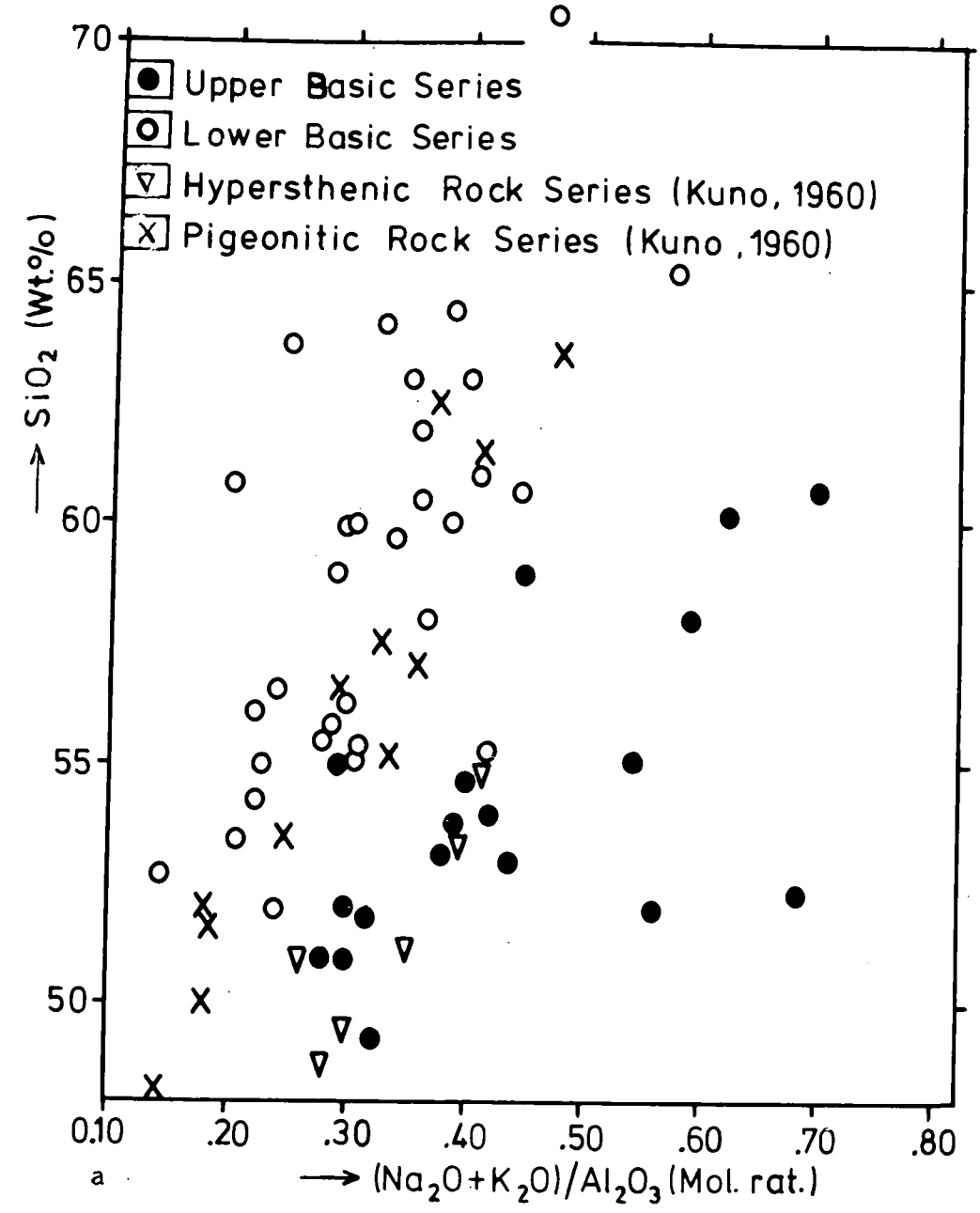

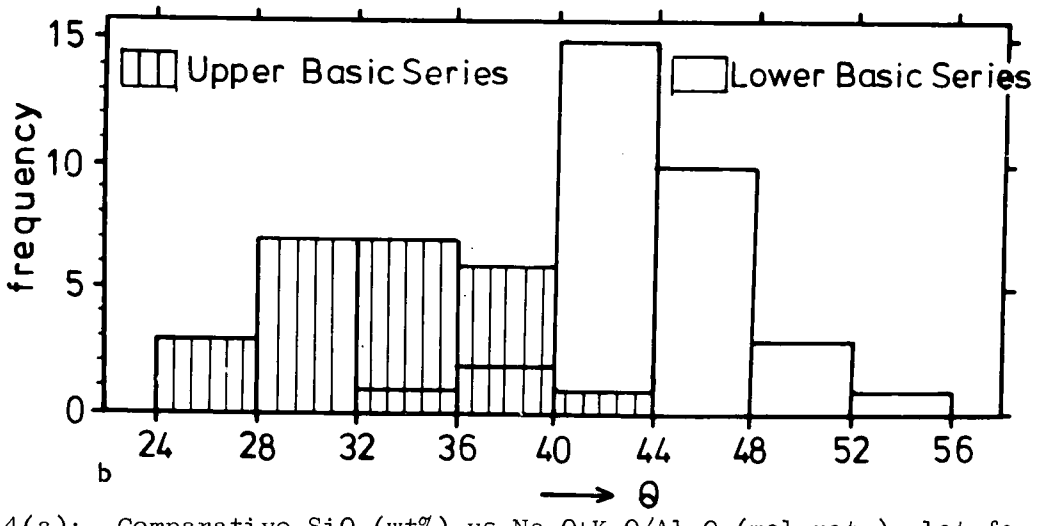

FIGURE 3.4(a): Comparative SiO_2(wt%) vs.Na_2O+K_2O/Al_2O_3(mol.rat.) plot for the northern Harsit and Japanese basic volcanic rocks.

FIGURE 3.4(b) Distribution of θ values in the Lower and Upper Basic Series

Chapter 2. Japanese lavas are also plotted in Figure 3.4a. These plots again show that the Lower Basic Series are similar to the pigeonitic series (Kuno,1960, p.125; Sugimura,1960 p.145), and the Upper Basic Series to the Hypersthenic series Kuno,1960,pp.125, 140).

Sugimura (1960, 1968) has derived an index, the Θ index which allows comparison of sub alkaline rocks in terms of alkalis, silica and alumina. He has shown that Θ usually gives a constant value for basaltic and andesitic rocks of one volcanic source. In Figure 3.4b a 'Θ' histogram of the Harsit basic rocks reveals a clear separation of the two series. Mean values are shown in Table 3.2, where they are compared with Θ values of volcanics from Japan. The data confirm the striking similarity between Pigeonitic (tholeiitic) lavas and the Lower Basic Series and between the Hyperstenic (calc-alkaline) rocks and the Upper Basic Series.

The tholeiitic and calc-alkaline affinities of the Lower and Upper Volcanic Cycles respectively can be further verified by using the alkaline-lime index of Peacock (1931). The Lower Volcanic Cycle have an index of 65 and should be termed a "Calcic Series". The andesites of such suites have very calcic plagioclase and according to McBirney 1969, p.503 "... are typical of volcanic belts rising from moderately deep seas or very near the edge of thin continental crust in regions such as Mariana, Japan and Antilles". The Upper Volcanic cycle with an index of 58 are termed "calc-alkaline". McBirney (1969, p.504) states that "... most andesitic volcanoes near continental margins, that are visibly underlain by considerable thicknesses of sialic crust erupt lavas that belong to the calc-alkaline series".

The difference in the K_2O contents of the two volcanic cycles, shown in table 3.1 is highly significant. No gradations occur between the two, although spatially the series overlap.

The formation and significance of K-rich volcanic rocks have been

Table 3.2: Θ values for Turkish and Japanese volcanic rocks (after Egin et al, in print)

Area	Magma Type	Mean Θ value*	Standard error**	Reference
Harşit, Lower Basic Series	Tholeiitic	43.61	0.64	Present study
Harşit, Upper Basic Series	Calc-alkaline	33.24	1.04	Present study
Izu-Hakone	Tholeiitic	43.05	0.50	Kuno (1968)
Tarumai	Tholeiitic	45.8	-	Sugimura (1960)
Tori-Sima	Tholeiitic	42.1	0.20	Kuno (1960)
Amagi	Calc-alkaline	36.7	0.40	Kuno (1968), Miyashiro (1974)
Kayatokage	Calc-alkaline	35	-	Kuno (1960)
Ontake	Calc-alkaline	32	-	Kuno (1960)
Genbuda	Alkaline	28	-	Sugimura (1960)
Tosima	Alkaline	21	-	Sugimura (1960)
Penghu	Alkaline	30.1	-	Sugimura "

* All Θ values except those for Harşit volcanics are from Sugimura (1960, 1968)

** $(d^2/n)^{\frac{1}{2}}$ where d = standard deviation, n = number of samples.

reported from various parts of the world. Moore (1962) pointed out that in Cenozoic rocks of the western United States, K is least abundant, relative to total alkalies, in a zone along the Pacific coast becoming more abundant towards the east where the continental crust thickens. Moore concluded that, in the east, they acquired their high K/Na ratios from the crust by melting and contamination. In New Zealand, where a continental crust underlies the volcanic belt, Ewart and Stipp (1968) have invoked that the origin of the andesitic to rhyolite suite is consistent with a hypothesis involving assimilation of Triassic to Jurassic eugeosynclinal greywacke and argillite sediments. Hypotheses relating the formation of the Japanese calc-alkaline (Hypersthenic) rocks to contamination of magmas with geosynclinal and/or granitic material have been proposed by Aoki and Oji (1966) and Kuno (1968b). In general, in the generation of calc-alkalic rocks, sialic or granitic contamination of basaltic magma is a prerequisite. This is followed by fractional crystallisation and the generation of more evolved calc-alkaline members (Kuno, 1950; Tilley, 1950).

The Pontid Volcanic Belt and remnant Pontian Land basement rocks,Figure 1.2 clearly represents a magmatic arc, underlain by a sialic crust. There is however little or no data related to the thicknesses of the continental crust (Neprochnov et al, 1974; Brinkmann, 1972, 1976), although it probably becomes thinner towards the North Anatolian Fault, near to the proposed trench (see Chapter 1), where it is replaced by mantle derived ultramatic rocks (Brinkmann,1972, p.622, Fig.2).

If contamination of basic magmas by assimilation of upper crustal material, or by mixing with acid rocks, plays a part in the production of the Harsit volcanics, the theory must apply equally to both the Lower and Upper Volcanic Cycles, since their distribution seems unrelated to position in the arc. Assimilation of basement rocks by rising magma would not adequately explain the enrichment of K, Ba, Rb etc. in the Upper Volcanic Cycle relative to the Lower Volcanic rocks. This, however, may be

explicable in terms of a different source material and fractionation stage for each volcanic unit as discussed below.

TiO_2 levels and variations in the two volcanic cycles are comparable. Figure 3.5 shows that both series have TiO_2 contents compatible with island arc basalts and andesites (Pearce and Gale,1977).

There is no significant differerence in the MnO distribution of the two volcanic cycles (Table 3.1). The high contents in some Lower Basic rocks, apparently unaffected by mineralisation, are believed to be due to the relatively high mobility of this element.

P_2O_5 shows a tendency to concentrate during the early part of the main stage of crystallisation, presumably as apatite. The relatively high P_2O_5 content of the Upper Basic Series (Table 3.1) may be attributed to the presence of hornblende and biotite, since hydrous silicates may accept more phosphorus than anhydrous ones, although the difference is small (Anderson and Greenland,1969). In the Upper Volcanics P_2O_5 tends to remain constant until a silica level of approximately 60% is reached, followed by a sharp decrease (Table 3.1). This pattern is similar to that of CaO, and may indicate that fractionation of apatite, like plagioclase, did not take place until a relatively late stage. In the Lower Volcanics the low P_2O_5 level are attributed to early fractionation of this element, yielding a melt low in P_2O_5.

3.3 Trace Elements

In recent years, studies related to the alteration of ocean-floor basalts (Cann, 1970a) and volcanics subject to metamorphism or extensive alteration (Floyd and Winchester, 1975, 1978; Winchester and Floyd, 1977; Whitehead and Goodfellow, 1978) have revealed that the trace elements Ba, Rb and, to a lesser extent, Sr have been significantly redistributed. Other elements, such as Ti, Zr, Y, Nb, P, Cr and Ni are generally considered to remain inert during secondary processes (Pearce and Cann, 1973). These

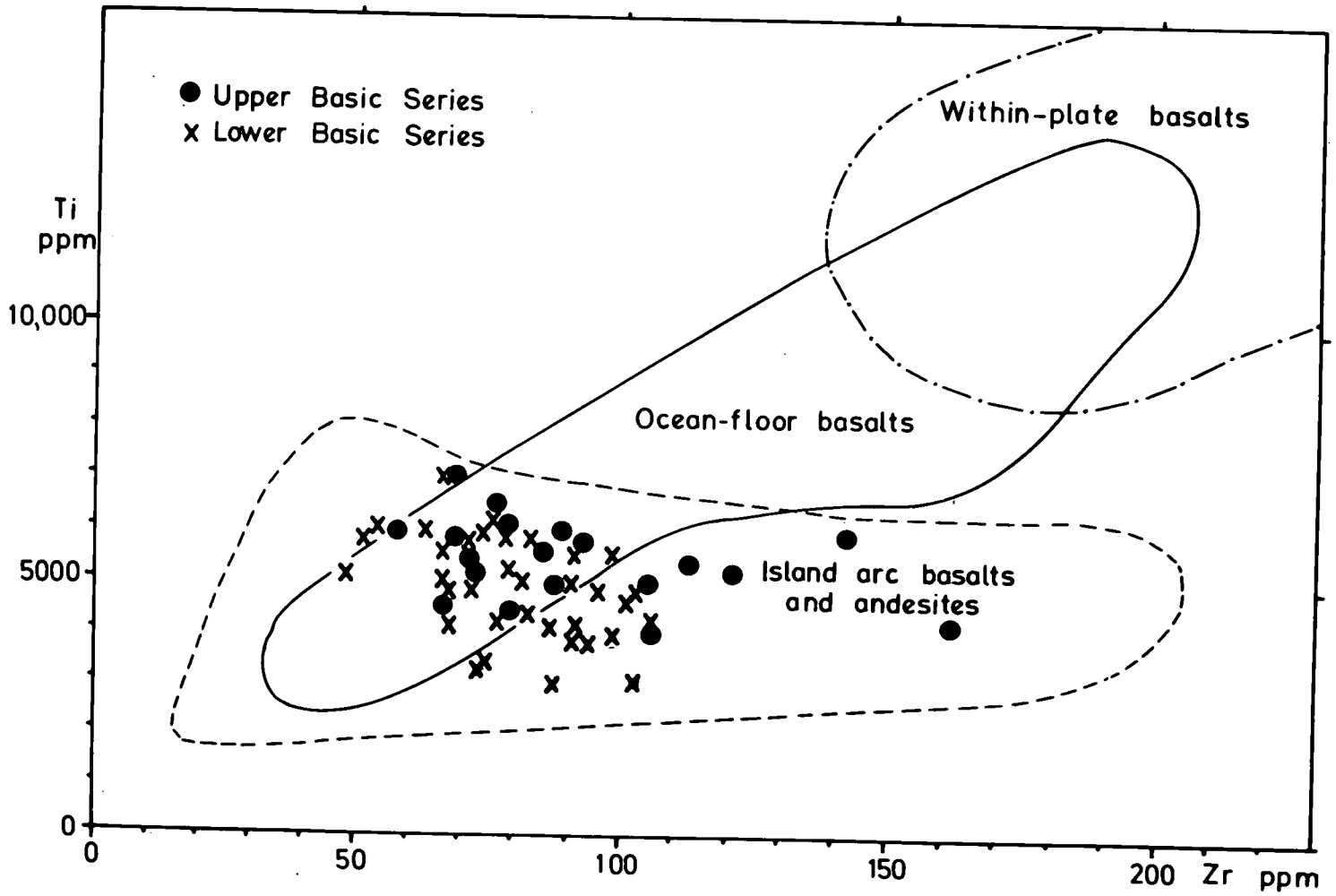

FIGURE 3.5: Ti vs. Zr Field boundaries after Pearce and Gale (1977)

immobile elements can be used satisfactorily to discriminate between subalkaline and alkaline basaltic rocks. Distinction between tholeiitic and calc-alkaline series is less certain due to insuffient data (Winchester and Floyd, 1977). The Harsit Volcanic rocks show varying degrees of chemical weathering and are thus mainly discussed in terms of the immobile trace elements. The present study shows that significant distinctions may be obtained between tholeiitic and calc-alkaline rocks using Nb, Y and Zr contents.

Taylor and White (1966) and Prinz (1968) have shown that the large cations; K, Rb, Ba, Ca, Sr and Na, the ferromagnesian elements; Cr and Ni, and the chalcophile element; Cu give valuable information relating to the course of crystallisation, and to source material.

The major differences in the trace element levels of each volcanic unit are shown in Table 3.1. Significant differences occur between the Lower and Upper Basic Series. Ba, Nb, Zr, Sr, Rb, Cu, Ni and Cr are higher in the Upper Basic Series. The enrichment of the above elements from tholeiitic to calc-alkaline and shoshonitic rocks is well established in island arcs (Jakes and Gill, 1970; Pearce and Cann, 1973). Table 3.3 summarises the trace element contents of rocks with tholeiitic, calc-alkaline and shoshonitic affinities.

In a general sense, in both volcanic cycles Ba, Rb and Zr increase with silica. This trend would normally result from fractional crystallisation of basaltic magma (Taylor 1969). An exponential decrease in the levels of Cr, Ni and Cu together with an increase in Sr, followed by a sharp decrease when the rocks become acidic in composition, are important characteristics of the Upper Volcanic Cycle (Table 3.1). This series also shows Nb enrichment in later differentiates while Nb is substantially constant in the Lower Volcanic Cycle.

Of the trace elements Ba shows the greatest variation, particularly

TABLE 3.3: Trace element abundances in volcanic rocks from well-known volcanic terrains

	1	2	3	4	5	6	7	8	9	10	11	12	13	14	15	16	17
SiO_2	58.09	51.57	56.15	57.49	-	52.76	59.77	59.50	51.04	59.98	-	-	61.1	53.41	57.30	53.94	53.74
Rb	12	5	-	11	17	14	43	31	49	124	135	140	31	62	80	115	75
Ba	145	75	194	162	244	205	366	270	349	747	720	820	320	398	569	1217	1000
Sr	230	200	214	290	450	280	252	385	346	270	420	425	314	515	634	459	700
Ni	22	30	89	5	84	6	7	18	145	22	30	2	38	73	25	6	20
Cr	30	50	199	11	160	104	22	56	410	62	85	12	66	200	111	24	30
Zr	80	70	160	87	138	62	83	110	141	227	180	300	115	83	105	92	40
Nb	-	-	-	1	-	2	3	4.3	11	14	-	-	4.5	4	4	4	-
Y	-	-	-	24	30	20	30	21	27	40	-	-	23	21	21	22	-

1. Trace elements in developed island ars, 85% tholeiitic (Jakes and White, 1972a)
2. Tholeiitic basalt (Ibid)
3. Avarage archaean, tholeiitic volcanic rocks, Canada. (Baragar and Goodwin,1969)
4. St.Kitts tholeiites, Lesser Antilles (Brown et al, 1977)
5. "All tholeiites" mean (Prinz, 1968)
6. Lower Basic Series, basalts, northern Harsit river (Egin et al, in print)
7. Lower Basic Series, andesites, northern Harsit river (Ibid)
8. Avarage andesite,calc - alkaline (Taylor 1969)
9. Calc-alkaline basalt of southern outcrop, English Lake District (Fitton, 1971a)
10. Calc-alkaline andesite of southern outcrop, English Lake District (Ibid)
11. Andean, calc-alkalic andesite (Sieger et al,1969)
12. Intracontinental andesite, Carpathian (Jakes and White, 1972a)
13. Hypersthenic rock series, andesite (Taylor and White, 1966)
14. Upper Basic Series, basalts, northern Harsit river (Egin et al, in print)
15. Upper Basic Series, andesites, northern Harsit river (Ibid)
16. Upper Basic Series, dolerites, northern Harsit river
17. Shoshonite (Jakes and White, 1972a)

amongst the statistically higher values of the Upper Volcanic Cycle. The highest Ba values for basic rocks occur in the intrusive dolerites (Table 3.3) and are comparable with levels found in shoshonitic rocks. Although many dolerites are near to mineralised areas, sample 184 and 186 are at some considerable distance from the mineralisation. This suggests that contamination from underlying barytic beds, during the course of intrusion, is unlikely. Had such contamination occurred the dolerites might also have been enriched in Mn or Fe (Chapter 8).

The behaviour of Rb is similar to that of K and Ba. The element being enriched in late fractionates. According to Jakes and White (1970) tholeiitic island arc rocks have high K/Rb ratios when compared to calc-alkaline and shoshonitic types, a feature which is not shown by the Harsit volcanics. The plot of K against Rb shown in Figure 3.6 reveals considerable scattering of values, mostly in the basic members of each series: the Lower Basic Series have a range of K/Rb from 95 to 790 and the Upper Basic Series from 175 to 500. The values of the ratio for the Lower Basic Series are considerably lower than for the tholeiitic rocks discussed by Jakes and White (1970, table 2), whose K/Rb ratios vary between 510 and 1070. Since the K contents are normal, the generally low K/Rb ratios, compared with the other tholeiitic suites, must be due to relatively high Rb contents. Brown et al (1977) attributed low K/Rb ratios in the island arc tholeiites of the Lesser Antilles to a high level fractionation of primary melts, with amphibole among the separating phases, yielding residual liquids with low K/Rb ratios.

Figure 3.6 also shows that K/Rb ratios tend to decrease as the K content increases from the Lower to the Upper Volcanic Cycles. Dickinson and Hatherton (1967) and Jakes and White (1970) have shown that increase in K content of lavas across island arcs, in a direction away from the ocean, is accompanied by a decrease in the K/Rb ratios. The present study suggest

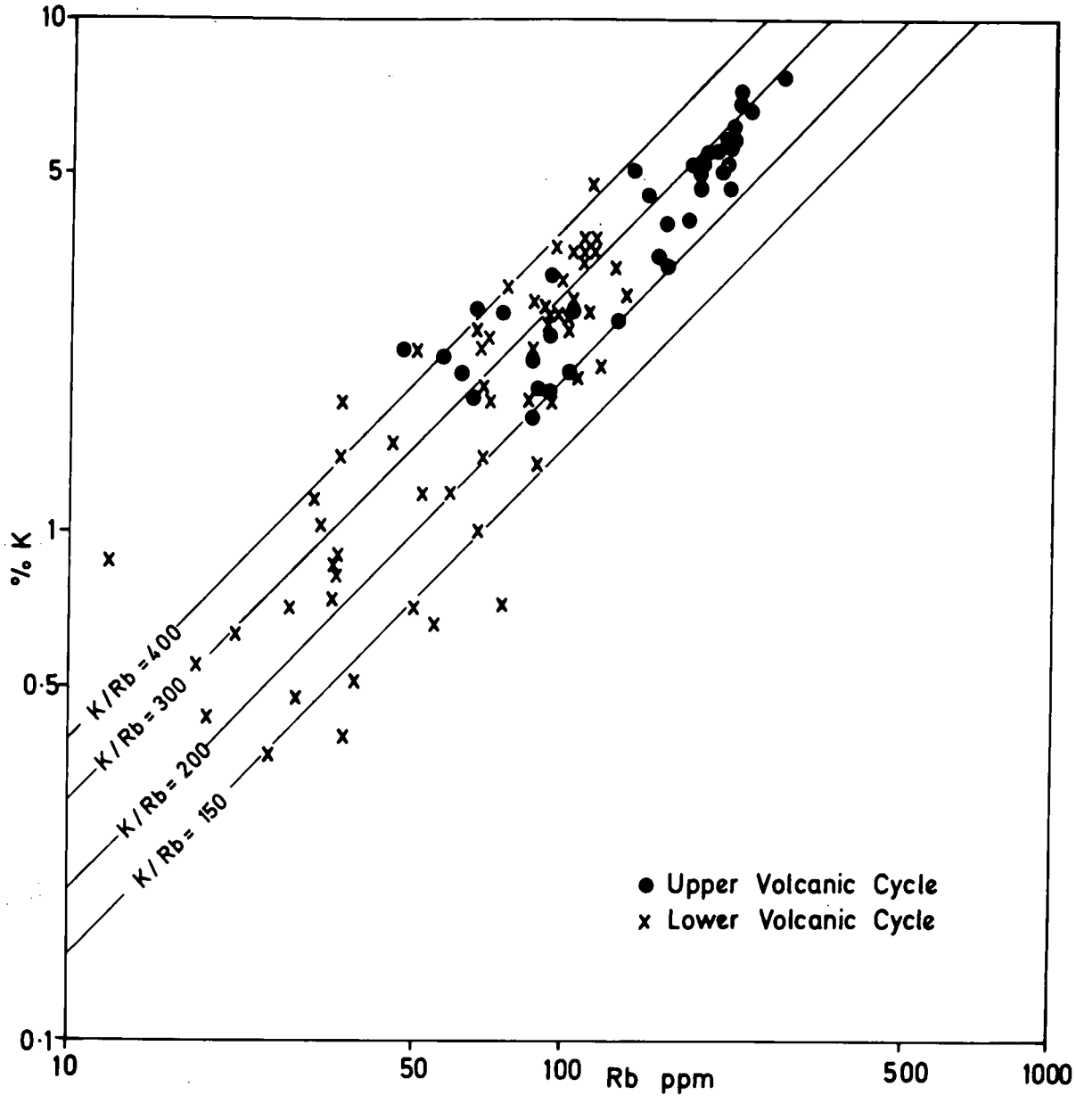

FIGURE 3.6: Kvs. Rb for volcanic rocks from the northern Harsit river area

that similar variation in K, and K/Rb ratios, can also occur in time.

Goldschmidt (1954) stated that Zr increases as differentiation proceeds from mafic to silisic rocks, while Chao and Fleischer (1960) have shown that more Zr is more soluable in alkalic magmas than in tholeiitic magmas. The low and high Zr contents of the Lower and Upper Volcanic Cycles respectively (Table 3.1) are in accordance with this. Taylor (1969) pointed out that large highly charged cations (e.g. Zr,Nb) are enriched in volatile rich magmas. Enrichment of those elements only occurs in the Lower Volcanic cycle in the late stage rhyolitic breccias where there is a large increase relative to the dacitic lavas. In the Upper Volcanics progressive enrichment of Zr and Nb takes place throughout crystallisation and may be related to a higher water content in the magma. Differentiation of the Lower Volcanic Cycle is essentially a process involving a dry magma. In such a situation enrichment of incompatible elements into residual liquids will be minimal. The Upper Volcanic Cycle conversely has formed from a much wetter magmas with the resultant, pronounced fractionation of incompatibles and their steady enrichment throughout crystallisation. These facts suggests that the mineralisation, associated with the highly pyroclastic rhyolitic rocks of the waning stage of the Lower Volcanic cycle may suggest that addition of water to this magma was a late stage event, responsible for both the explosive nature of the rhyolitics and the addition of ore components. Some significance may well attach to the correlation between these rhyolites, rhyolitic breccias the mineralisation, and the dominant fracture pattern. The fracture pattern providing channel ways for circulating hydrothermal fluids (Chapter 5.1).

In igneous rocks Sr is closely associated with Ca, its distribution being strongly controlled by that of plagioclase (Prinz, 1968). In the Lower Volcanic rocks Sr decreases smoothly when the rocks become andesitic-dacitic in composition. In the high Sr containing Upper Basic Series, Sr

increases from basalts to andesites when a sudden drop in the Sr level occurs and low amounts persist throughout the acidic members (Table 3.1). In the latter crystallisation and subsequent removal of plagioclase only took place at a late stage, possibly due to magma generation at depths where plagioclase was unstable, as suggested by Dostal et al (1977). Yoder and Tilley (1962) have also shown that high PH_2O will supress plagioclase crystallisation in basic magmas. In the Lower Basic Series Sr depletion may be explained by its incorporation into early formed plagioclase yielding a Sr impoverished melt and subsequent Sr poor products. Taylor (1969) has suggested that fractional crystalliation would produce low K/Rb, Ba/Rb and high Rb/Sr, Ba/Sr ratios. The plot of Sr versus Rb in Figure 3.7 shows a clear separation between the rocks of the Lower and Upper Volcanic Cycles. The Rb/Sr ratio, however, increases from basaltic to dacitic to rhyolitic rocks in both series, indicating the effects of independent fractional crystalliation in each volcanic cyle. Both cycles show trends in their basicseries which are closely similar to those reported by Brown et al (1977) for basalts and andesites from the Lesser Antilles, and overall trends similar to those given for Icelandic rocks by Johanneson (1975). In the basic members the trends are produced by increasing Rb with virtually constant Sr and in the acidic members by a sharp decrease in Sr at near-constant Rb (Figure 3.7). The absence of significant amphibole in the basic rocks, particularly in the Lower Basic Series, mitigates against amphibole fractionation as a controlling mechanism for Rb build up as advocated by Brown et al (1977). Plagioclase does not seem to have affected Sr levels in the residual liquids until the more acid, dacites-rhyodacites crystallised, when Sr depletion is very marked.

Ni is significantly higher in the basic lavas of the Upper Volcanic Cycle than in their Lower Volcanic Cycle counterparts (Table 3.1) although intrusive dolerites of the UpperVolcanics have low Ni values (Table 3.3).

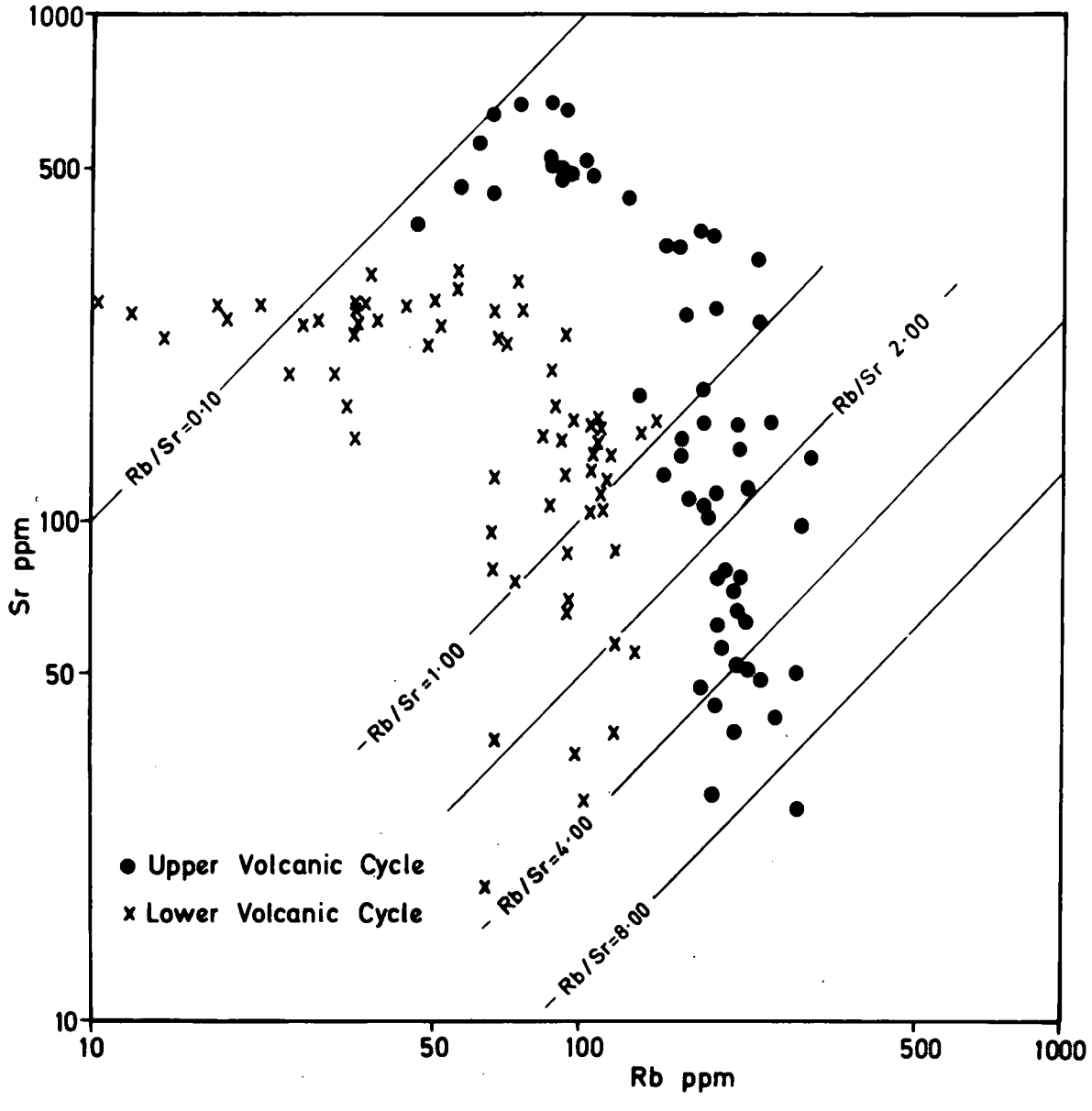

FIGURE 3.7: Logarithmic plot of Sr vs.Rb for volcanic rocks from the Lower and Upper Volcanic Cycles

The exponential decrease in Ni with increasing silica content is due to its preferential incorporation in olivine and pyroxenes (Taylor,1965; Burns 1969/1970). Early crystallisation and removal of these phases causes Ni depletion in residual liquids resulting in very low levels in most of the Lower Volcanic Cycle and in the dacites and rhyodacites of the Upper Volcanics. The low Ni (and Mg,Cr) contents of the intrusive dolerites is attributed to a prolonged period of crystallisation, although the data is too limited to draw any firm conclusions. Green and Ringwood (1967) proposed a mechanism such that the abundances of "incompatible elements; K,Ti, P,Ba, Rb,Sr" in magmas, can be explained by the interaction of liquid with wall rocks. They pointed out that interaction with wall rocks may promote some 5-20% pyroxene crystallisation. The validity of the enrichment of incompatible elements by this process has recently been questioned by Gast (1968) and found to be inadequate. However, it may be argued that due to the prolonged period of crystallisation these intrusives may show marked crystal fractionation. Removal of pyroxenes and olivines would then deplete the liquid fraction in Ni (and Mg,Cr) and causing relative enrichment of Ba,Rb,Zr. The high Ni content of the Upper Basic Cycle lavas, however, presumably derives from an ascending magmatic liquid from which Ni-rich phases such as olivine and pyroxene are not removed until a late stage in the crystallisation history, in a similar manner to late stage apatite and plagioclase fractionation.

Cr has a similar distribution pattern to Ni in the Harsit volcanics, with positive correlation between Cr, Ni and Mg, particularly in the Upper Volcanic Cycle. Four lower basic lava samples however show anomaliously high Cr contents of 130 to 150 ppm with no equivalent increases in either MgO or Ni. The Cr enrichment shown by the four samples can be attributed neither to their unfractionated nature nor their accumulative origin, indeed sample 242, with 130ppm Cr, is aphanitic. Cr is most likely to be located

in pyroxene and magnetite(Prinz ,1968). Olivine does not readily take Cr^{3+} into its structure, although common inclusions of chrome-spinel in olivine allow subtraction of Cr from the liquid (Gast,1968). The low Ni contents of 0 to 23 ppm in these samples suggest that pyroxene is not responsible for enhanced Cr levels. The Lower Volcanic Cycle show iron enrichment relative to the Upper Volcanics as little magnetite is formed during the early stages of crystallisation. Consequently Cr may remain in the melt causing little Cr enrichment (like iron), unless it can be shown that Cr is incorporated in pyroxene or olivine as chrome-spinel inclusions.

The validity of the argument may be supported by the Zn distribution of the volcanics (Table 3.1). The higher Zn content of the Lower, relative to the Upper, Basic Series is believed to be the direct effect of iron enrichment in the former. Early formed magnetite in the Upper Volcanic Cycle, thus creates sites for Zn substitution in the magnetite structure (cf.Taylor, 1965).

Cu is significantly lower in the Lower relative to the Upper Basic Series (Table 3.1). The lack of a positive correlation between S and Cu suggests that early formed sulphides have little affect on the fractionation of Cu in either series. Cu levels found in the Lower Basic Series are anomaliously low for tholeiite whose median value is 123 ppm according to Prinz (1968,p.278). The presence of Cu mineralisation, associated with the rhyolites and rhyolitic tuffs and breccias of the waning stage of the Lower Cycle, suggests the possibility that the lower Cu contents in the underlying lavas are the result of leaching by the mineralising fluids.

The tholeiitic and calc-alkaline affinities of the Lower and Upper Volcanic Cycles, respectively, are further substantiated using immobile trace elements.

Figure 3.8 shows a Ti:Zr:Sr plot similar to that developed by Pearce

FIGURE 3.8: Ti-Zr-Sr plot for rocks from the Lower and Upper Basic Series. Field boundaries after Pearce and Cann (1973)

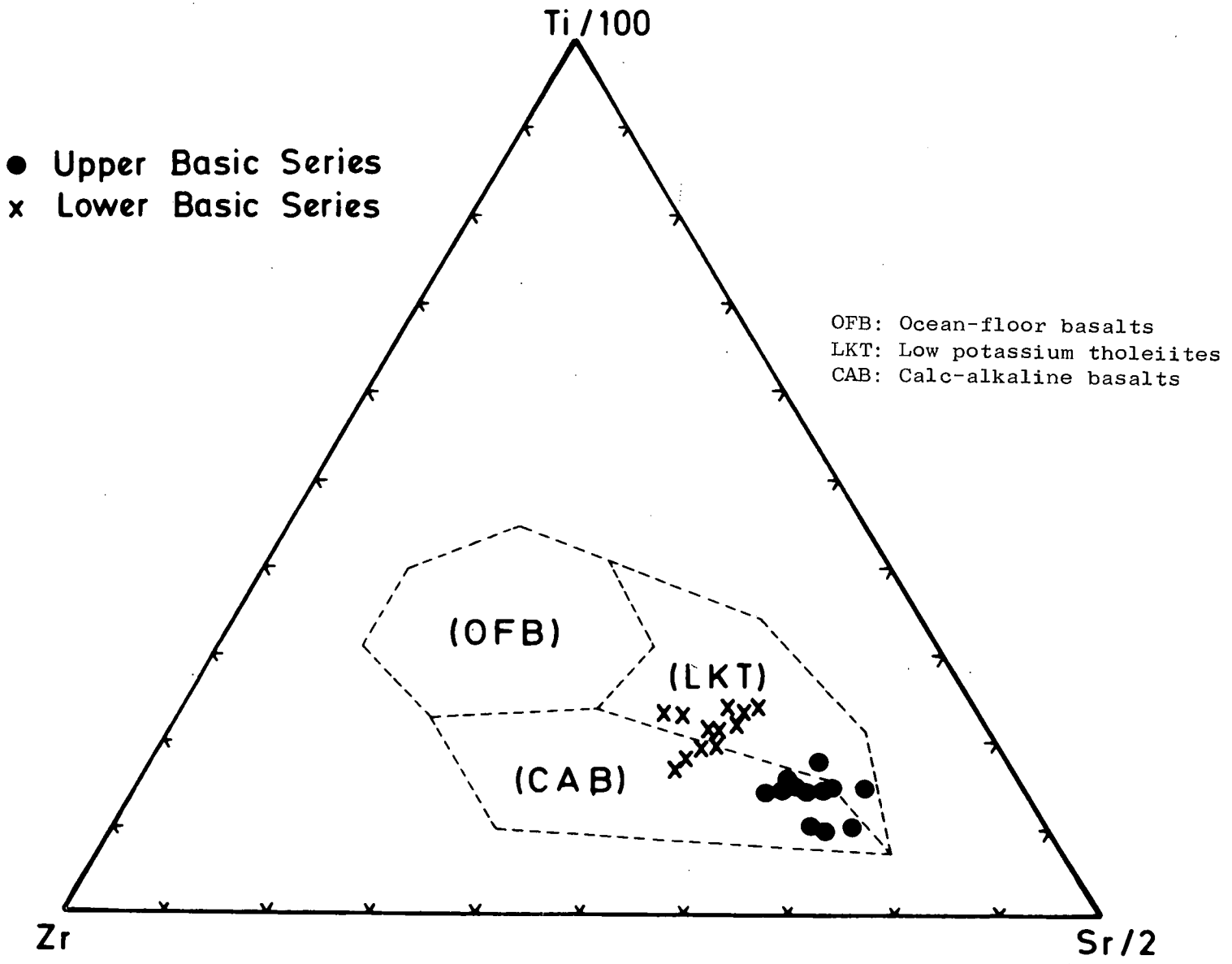

and Cann (1973). Basalts of the Lower Volcanic Cycle plot substantially in the tholeiitic field whereas basalts of the Upper Volcanic unit are predominantly calc-alkaline.

Whitehead and Goodfellow (1978), using a Nb:Y:Zr ternary plot, have shown that ocean-floor tholeiitic basalts can be separated efficiently from alkaline basalts, while Pearce and Cann (1973) have used Y/Nb ratios to distinguish between magma types. They demonstrated that the ratio increases progressively from alkalic through calc-alkaline to tholeiitic types although some degree of overlap occurs. Figure 3.9 (a) and (b) suggests that the Nb:Y:Zr plot, will distinguish between island-arc tholeiitic, calc-alkaline and alkaline basalts and andesites with over 90% certainty regardless of their degree of alteration. In Figure 3.9(a) respective fields for each suite are delineated using available published data, presented in Table 3.4. Basalts and andesites from the Harsit volcanics, including altered samples, are plotted in Figure 3.9(b). They plot within the appropriate island-arc tholeiitic and calc-alkaline fields.

3.4 Petrogenesis

Geochemical data for volcanic rocks from the Pontid Belt are very limited. Tugal (1969) has presented a number of analyses from the area around Lahonos, 20 km southwest of the Harsit river. Akinci (1974) has also analysed volcanics from the Bulancak area some 50 km west of the present area. The analyses presented by Tugal are inconclusive since they probably include material which has been altered both by weathering and mineralising fluids. Akinci attempted to separate his Lower Basic Series and the young basic dykes, concluding that the Lower Volcanic Cycle was calc-alkaline and the latter, tholeiitic. Re-examination of his data suggests that they could readily be re-interpreted in the opposite sense. Peccerillo and Taylor (1976,1977) have analysed a limited number of volcanic rocks from the western Pontids. Their analyses are far too few to draw any firm

FIGURE 3.9a: Nb-Y-Zr plot. A, B and C correspond to the field of tholeiitic, calc-alkaline and alkaline basalts and andesites respectively. Sources of data are shown in table 3.4.

FIGURE 3.9b: Nb-Y-Zr plot for rocks from the Lower and Upper Basic Series.

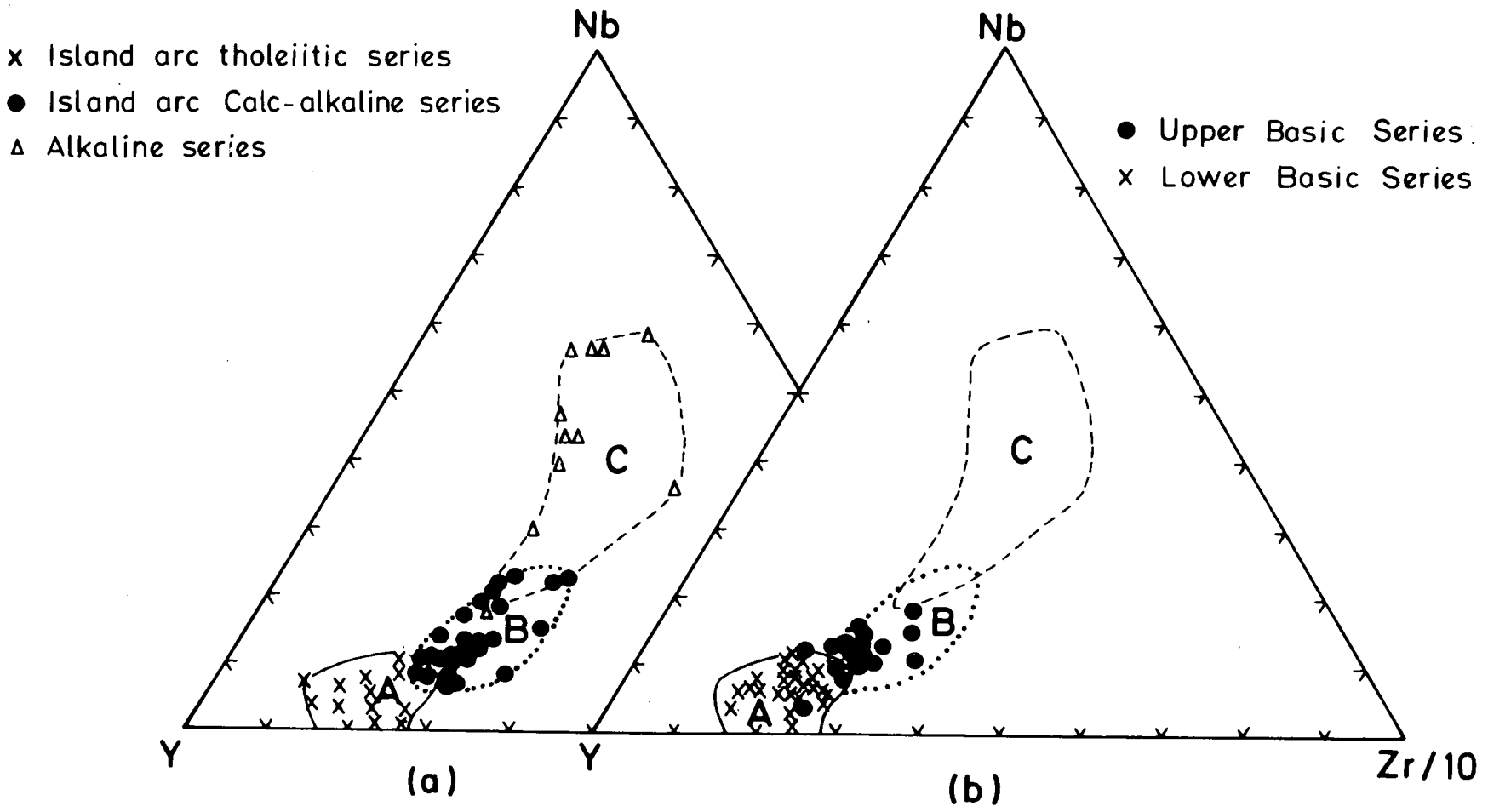

TABLE 3.4: Distribution of the Zr, Y, Nb for characterising the different magma types

Magmatic Suite	Area	Zr	Y	Nb	Reference
LKT	Izu arc (Oshima)	44	21	1	1
LKT	Tonga arc (Falcon Island)	33	17	1.5	1
LKT	Marianas arc (Guam)	52	16	2.5	1
LKT	Fiji (Viti Levu)	68	22	0	2
LKT	South Sandwich Island	44	18	2	1
LKT	Saipan andesite	90	25	0.3	3
T	Niva Fo'ou (N111)	93	30	3.7	4
T	Tafahi (T116)	7.6	6	0.56	4
T	Taoul (7128)	16	9.4	0.45	4
T	Mccarley (10380)	37	13	0.61	4
T	L'Esperance (14840)	40	18	0.76	4
T	Lesser Antilles (St.Kitts)	87	24	1	5
T	Lower Basic Series,Harsit	79	27	2,8	present
CA	Java arc	107	24	3.5	1
CA	Lesser Antilles (St.Lucia)	90	23	3	1
CA	Lesser Antilles (Dominica)	90	24	4	5
CA	Japan	64	15	2	1
HCA	Japan (12623)	46	13	2.1	6
HCA	Japan (12620)	108	24	3,9	6
HCA	Japan (12622)	117	26	2.9	6
HCA	Japan (12625)	120	25	5	6
HCA	Japan (12616)	100	22	2.6	6
HCA	Japan (12618)	115	23	4.5	6
HCA	Japan (12614)	125	25	4.3	6
CA,basalt,mean	-	106	23	2.5	1
HAB	-	126	25	5.6	7
HAB	-	100	20	4	3
CA,low Si andesite	-	92	22	3.7	3
CA, andesite	-	110	21	4.3	3
CA,andesite	-	126	25	4.6	7
CA	Upper Basic Series (Harsit)	90	22	4.0	present
MA,olivine basalt	-	234	32	48	7
MA,trachybasalt	-	282	38	87	7
MA,hawaaite	-	277	36	42	7
MA,mugearite	-	391	48	66	7
MA,trachyandesite	-	448	46	118	7
A	Lesser Antilles (Grenada)	125	24	8	5
A	Tetagouche,group B, Noranda	220	34	24	8
SA, phonolite	-	839	44	178	7
SA, basanite	-	330	31	84	7
SA,	Tetagouche, group C, Noranda	316	38	54	8

LKT = Low K. tholeiite
T = Tholeiite
CA = Calc-alkaline
HCA = Hypersthenic (Calc-alkaline)
HAB = High Al-basalt
MA = Mildly alkaline
A = Alkaline
SA = Strongly alkaline

References

1 = Pearce and Cann (1973)
2 = Gill (1970)
3 = Taylor (1969)
4 = Ewart et al. (1977)
5 = Brown et al (1977)
6 = Taylor and White (1966)
7 = Winchester and Floyd (1977)
8 = Whitehead and Goodfellow (1978)

conclusions, and indeed the location of the samples may well be doubtful, as they come from areas which have not been mapped in detail.

The chemical evidence presented above clearly distinguishes the two Volcanic Cycles and any proposed model for the generation of the Pontid magmatic arc magmas must account for the following factors.

a) The chemical difference is in time with variation from an Upper Cretaceous, tholeiitic, Lower Volcanic Cycle to an early Tertiary (Eocene?) calc-alkaline, Upper Volcanic Cycle.

b) Iron enrichment is shown only by the Lower Volcanic Cycle, but higher levels of K, Rb, Ba, Sr, Cr and Ni occur in the Upper Volcanic Cycle.

c) The preponderance of pyroclastics and the presence of hornblende and biotite in the Upper Basic Series, as revealed by the field occurrences and petrography.

d) The low K/Rb ratios of the Lower Volcanic Cycle when compared to known tholeiitic rocks.

e) Fractional crystallisation of the Upper Volcanic Cycle at a high level, and the presence of a "silica gap" in the unit.

Compositional variation can occur with time and stratigraphic level in island arcs. The earliest rocks are tholeiitic, followed by calc-alkaline rocks, erupted along with tholeiites, and finally, in the latest stages of the development of an island arc, shoshonitic rocks appear. (Baker, 1968; Gill, 1970; Jakes and Gill, 1970; Jakes and White, 1972a). The Pontíd volcanic rocks must follow this pattern. Lateral variation perpendicular to the arc-axis, observed for example in Japan (Kuno, 1966, 1968 a,b; Sugimura,1968), can not be confirmed on the basis of the present study. The 1:500,000 geological map of Turkey shows that the Upper Volcanic Cycle has an irregular distribution, occurring both to the north and south of the Lower Volcanics (Gattinger et al,1962; Goksu et al,1974).

The source materials for island arc rocks have been discussed in

detail by Green and Ringwood (1967), Ringwood (1969), Fitton (1971b), Jakes and White (1972b) and Wyllie (1973). Oceanic crust formed during the development of the Lias-Dogger Trough in the Tethyan Ocean, described in Chapter 1, may be used as the initial source material for Pontid Volcanism. Gass (1977) has described oceanic crust as composed of thin Layer 1 sediments followed downward by the pillow lavas and dykes (hornblende bearing, Cann 1970b) of Layer 2, sheeted dyke complex, then mafic, cumulate gabbros of Layer 3. At the commencement of Middle to Upper Cretaceous subduction the uppermost part of this succession, particularly the sediments, would be scraped of in the trench (Dewey and Bird, 1970). Layer 2 would be transformed through progressive metamorphism, to 'dry' amphibolite as the ocean crust descended beneath the trench (Fitton, 1971b). Melting of the surface layer of the slab starts when amphibolite begins to breakdown at about 12 Kb ($\sim$ 40 km, Fitton, 1971b, Figures 1 and 2). Breakdown of amphibole provides water for magma generation and releases alkalies. According to Boettcher (1973) most of the Na_2O becomes incorporated into the melt and most of the K_2O released through amphibole breakdown is incorporated into biotite. This process may well account for the formation of the Upper Cretaceous, tholeiites of the Lower Volcanic Cycle. At this stage, release of water and alkalies was negligible with the Na_2O content of the derived magmatic liquid being greater than K_2O. Iron enrichment, due to low water and pO_2 and relatively low contents of cations such as K, Rb and Ba, compared to the Upper Volcanic Cycle, may also be expected in this process. Gast (1968) has shown that the concentrations of K and Rb and the ratio of K/Rb in liquids and residues produced by partial melting of amphibolite at the mantle temperatures and pressures are significantly different from their values in the amphiboles. The liquids are enriched in Rb relative to K. This feature could explain the relative enrichment of Rb in the Lower Volcanics and the subsequent low K/Rb ratios of these rocks.

Final closure of the Tethyan Ocean took place in the early Tertiary, the subducted slab sinking into a higher pressure regime (a 15 kb increase in pressure can be created in 1/4 m.y. in a plate descending at a rate of 9 cm/year). At this stage amphibole continued to melt but was now probably joined by mica owing to the higher pressure. Final breakdown of amphibole and decomposition of micas released additional water and K during the generation of magmas (Boetcher 1973). This stage, presumably represent the initiation of the Upper Volcanic magma. This would produce a 'wet' magma preventing iron enrichment in the resultant rocks due to incorporation of iron into early magnetite. High water contents supress plagioclase crystallisation in basic magmas (Yoder and Tilley,1962) resulting Sr enrichment until the water is released. A drop in pressure as the liquids rise from their source region would lower the solubility of water in the magma and lead to water saturation (Fitton, 1971a). Until water escapes through explosive volcanism, removal of phases by crystal setting is unlikely. The thick breccia and tuff horizons in the Upper Basic Series, for example near Evliya Tepe (Plate 3.1) are clear indications of their explosive nature. No comparable pyroclastics being observed in the Lower Basic Series. Explosive escape of water would subsequently lead to the formation of plagioclase and restore crystal setting of silicates, resulting in the sharp drops in the levels of constituents such as Ca and Sr between basic and acidic rocks. This has been termed "high level fractionation". The occurrence of hornblende and a little biotite in the Upper Volcanic andesitic rocks is a well known characteristic of the calc-alkaline suite (Jakes and White, 1972b). They probably reflect the high water content of the magmas since not only are they hydrous but K and related cations are more abundant relative to the early melting of the oceanic crust.

Upward migration of water-rich vapour, derived from melting of a

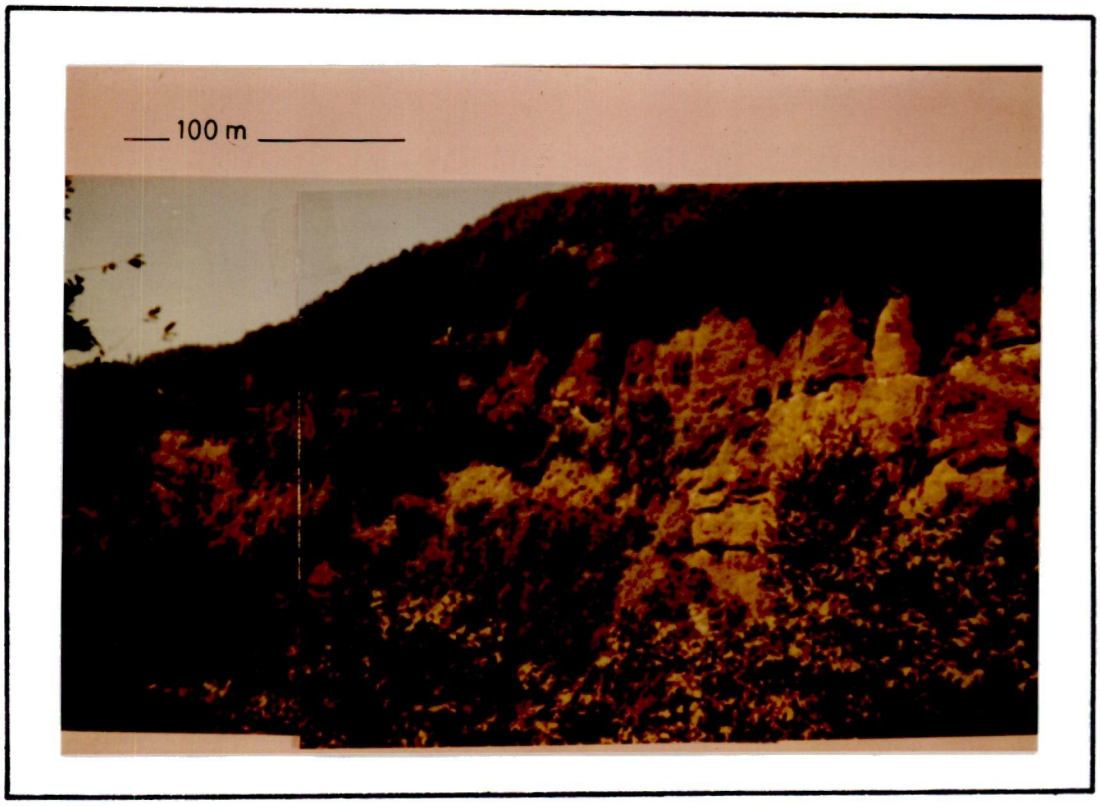

Plate 3.1: Breccia and tuff horizons near Evliya Tepe

subducted oceanic crust slab at higher pressures, could cause partial melting of mantle peridotite (Hamilton,1969; McBirney,1969). The temperature in mantle peridotites above the subduction zone is expected to be higher than within the downgoing slab (Wyllie,1973, Figure 5). Kushira (1973) has shown that in the presence of upward migrating water the solidus of "lherzolite" is significantly lowered such that it would partially melt, yielding a liquid relatively rich in K_2O. Substantially higher K_2O contents in the Upper Volcanic Cycle thus may further be expected through contamination from the partial melting of mantle material. The relatively high Cr and Ni values may also reflect a contribution from the mantle, since their content in liquids produced by partial melting do not vary with the degree of melting (Gast,1968).

Contamination by the Pontid granitic basement cannot however be ruled out in the formation of either units although it may be of minor importance. The presence of strained quartz as xenocrysts in the lavas may be an indication of assimilation or hybridisation at depth.

CHAPTER FOUR

MINERALISATION

4.1 Introduction

The general relationship of ores to specific magmatic series, especially to rocks of the tholeiitic and calc-alkaline series from orogenic belts, has been well documented in recent years (Guild 1972a,b; Jakobsen, 1975; Mitchell and Garson, 1976). Sawkins (1972) stated that convergent plate boundaries are areas of prime importance for sulphide ore body generation, where ore deposition appears to be related to subduction-initiated acid magmatism. In a broad sense, ore deposition at convergent plate boundaries can be subdivided into two sub classes. They are: Kuroko-type, stratiform, volcanogenic, massive sulphide deposits related to submarine island arc volcanism and Andean or Cordilleran porphyry-type deposits related to shallow acid intrusions. Although the two types of ore-deposit are relatively distinctive, they can occur together in both environments. Titley (1975) reported the occurrence of both types of deposit in the Phillipines island-arc, whereas in Ecuador, volcanogenic, exhalative, strata-bound sulphide deposits have been reported by Goossens (1972). Vein-type base metal deposits, however, may be present at convergent plate boundaries while subduction was active (Sillitoe, 1977).

4.2 The Pontid Metallogenic Province

The global metallogenic unit, the Tethyan-Eurasian Metallogenic belt, described by Grant (1974) and Jankovic (1977) is almost 10,000 km long. It extends from south eastern Europe through the eastern Pontids, the lesser Caucasus, Iran, south east Afghanistan, eventually reaching the Himalayas. From the Himalayas the belt continues southeast wards linking with the Pacific metallogenic belt. The metallogenic unit developed during the Mesozoic and Tertiary as a result of compressional

plate motions between the Eurasian and the Afro-Arabian-Indian plates which in turn led to the development of magmatic activity and associated mineralisation. The belt contains porphyry Cu-Mo deposits, strata-bound, volcanogenic, massive sulphide deposits, polymetallic and Cu-Au vein deposits, exhalative Mn deposits and skarn type mineralisation. Type localities and characteristics of these deposits have been described by Supercanu (1971), Akinci (1974), Grant (1974) and Jankovic (1977).

Figure 4.1 and Table 4.1 summarise the available data on the ore-deposits of the Black Sea Metallogenic and Volcanic Province (the Eastern Pontids). The five types of ore-deposit, mentioned above, may be classified into two main genetic categories, based on the age relationships, host rocks and mineral parageneses. The two categories are:

1. Deposits associated with the Upper Cretaceous, tholeiitic, "Lower Volcanic Cycle".
2. Deposits related to the Tertiary, acid intrusives.

A brief summary of each type of deposit is presented below, special attention being given to massive sulphide deposits from the study area which are described for the first time.

4.3 Ore deposits associated with the Upper Cretaceous, tholeiitic, Lower Volcanic Cycle

Three of the five types of ore-deposit occur within the upper part of the Lower Volcanic Cycle. They are:

a. Massive sulphide deposits
b. Vein-type sulphide deposits
c. Exhalative manganese ores

All three types are concentrated in the dacitic-rhyolitic lava, tuff and breccia formations, as opposed to the Upper Cretaceous dacite lavas. The host rocks, as described in Chapter 2 are pyroclastic products of submarine acid volcanism.

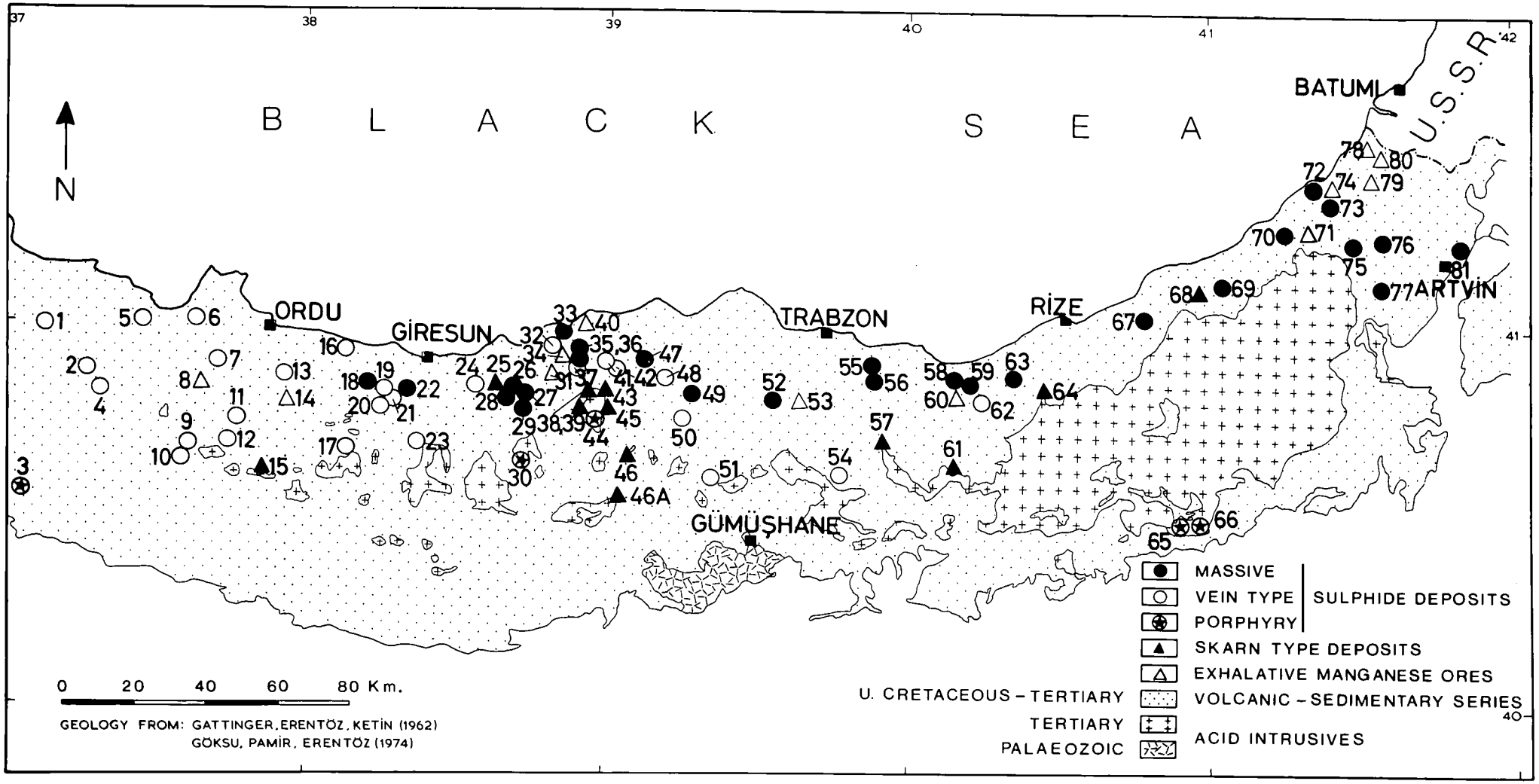

FIGURE 4.1: Distribution of mineral deposits in the eastern Pontid Volcanic and Metallogenic Province

TABLE 4.1: List of the mineral deposits in the eastern Pontids

NO	LOCATION	TYPE	WALL ROCK	AGE	COMPOSITION	REFERENCE
1	Tekkiraz	Vein	Pyroclastic rocks ?	?	Ga.,pyr.	MTA Publ.133,(1972)
2	Karadere	Vein	Andesitic pyroclastics	Tertiary	Pyr.,cpyr.,sph.	Vujanovic (1974)
3	Bakircay-Amasya	Porphyry	Granite,granodiorite	Eocene	Cpyr.,moly.	Snelgrove (1971)
4	Patlak	Vein	Andesite ?	?	Cpyr.,pyr.	MTA Publ.133 (1972)
5	Gozevi-Baskoy	Vein	Andesitic,dacitic tuffs	U.Cretaceous	Cpyr.,pyr.,ga.,sph.	Gumus (1970)
6	Arpalik-Abazadag	Vein	Dacitic tuffs	U.Cretaceous	Ga.,sph.,pyr.	MTA Publ.133 (1972)
7	Aytepe	Vein	Rhyolitic,dacitic pyroclastics	U.Cretaceous	Pyr.,ga.,sph.,fahl., cpyr.	Vujanovic (1974)
8	Geci	Exh.Sed.	Andesitic,dacitic tuffs	U.Cretaceous	Mn.Oxides	Gumus (1970)
9	Zevli-Okcubel	Vein	Andesite ?	?	Pyr.,cpyr.	MTA Publ.133 (1972)
10	Bulut-Hülul	Vein+Exh.Sed.	Dacitic rocks	U.Cretaceous	Pyr.,cpyr.,bary.,ga., psil.	Ditto
11	Damarli Maden	Vein	Andesite-rhyolite	?	Ga.	Ditto
12	Karakiraz-Kavak	Vein	Dacite	Mesosoic ?	Ga.,sph.,cpyr.	Gumus (1970)
13	Tifi-Hoben	Vein	?	?	Gpyr.,ga.	MTA Publ.133 (1972)
14	Akoluk	Exh.Sed.	Andesitic-dacitic tuffs	U.Cretaceous	Pyrol.,psil.	Gumus (1970)
15	Mahmat-Gumele	Skarn	Andesite ?	Eocene	Spec.,spyr.	MTA Publ.133 (1972)
16	Piraziz	Vein	Rhyodacitic pyroclastics	U.Cretaceous	Polymetallic	Barnard (1970)
17	Kirazoregi	Vein	Dacitic pyroclastics	U.Cretaceous	Ga.,sph.,cpyr.,pyr.	Oner and Iwao (1974)
18	Darikoy	Massive	Rhyolitic pyrolastics	U.Cretaceous	Polymetallic	Ditto
19	Bulancak	Vein	Rhyodacite	U.Cretaceous	Polymetallic	Akinci (1974)
20	Kornali Dere	Vein	Rhyodacitic ?	U.Cretaceous	Ga.,sph.,cpyr.	Ditto
21	Uzumluk	Vein	Altered rhyodacite	U.Cretaceous	Ga.,sph.,pyr.	Akinci (1974)
22	Akkoy	Massive	Brecciated porphyritic dacite/dacitic tuff	U.Cretaceous	Polymetallic	Ditto
23	Madenkoy-Yavuzkemal	Vein	Rhyodacitic	U.Cretaceous	Pyr.,cpyr.±ga.±bary.	Ovalioglu (1969)
24	Yirdincik	Vein	Dacitic,andesitic pyroclastics	U.Cretaceous	Polymetallic	Oner and Iwao (1974)
25	Yaglidere-Catak	Skarn	Silicified limestone	Eocene	Spec.,mag.,pyr.,cpyr.	Kayaalp M.(pers.Comm.)
26	Lahanos	Massive	Dacite/dacitic rhyolitic tuffs	U.Cretaceous	Polymetallic	Tugal (1969)
27	Kizilkaya	Massive	Rhyolitic,dacitic tuff breccia	U.Cretaceous	Polymetallic	Ditto: Oner & Iwao (1974)
28	Killik	Massive	Rhyolitic tuff,breccia	U.Cretaceous	Sph.,cpyr.,ga.,pyr.	Ditto
29	Kepcelik	Massive	Dacitic Tuff	U.Cretaceous	Cpyr.,pyr.,sph.,ga.	Kayaalp M.(Pers.Comm.)
30	Emeksan	Porphyry	Granite-Grandodiorite	Eocene	Moly.,cpyr.,pyr.	Dogan,R. (Pers.Comm.)
31	Guce-Kemaliye	Exh.Sed.	Dacitic rocks	U.Cretaceous	Mn.Oxides	
32	Yalc	Vein,massive ?	Dacite/dacitic tuffs	U.Cretaceous	Pyr.,cpyr.	
33	Harsit-Koprubasi	Massive	Rhyolite/rhyolitic tuff, breccia	U.Cretaceous	Polymetallic	
34	Arslancik	Exh.Sed.	Dacite,dacitic tuffs	U.Cretaceous	Mn.Oxides,bary.	

(cont.)

(Table 4.1, cont.)

NO	LOCATION	TYPE	WALL ROCK	AGE	COMPOSITION	REFERENCE
35	Harkkoy	Massive	Rhyolite/rhyolitic tuff, breccia	U.Cretaceous	Polymetallic	
36	Israil	Massive	Dacitic,rhyolitic tuffs	U.Cretaceous	Pyr.,cpyr.,ga.±sph.	
37	Yersuyu Dere--Keten Cukuru	Massive	Rhyolitic tuff,breccia	U.Cretaceous	Pyr.,cpyr.,sph.,bary.	
38	Basboynu Yolu	Skarn	Granite/limestone	Eocene	Spec.,mag.,cpyr.,pyr.	Kayaalp M.(pers.Comm.)
39	Gudul	Skarn	Granite/spilite ?	Eocene	Spec.,mag.,ga.,cpyr.	MTA Publ.133 (1972)
40	Kale Tepe	Exh.Sed.	Dacite,dacitic tuff	U.Cretaceous	Pyro.,psil.	
41	Eseli	Vein,massive	Dacitic pyroclastics	U.Cretaceous	Pyr.,cpyr.,sph.	Durukal (1969)
42	Danisment-Siezlik	Vein,massive	Dacites	U.Cretaceous	Polymetallic	MTA Publ.133 (1972)
43	Girlak Maden	Skarn	Limestone	Eocene	Cpyr.,sph.,ga.	Ovalioglu (1969)
44	Kosemusa-Catalkoy	Porphyr ?	Granite	Eocene	Cpyr.,pyr.±moly.	MTA Publ.133 (1972)
45	Kelete	Skarn	Granite/marble	Eocene	Cpyr.,pyr.,spec.	Acar E.(pers.Comm.)
46	Egrikar-Deregozu	Skarn	Granite	Eocene	Mag.,mar.,hem.,cpyr.	Ovalioglu (1969)
46A	Torul	Skarn	Limestone	Eocene	Mag.,cpyr.	Hamamcioglu & Sawa (1971)
47	Sadi Yaylasi	Massive	Tuffs ?	U.Cretaceous	Sph.,ga.,cpyr.	MTA Publ.133 (1972)
48	Alacadag	Vein	Biotite dacite	U.Cretaceous	Ga.,sph.,cpyr.,pyr.	Ha m amcioglu & Sawa (1971)
49	Ken Maden	Massive	Dacite lava,tuff,breccia	U.Cretaceous	Polymetallic	Oner and Iwao (1974)
50	Fol Maden	Vein	Dacite,andesite	U.Cretaceous	Ga.,sph.,cpyr±pyr.	Kieft (1956)
51	Zigana	Vein,massive ?	Dacite	U.Cretaceous	Polymetallic	Ryan (1960)
52	Yaylabasi	Massive	Fine tuff,mudstone	U.Cretaceous	Bary.,sph.,ga.,cpyr.	Oner and Iwao (1974)
53	Ocakli-Kucukyazlik Yemisli-Abdulaliler	Exh.Sed.	Andesitic tuff,breccia	U.Cretaceous	Mn.Oxides	Ditto
54	Kiran Maden	Skarn	Limestone	?	Pyrol.	Gumus (1970)
55	Kankoy	Massive	Dacitic,rhyolitic pyroclastics	U.Cretaceous	Pyr.,cpyr.	Oner and Iwao (1974)
56	Kalafak-Hatipli	Massive ?	Silicified dacitic pyroclastics	Eocene ?	Pyr.,cpyr.±sph.±ga.	Ditto
57	Ayven-Dagbasi	Skarn	Granite/limestone	Eocene	Ga.,pyr.,cpyr.,mag.	Ovalioglu (1969)
58	Bastimar	Massive .	Altered dacite	U.Cretaceous	Cpyr.,pyr.,sph.	Oner and Iwao (1974)
59	Kutlular	Massive	Dacitic tuff	U.Cretaceous	Cpyr.,pyr.,sph.	Cagatay (1977)
60	Pirki	Exh.Sed.	Dacitic,andesitic tuff	U.Cretaceous	Mn.Oxides	Gumus (1970)
61	Cimildag	Skarn	Limestone ?	?	Fe,S.	Ditto
62	Kotarak Dere	Stockwork, massive	Dacitic,rhyolitic tuff	U.Cretaceous	Polymetallic	Cagatay (1977)
63	Curpinar	Massive,dissem.	Dacitic,rhyolitic pyroclastics	U.Cretaceous	Polymetallic	Oner and Iwao (1974)
64	Hayrat	Skarn	Granite	?	Mag.,cpyr.	MTA Publ.133 (1972)
65	Bakircay	Porphyry	Tonolite	Eocene	Cpyr.,moly.,pyr.	Taylor (1977)
66	Ulutas	Porphyry	Quartz-mon zonite	Eocene	Cpyr.,moly.,pyr.	Taylor (1977)
67	Madenkoy-Latum	Massive	Dacitic,rhyolitic tuffs	U.Cretaceous	Polymetallic	Cagatay (1977)
68	Pilarcivat	Skarn	?	?	Pyr.,mag.,cpyr.	Ditto
69	Tunca	Massive	Rhyodacitic pyroclastics	U.Cretaceous	Polymetallic	Ditto
70	Sivrikaya	Massive ?	Rhyodacite and tuffs	U.Cretaceous	Cpyr.,sph.,bary.	Koprivica (1976)

(cont.)

(Table 4.1, cont.)

NO	LOCATION	TYPE	WALL ROCK	AGE	COMPOSITION	REFERENCE
71	Abuhemsin	Exh.Sed.	Dacite	U.Cretaceous	Mn Oxides	Koprivica (1976)
72	Peronit	Massive	Rhyodacitic,dacitic pyroclastics	U.Cretaceous	Sph.,cpyr.,ga.,pyr.	Cagatay (1977)
73	Kutonit	Massive	Rhyodacite	U.Cretaceous	Pyr.,cpyr.,sph.	Ditto
74	Pernonit	Exh.Sed.	Rhyodacite,dacite	U.Cretaceous	Pyrol.,polianite	Kraeff (1963)
75	Akarsen	Massive	Rhyolitic pyroclastics	U.Cretaceous	Pyr.,cpyr.,sph.,ga.	Vujanovic (1974)
76	Murgul	Stockwork massive	Dacitic,rhyolitic ? pyroclastics	U.Cretaceous	Cpyr.,pyr.,sph.,ga., ±sulphosalts	Tugal (1969), Cagatay (1977)
77	Petek	Stockwork massive	Rhyolitic pyroclastics	U.Cretaceous	Pyr.,cpyr.,ga.,sph.	Vujanovic (1974)
78	Daricali	Exh.Sed.	Dacite, tuffs ?	U.Cretaceous	Mn.-Fe.Oxides	Koprivica (1976)
79	Korucular	Exh.Sed.	Dacitic,rhyolitic rocks	U.Cretaceous	Mn.Oxides	Gumus (1970)
80	Yukari Sahinler	Exh.Sed.	Dolerite-basalt	Tertiary ?	Mn.-Fe.Oxides	Koprivica (1976)
81	Zinkot	Massive ?	Rhyolitic rocks,chert ?	U.Cretaceous	Polymetallic	Hamamcioglu & Sawa (1971) Cagatay (1977)

ABBREVIATIONS:

Cpyr - Chalcopyrite; Ga - Galena; Hem - Haematite; Pyr - Pyrite; Sph - Sphalerite; Moly - Molybdenite; Psil - Psilomelane; Pyro - Pyrolusite; Bary - Barite; Spec - Specularite; Mag- Magnetite; Pol - Polianite; Exh.Sed - Exhalative Sedimentary

4.3.1 Massive sulphide deposits

These deposits may be polymetallic, containing lead and zinc sulphides, together with varying amounts of sulphosalts and sulphates. Included in these would be deposits such as Darikoy, Akkoy and Harsit-Koprubasi. Alternatively the ore may comprise major amounts of pyrite, together with minor associated copper, lead and zinc sulphides, exemplified by Israil, Yalc and the Lahanos mines (Fig.4.1, Table 4.1).

The massive sulphide deposits exhibit morphological and mineralogical zonation strikingly similar to that shown by the Japanese Kuroko ores (Ishihara,1974). Ideally an ore-body would consist of the following sequence:

Top Mn-bearing tuffs and tuffaceous sedimentary rocks
Hematitic beds
Barite
Strata-bound, massive ore
Stockwork and disseminated ore
Gypsum and/or dolomite

Bottom Rhyolitic lavas, tuffs and breccias

Based on the observations in the study area the ideal, or complete, massive ore-body would comprise, from bottom to top, the following sequence. The lowermost horizons comprise disseminated pyrite contained in rhyolitic lavas. This is followed by dolomite and/or gypsum horizons, noted in several drill-cores during the present study. Approximately 6,000 m of diamond-drilling was carried out, within a 500 x 500 m area around the Harsit-Koprubasi mine, and elsewhere in the study area. M.T.A. core logs, however, failed to indicate the presence of the gypsum and dolomite horizons. The upwards sequence continues with development of pyrite-quartz veinlets, extensive pyrite and chalcopyrite stockwork, and, to a lesser extent, disseminated ore. The stockwork ore occasionally contains sphalerite, galena and sulphosalts. Strata-bound, lenticular, massive ore (plates 4.1 and 4.2) overlies the stockwork mineralisation. Its lateral extension is usually less than that of the stockwork horizons, and its

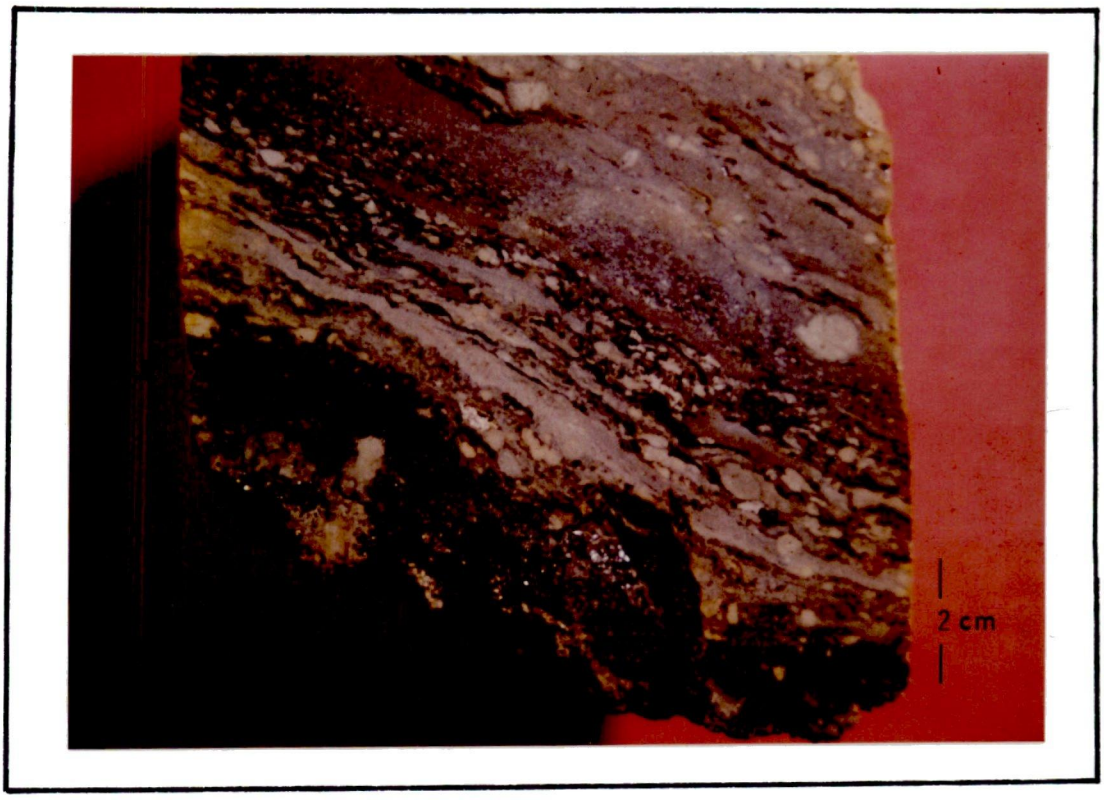

PLATE 4.1: Massive ore/hanging wall-tuff contact (Harsit-Koprubasi mine, borehole 68, 29m)

PLATE 4.2: Hanging wall pyroclastic rocks containing lenticular massive ore fragments (Harsit-Koprubasi mine, borehole 68,27m)

thickness may vary between 0.20 and 15 metres. The ore consists mainly of sphalerite, chalcopyrite, pyrite, galena and various sulphosalts in a quartz and barite gangue. On top of the massive ore, orpiment and possibly realgar, together with colloform and framboidal pyrite, sphalerite and tetrahedrite occur. Discontinuous barite lenses, in the tuffs, cap the massive ore bodies and these are overlain in turn by hematite and goethite bearing tuffs, in the form of thin lenses, whose dimensions are greater than the massive ore. The hanging wall finally comprises the Mn-oxide or hydroxide bearing tuffs and tuffaceous sedimentary series.

It is not common however to see the whole zonal sequence in any given deposit, although the succession is complete, except for the gypsum and ill-defined barite lenses, in the Harkkoy mine. In the Harsit-Koprubasi mine, however, stockwork ore of pyrite, sphalerite and galena has dominance over pyrite-chalcopyrite ore, presenting an ill-defined "mineralogical zonation." The other consituents of the massive ore, however, are ideally developed.

The valley of the Yersuyu river at Ketencukuru (Fig.2.1) reveals a good section of a massive type ore body. In this locality the emplacement and subsequent disposition of the "host rock" is controlled by NE-SW and NW-SE faults respectively (Fig.2.2, section E-E^1). On the west bank of the river Harsit, a NW-SE striking fault downthrown a few hundred metres to the east exposes the host-rock dacitic-rhyolitic lava, tuff and breccia formation against the Lower Basic Series. The host rock is overlain by the tuffaceous sedimentary unit and near to the contact between the two units a small outcrop of massive ore occurs. Further NW-SE step faulting forms a graben in the Harsit river valley. Rhyolitic lavas, found in the valley bottom, contain disseminated, euhedral pyrite crystals. To the north west, towards Ketencukuru, the lavas gradually change to breccias containing angular to rounded rhyolitic fragments. These are succeeded by tuffs in which occur 5-10 m thick massive dolomite lenses. The tuffs

are approximately 100 m thick and contain stockwork pyrite and chalcopyrite giving way, towards the top, to a stockwork of pyrite, sphalerite, chalcopyrite and galena. At the head of the valley, at Ketencuturu, small, massive ore outcrops of 1m thickness are followed by 0.5 - 1 m of massive barite ore, which are, in turn, overlain by further tuffs.

Similar zonation is well demonstrated by other deposits such as Lahanos (Tugal 1969) and Madenkoy/Cayeli (Cagatay, 1977). In general, the massive ore bodies occur as conformable lenses in the tuff horizon, approximately at right angles to the stockwork ore (Cagatay, op.cit.). The footwall almost always displays widespread alteration halos which are characterised by argillization and extensive silicification. The hanging wall tuffs and/or volcanics however, exhibit only limited alteration.

4.3.2 Vein-type sulphide deposits

Mineralisation of vein type is the least well-known in the region. The deposits occur as networks of veins and veinlets usually associated with dacitic-rhyolitic rocks of Upper Cretaceous age. An extensive study by Akinci (1974) showed that at Bulancak the sulphide deposits occur as fissure-filling, Pb-Zn-Cu sulphide veins of subvolcanic, hydrothermal type. Akinci considers that the veins are related to post-Eocene igneous activity and are similar to veins associated with Neogene volcanism in Japan. Vein-deposits described by Kraeff (1963) in the Hopa-Murgul region contain either Cu sulphides and pyrite or Cu and Zn sulphides and pyrite, and are associated with the Upper Cretaceous albite-dacite 1. The overlying unit of Turonian-lower Campanian Hippuritic limestone is free from mineralisation. Polymetallic veins at Piraziz are associated with effusive rocks and tuffs. They belong to the plutonic or sub-volcanic deposit type of Barnard (1970). The veins are emplaced in altered dacitic pyroclastics.

The mineralogy of the vein-deposits is similar to that of the massive

sulphides. They are, however, lacking in gypsum and contain lesser amounts of barite (Table 4.1).

The influence of major lineaments on the emplacement of ore veins has been demonstrated in the studies of Pollak (1968), Gumus (1970), Snelgrove (1971) and particularly Akinci (1974). Akinci supported a single, extended period of mineralisation for the sulphide deposits in the Tekmezar and Darikoy (Bulancak) areas. He showed, convincingly, that the ore bearing fluids rose along NW-SE trending faults.

Consideration of Table 4.1 together with brief examples, outlined above, indicates that the vein-type sulphide deposits are concentrated in the Upper Cretaceous dacitic-rhyolitic rocks. The rocks that overlie the deposits are free from mineralisation. A predominant structural feature of the Upper Volcanic Cycle is perfect vertical, or subvertical, columnar jointing. These joints would provide ideal channelways for the rising ore fluids and so absence of mineralisation suggests that generation of ore-forming fluids was prior to the formation of the Upper Volcanic Series. Oner and Iwao (1974) have furthermore pointed out that "... the intrusions of granitic rocks (Tertiary, Eocene) seem to have brought no fruitful mineralisation." This suggests, in turn, that volcanic processes have initiated the massive and vein-type mineralisation of the region.

The vein and stockwork type deposits described by Sawa and Altun (1977), and placed by them in a different genetic class from the massive ores, occur in rhyolitic domes, have pyrite-chalcopyrite associations and resemble the stockwork part of the massive sulphide deposits. This category may be interpreted as feeders to massive ore rather than a different genetic class of vein-type deposits. Re-interpretation of these "veins" may lead to location of massive deposits. This is exemplified in the vicinity of Ketencukuru, in the study area, which had

previously been described as pyrite-chalcopyrite vein occurrences by Kieft (1956).

4.3.3 Exhalative manganese mineralisation

Manganese deposits in the study area occur in the upper part of the Lower Volcanic Cycle in the dacitic-rhyolitic lava, tuff and breccia. A similar stratigraphic level is shown by the deposits of the abandoned Peronit mine (74, Table 4.1) whose annual output was 2000 tons, with an average of 48% Mn (Kraeff 1963). Although Mn deposits are numerous in the region (Fig.4.1 and Table 4.1) they are usually uneconomic with reserves of 1000 tons or less (Cagatay, 1977).

Manganese ores may occur massive, associated with fine opal or chalcedony and radiolarian cherts, as observed in the Guce area, or they may be nodular and botryoidal associated with opal, chalcedony and minor hematite, as found in the vicinity of Kale Tepe (Fig.2.1). Their main characteristic is their intimate association with volcanic material, cherts and cherty sediments, the latter owing their formation to submarine volcanism, as proposed by Shatskiy (1966). They are closely similar to Mn deposits from Japan and Indonesia which have been classified as exhalative-sedimentary, the manganese being contributed by volcanic hot springs, discharging directly onto the sea floor (Stanton, 1972).

4.4 Ore deposits related to Tertiary acid intrusives

Two ore-deposit types comprise this category, their distribution being shown in Fig. 4.1 and Table 4.1. They are:

a) Porphyry Copper - Molybdenum deposits

b) Skarn-type ore deposits

4.4.1 Porphyry copper-molybdenum deposits

Exploration for this type of mineralisation has recently been started in the region following discoveries in adjacent areas such as the Sredno-Gora province of Bulgaria (Bogdanova and Bogdanov, 1974), Chalkidiki in Northern Greece and Sar Chesmah in Iran (Snelgrove, 1971). Taylor (1977)

showed that the Bakircay and Ulutas porphyry copper prospects of the eastern Pontids, are related to Eocene tonalitic and quartz-monzonitic intrusions, emplaced in coeval volcano-sedimentary piles. He concluded that the Bakircay deposit represents the deeper parts of an upright column of porphyry mineralisation, while Ulutas is more typical of the upper parts of such a column, thus explaining the difference in their petrology, structure and the alteration patterns. Research in progress on the Emeksan-Esenlidere molybdenum deposits shows them to be intimately associated with quartz-monzonite and microgranitic stocks of Tertiary age, emplaced along NE-SW lineaments. Mineralisation is accompanied by well defined alteration halos in which the inner part is represented by K-feldspar followed outwards by sericitic and propylitic alteration (Dogan R.,pers.comm).

4.4.2 Skarn-type ore deposits

These deposits occur at the contact between the Tertiary granites and older volcano-sedimentary formations. Vujanovic (1974) has demonstrated two phases of mineralisation. The first phase involves the formation of magnetite, specularite and hematite in a contact aureole. They are closely associated with the metamorphic and metasomatic development of the actinolite, wollastonite, garnet and epidote. The second phase is characterised by the sulphide minerals pyrite and chalcopyrite together with rare galena and sphalerite. Tugal (1969) has pointed out that skarn-type mineralisation and/or emplacement of the intrusives is accompanied by chloritisation and calcification of the host rock.

Deposits of skarn-type are generally small and uneconomic, they are thus probably the least attractive prospects in the region.

4.5 Stratigraphic control of massive sulphide deposits

Massive sulphide deposits in the region occur in the upper part of the tholeiitic Lower Volcanic cycle, in the dacitic-rhyolitic lava, tuff and breccia formation. These mineralised pyroclastic rocks are usually overlain by the tuffaceous sedimentary unit which marks a division between the two major episodes of volcanism in the eastern Pontids. It is not

uncommon, however, for the Upper Basic Series to cap the mineralisation where the sedimentary unit is missing. This association has been described by Cagatay (1977) at the Madenkoy/Cayeli deposit.

The "host-rock" dacitic-rhyolitic lava, tuff and breccia formations unconformably overly the dacite lavas of the Lower Volcanic Cycle as seen for example, at the Harkkoy mine. The host rock shows close spatial association with the dominant fracture system of the area (Fig.2.1) whereas the dacites are true lava flows with a more widespread distribution. The fundamental difference between the two units lies in the high proportion of pyroclastic rocks and explosive volcanism in the host-rock when compared with the dacites. In addition there is a pronounced petrological difference between the two units. The differentiation index, represented by the sum of normative Q, Or, Ab, Lc, Ne, Kp (Thorton and Tutle, 1960), has been calculated for both units using the least altered samples. Table 4.2 and Fig.4.2 illustrate the general tendency for lower values in the dacites than in the host rock, in very good agreement with the results obtained from Japanese acid volcanic rocks by Tatsumi and Clark (1972). The data implies that the dacitic-rhyolitic lava, tuff and breccia host-rock formation is more differentiated than the older unmineralised dacite, if they are derived from a common parent.

Detailed studies of the Harsit-Koprubasi and Harkkoy mine areas (Chapter 5) reveal that dome-shaped rhyolites are closely related to the occurrence of the ore deposits, while volcanics both underlying and overlying the host-unit are unmineralised. Sawa and Altun (1977) have reported that ore pebbles occur in the Upper Cretaceous-early Tertiary sedimentary rocks which underlie the Upper Basic Series, while detrital barite can be seen in mudstones overlying ore and massive barite at the Yaylabasi mine (D.M.Hirst, pers.comm). In the Harsit river area lenses of reworked barite are found conformable to the bedding planes of

TABLE 4.2: D.I.* values for the northern Harsit area and Japanese acid volcanic rocks

		Northern Harsit river area volcanics		Kosaka mine - Japan **		Tsuchihata Mining area - Japan **	
		Dacite	Dacitic-rhyolitic lava, tuff and breccia = host rock	Older volcanic rocks	Lava dome volcanic rocks = host rock	Older volcanic rocks	Lava dome volcanic rocks = host rock
Differentiation Index (D.I.)*	Range	66.2-87.3	75.5-97.6	78-91.8	83 - 92	62-88	85-90
	Mean	79.17	87.25	84	87	74	88
	S.d	5.56	5.34	-	-	-	-
	P.	27	31	-	-	-	-

* D.I., defined by Thornton and Tutle (1960)

**Data from Tatsumi and Clark (1972)

S.d: Standard deviation

P : Population

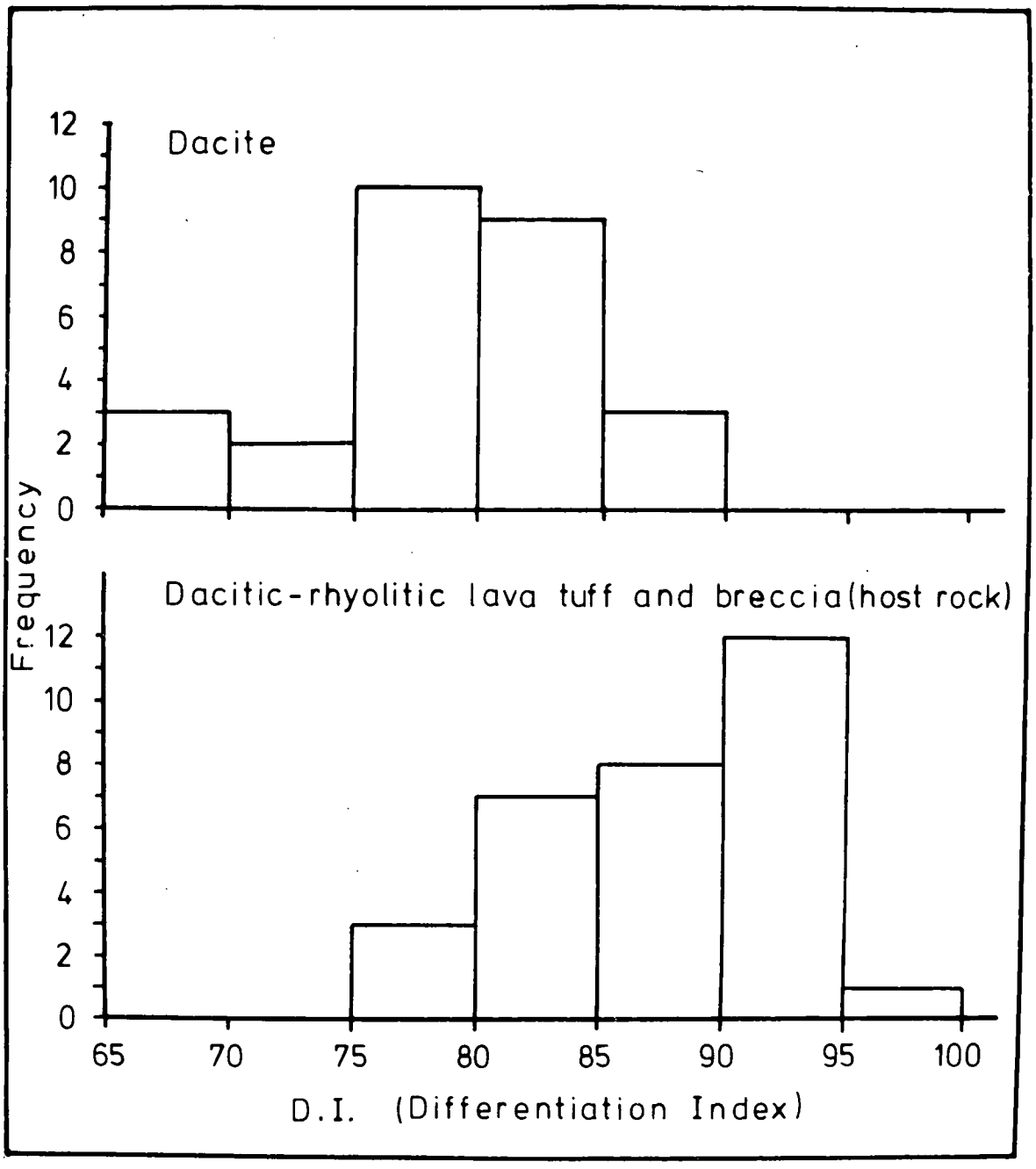

FIGURE 4.2: Differentiation Index (D.I.) histogram for the Lower Volcanic Cycle dacite and host rock

radiolarian cherts overlying massive ore at the Harsit-Koprubasi mine. Clearly ore-deposition pre-dated sedimentation in all these areas. The complete absence of hydrothermal alteration in the Upper Cretaceous limestones at the Israil mine (Kieft, 1956) is further proof that mineralisation was confined to the period occupied by formation of the dacite-rhyolitic lava, tuff and breccia.

4.6 Tectonic control of sulphide ore deposits

Kronberg (1970) considers that the tectonic movements which produced the block faulting in the eastern Pontids probably began during the Lias, but continued throughout the Alpine orogency (Cagatay, 1977). According to Schultze-Westrum (1961) there are still movements of the order of centimetres per year in the Tirebolu area, presumably reflecting recent reactivation of these faults.

The dominant fault pattern in the eastern Black Sea region is NE-SW and NW-SE (Schultze-Westrum, 1961), although Kronberg (1970) noticed a weak development of N-S orientated faults. Faults with this strike are well developed to the south of Kovancik Mah. (Fig.2.1) and indeed the rose diagram shown in Fig.4.3strongly suggests that N-S, together with NW-SE and NE-SW, are the major fault directions in the northern Harsit river area. The northern part of the Harsit river forms a deep valley running approximately N-S and is one of the major lineaments visible in aerial photographs of the region. Fault control of this valley can be demonstrated approximately 1-2 km south of Aslancik and north of Kuskaya (Fig.2.1), while the ore horizons in the Harsit-Koprubasi mine are sharply cut off at the E and NE bank of the river. Lithological differences across the river to the north of Kuskaya near Koprubasi (Fig.2.1), and between the Harsit-Koprubasi mine and Kaan Tepe (Figs.5.1 and 5.2) further support the influence of faults in determining the course of the river. Although N-S faults seem subordinate to NE-SW and

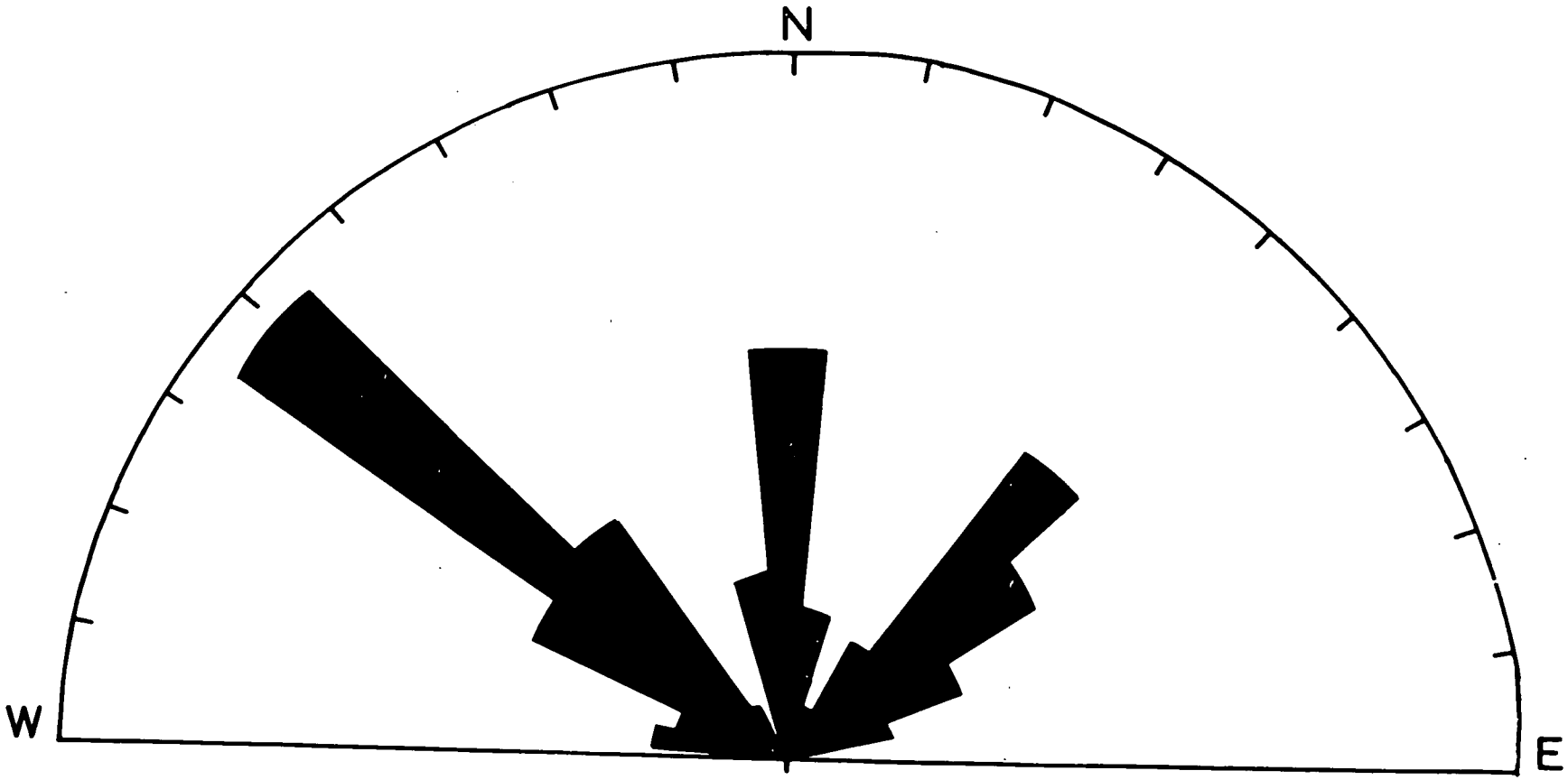

FIGURE 4.3: Fault strike. Measured from the 1:25 000 scale geological map of the northern Harsit river area (207 measurements)

NW-SE faults in their relationship to the emplacement of the volcanics, the data obtained from the Harsit-Koprubasi mine indicates that a volcanic centre which produced pyroclastics and mineralisation lies close to the west bank of the Harsit river (see Chapter 5.1). The occurrence of this, the biggest mine in the study area (Harsit-Koprubasi), and of Mn deposits near Aslancik, suggest that N-S faults are worthy of attention in the search for ore deposits in the region.

It is now commonly accepted that in the eastern Pontids, faults facilitated magmatic activity (cf Tugal, 1969; Oner and Iwao, 1974; Popovic, 1975; Cagatay, 1977) and the localisation of ore-forming solutions (Pollak, 1968; Gumus 1970; Snelgrove 1971; Akinci, 1974). The spatial association of igneous rocks with NE-SW and particularly NW-SE trending faults is well demonstrated in the northern Harsit river area by the distribution of quartz-feldspar porphyries in the south and southwest, and of dolerite sheets and particularly the rhyodacites of the Upper Volcanic cycle in the north (Fig.2.1). Although direct control of mineralisation by faulting, in the sense demonstrated by Akinci at Bulancak, is lacking, the dacitic-rhyolitic lavas, tuffs and breccias of the host rock show close spatial distribution with this conjugate fault pattern. This is well demonstrated in the Ketencukuru region, near Yalc Tepe, to the west and south of Caldagi, near Kovancik and indeed in the vicinity of Koprubasi and Harkkoy (Fig.2.2). It is perhaps relevant that the host-rock horizon does not occur in the relatively unfaulted area in the east and northeast of the study area (Fig.2.1). Here the sedimentary series and/or the Upper Basic Series directly overlie the barren dacites of the Lower Volcanic Cycle. Localisation of the host-rocks may thus be achieved by considering the conjugate NE-SW and NW-SE fault patterns which have been derived from the compressional Alpine movements. The relatively weak development of N-S striking faults

supported by the N-S disposition of the major river valleys could reflect a transcurrent fault system, developed during the formation of the Lias-Dogger trough. If they represent reactivation along such fractures the faults are probably deep-seated. They may thus facilitate both intrusion and provide pathways for uprising magma to form extrusive lavas. Intersection of the major lineaments could thus produce channelways, both for magmatic activity and for introduction of ore-forming fluids.

CHAPTER FIVE

DESCRIPTION OF INDIVIDUAL DEPOSITS

5.1 The Harsit-Koprubasi Mine

5.1.1 Introduction

The mine is situated 2.5 km east of Tirebolu in Koprubasi township. This is the only deposit in the study area on which drilling has been completed and for which present mine reserves and ore grades are accurately known. Ore reserves in the deposit are estimated to be 9,800,000 tons grading at 2.56% Zn, 1.77% Pb and 0.33% Cu (MTA News,1977). The deposit is also estimated to include 416 tons of Ag and 690 tons of Cd (Acar,1974).

A 1:2000 scale geological map of the area surrounding the Harsit-Koprubasi mine has been made. This is shown in Figure 5.1. Although the general characteristics of the geological formations in the northern Harsit river area were described in Chapters 2 and 3, the following units from this sequence, occurring within the area covered by Figure 5.1, are discussed briefly in relation to the mineralisation.

	5.	Terrace - alluvium
Upper Volcanics	4.	Dacite - rhyodacite
	3.	Dolerite sheets
Lower Volcanics	2.	Tuffaceous sedimentary series
	1.	Dacite-rhyolitic lava, tuff and breccia

5.1.2 Dacitic-rhyolitic lava, tuff and breccia

Pyroclastics and lavas of rhyolitic composition constitute this extensively altered unit. There is general agreement on the definition of the host rock for Vujanovic (1972) has termed it "rhyodacitic volcanic breccia" whereas Acar (1976) has used the term "dacitic pyroclastics". Available diamond drill cores were carefully examined both petrographically and chemically in order to give more precise information on the nature of the host rock than the broad term "tuff and breccia", used previously in core-logging by M.T.A. The sections shown in Figures 5.4 and 5.5 are based on data derived from the borehole cores, whose locations are shown in Figure 5.3.

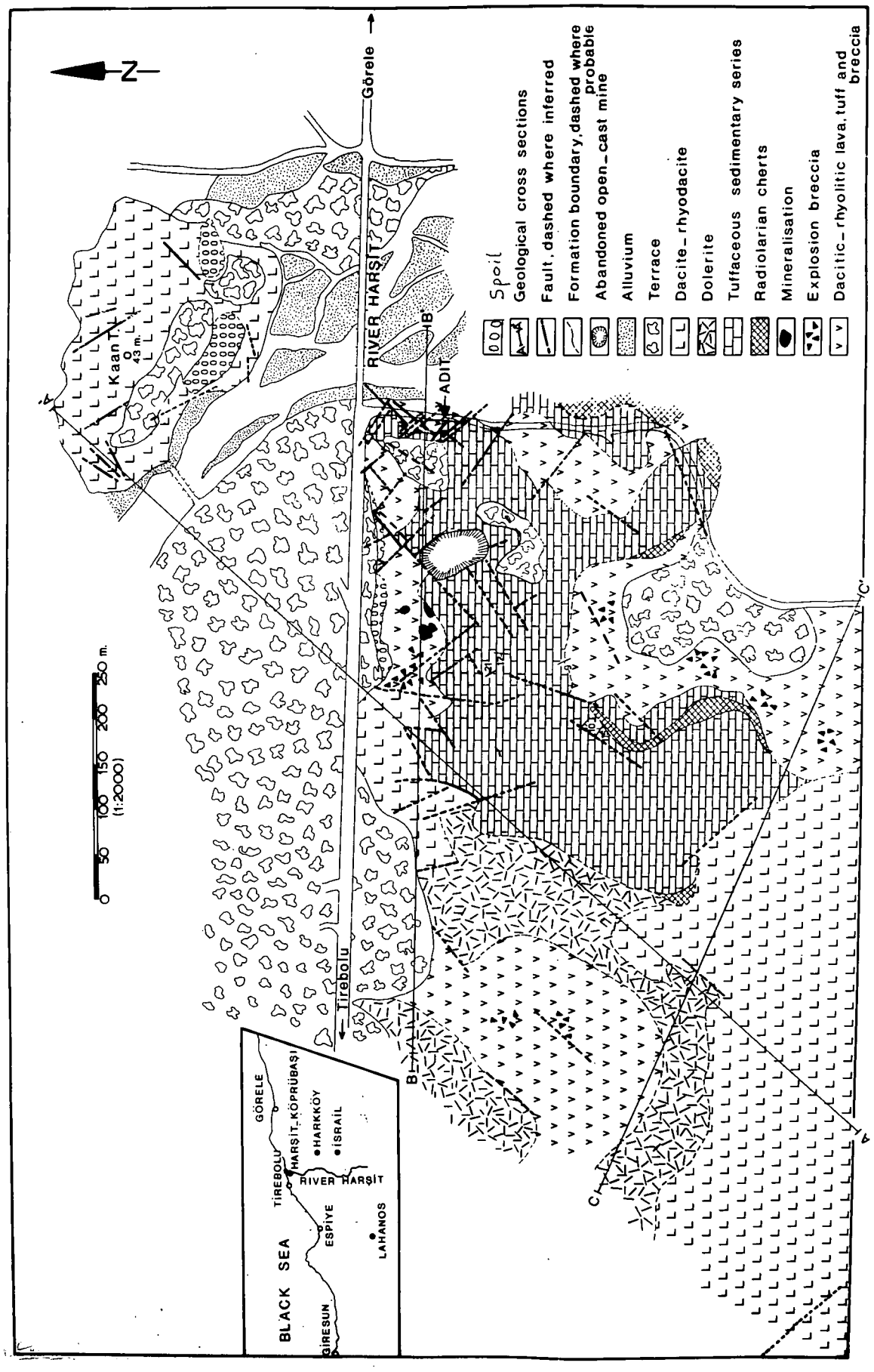

FIGURE 5.1: Geological map of the Harsit-Koprubasi mine area

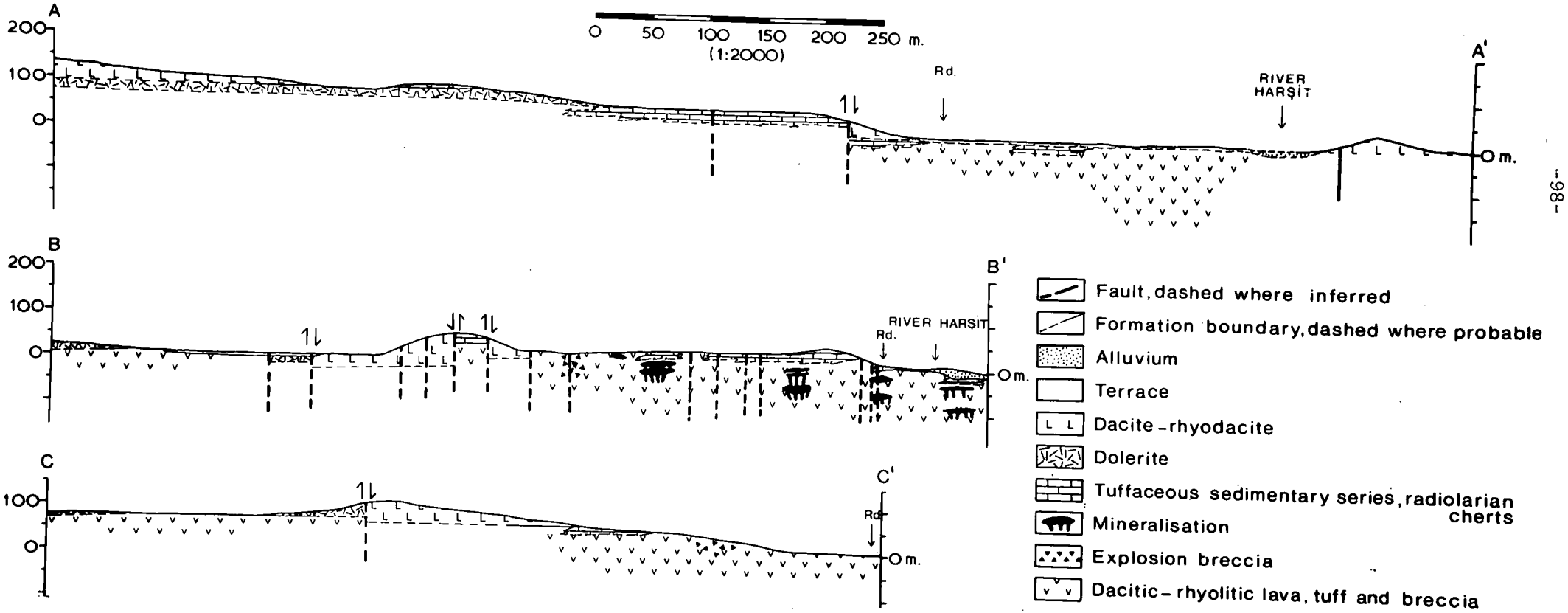

FIGURE 5.2: Geological cross-sections from the Harsit-Koprubasi mine area

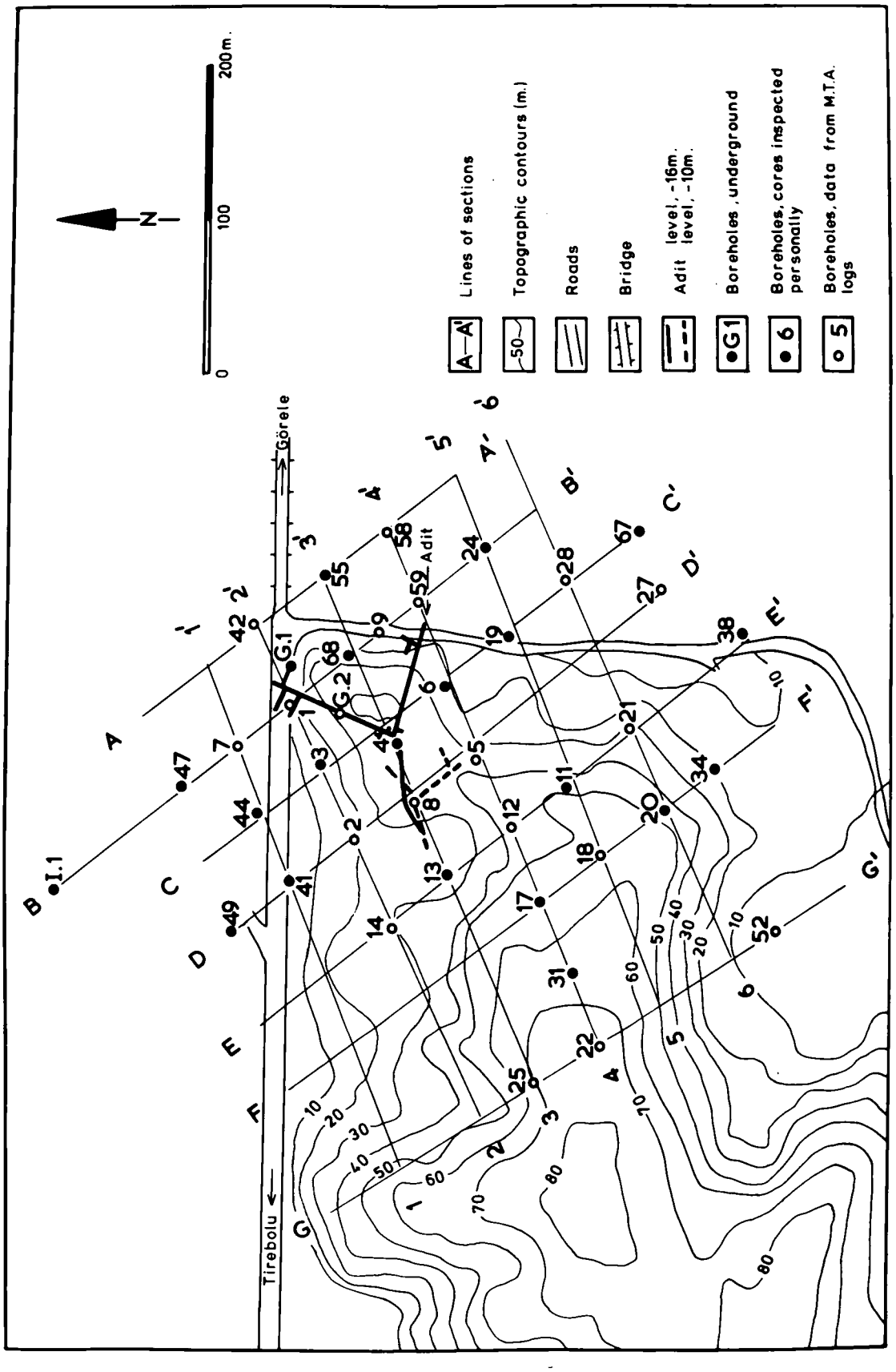

FIGURE 5.3: Topographical map showing the location of the boreholes in the Harsit-Koprubasi mine area

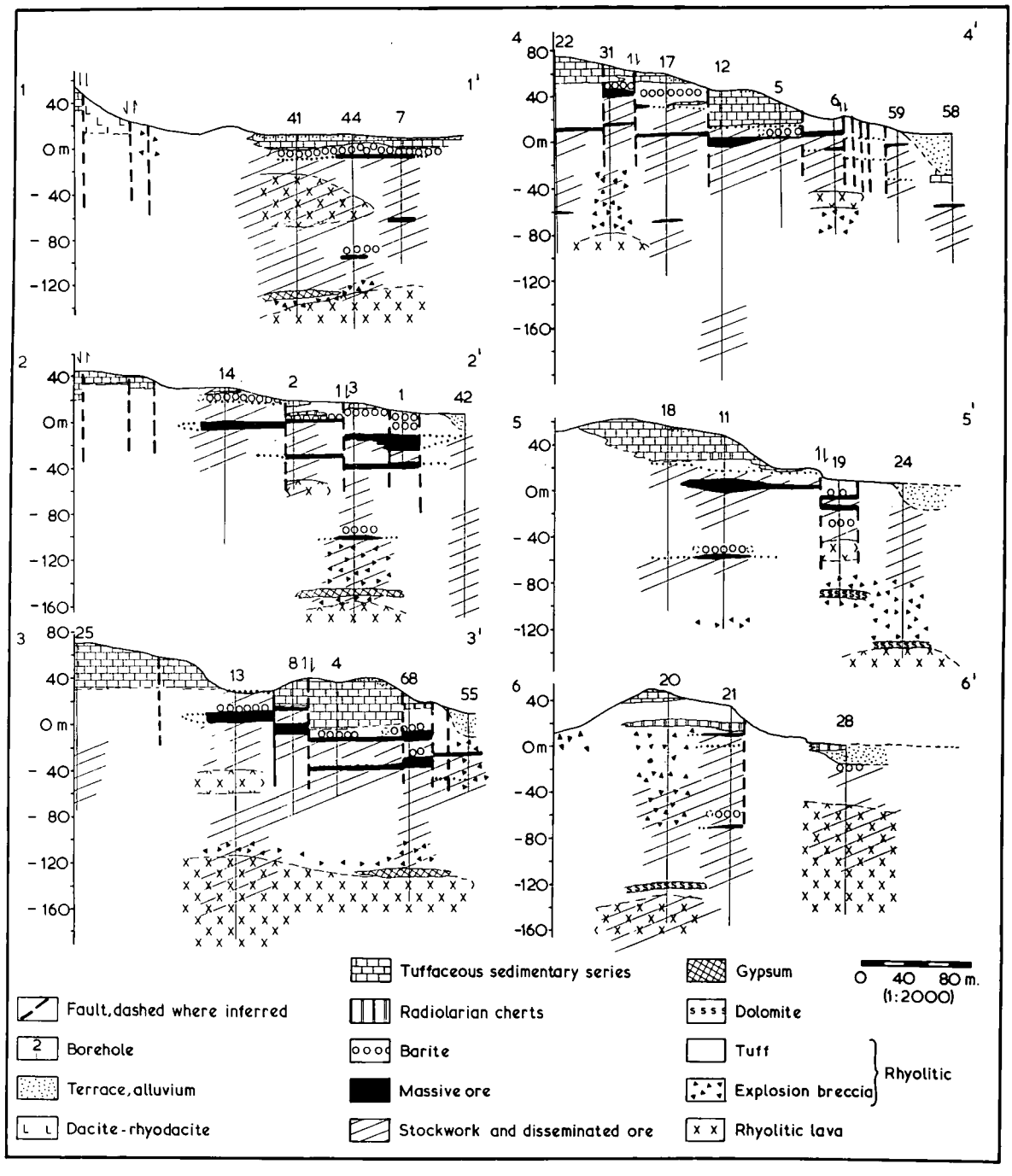

FIGURE 5.4: Geological cross-sections across the Harsit-Koprubasi boreholes

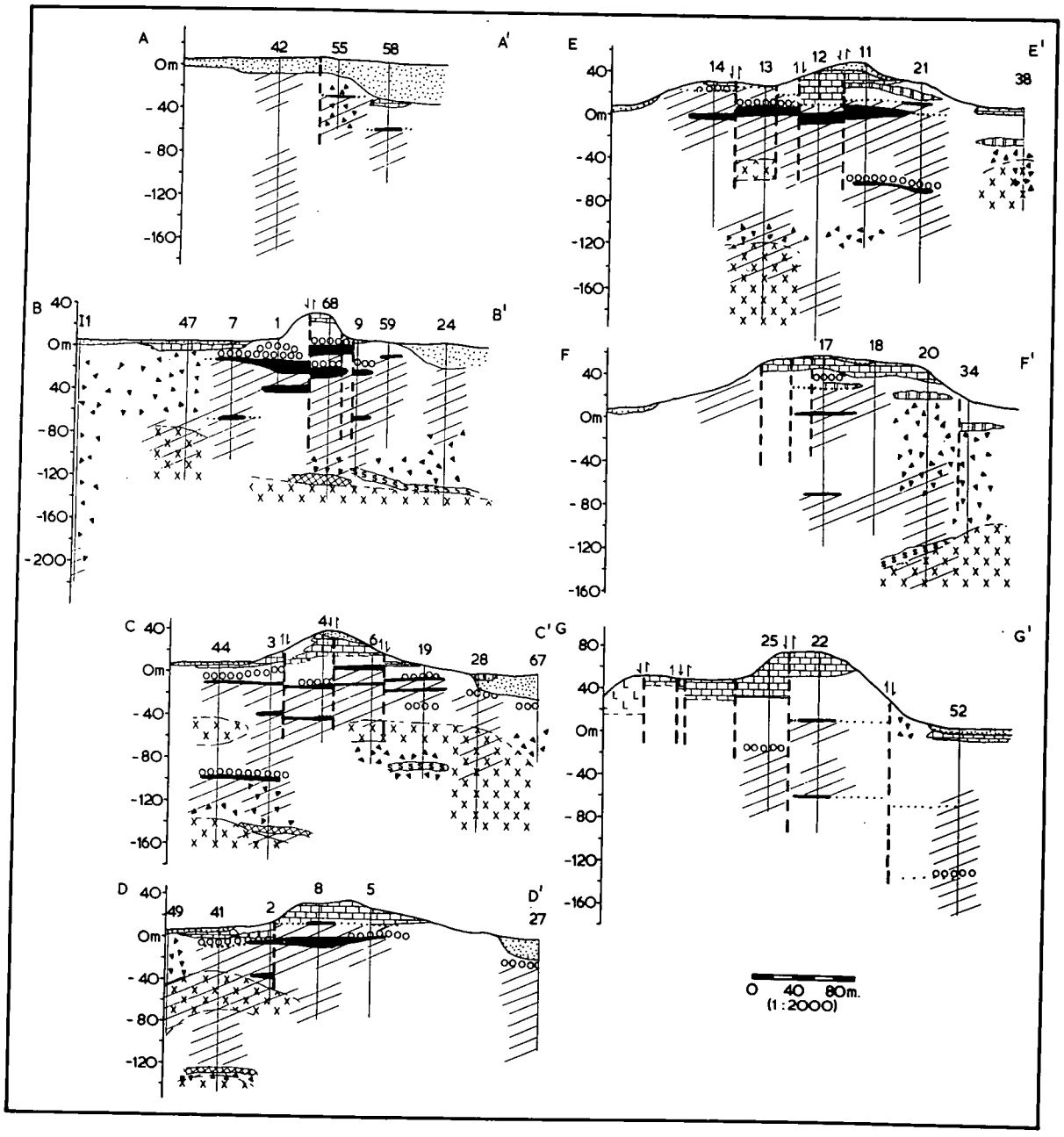

FIGURE 5.5: Geological cross-sections across the Harsit-Koprubasi boreholes (Symbols as in Figure 5.4)

Lavas generally occur towards the base of the sequence, they are of fine grain-size and contain sericitized plagioclase, orthoclase and biotite laths, together with quartz, aligned in a fine-grained matrix. Due to the silicification, a mosaic texture is usually superimposed on the original texture of the rhyolites. The borehole sections demonstrate that more than one rhyolite horizon may occur in the vertical section. Although some correlation between them has been established, limited data and short drill holes has reduced the extent of lateral correlation. However, some rhyolite, which apparently occurs within the explosion breccias (Figure 5.4., section 4.4., borehole 6), may well be large fragments broken off during the volcanic eruption.

The rhyolites are succeeded usually by breccias, termed "explosion breccias". They contain angular to rounded lava fragments, ranging in size from a few mm to a few cm in diameter, contained in a fine-grained, tuffaceous matrix. The thickness of the breccia formation varies, but is usually approximately 40 m. Breccias reach an unusual thickness of around 100 m in borehole I-1, they grade upwards into more tuffaceous material which also reaches some 100 m in thickness. Over 200 m of drilling has failed to confirm the presence of rhyolite underlying the unit at this point (Figures 5.4 and 5.5). The variation in thickness and lateral extent of the breccia horizons is remarkable. The thick breccia formations seen in boreholds I-1 and 47 thin towards boreholes 49 and 44, while thick breccias shown by boreholes 20 and 34 also thin outwards, for example, towards borehole 31 (Figure 5.3). The rhyolites are not always overlain by explosion breccias, as seen for example in cores 41 and 2 (Figure 5.4). This presumably reflects a limited development of volcanic centres, if the explosion breccias are considered to be the first material erupted from such a centre. Tuff and tuff-breccias occupy the upper parts of the succession, the latter being a gradation between the tuffs and the explosion breccias.

5.1.3. The tuffaceous sedimentary series

This unit consists of marls, some limestone and sandstone, mudstone and radiolarian cherts with or without an admixture of varying amounts of volcanic ash. Towards the top of the pyroclastic unit, the sequence of discontinuous, lenticular, radiolarian cherts (Figures 5.4 and 5.5) with the same bedding planes as the tuffs suggests that sedimentation was contemporaneous with the waning stage of volcanism.

The thickness of the unit varies between 1 m and 50 m. The variation occurs within short lateral distances and may be explained in terms of limited basin development resulting from the uprising rhyolites.

Stratigraphically, radiolarian cherts and mudstones occupy the lowest part of the unit. The following species, found in the unit support an Upper Maestrichtian (Upper Cretaceous) age (A.T.S. Ramsay, pers.comm.)

Heterohelise americana
Globotruncana mayaroensis
Globotruncana gansseri
Heterohelise sp.

5.1.4 Dolerite

Dolerite overlies the host rock and the tuffaceous sedimentary series in the form of a sheet whose thickness is approximately 30-40 m. The exposures are usually very poor and covered with thick vegetation. Contact relations to the tuffaceous sedimentary series support post Upper Cretaceous emplacement. No upper age limit can be deduced although Acar (1976) has ascribed a Palaeocene-Eocene age to these rocks.

5.1.5 Dacite-rhyodacite

This usually fresh, well jointed unit is the final volcanic product, it always forms the topographic heights in the mine vicinity. Kaan Tepe, north east of the mine adit, is formed from this unit, as seen in Figure 5.1, whereas to the west at the same topographical level is the host rock (Figure 5.2). This suggests that the Harsit river, to the southwest and west of Kaan Tepe, is fault controlled.

5.1.6 Mineralisation

The Harsit-Koprubasi deposit is a polymetallic ore body consisting of massive ore usually underlain by stockwork and disseminated ore. This two-fold subdivision has been described previously by Vujanovic (1974) who used the terms high grade and low grade, and by Acar (1974) who described the two types as rich-massive and poor-stockwork. Figures 5.4 and 5.5 show that three levels of massive ore, exclusively associated with tuffs, occur in the area. The stockwork and disseminated ore, however, may be present not only in the tuffs but also in the breccias and/or rhyolites. Gypsum and/or dolomite, when present, are confined to the lowermost horizons of the stockwork part of the ore body. Lateral correlation between each of the three levels of massive ore is mainly based on the distribution of barite and of the tuffaceous sedimentary series. The barite usually overlies the ore horizon, whereas the sedimentary series is always found at the top of a thick pyroclastic unit above the uppermost massive ore and barite horizons.

The thickness and lateral extent of each of the three massive ore levels are shown in Figure 5.6, they are referred to as ore bodies A, B and C from the top downwards. From Figure 5.6 it is evident that the maximum thickness of each massive ore lens occurs approximately 100 m northwest of the adit. A second, less well defined maximum is present to the southwest of the adit. The lateral distribution of ore-body A shows some elongation in a N-S direction whereas ore-bodies B and C have a tendency to NW-SE alignment thus following the dominant fault strike direction in the area, previously shown in Figure 4.3.

The thickness of the massive ore reaches 15 m in ore body A. The deposit thins outwards forming a lens shaped ore-body. At this level ore reappears to the southwest where it reaches a maximum recorded thickness of 6 m. From the borehole data available it is not clear whether this is part of ore-body A or part of a separate anddiscrete lens

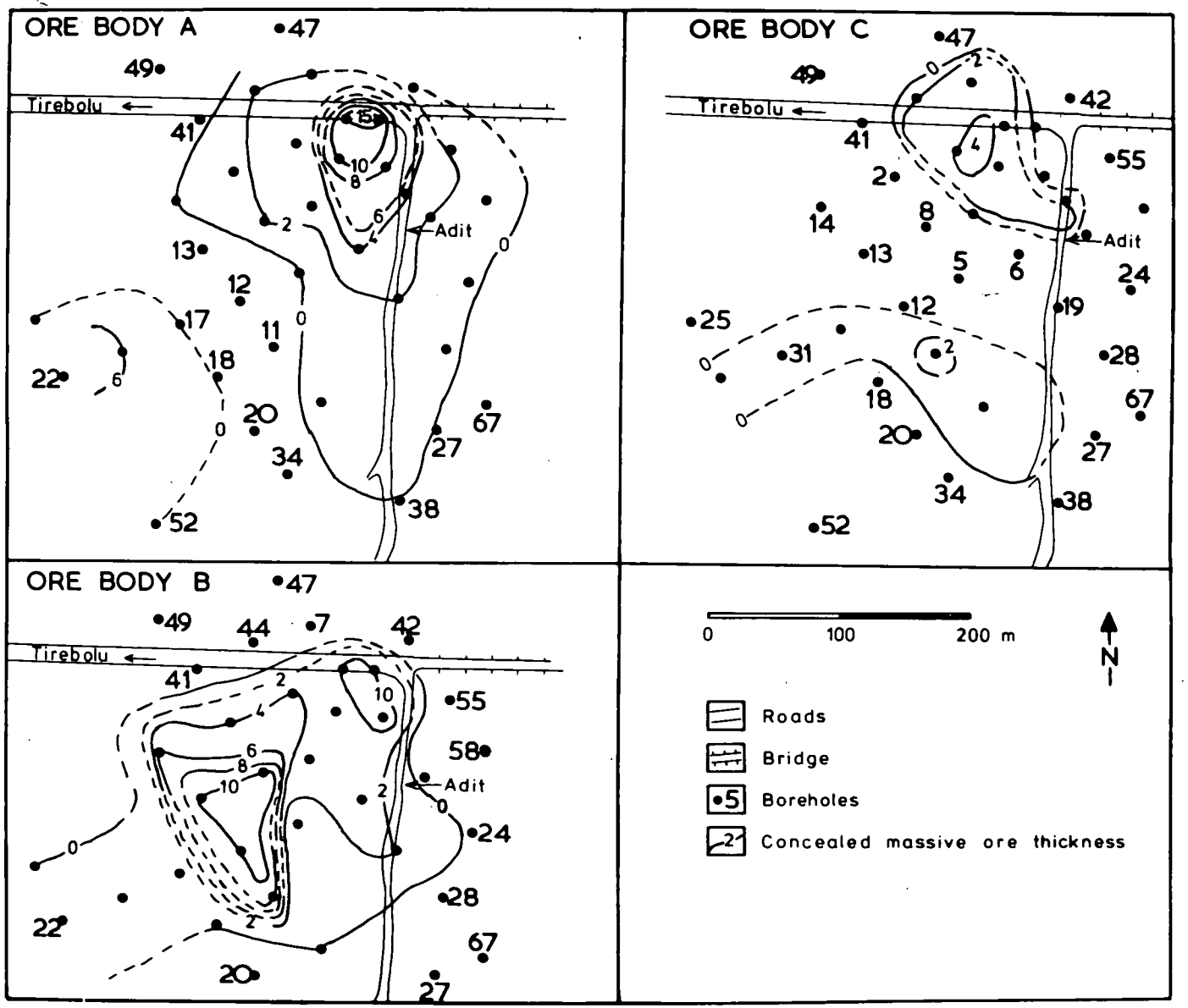

FIGURE 5.6: Thickness and lateral extent of the three massive ore-levels in the Harsit-Koprubasi mine area

occupying the same stratigraphic level. The thickness of stockwork ore associated with each massive ore level does not usually exceed 20-30 m. Thick stockwork ore are occasionally seen, for example, in boreholes 41, 3 and 68, where they underly massive ore of level A, and in boreholes 11 and 13 where they underly levels B and C respectively. They may represent feeders to their respective overlying massive ore bodies (Figures 5.4 and 5.5).

The presence of three massive ore-zones within the same pyroclastic sequence is not an unusual feature for massive sulphide deposits. In Noranda province, Canada, Sinclair (1971) has demonstrated that the Horne mine is stratigraphically succeeded by the No.5 zone, both having formed independently within the same, volcanic, marine environment as a result of fumarolic and solfataric activity. In the Kuroko deposits of Japan, Hirabayashi (1974) has identified "shallower and deeper level" orebodies and has concluded that "at least three cyles of mineralisation" have occurred.

The information available from cores in the Harsit-Koprubasi mine area suggests that the presence of three ore-bodies may be explained either by the occurrence of at least two independent rhyolites (Figures 5.4 and 5.5), or by migration of volcanic centres and their subsequent vulcanism. The result of both mechanisms would be the same: production of pyroclastic material and ore fluids.

Zonation in the mine is morphological rather than mineralogical with massive ore underlain by stockwork ore which is followed downward by disseminated ore. Mineralogical zonation, as described in chapter 4.3.1, is ill-defined except for the obvious mineralogical differences between the massive and stockwork ores. Within the stockwork zone, however, some variation may be seen in the lowermost horizons. In boreholes 20-180 m, 11-80 m (Figure 5.7b) and 44-150 m the veins contain quartz, pyrite and chalcopyrite while in boreholes 24-76 m and 47-110 m pyrite veins and

disseminations occur and in borehole H3-112 m and 138 m the veins contain quartz only.

5.1.7 Geochemistry

In common with most world-wide massive sulphide deposits, mineralised outcrops, or surface exposures of the massive ore, are virtually absent in the area. Establishment of the pattern of variation or enrichment of elements in various parts of the pyroclastic pile would thus facilitate exploration and provide information regarding the stratigraphic and structural features of the ore body. The latter become particularly important in steeply dipping massive ore, such as the lenticular-shaped massive deposits of the Madenkoy/Cayeli deposit which dips at about 50^{o} NNW (Cagatay 1977).

Borehole core samples were analysed for Si, Al, Fe, Mg, Ca, Na, K, Ti, Mn, P and Ba, Nb, Zr, Y, Sr, Rb, Zn, Sb, Cd, Ag, Mo, Cu, As, Pb and S by X-ray fluorescence Spectrometry. The results and analytical techniques are given in Appendix 1.

The results of these analyses are plotted in Figures 5.7 a-e. The plots show that the distribution of the elements is largely controlled by the type and relative amounts of ore and gangue minerals. The massive ore is enriched in S, Zn, Cd, Pb, Ag, Sb and Mo whereas Fe and Cu show a relative enrichment in the stockwork ore. Comparison of the successive massive ores indicates that the lower ore, level C, is relatively enriched in Fe and Cu and depleted in Sb, Mo and As (Figures 5.7a,b,d and e). As is usually enriched in the tuffs and tuffaceous sedimentary series overlying the ore-bodies, as shown by Figures 5.7a, c and e. It is usually accompanied by Ba, Fe and Mn (Figures 5.7a, c and e) or by Fe (Figures 5.7b).

The co-variance between the elements is usually well pronounced. The similarity between the Zn and Cd distributions illustrates the substitution of Zn by Cd as shown in figures 5.7.a to e. A co-variance

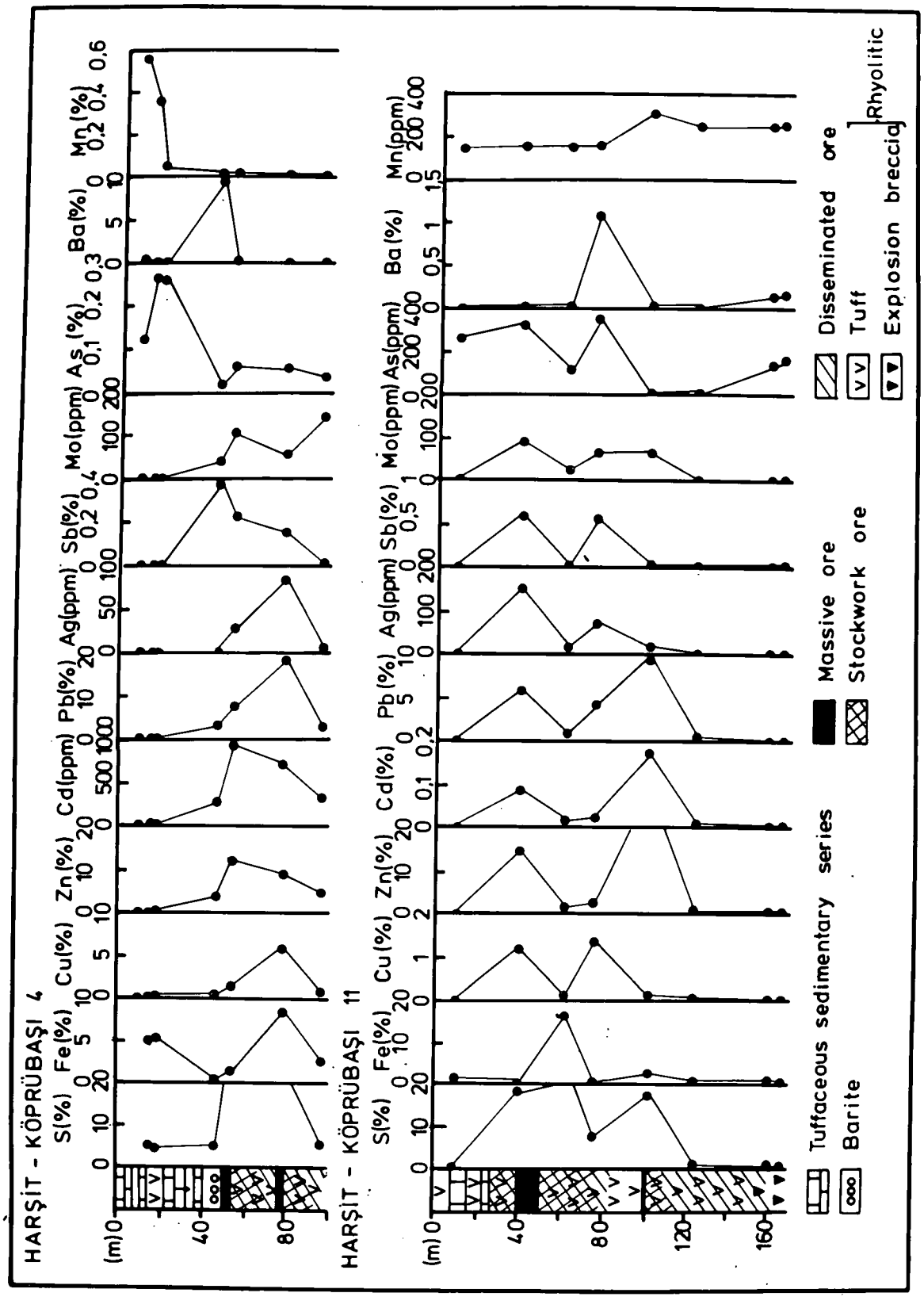

FIGURE 5.7(a) and (b): Geochemical data for boreholes 4 and 11, respectively (Harsit-Koprubasi mine)

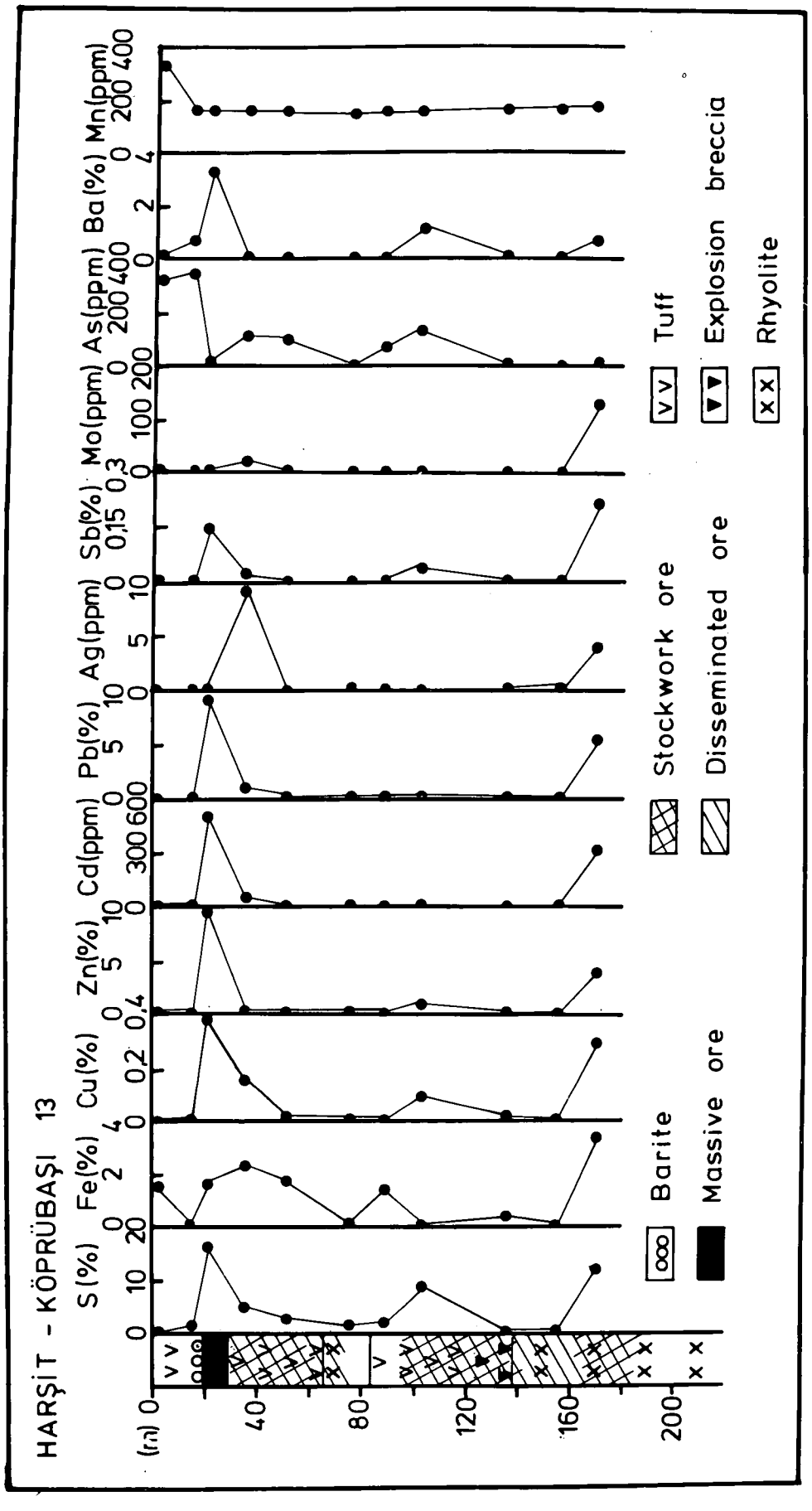

FIGURE 5.7(c): Geochemical data for borehole 13 (Harsit-Koprubasi mine)

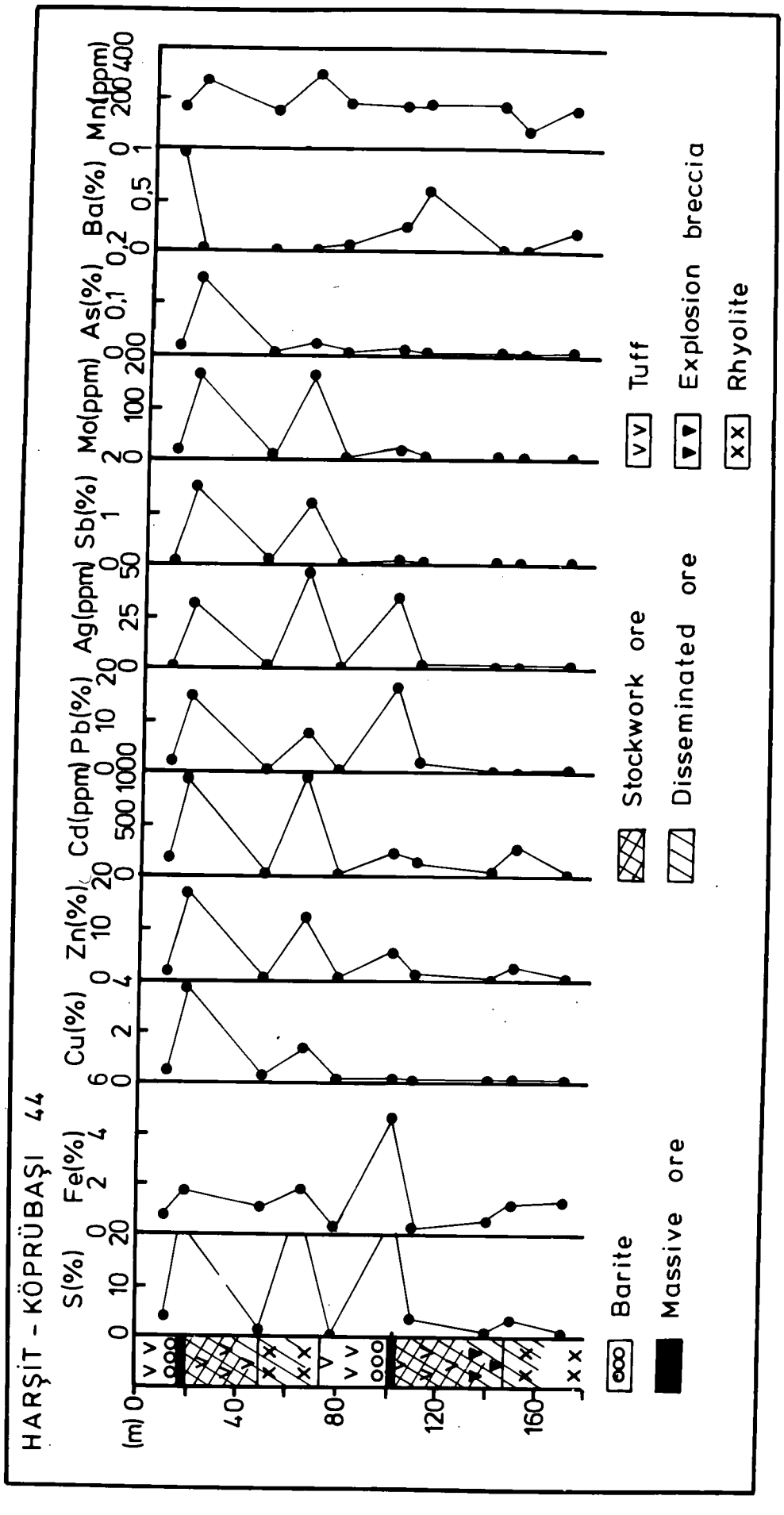

FIGURE 5.7(d): Geochemical data for borehole 44 (Harsit-Koprubasi mine)

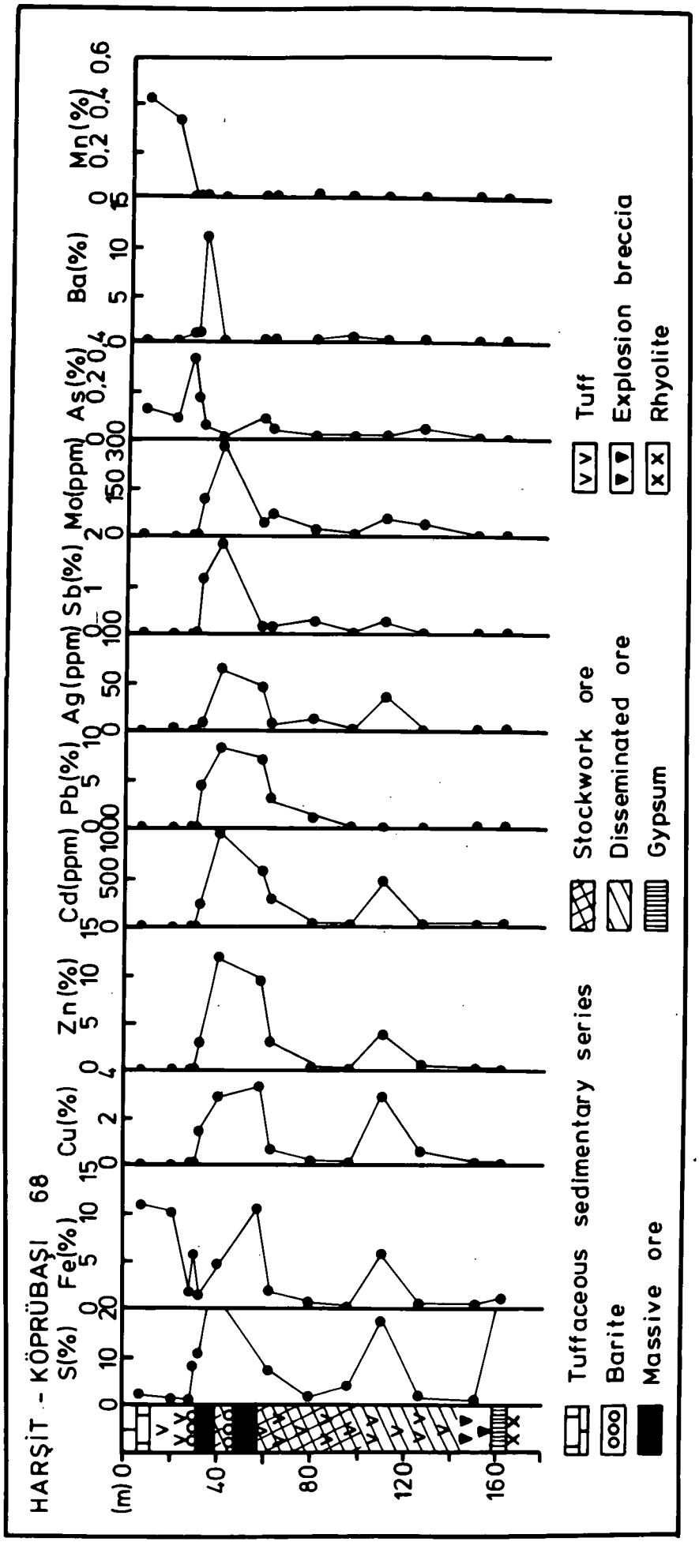

FIGURE 5.7(e): Geochemical data for borehole 68 (Harsit-Koprubasi mine)

between Ag and Pb (Figures 5.7 a, d and e) and Ag and Sb (Figures 5.7 b and e) may suggest that Ag is incorporated into the galena and tetrahedrite structures, respectively.

Results obtained from the Harsit-Koprubasi mine, as well as from the Harkkoy deposit described below, strongly resemble data obtained from the volcanogenic massive sulphide deposits of Madenkoy/Cayeli by Cagatay (1977) and from the Kuroko deposits of Japan by Tono (1974). The use of elements such as Ba, Mn, and Fe as geochemical indicators is considered in Chapter 8.

The distribution of Nb and Zr in the volcanic rocks closely associated with the ore-bodies, Figure 5.8, shows a 2 to 4 fold enrichment in explosion breccias when compared to the rhyolite lavas or the succeeding tuffs. These elements are not sensitive to alteration and metamorphism (Cann,1970; Pearce and Cann, 1973; Floyd and Winchester, 1975, 1978 and Winchester and Floyd, 1977) nor are their contents liable to modification during devitrification (Smith and Bailey, 1966).

The chilling affect of cold water on silicate melts is known to cause rapid and intense shattering (McBirney, 1963). The explosion breccias are thought to be derived from hot ascending magmatic liquids (e.g. rhyolitic melts) which come in contact with evolved sea-water. The poor grading and sorting of the breccias suggests that they were not thrown high above the sea-floor, but may have been derived from shallow-emplaced rhyolites under the sea-floor.

The explosive activity may also be related to the sudden release of gas which occurs when gas-charged magma moves into a highly fractured zone (Wright and Bowes, 1968). The host rock horizon and overlying tuffs are closely associated with the dominant fault pattern and are themselves extensively faulted (Figures 2.1, 5.1 and 5.9). The gas-charged magma may well be derived from a suite which has evolved by a crystal-liquid fractionation process; for example the fractional crystallisation of the Lower Volcanic Cycle (Chapters 2 and 3). Neither Nb nor Zr are readily

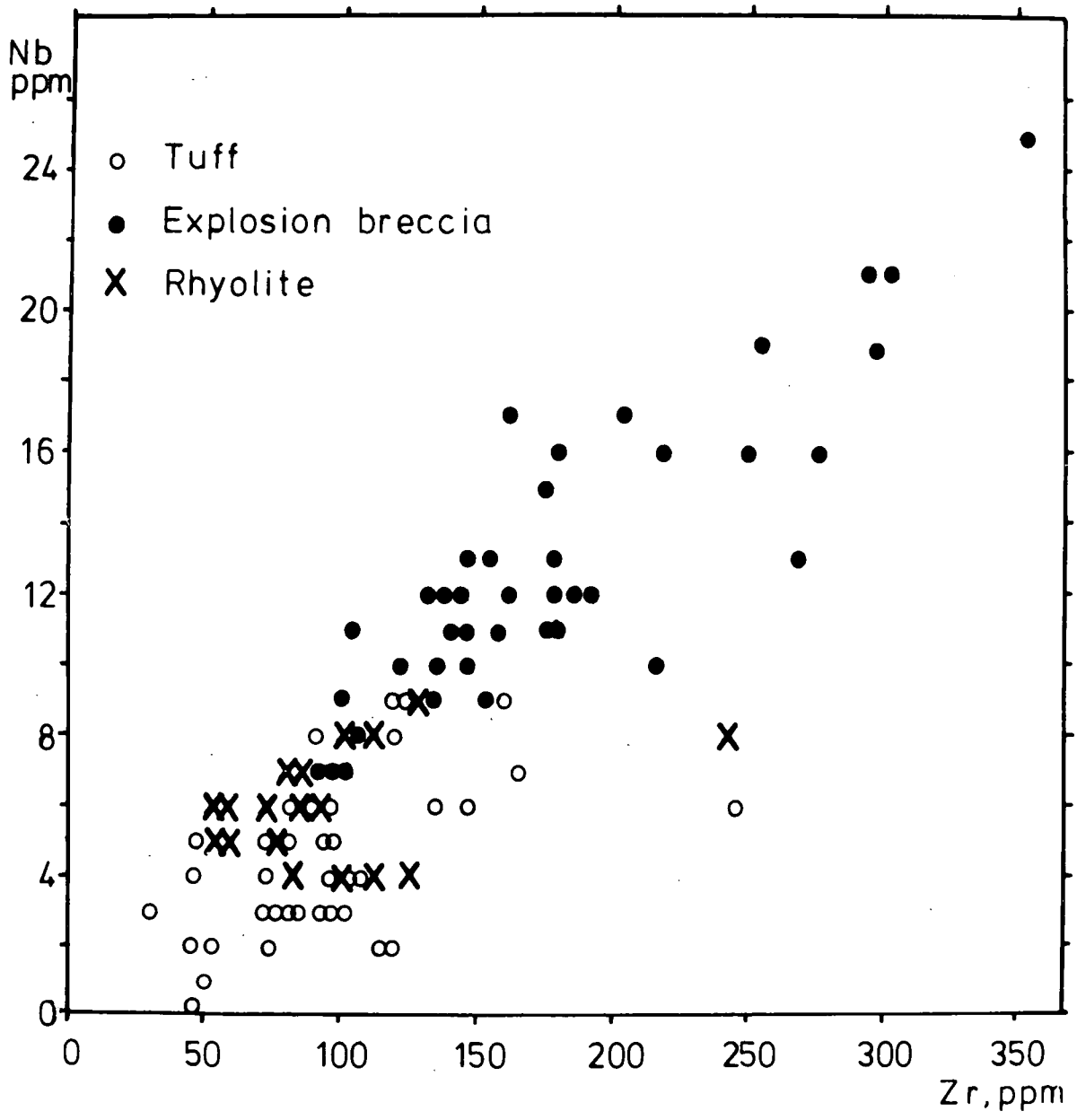

FIGURE 5.8: Nb vs. Zr plot for the host-rock

incorporated into minerals such as olivine, pyroxene or feldspar and thus encrichment of these elements in magmas does not take place in the early stages of fractionation (cf.Goldschmidt,1954).

According to R.Macdonald of Lancaster University (pers.comm.) the distribution of these geochemical tracers between the explosion breccias and the tuffs may suggest a zoned magma chamber. The former could result from a magma column enriched upward in Nb and Zr by diffusional processes. This was erupted and the chamber filled with a less evolved magma which produced the tuffs.

Although very little information is available in the literature relating to such a diffusional model the high contents of Nb and Zr in the explosion breccias could be used to trace volcanic centres. Due to the close time and space association of such centres with the mineralisation, these geochemical tracers may further determine the proximity of ore-bodies.

5.2 The Harkkoy Mine

5.2.1 Introduction

The Harkkoy deposit is situated approximately 8 km SSE of Koprubasi township. The first mining activity in the area is believed to be drilling by a British company before the first world war (Kieft,1955). More recently, geological work in the mine vicinity was initiated by M.T.A. in the 1950's, as a part of the regional study of the Tirebolu region. A brief summary given by Kieft (1955) describes the following geological units:

d. Upper Cretaceous tuff, limestone and marl

c. Silicified and kaolinised masses found in the vicinity of ore bodies

b. Dacite

a. Basalt

Because of limited surface exposure Kieft (1955) was unable to locate the host rock. He speculated that the ore may occur between the

dacites and the overlying tuff-limestone horizons. Lob (1960) described the ore-body as being of "hydrothermal-subvulkanischen" type, and presented the following grades as typical of the massive ore:

Pb = 5.00% (wt)
Cu = 1.87% "
Zn = 13.75% "
Fe = 10.26% "
S = 19.52% "

More detailed studies, started by M.T.A. after 1974, suggest a total reserve of 3,000,000 tons of pyrite ore (M.T.A. News, 1978).

5.2.2 Geology

The geological map and cross-section of the area, shown in Figures 5.9 and 5.10, are based on the 1:10.000 topographical map. Three borehole cores have been examined and chemically analysed (Figure 5.11 a,b and c), but information from other cores has been supplied (Akinci, pers.comm.)

The following formations were observed in the vicinity of the ore-deposit. They belong to the Lower Volcanic Cycle and are arranged in stratigraphically descending order:

Lower Volcanic Cycle
(6. Sedimentary and tuffaceous sedimentary series
(5. Hematitic beds
(4. Rhyolitic tuff and breccia
(3. Rhyolite
(2. Dacite
(1. Andesite and basalt

Units 1 and 2 are lava flows. They exhibit similar characteristics to those lavas previously described from unmineralised parts of the study area. It is important to note however, that neither the andesites and basalts which occur approximately 200 m NE of the mineralised rhyolite, nor the dacite outcropping in Maden Dere are mineralised (Figure 5.9). The rhyolite of unit 3 may be distinguished from the overlying tuffs and breccias, and the underlying dacite, by the alignment of quartz, feldspars and biotite, and by its mosaic texture developed as a result of silicification. This type of alteration probably led Kieft (1955) to introduce the term "silicified and kaolinised masses". It is apparent from Figures 5.9 and 5.10 that the rhyolites usually have faulted contacts with further strong

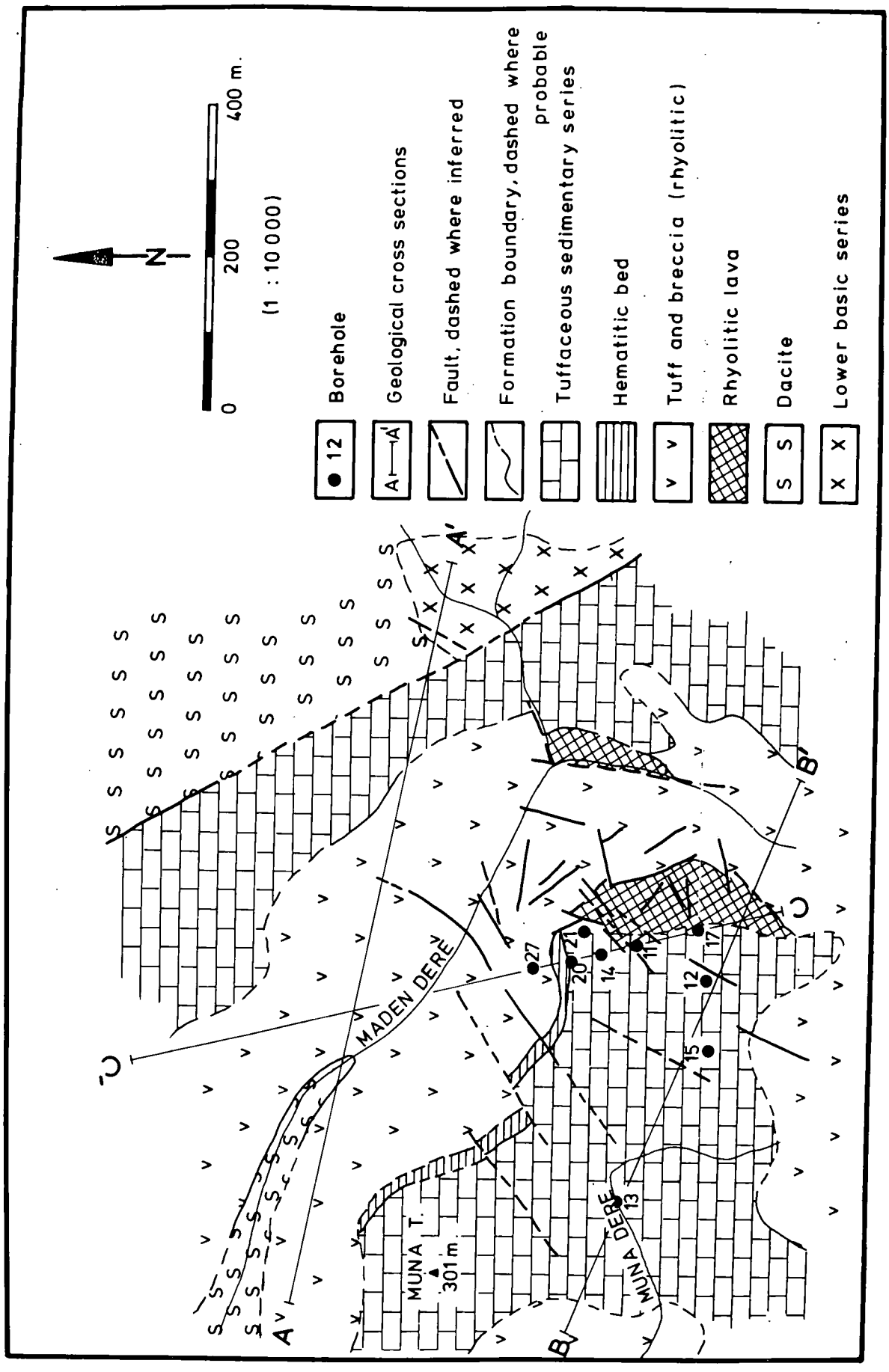

FIGURE 5.9: Geological map of the Harkkoy mine area

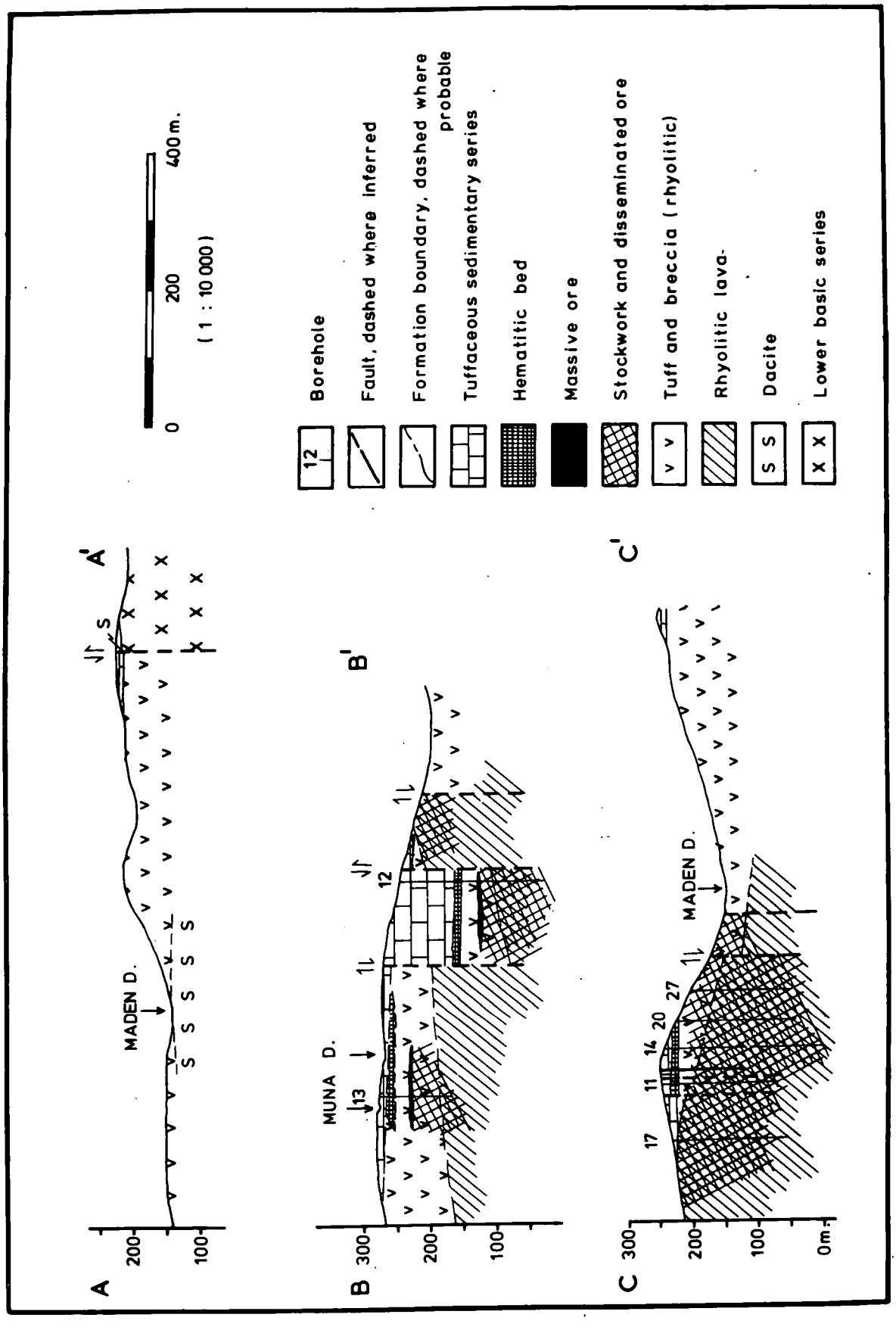

FIGURE 5.10: Geological cross-sections from the Harkkoy mine area

faulting in their immediate vicinity, when compared to the other geological units in the mine area. The magmatic liquids which formed the rhyolites follow the major fracture system, as described in Chapter 4.6. The strongly faulted area thus formed an ideal weak zone for rhyolitic emplacement. The concentric arrangements of some faults, however, suggests that they may have developed in an attempt to accommodate the volume increase resulting from an uprising dome of rhyolitic magma.

Explosion breccias, described from the Harsit-Koprubasi mine, seem to be absent at Harkkoy. The tuffs are also thinner and do not exceed a maximum of 70m, this being only about half their thickness at Harsit-Koprubasi.

The hematitic beds consist of hematite and/or goethite mixed with tuffs. They reach a thickness of 20-25 m and give way upwards to the tuffaceous sedimentary and sedimentary series which have closely similar characteristics to those described from Harsit-Koprubasi mine area.

5.2.3 Mineralisation

The Harkkoy ore body is a pyritic Cu, Zn, Pb massive sulphide deposit associated with rhyolite and rhyolitic tuffs. The orebody consists of pyrite-chalcopyrite-quartz stockwork ore overlain by massive, chalocopyrite rich Zn-Pb ore. The stockwork ore gradually changes to disseminated pyrite and unmineralised rhyolite, it is often associated with dolomite which occurs both disseminated and in small veins. Although stockwork ore may occur both in the rhyolites and the overlying tuffs, the massive ore is always found towards the top of the tuff horizons. As shown in Figures 5.10 and 5.11 b the massive ore is relatively thin, reaching a maximum thickness of 2 m compared to the maximum of 15 m in the Harsit-Koprubasi mine. It is also evident from Figure 5.10 that the massive ore, so far discovered by drilling at Harkkoy, occurs within the thick pile of tuffs. No massive ore is seen in cores 11, 14 and 17 where the tuffs are thin and situated near the culmination of the rhyolite dome. The distribution

of pyroclastic material tends to increase away from this flat dome and hence the relatively unfaulted areas to the east and, particularly, northeast of Maden Dere have a thick tuff sequence. These areas suggest themselves as promising places to search for further extensions of the massive ore body.

Absence of faulting in the area would be an added bonus as the evidence from the Harsit-Koprubasi mine shows that late faults have caused considerable disruption of the ore-body (Figure 5.5, section $2-2^{1}$).

Widespread, lenticular barite has not been observed in the area, unlike Harsit-Koprubasi. Acar (1976) however, has recorded baritic mineralisation between the ore body and the overlying hematised tuffs.

5.2.4. Geochemistry of the Ore-body

The distribution of various elements in vertical sections from cores 11, 12 and 14 are presented in Figures 5.11 a, b and c. In a general sense Zn, Cd, Pb, Ag, As, Ba and Mn increase from bottom to top, whereas there is a tendency for Fe and Cu to increase downwards. The distinction between the massive ore and the underlying stockwork and disseminated ore is difficult because of the limited data on the massive ore. However, data shown in Figure 5.11b together with that of Lob (1960), suggests that massive ore is enriched in Zn, Pb, Cd, Ag(?) and As, whereas stockwork horizons contain more Fe, Cu and Mo. There is a conspicuous enrichment of Fe, As, Ba and Mn in the tuffaceous sedimentary series, as seen in Figure 5.11a, b and c. Fe is clearly incorporated into hematite and goethite but in this zone As seems unrelated to any sulphide phase, although in the massive ore it derives from bournonite and presumably also from tennantite and enargite. Ba may be concentrated in barite and Mn in various oxides, although thin section examination suggests that they also probably occur as dispersed elements since no barite or Mn oxides could be identified. The elements are therefore most probably occurring in adsorbed sites on the various clay minerals present within the tuffaceous sediments.

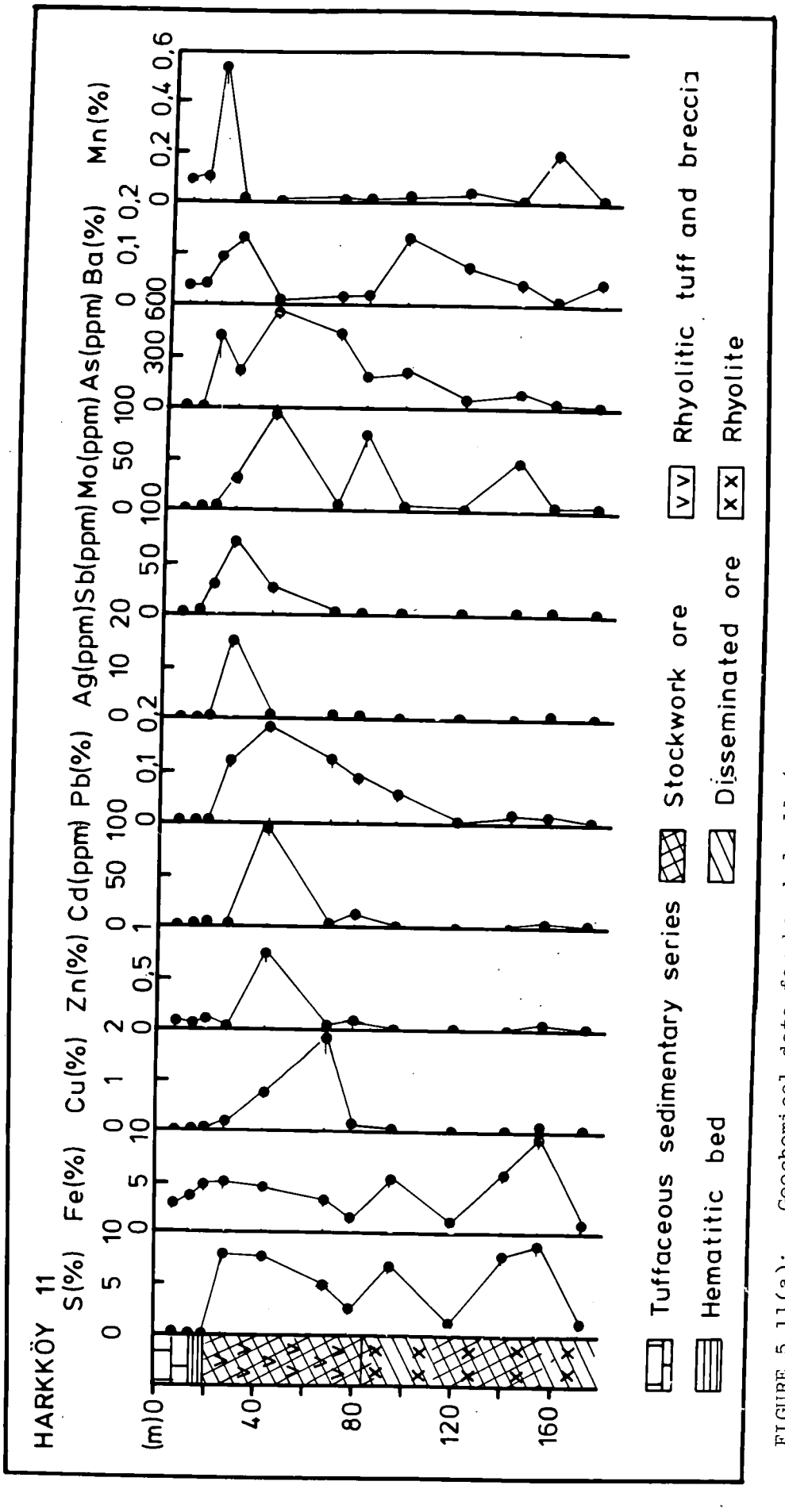

FIGURE 5.11(a): Geochemical data for borehole 11 (Harkkoy mine)

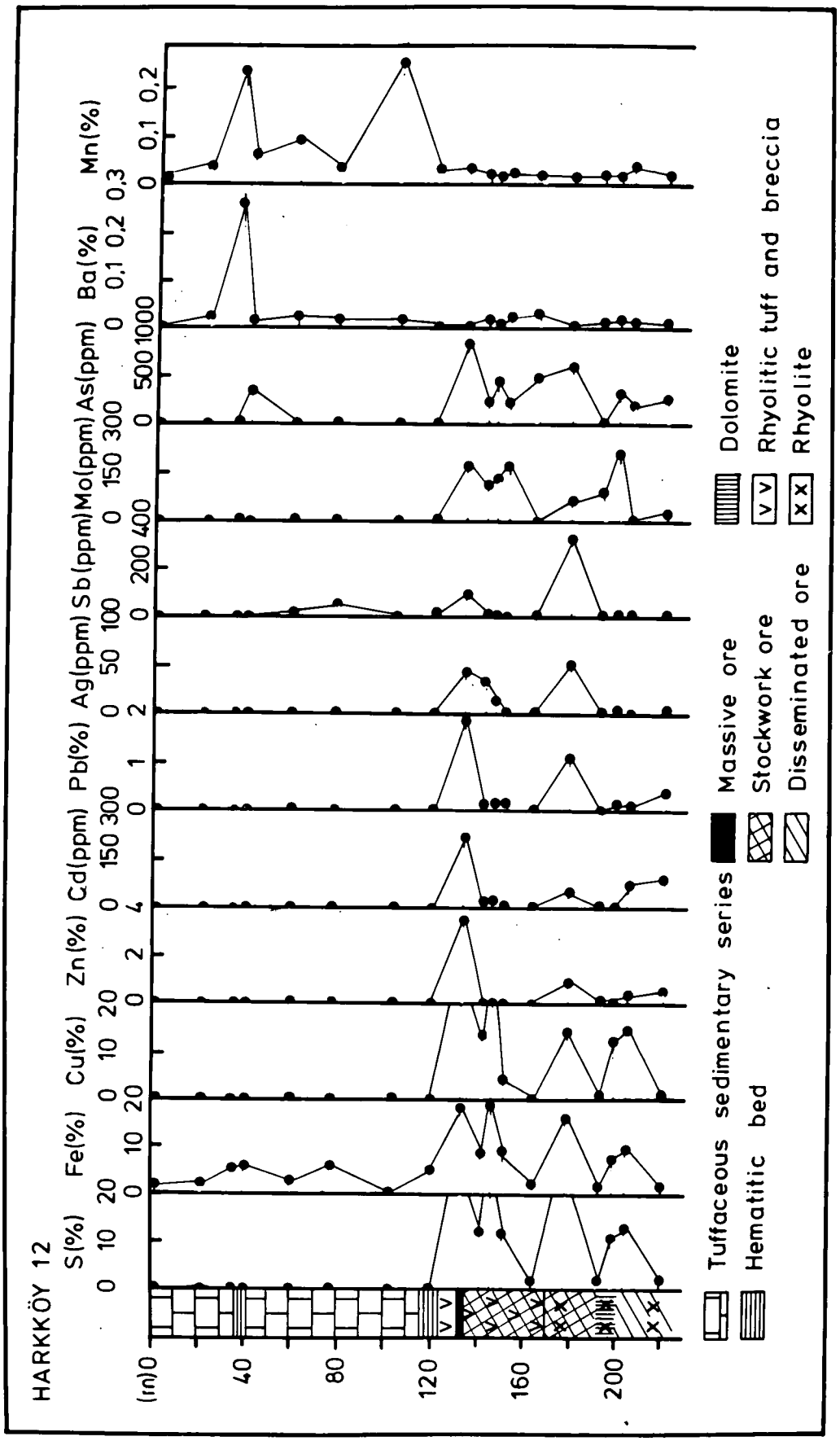

FIGURE 5.11(b): Geochemical data for borehole 12 (Harkkoy mine)

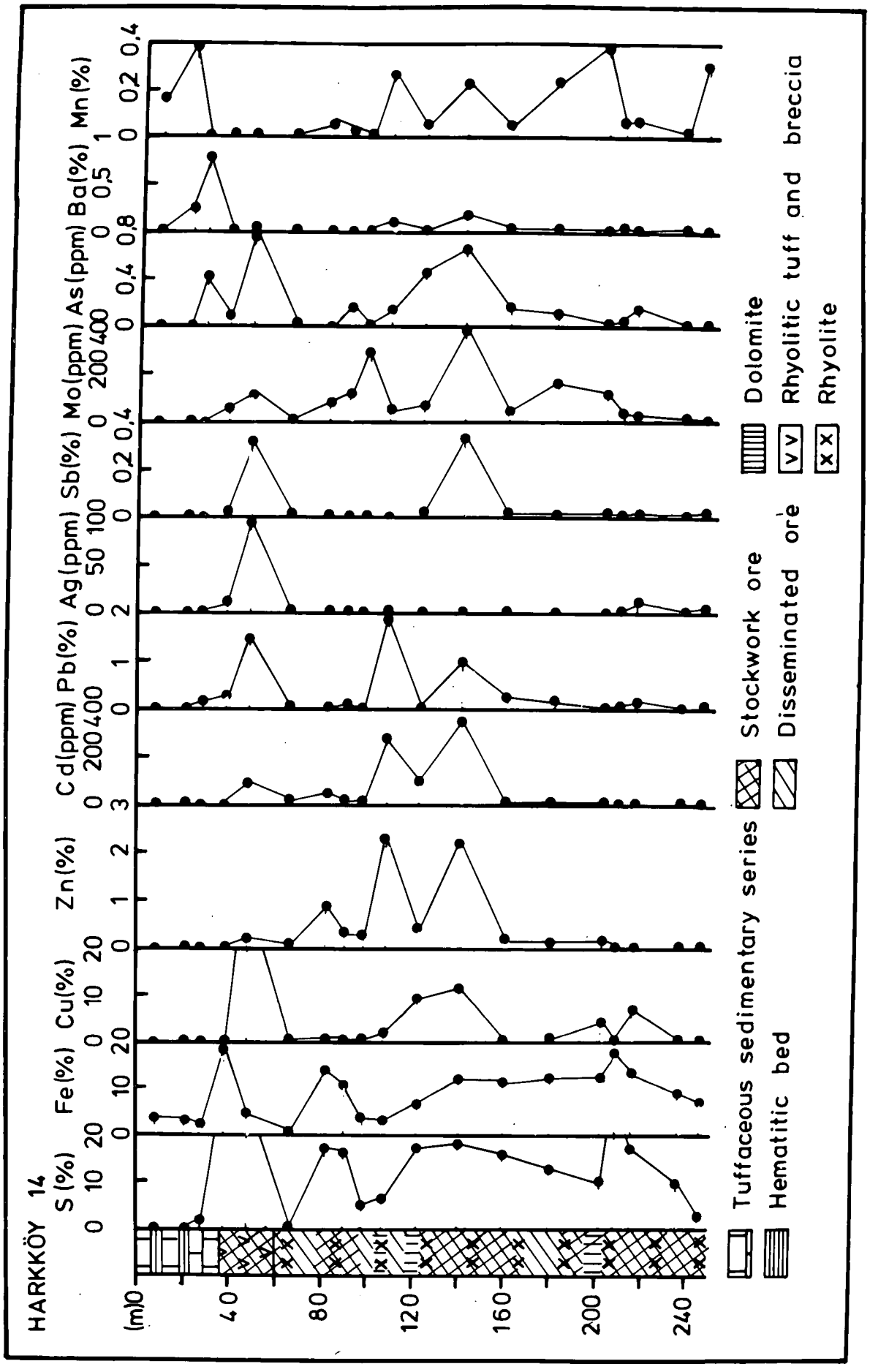

FIGURE 5.11(c): Geochemical data for borehole 14 (Harkkoy mine)

In core 11 (Figure 5.11a), from the bottom to the top of the sequence, the following order is observed. The sequence of sulphides commences with Fe and S, presumably reflecting pyrite. This is followed by Fe, Cu (Pb), S, then Fe, Zn, Pb,(Cu),S and finally Fe, Pb with Ag and Sb. The latter zone is accompanied by a culmination in Ba and closely overlain by a zone in which S levels fall to near zero, but Fe and particularly Mn are enriched. Some elements clearly substitute for major elements, this is obvious in the co-variance of Cd and Zn. Ag and Sb show co-variance and are presumably incorporated into Pb bearing minerals near the end of the sequence of sulphide deposition. Mo and As also follow Pb fairly closely and are presumably mainly present in galena, although the distribution of Mo in the lower part of the core suggests additional control by pyrite. The sequence of sulphides suggests deposition related to order of solubility, the order being generalised as Fe$<$Cu$<$ Zn$<$ Pb. The sequence is completed by a change in the oxidation state, the cessation of sulphide deposition, and deposition of Fe and Mn oxides.

The sequence is closely similar in core 12 (Figure 5.11.b), although Fe, Cu and S are co-variant throughout suggesting that chalcopyrite, rather than pyrite, is the dominant Fe-bearing sulphide. The Zn-Cd co-variance is again very evident, with Zn essentially confined to the massive ore. Ag and Sb again show co-variance with Pb but Mo and As seem to be most closely associated with chalcopyrite. In the overlying S-deficient zone, Fe, Mn and Ba are clearly enriched and As shows a small culmination in the hematitic bed.

Variation in core 14 (Figure 5.11c) is rather similar to that in core 11, although Cu and particularly Pb and Zn are more co-variant.

CHAPTER SIX

ORE MINERALOGY

A number of polished specimens from each mineralised locality have been examined. The specimens were mostly from borehole cores and accessible underground workings, although a few were obtained from mineralised outcrops. X-ray diffraction (X.R.D.) and electron probe microanalysis (EPMA) techniques were used in the identification of mineral phases and in the measurement of the trace element variations in certain minerals. Details of the techniques are given in Appendix 2.

6.1 Distribution of mineral species

Table 6.1 shows the occurrence, abundance and distribution of sulphides, sulphates, oxides and carbonates in massive sulphide deposits of the northern Harsit river area. The mineralisation is shown in relation to variations in the lithology of the host-rock. The information in Table 6.1 is compounded from observations on a number of deposits in the area since, as explained previously, no single deposit shows the complete zonal sequence. The zonation is similar to those described for the Cayeli deposits by Cagatay (1977) and for the Lahanos mine by Tugal (1969). The sequence also shows many close similarities to the distribution of mineralisation in Japanese Kuroko deposits as described by Ishihara (1974) and first noticed by Tugal (1969). Cagatay (1977) has compared the ones at Cayeli with the Kuroko deposits terming the massive ore - Black ore (Kuroko) and stockwork ore - Yellow ore (Oko) deposits. The generalised terms Black Ore and Yellow Ore have been used in this study. The term "Black ore" is used to encompass the massive part of the orebody when it consists of sphalerite, pyrite, galena, chalcopyrite and sulphosalts. Use of the term "massive pyritic ore", for example in describing the deposits at Lahanos (Tugal,1969), Israil, Yalc Tepe and Yarmaden, implies the importance and abundance of the named mineral. The term "Yellow ore" has

Lava	Breccia	Tuff	Sediments		Lithology / Minerals	Pyrite FeS_2	Chalcopyrite $CuFeS_2$	Sphalerite ZnS	Galena PbS	Digenite ? Cu_9S_5	Chalcocite ? Cu_2S	Covellite CuS	Bornite Cu_5FeS_4	Realgar AsS	Orpiment As_2S_3	Tetrahedrite / Tennantite $(Cu,Fe)_{12}(Sb\text{-}As)_4S_{13}$	Bournonite $PbCuSbS_3$	Enargite Cu_3AsS_4	Electrum (Au,Ag)	Hematite Fe_2O_3	Goethite FeO.OH	Manganite ? MnO.OH	Pyrolusite ? MnO_2	Psilomelane $(Ba,H_2O)_2Mn_5O_{10}$	Dolomite $(Ca,Mg)CO_3$	Siderite $FeCO_3$	Ankerite $Ca(Fe,Mg,Mn)(CO_3)_2$	Malachite $Cu_2(OH)_2CO_3$	Azurite? $Cu_3(OH)_2(CO_3)_2$	Barite $BaSO_4$	Gypsum Ca $SO_4.2H_2O$	Quartz SiO_2
		2	2		Tuff and Tuffaceous Sedimentary Series										+					2-3	2-3	+	+	1								1
		3		massive ore body	Barite horizon																									3		1
	+	3			Strata-bound massive ore	2	1	3	2	+	+	+	+	+	+	1-2	1-2	+										+	+	1		2
1	1	2			Stockwork and disseminated ore	3	2	1	1	+	+	+	+			+		+	+?											+		3
2	2	2			Gypsum - dolomite	+	+																		1	+	+				1	2
3	+				Rhyolite	1-2	+																									2

1, 2, 3 : Relative abundances
\+ : Present

TABLE 6.1: Occurrence, abundance and distribution of mineral species in the study area

been used to describe a chalcopyrite-pyrite ore occurring mostly in stockwork and/or disseminated form, seen for example in the cores from the Harkkoy mine: many of the siliceous, pyritic stockworks however would be more appropriately termed "Keiko" ores, if direct comparison with the Japanese examples is to be maintained.

6.2 Suphides

6.2.1 Pyrite

Pyrite is by far the most abundant sulphide mineral and occurs throughout the deposits in all zones up to the barite horizon. Its abundance and form, however, may vary both between and within ore bodies.

Euhedral to subhedral pyrite is most common since the "formation energy" of pyrite is greater than that of other sulphide minerals (Ramdohr, 1969).

Colloform pyrite does occur, but is exclusively confined to the upper parts of the massive black ore which also contains considerable barite (Plate 6.1). Under the microscope it shows pellet, framboidal and zonal textures and appears to be similar to the "mineralised bacteria", described by Ramdohr (1969, fig.116). The occurrence of colloform pyrite has been reported in many of the massive sulphide deposits investigated in the Pontid metallogenic province. It occurs in ore Zone III, the upper part of the massive pyritic ore, at Lahanos (Tugal,1969) and is intimately associated with the Black ore at Cayeli (Cagatay, 1977). In the Bulancak sulphide veins, however, Akinci (1974, p.103) stated that "no form of colloidal pyrite was seen".

The origin of colloform textures has been extensively discussed by Bastin (1950), Edwards (1965), Rickard (1970) and Kribek (1975) with general acceptance that they represent open space precipitation. Kribek (1975) discussed the origin of framboids, based on laboratory experiments. He concluded that sulphidation (oxidation) of metastable spherical grains of

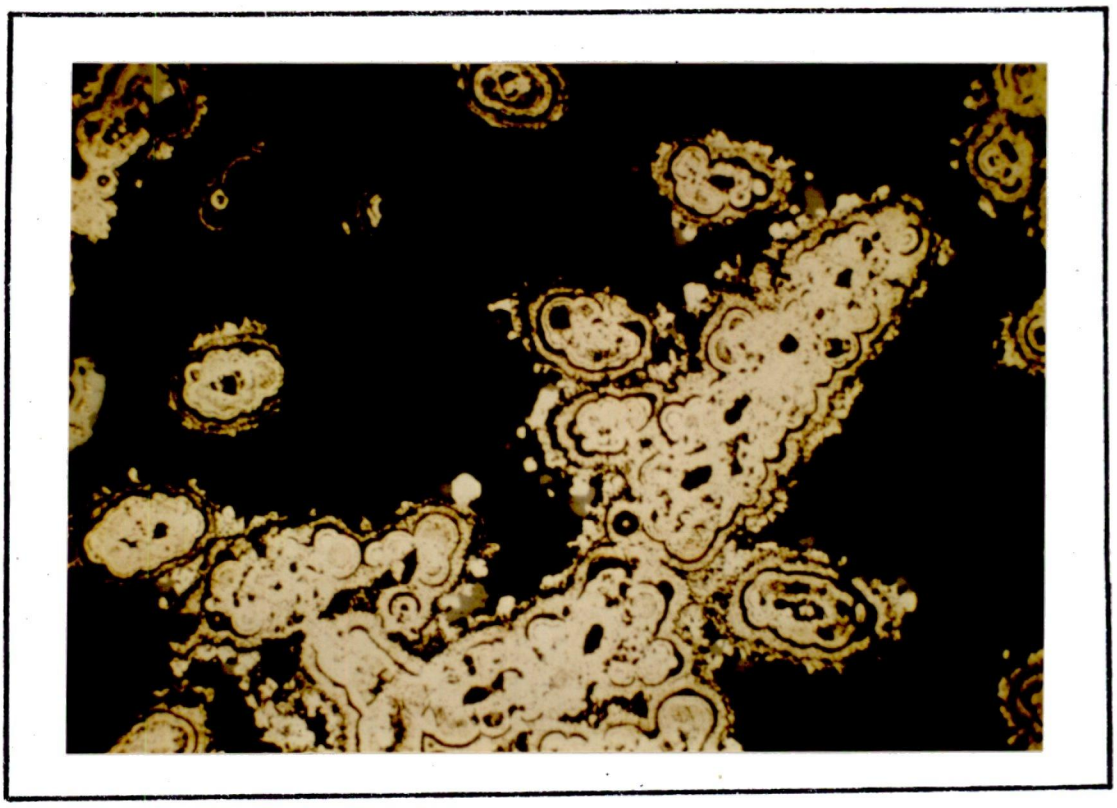

PLATE 6.1: Colloform pyrite (sample 405, Harsit-Koprubasi mine adit, level, -10) 100x.

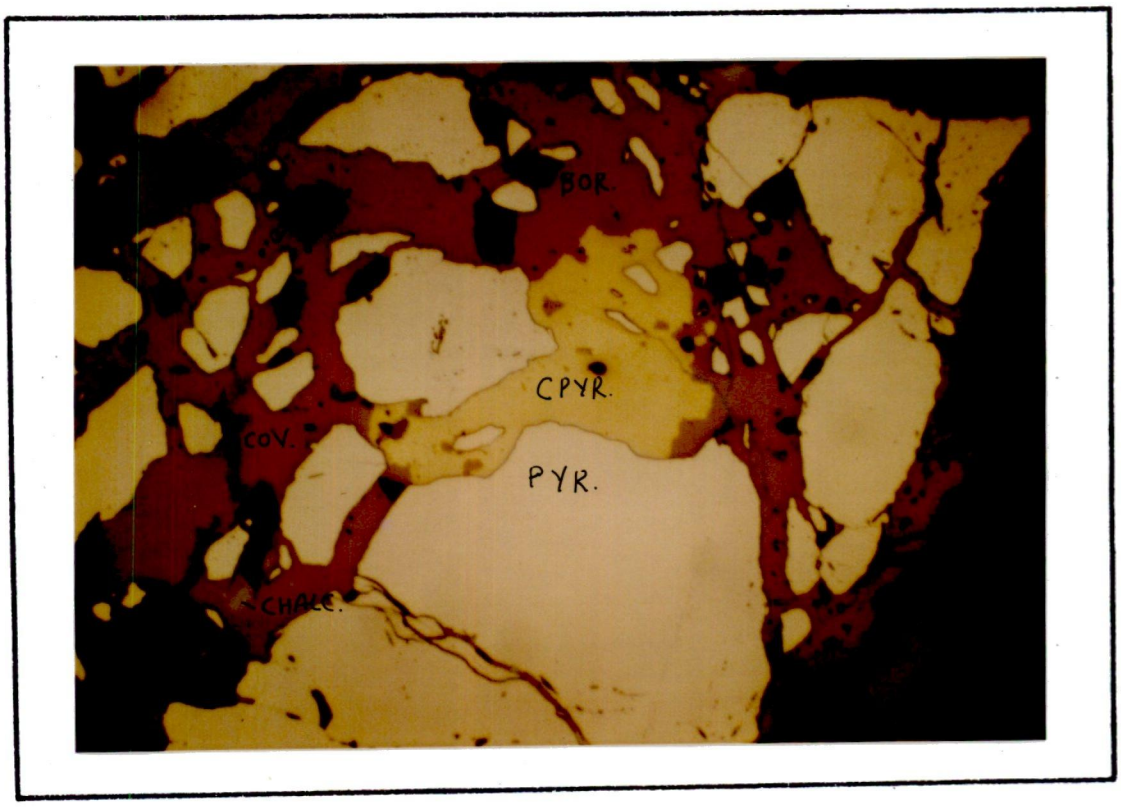

PLATE 6.2: Cataclastic pyrite replaced by chalcopyrite, bornite, chalcocite(?) and covellite (Harkkoy mine, borehole 14, 47.55 m) 100X

sulphur, initiated either by the oxidation of hydrogen sulphide or by the action of micro-organisms, may precipitate framboidal pyrite. Watanabe (1974) has also ascribed the formation of colloidal textures observed in Kuroko ores to an increase in the oxidation state of the ore fluids.

Pyrite commonly exhibits a cataclastic texture (Plate 6.2) of euhedral to subhedral grains. Angular fragments of pyrite (and in places chalcopyrite) are scattered in a matrix of chalcopyrite, bornite, sphalerite and covellite. Watanabe (op.cit.) interprets such fragmental textures in the Kuroko ores, as due to redeposition and transportation during sliding and slumping of local submarine lavas during and after the precipitation of the ore minerals. The occurrence of brecciated ore fragments in the Harsit-Koprubasi mine black ore (Plates 6.3 and 6.4) may support this theory of redeposition. Additionally, however, it may be proposed that co-eval, or post-ore deposition, volcanism may also produce fragmental and cataclastic textures (Plate 6.5). The occurrence of such textures in relatively undisturbed (unfaulted) parts of the ore body may rule out the possibility of fault brecciation.

The grain-size of pyrite varies between the euhedral and colloform types. The former are largest at the bottom of an orebody where they reach 1-2 mm in diameter in the disseminated ore. In the stockwork, the grain-size averages about 100μ in diameter, while in the massive ore the average dimensions fall to around 50μ. Colloform pyrite is of extremely fine grain-size.

A series of electron probe analyses were carried out on pyrite grains of euhedral to subhedral and collform type. Individual analyses are shown in Table 6.2., and Table 6.3 summarises the results obtained from the two varieties. Application of the Wilcoxon Rank Sum Test (Wilcoxon & Wilcox, 1964) reveals significant differences in the major and minor element contents of the well crystalline and colloform types.

Differences in levels of the major elements Fe and S, and in the trace

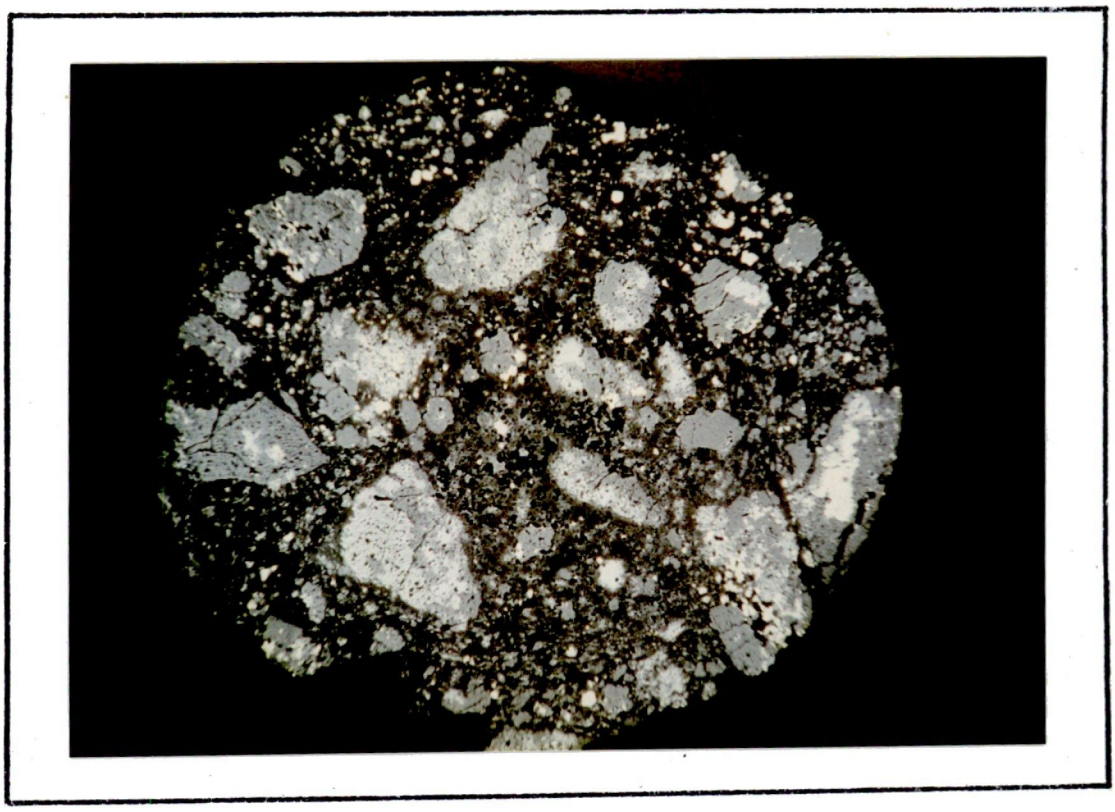

PLATE 6.3: Ore breccia (sample 438, Harsit-Koprubasi mine adit, level - 10)

PLATE 6.4: Ore breccia (sample 112, northern Harsit river area.)

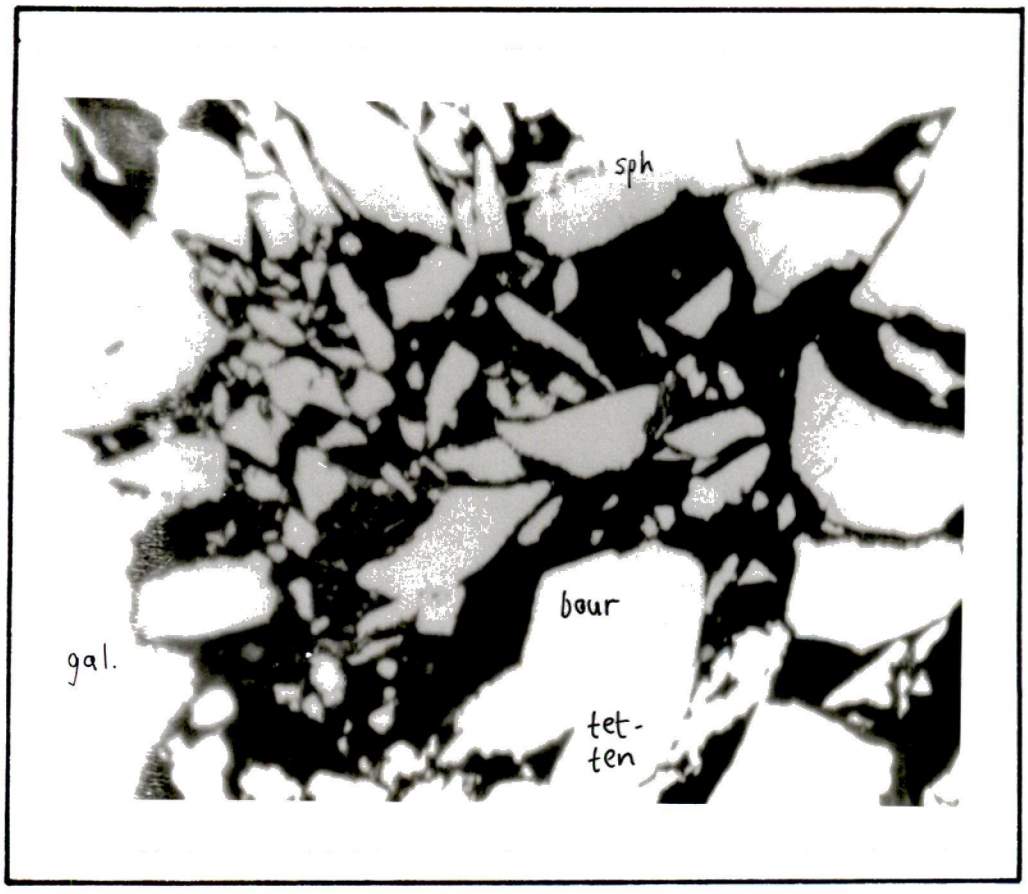

PLATE 6.5: Cataclastic texture in galena, sphalerite, tetrahedrite and bournonite (sample 437, Harsit-Koprubasi mine adit, level, -10) 100X

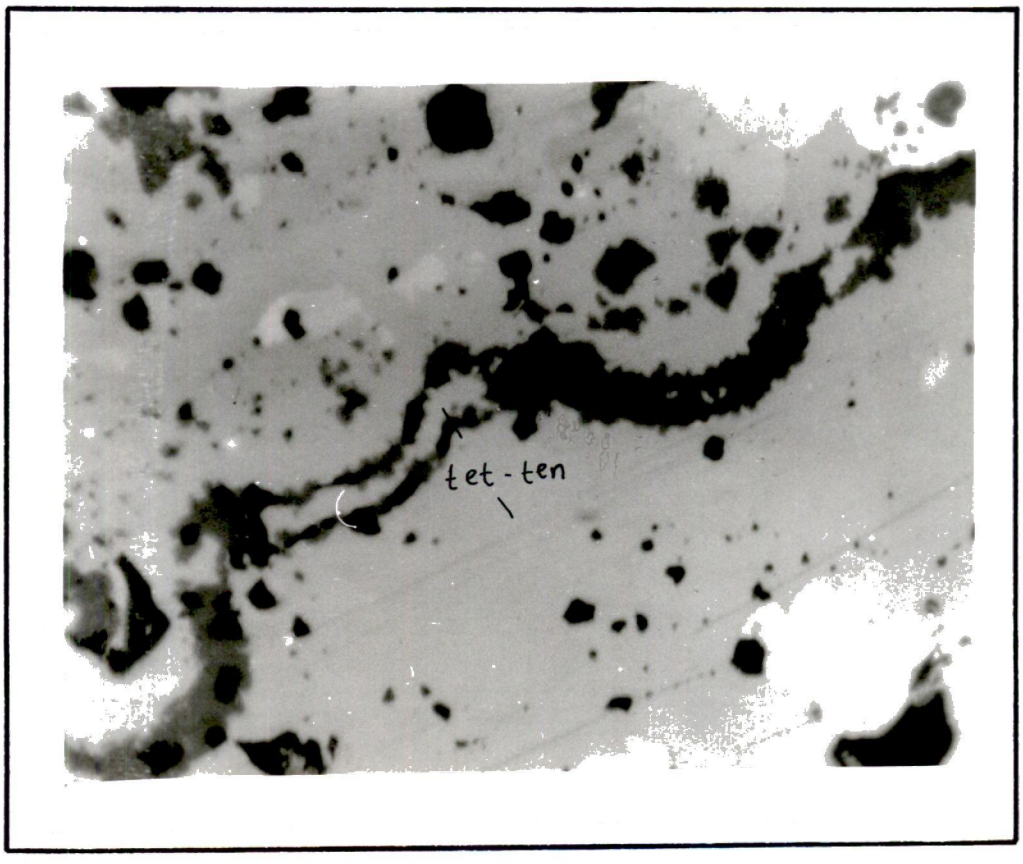

PLATE 6.6: Colloform intergrowth of sphalerite, tetrahedrite-tennantite and galena (sample 435, Harsit-Koprubasi mine adit, level, -10) 100X

COLLOFORM PYRITE

Sample No.	Fe*	S*	As	Se	Cr	Cu	Zn	Co	Ni	Total*
H11-44m	45.93	53.69	5060	-	-	n.d.	n.d.	1070	630	100.30
H11-41m	45.31	53.71	7600	-	210	n.d.	n.d.	1450	1820	100.13
H13-19m	45.20	49.66	4470	-	-	550	680	610	1360	95.63
H13-21m	44.41	51.22	6040	-	-	3740	1530	1480	2930	97.20
H27-21m	44.93	53.14	2150	-	240	2020	-	1590	750	98.75
H31-22m	42.50	54.33	11330	400	-	8360	11870	1240	810	100.23
H41-16m	44.07	52.40	18100	-	-	11230	2450	1030	790	99.83
H68-38m	45.50	53.40	8380	-	-	n.d.	n.d.	600	-	99.79
H68-48	46.47	52.03	11190	-	-	1760	1880	1480	1350	101.26
112	43.28	52.92	7780	-	-	n.d.	n.d.	1080	530	97.14
112A	45.32	53.37	-	-	-	n.d.	n.d.	-	650	98.76
405	44.81	51.64	11340	-	320	n.d.	n.d.	1150	780	97.81
405A	45.46	51.21	19200	-	390	n.d.	n.d.	-	-	98.63

EUHEDRAL PYRITE

HG2-11m	45.39	52.07	270	750	-	1280	-	2070	720	97.97
H4-53m	47.24	52.26	5080	-	-	1230	660	1390	560	100.39
H13-19m	45.56	52.07	6550	-	-	1650	310	1770	-	98.66
H13-24m	44.42	54.38	810	270	-	-	-	2120	-	99.12
H19-24	46.74	52.91	2580	-	200	-	-	990	670	100.09
H44-16m	46.40	54.43	3650	-	-	-	-	860	-	101.28
H47-102m	46.32	53.90	5070	-	-	n.d.	n.d.	990	350	100.86
H68-48m	46.80	52.48	1820	-	430	870	950	1330	720	99.89
H68-49m	46.98	52.88	-	380	-	-	2070	840	-	100.19
H68-54m	46.65	51.25	1310	380	-	990	1340	1370	490	98.48
HRK11-30m	46.50	52.47	-	260	460	1190	-	1390	860	99.39
HRK11-43m	46.82	54.28	2740	-	-	720	-	670	-	101.51
HRK12-141m	46.94	52.69	-	-	-	-	700	1940	-	99.89
HRK12-148	45.24	53.30	-	660	-	1240	920	1590	870	99.07
HRK14-47m	45.55	53.32	-	470	290	2800	940	1350	320	99.49
HRK14-148	47.60	52.56	-	-	-	570	230	1230	420	100.41
165	45.60	53.87	-	790	-	-	-	1440	410	99.73
165A	47.12	53.90	-	700	-	840	400	1620	1340	101.51
216	45.44	53.74	-	-	-	n.d.	n.d.	-	-	99.18
216A	46.08	53.64	-	880	-	6680	-	970	540	100.63

* wt percent, otherwise in ppm
n.d. not determined
- below the detection level
H Harsit-Koprubasi borehole sample
HG Harsit-Koprubasi adit borehole, level - 16 m
HRK Harkkoy mine
112 surface sample

TABLE 6.2: Electron probe microanalyses for pyrites

Elements	Euhedral Range	Colloform Range	W.R.S.T.
Fe*	44.42 - 47.60	42.50 - 46.47	0.01
S*	51.52 - 54.44	49.66 - 54.33	0.05
As	n.d. - 6550	n.d. - 19200	0.01
Se	n.d. - 790	n.d. - 400	0.05
Cr	n.d. - 460	n.d. - 390	-
Cu	n.d. - 6680	1760 - 11230	0.01
Zn	n.d. - 2070	680 - 11870	0.01
Co	n.d. - 2120	n.d. - 1590	0.10
Ni	n.d. - 1340	530 - 2930	0.01
Co/Ni	1.06 - 10.60	0.30 - 4.61	0.01

W.R.S.T. Two-sided Wilcoxon Rank Significance Test probability levels (Wilcoxon and Wilcox 1964), only values up to a probability level of 0.10 are included.

* Wt percent, otherwise in ppm

n.d. below the limit of detection

TABLE 6.3: Comparative electron probe microanalysis results for well crystalline and colloform pyrites

elements Cu and Zn, are attributed to the extremely fine grain-size of the colloform pyrites. The apparent higher Cu and Zn contents of the colloform pyrite may be readily explained by contamination from PbS and ZnS present in the black ore which is intimately associated with the colloform pyrite. Cu and Zn, which are not readily accepted into the crystal structure of pyrite, thus most probably occur as "mechanical admixtures" (Ramdohr, 1969, p.779).

Pyrite can contain substantial Ni and Co substituting for Fe (Stanton, 1972). Examples given by Fleischer (1955) indicate that pyrite of sedimentary origin is characterised by low Co contents and Co/Ni ratios less than one, whereas pyrite of hydrothermal origin has high Co values (400-2400 ppm) and Co > Ni. Fleischer suggests however that Co content and the Co/Ni ratio must be used with considerable caution in determining the origin of pyrite. A similar study by Davidson (1962) also showed that Co/Ni ratios may be used to distinguish sedimentary and magmatic hydrothermal ores, while Loftus-Hills and Solomon (1967) have demonstrated from Tasmanian examples, that a clear distinction may be established between sedimentary pyrite and all other pyrite (hydrothermal). Tono (1974) has compared Co/Ni ratios of silicified (Co/Ni= 22) and Oko(Co/Ni=3) ore in Kuroko deposits which indicate a downward increase sympathetic with the temperature variation shown by these ores. The observed variation in Co and Ni and the difference in the Co/Ni ratio between euhedral pyrite, which occurs in the lower parts, and colloform pyrite, found in the upper part of the orebodies, is thus compatible with that shown by the Kuroko deposits.

However, examination of tables 6.2 and 6.3 shows that the Co/Ni ratio is more significantly changed (0.01 level) by the increase of Ni in colloform pyrite. It is therefore necessary to find a source for Ni and to decrease Co levels in the upper part of the ore body, as compared to

the lower stockwork zone. The deep sea clays are characterised by excess amounts of Ni and the oceanic basalts by their high Ni content (Taylor,1969). By analogy to these, a possible interaction between the ascending hydrothermal solutions with a high Co/Ni ratio and the sea water with a Co/Ni ratio of 0.05 may well be an answer to the change in the ratio within the ore body as discussed in Chapter 7. Therefore variation in Co/Ni ratios within an ore suggests that simple Co/Ni ratios for a deposit have little meaning in the classification of volcanogenic sulphide deposits, as attempted by Cagatay (1977, p.10).

The higher As contents of the colloform pyrite are similar to the values observed in colloform pyrite by Ramdohr (1969). Hawley (1952) has demonstrated that in the Porcupine veins, Ontario, low temperature pyrite contains more As than its high temperature counterpart, while Talluri (1951) has shown that pyrite in eruptives is enriched in As relative to sedimentary pyrite. Malakhov et al (1974) showed that pyrite from the syngentic upper parts of the Makansky deposits of the southern Urals contains more As than the epigenetic veins.

The geochemistry of Se is closely related to that of sulphur although Howard (1977) states that Se is concentrated in high temperature sulphide ore deposits, thus accounting for its enrichment in the epigenetic veins of the Makansky deposits described by Malakhov et al (1974). Loftus-Hills and Solomon (1967) have concluded that in some major provinces the Se/S ratio may be a useful indicator of ore genesis.

In the northern Harsit river area Se is relatively depleted in the colloform pyrite (Table 6.3). Stanton (1972,p.172) has stated that "sulphur and selenium show many similarities of chemistry and general association. However one dissimilarity stands out: whereas sulphur is abundant in the water of oceans, selenium is....conspicuously absent." The change in the oxidation state of the ore fluids, or oxidation of

hydrogen sulphide necessary for precipitation of colloform pyrite, may be facilitated by the contact or mixing of ore fluids with sea water. Such interaction would be likely to yield low Se-bearing pyrite due to the dilution effect of low Se sea-water. The abundance of barite, in close association with colloform pyrite, may also support a change in the oxidation state of the ore-forming fluids, or mixing of sulphate-bearing sea-water with Ba-carrying ore fluids.

6.2.2. Chalcopyrite

The abundance of chalcopyrite varies both geographically and stratigraphically. It is usually the major constituent after pyrite, in the stockwork ore (Yellow ore). In sphalerite rich-veins it forms droplets resulting from immiscibility during cooling (Ramdohr,1969). Chalcopyrite usually replaces euhedral pyrite and occurs together with enargite and bornite forming the following common association:

Pyrite+chalcopyrite+bornite+enargite±native gold.

Chalcopyrite is less common in the massive ore and when present is of small grain-size, averaging approximately 50μ in diameter. It shows no replacement features in the massive ore. The association: Sphalerite + tetrahedrite + tennantite + pyrite + galena + chalcopyrite + bournonite is characteristic. Most of the chalcopyrite appears to have formed either contemporaneously with, or later than, the pyrite. It may well form earlier than most of the other massive ore constituents shown in Table 6.1.

Electron-probe analyses of chalcopyrite are presented in table 6.4, although limited, show general agreement with trends established for the trace elements in pyrite. Co/Ni ratios in chalcopyrite from the uppermost horizons of massive ore (Co/Ni 0.68 and 1.44) are low when compared to those in chalcopyrite from stockwork ore (Co/Ni 1.23 - 3.55), while Se levels were below the detection limit in the massive ore of the higher stratigraphic horizons. The generally high As contents are closely

Sample No.	Cu*	Fe*	S*	As	Se	Cr	Zn	Co	Ni	Total*	Comments
CHALCOPYRITE											
H 19/24m	33,18	29,84	34,15	3760	-	-	1990	1560	1080	97,99	massive
H 69/54m	35,63	29,41	35,86	2220	-	-	1690	520	760	101,44	"
H 68/65m	33,05	29,09	35,41	-	-	-	2040	710	-	99,85	stockwork
HRK 11/30m	34,33	30,00	34.52	4940	-	-	1080	710	430	99,11	"
HRK 12/141m	33,17	30,10	33.67	6590	510	500	5610	1070	470	98,89	"
HRK 12/148m	34,96	30,89	34,69	6150	1500	430	1390	1940	1570	101,84	"
HRK 14/148m	34,61	30,35	34,00	-	-	210	1800	1430	760	99,38	"

SPHALERITE	Zn*	S*	Cd	Fe	Cu	Mn	Sb	Hg	Ag	Pb	Se	Total*	Comments
70 A	66,12	32,74	5060	3280	n.d.	-	n.d.	n.d.	n.d.	n.d.	n.d.	99,70	massive
H 19/24m	65,40	31,67	5540	2710	2410	1060	1580	-	-	540	-	98,47	"
H 68/44m	66,21	32,10	4940	3860	550	-	n.d.	n.d.	n.d.	n.d.	n.d.	99,25	"
H 68/48m	66,15	32,03	5500	1050	-	770	n.d.	n.d.	n.d.	n.d.	n.d.	98,91	"
H 44/103m	66,75	32,50	6250	5940	230	550	n.d.	n.d.	n.d.	n.d.	n.d.	100,55	stockwork
H 68/59m	65,27	32,84	4150	9200	9860	1100	n.d.	n.d.	n.d.	n.d.	n.d.	100,55	"

TETRAHEDRITE	Cu*	S*	Sb*	As*	Zn*	Ag*	Bi	Pb	Fe	Cd	Se	Mn	Total*
H.G.10	36,21	23,82	30,81	0,42	7,22	1,43	-	n.d.	1650	n.d.	n.d.	-	100,10
H17/58m	36,96	22,94	27,91	2,35	7,31	1,82	n.d.	2220	1420	-	-	n.d.	99,69
H19/19m	37,11	23,10	29,14	1,06	7,06	1,30	n.d.	n.d.	2890	-	-	420	99,11

ENARGITE	Cu*	S*	Sb*	As*	Zn	Ag	Bi	Pb*	Fe	Cd	Se	Mn	Te	Sn	Total*
H 17/58m	44,06	30,70	0,78	19,19	-	-	n.d.	3,71	2280	-	-	-	n.d.	n.d.	98,70
H 7/25m (A)	46,83	31,12	4,13	17,17	830	n.d.	n.d.	n.d.	740	-	-	-	-	n.d.	99,96
H 7/25m (B)	46,64	30,21	7,57	15,45	-	-	-	n.d.	1500	n.d.	n.d.	n.d.	n.d.	-	100,04
HRK 14/47,55m.A	48,10	33,15	-	18,52	n.d.	-	n.d.	n.d.	9500	n.d.	n.d.	n.d.	n.d.	n.d.	100,73
HRK 14/47,55m.B	48,75	34,56	-	17,05	n.d.	-	n.d.	n.d.	-	n.d.	n.d.				100,37

- : Below the detection limit
* : in percent, otherwise in ppm
H : Harsit-Koprubasi Borehole number
HG : Harsit-Koprubasi adit specimen, level-16m
HRK : Harkkoy mine borehole number
n.d. : not determined
70A : surface specimen

TABLE 6.4: Electron probe microanalyses for various sulphide and sulphosalt minerals

comparable to those found in the Shakanai Kuroko deposits by Nishiyama (1974). They may result from exsolution of As minerals within the chalcopyrite (Edwards,1965). Chromium levels are higher in chalcopyrite than co-existing pyrite as shown by Shimazaki (1974) for Kuroko ores. Cr has only been detected in the lower stockwork chalcopyrite (Table 6.4) of Harkkoy 12 and 14 borehole cores.

6.2.3 Sphalerite

Sphalerite is the most abundant sulphide in the massive ore, although it is virtually absent in the stockwork ore of Harkkoy mine. It is usually found in subhedral to anhedral grains varying in size between 20 and 800μ , but being mostly near to 80μ in the massive ore. Occasional colloform intergrowths of sphalerite with galena and tetrahedrite occur in the upper, massive, black ore, Plates 6.6, 6.7 and 6.8 again pointing to a change in the physico-chemical parameters as discussed for colloform pyrite. Most of the sphalerite is dark brown, but yellow-green to red coloured varieties are present, sometimes showing alternate bands of yellow and red in thin discs prepared for fluid-inclusion studies. Exsolved blebs of chalcopyrite in sphalerite occur in minor amount, while replacement involves sphalerite for pyrite. The relationship between sphalerite and other massive ore constituents is not clear.

Sphalerite analyses are shown in Table 6.4. Barton and Toulmin (1966) have shown that, except for very Fe rich varieties, the Fe content of sphalerite is a function of aFes and temperature, provided the relationship is unaffected by the other components of the system, such as MnS and CdS. Their studies in the Zn-Fe-S system, however, only consider the use of sphalerite as a geothermometer above 580^{o}C, although Yui and Czamanski (1971) have obtained values below 300^{o}C from sphalerite from Iimori mine by extrapolation of the original curve produced by Barton and Toulmin (1966, fig.14). No attempt was made to use the sphalerite geothermometer

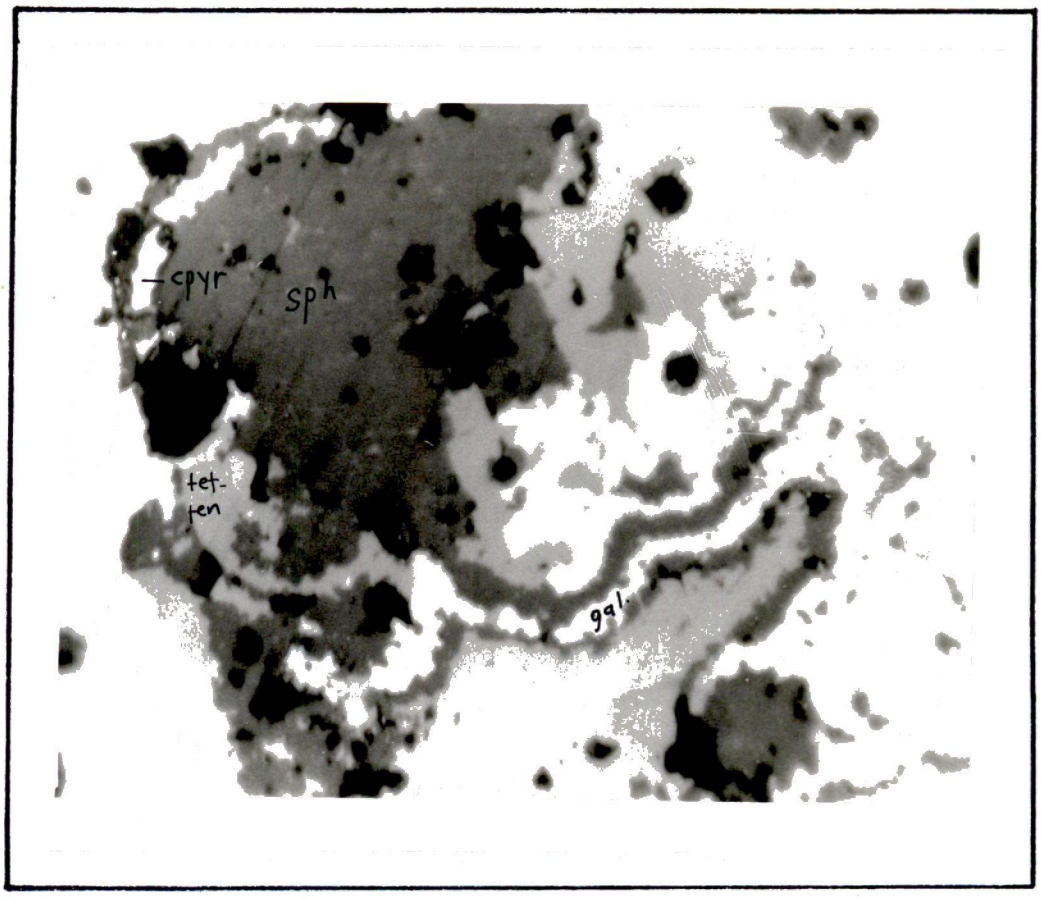

PLATE 6.7: Colloform intergrowth of sphalerite, tetrahedrite - tennantite, bournonite, galena and chalcopyrite (sample 435, Harsit-Koprubasi mine adit, level, -10) 56X

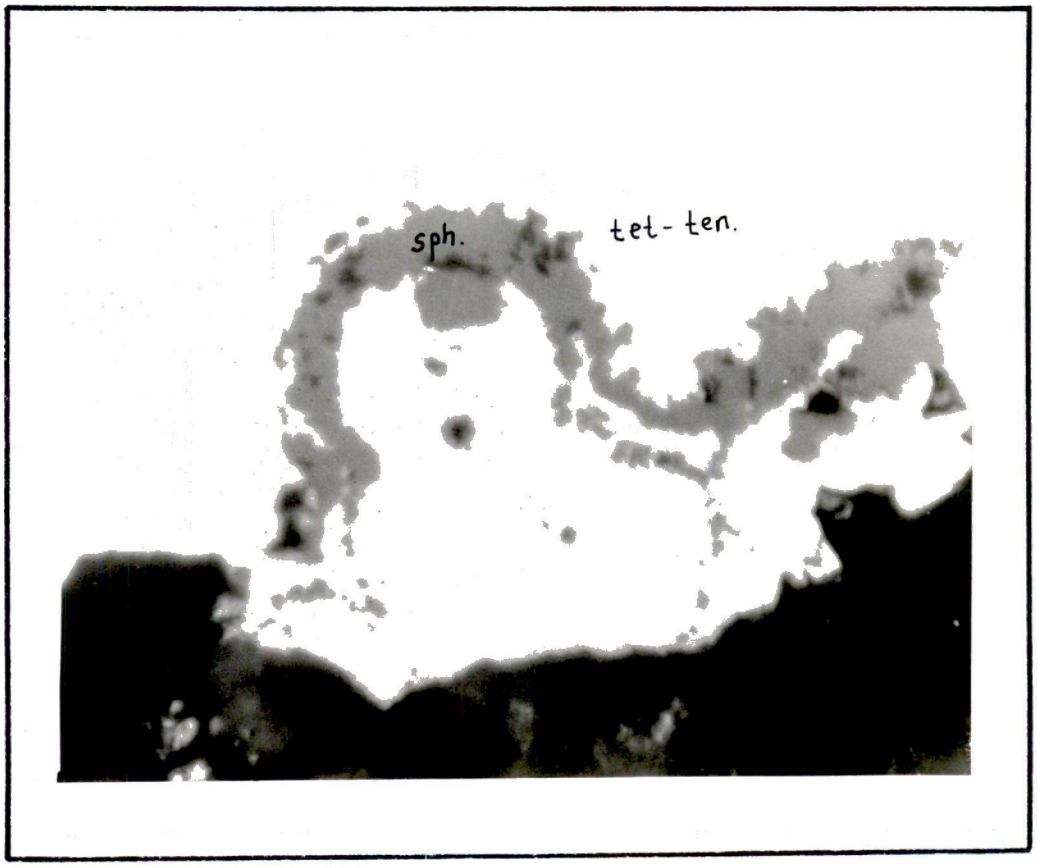

PLATE 6.8: Sphalerite, tetrahedrite-tennantite colloform intergrowth (sample 435) 450X

since Barton and Toulmin (1966,p.816) consider that "equilibrium cannot be quantitatively extrapolated to lower temperatures from the presently available data and therefore quantitative geothermometry....is not feasible." The data obtained from the fluid inclusion studies of sphalerite from the study area yield temperatures below 300°C. The iron content of sphalerite varies between 0.1 and 0.9 wt% with the tendency for the higher values to occur in the stockwork ore. The variation may be attributed to a change in the sulphur fugacity (Barton and Toulmin, 1966; Nash, 1975), and/or temperature (Barton and Skinner, 1967). The data is too limited to attribute the variation to a particular aspect of the ore forming fluids, however, the generally low Fe content is similar to values obtained from Kuroko deposits, from Bulancak mine and from Binnatel mine where the data are in agreement with the temperatures of less than 300°C obtained from fluid inclusion studies (Urabe,1974; Akinci,1974; Graeser,1969).

Acar and Akinci (1975) found a linear correlation between Cd and Zn contents as a result of systematic analysis of material from the Harsit-Koprubasi mine. The high Cd levels in the analysed sphalerites shown in Table 6.4 are in agreement with their study and imply that Cd may be an economic by-product of the ores.

6.2.4 Galena

Galena is commonly found in the massive ore where it usually occurs as rounded grains of 50-60 μ diameter. It shows no replacement features (plate 6.9). Electron probe analysis of galena from the Harsit-Koprubasi mine, borehole 19, at 24 m gave the following result:

PbS, H19-24m(Wt%)	Theoretical (Palache et al.1944)
Pb = 84.97	86.60
S = 13.00	13.40
Mn = 0.049	-
Zn = 0.090	-
Sb = 0.103	-
Total = 98.21	100.00

Cu, Fe, Hg, Cd, Ag, Se, As were not detected.

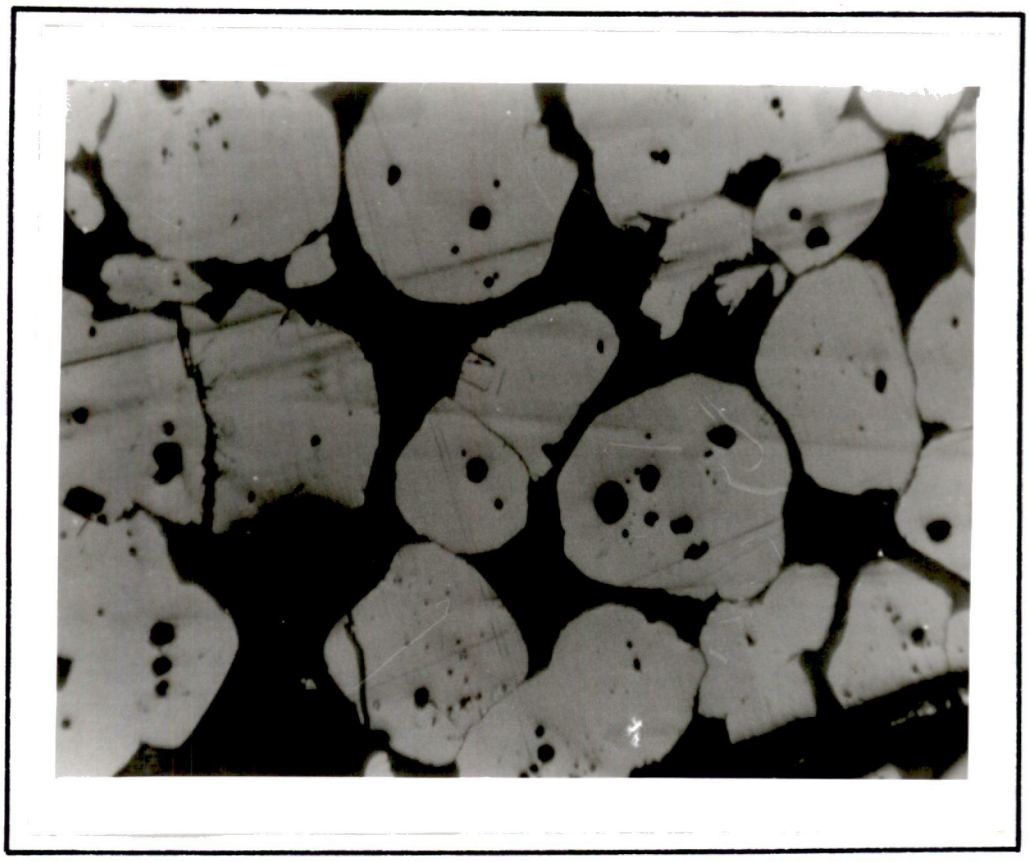

PLATE 6.9: Photomicrograph showing rounded galena with no replacement feature (sample 447, Harsit-Koprubasi mine adit, level,-10) 56X

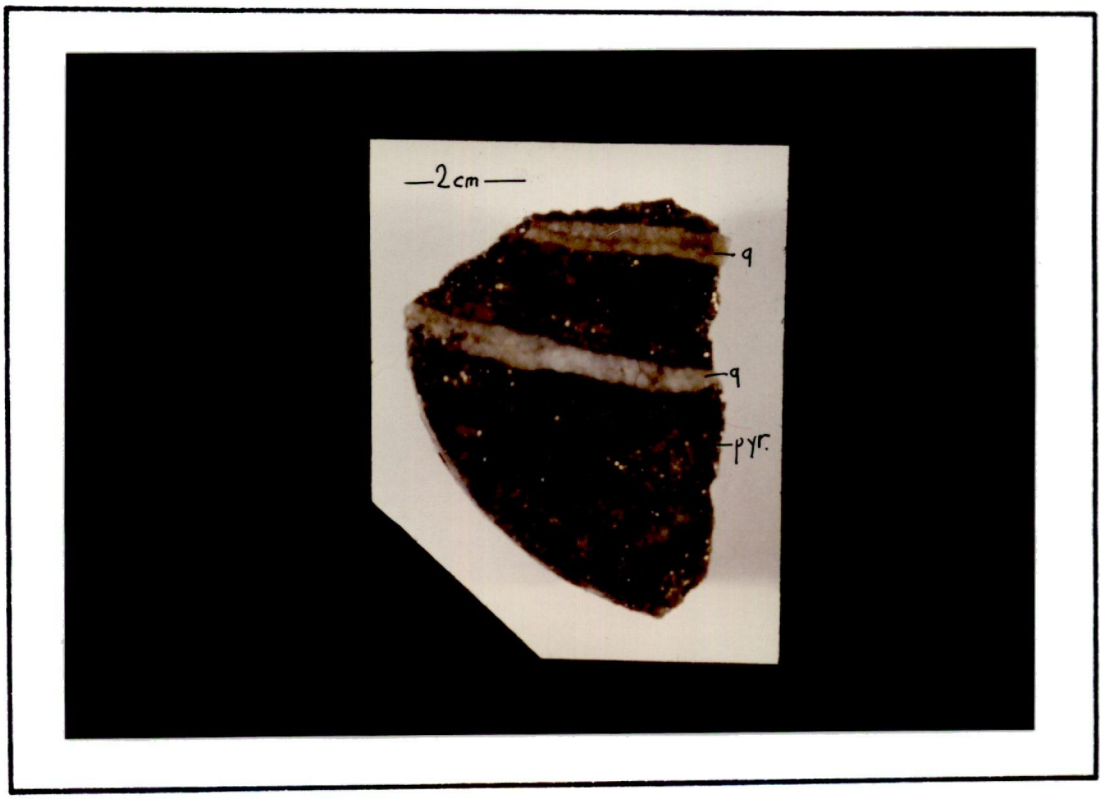

PLATE 6.10: Pyrite, chalcopyrite, quartz veins (Harkkoy mine, borehole 12, 165m)

6.2.5 Bornite

Bornite only occurs in a few specimens, in small quantities, being associated with chalcopyrite, pyrite, sphalerite and covellite and possibly with chalcocite and digenite. The following electron probe analysis, obtained from Harkkoy mine, borehole 14, at 47.55 m, gives the composition of bornite:

Cu_5FeS_4, HRK 14/47.55 m(Wt%)		theoretical (Palache et al,1944)
Cu =	61.76	63.33
Fe =	11.99	11.12
S =	25.44	25.55
Total =	99.19	100.00

As,Sb,Ag,Pb were not detected.

6.2.6 Enargite

According to Ramdohr (1969) enargite has the composition Cu_3AsS_4. As can be partly replaced by Sb although this is generally less than 7 wt%. With a greater proportion of Sb, the composition $Cu_3(As,Sb)S_4$ is reached and the mineral is termed stibioluzonite. The electron probe analyses shown in Table 6.4 reflect compositions near to enargite, for example H7, 25 m (A), based on 4 metal atoms, recalculate to $Cu_{2.92}Zn_{0.01}(As_{0.94}Sb_{0.13})S_{3.84}$. Enargite is only found in a few specimens but occurs in both the massive and stockwork ores, being generally associated with chalcopyrite, sphalerite, galena and tetrahedrite, and, to a lesser extent, pyrite. The grain-size is usually small, averaging 50-60 μ .

6.2.7. Orpiment

Orpiment is either confined to the uppermost part of the massive, black ore, or is found in small patches within the overlying tuffs. Specimen 326, from near to the Harsit-Koprubasi mine, consists of fine orpiment aggregates associated with tuffs. Electron probe analysis gave the following result:

As_2S_3, 326 Wt%		theoretical (Palache et al,1944)
As =	58.58	60.91
S =	40.11	39.09
Pb =	0.209	-
Total =	98.90	100.00

Sb,Ag,Cu,Zn,Cd,Se,Hg,Fe,Mn were not detected.

6.3 Sulphosalt minerals

Tetrahedrite - tennantite and bournonite are the dominant sulphosalts, occurring exclusively in the massive ore. The former, a major source of Ag, produces a level of 416 tons metallic Ag in the massive ore of the Harsit-Koprubasi mine (Acar, 1974). Springer (1969) has shown that the end members of the tetrahedrite - tennantite solid solution series do not usually occur naturally, while Hall (1972) and Yui (1971) have established a positive correlation between the Sb and As contents of the series. Electron probe analyses of material from massive ore horizons, show that the minerals are near to the tetrahedrite-end of the solid solution series, characterised by high Ag contents (Table 6.4). The ratio of chalcopyrite to tetrahedrite-tennantite in the massive ore is close to unity and thus both contribute substantial amounts to the Cu content of the ores.

The sulphosalts have similar textures and grain-size to sphalerite and galena, occurring interstitially, in an irregular form, between the other massive ore constituents. The colours of both tetrahedrite-tennantite and bournonite are very similar (pale greenish) but perfect polysynthetic twin lamellae with bluish-grey polarisation colours enable the latter to be distinguished from isotropic tetrahedrite-tennantite.

6.4 Gold

Gold was noted in one specimen only, from the Harkkoy mine (HRK Borehole 14 at 47.55 m) where it occurs as tiny rounded droplets in silicified tuffs. The gold shows high reflectivity, a whitish yellow colour and has an isotropic character which allows it to be distinguished from associated chalcopyrite.

6.5 Sulphates

6.5.1 Barite

Barite is the major gangue mineral of the massive ore where it occurs, together with quartz. Overlying the massive ore, it becomes the

dominant constituent. This zone may be monomineralic, consisting of minute barite crystals interstratified with the tuffs, or massive barite as seen for example in the roof of the adit forming the entrance to the Koprubasi mine. The thickness of this baritic ore varies from a few cm to a few metres. The mineral commonly forms lenses parallel to the bedding planes of the tuffs.

6.5.2 Gypsum

The presence of gypsum has only been confirmed by extensive X-ray diffraction studies of borehole core specimens from the Harsit-Koprubasi mine; gypsum was not recorded in previous studies by Vujanovic (1974) or Acar (1976). The mineral mostly occurs above the footwall rhyolites, being commonly associated with explosion breccias and silicified tuffs. It is extremely difficult to estimate the thickness or distribution of the mineral since most boreholes do not penetrate to sufficient depth, and the gypsum mainly occurs disseminated or in fine laminations. From studies based on Harsit-Koprubasi borehole cores H3, H44 and H68, the thickness may reach 7-8 m. Megascopically the mineral appears pinkish white, it may have been mistaken for calcite in previous studies. XRD shows that it is well crystalline.

6.6 Carbonates

6.6.1 Dolomite

Dolomite is the most common carbonate mineral. It is occasionally associated with ferroan dolomite and siderite, for example in the Harsit-Koprubasi borehole H24, at 134 m depth, where the carbonates reach 1 m in thickness and occur disseminated in the tuffs and breccias and as small veins. Dolomite also occurs in the massive form near Ketencukuru. Spatially the occurrence of dolomite is similar to that of gypsum in the Harsit-Koprubasi mine, although both minerals never occur in the same hand-specimen.

6.6.2 Malachite and Azurite

These minerals are found within the oxidation zone near the Harsit-Koprubasi mine adit. Malachite shows distinct bireflectance and purplish-grey polarisation colours, with characteristic green internal reflections whereas azurite is characterised by blue internal reflections and a cloudy appearance under crossed Nicols. The presence of both minerals has been further confirmed by X-ray diffraction.

6.7 Oxides

6.7.1 Quartz

Quartz is the principal gangue mineral. It occurs in the early quartz-pyrite veins and, less commonly, in the quartz-pyrite-chalcopyrite veins (Plate 6.10). The mineral is widespread in the extensive silicified envelope surrounding the ore bores where it appears as fine crypto-crystalline aggregates. The quartz veins are usually between a few mm and a few cm in thickness.

6.7.2 Hematite and Goethite

Hematite and Geothite are dominantly associated with hanging wall tuffs and radiolarian cherts. Hematite is only present in a few specimens as discrete blades or laths, otherwise it is mostly altered to goethite, producing the distinct red colouration of the hanging wall tuffs. The term "hematitic beds" therefore implies tuffs and associated sediments which contain both hematite and geothite. The minerals may form lenticular bodies parallel to the bedding planes of the tuffs (e.g. at Harkkoy) or radiolarian cherts (e.g. at the Harsit-Koprubasi mine). Colloform goethite-covellite intergrowths are present occasionally, mainly being associated with pyrite and chalcopyrite.

6.7.3 Manganese Oxides

Mn oxides in the area have either a close time and space relationship to the massive ore deposits or are closely associated with massive ore in time but not in space. The former consist of extremely

fine-grained, earthy, specks of pyrolusite and manganite, in the altered hanging-wall tuffs and cherts. The latter comprise high-grade, hard manganese ores with a botryoidal (Plate 6.11), structure, obviously of colloform origin (Plate 6.12). They occur in the uppermost part of the Lower Volcanic Cycle at the same horizon as the Mn-oxides associated with the massive ore bodies. Under the microscope both varieties comprise a fine, unidentifiable anisotropic mixture. X-ray diffraction studies reveal that the material is poor to well crystalline pyrolusite, psilomelane and minor manganite.

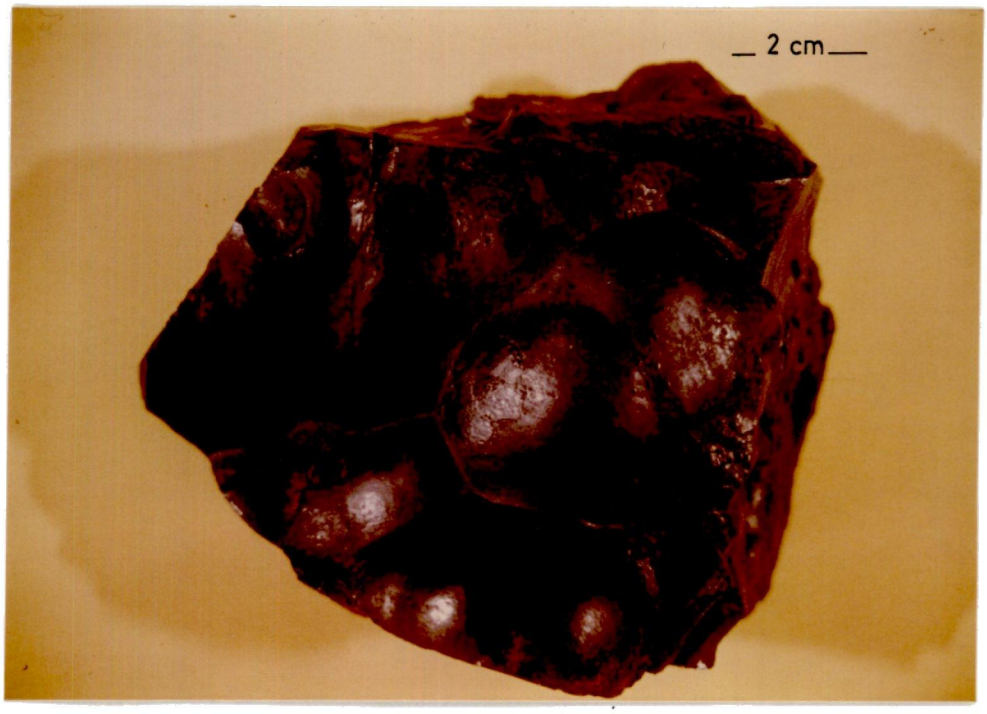

PLATE 6.11: Botryoidal manganese ore (sample 206, northern Harsit river area)

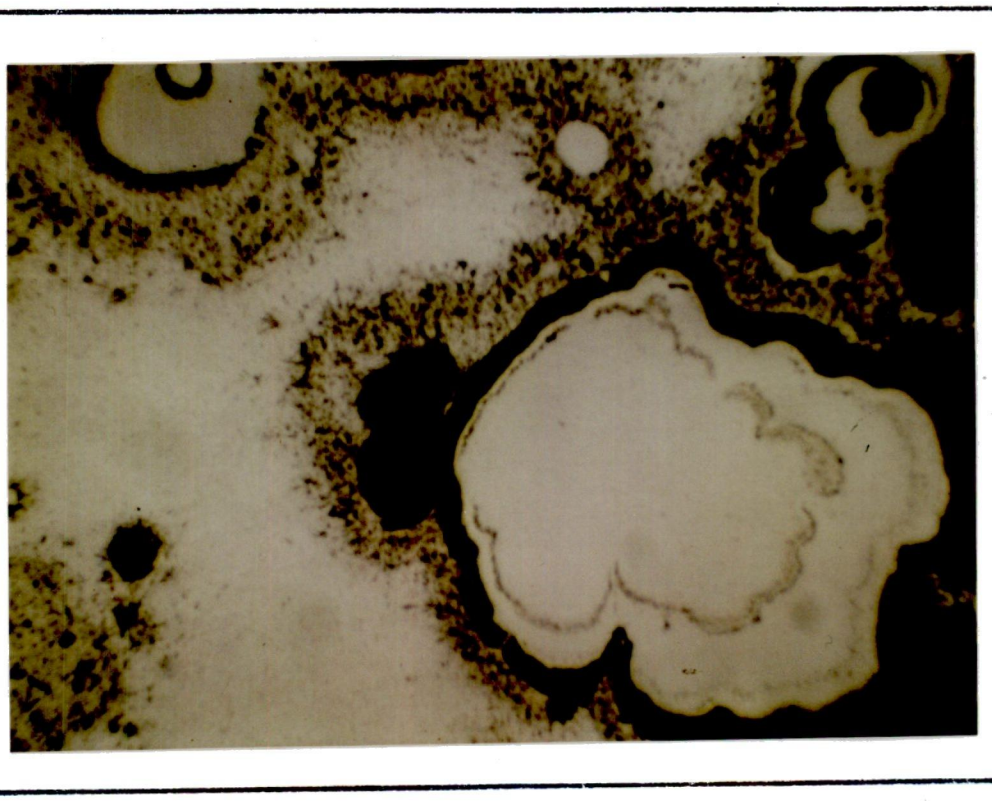

PLATE 6.12: Colloform intergrowth of the botryoidal manganese ore (sample 206, northern Harsit river area) 100X

CHAPTER SEVEN

CHARACTERISTICS OF THE MINERALISING SOLUTIONS

7.1 Introduction

Quantative evaluation of the nature and origins of ore forming fluids has always been a primary target for economic geologists. This chapter, based on the fluid inclusion studies and the patternof hydrothermal alteration, attempts to establish limits for some of the physicochemical parameters of the mineralisation. These include factors such as temperature, pressure and salinity of the mineralising fluids, and some thermodynamic parameters of the ore solutions and their constituent ions.

The use of fluid inclusions, especially in the determination of depositional temperature is particularly justified due to the limited applicability of the pyrrhotite-sphalerite geothermometer, pioneered by Barton and Toulmin (1966), and the restricted use that can be made of the distribution of minor elements between co-existing sphalerite and galena (Bethke and Barton, 1971). Studies based on the latter technique have shown that calculated temperatures scatter over a wide range, and do not agree with data from fluid inclusions. These unreliable data are presumably due to the difficulty in establishing that the sampling is confined to co-existing minerals and in elimination of the effects of post depositional re-quilibrium in the less refractory phase (Nash,1975). Fluid inclusion studies, however, particularly in recent years, have emerged as the most informative and dependable method (Sawkins, 1966; Roedder,1967)

7.2 Fluid inclusion studies

7.2.1 Types of inclusion

Distinctions between primary inclusions, formed at the time of growth of the surrounding part of the crystal, and secondary inclusions have been

given in the literature (Yermakov,1965; Roedder, 1965 and 1967). Inclusions which have grown parallel to crystal planes or to colour banding, and negative crystal shapes, are probably the most important criteria indicative of primary origin. Additionally, according to Roedder (1967), primary inclusions are large and sparsely distributed, while secondary inclusions from the same sample are small and very numerous.

The transparent minerals found in the ore-deposits of the northern Harsit river area are sphalerite, quartz and barite. Only a small number of measurements could be obtained from the quartz and barite, however, as the inclusions were either small and single phase, or unlikely to be of primary origin. Transparent sphalerite, in contrast, mostly yielded good, primary, fluid inclusions.

The fluid inclusions examined here were mainly aqueous inclusions containing a mobile vapour bubble, formed during cooling from the original trapping temperature as a result of thermal contraction of the host crystal and the trapped liquid (Rankin, 1978). The vapour bubble is usually water vapour, although additional volatiles such as CO_2 are sometimes present; the CO_2 appears black. The presence of CO_2 has only been confirmed by heating. Expansion of CO_2 (liquid) to a gas phase takes place rapidly below 31^{o}C on heating (Rankin, op.cit.), this is due to the high coefficient of thermal expansion of liquid CO_2 which is several times greater than that of water. Inclusions containing CO_2 are confined to the sphalerite stockwork ore from the Harsit-Koprubasi mine. Enjoji (1972) has indicated that inclusions of this type represent deposition from a gas phase, or from boiling fluids. They are most probably primary because of their rarity, and may thus represent a period of boiling of the ore fluids during their ascent.

A small number of inclusions contain opaque captive minerals similar to those described by Akinci (1974). Although positive identification of these minerals was not made, Akinci (op.cit.) has indicated

that they are mainly pyrite and chalcopyrite. No daughter salt minerals have been observed in any of the inclusions studied.

7.2.2. Experimental techniques

In order to estimate the homogenisation temperatures and the salinities of the ore forming fluids, disc-wafers of 0.5 to 1mm thickness, polished on both sides, were prepared from the ore and gangue minerals.

Fluid inclusions trapped at temperatures greater than about 70°C contain a vapour bubble at room temperature (Roedder, 1967). The homogenisation technique thus entails reheating the host mineral and its inclusion until the bubble just diappears, and the inclusion becomes a single homogenous phase.

Homogenisation temperatures were determined using a Leitz, model 350 microscope fitted with a 30 ohm, micro-furnace heating stage. The microscope has both UM 20/0.35 and H32/0.60 objectives and a 10X ocular. The current supply is regulated by a Rotary Regavolt rheostat. Temperatures are measured with a chromel-alumel thermocouple read directly on a 5000 series, Comark digital thermometer. The thermocouple was calibrated by heating organic compounds of known melting points; they are listed in Table 7.1. Heating rates during homogenisation varied from 5 °C/min to 1°C/min, as suggested by Smith (1974). Reproducibility of both standards and unknowns is better than $\pm$ 5°C. Some error, however, may be introduced due to the difficulty in estimating the homogenisation temperature in inclusions where the bubble migrates to a darkened corner, thus obscuring the view. This problem was minimised by recording homogenisation temperatures from several inclusions in the same sample. The homogenisation temperature (Th) is generally less than the true trapping temperature (Tt) of the inclusions, requiring a correction for pressure (Δ t) such that $T_t = T_h + \Delta t$.

In preceding sections evidence has been presented which indicates

Compound	Freezing point (^{o}C)
n-Decane	-29.7
Quinoline	-15.9
Benzonitrile	-13.0
Methylbenzoate	-12.3
Bromine	- 7.2
Butyric acid	- 6.5
Demineralised water	0
	Melting point (^{o}C)
Acetoxime	61-62
Benzoic acid	123
P-nitro aniline	147.5
Succinic acid	187
Anthracene	215
Hexachlobenzene	228
Gallic acid	263
Benzene hexachloride	310

TABLE 7.1: Standards used for thermocouple calibration

that sedimentation post dates the mineralisation. The distribution of the mineralisation and its close association with the dacitic-rhyolitic lava, tuff and breccia horizon has suggested that formation of the host rock and the mineralisation are contemporaneous. The effective pressure at the time of ore deposition must be therefore, the hydrostatic pressure resulting from the water column overlying the host rock. The micro-faunas found in the radiolarian cherts and mudstones of the sediments immediately overlying the host rock are pelagic or semi-pelagic. They have been examined by Dr.A.T.S. Ramsay of Swansea University who has identified the fauna as Upper Maestrichtian and suggested that they indicate water depths in excess of 700 m.

The well developed vesicularity in the underlying dacites, basalts and andesites of the Lower Volcanic Cycle may suggest however that the hydrostatic pressure was sufficiently low to allow escape of volatiles.

Further indirect evidence for water depth comes from the homogenisation temperatures and salinities of the fluid inclusions. Data presented by Ridge (1974, Figure 1) indicate that a homogenisation temperature of 228^{o}C coupled with a salinity of 5 wt% equivalent NaCl, the respective temperature and salinity shown by the massive ore, require a confining pressure equivalent to at least 280 m of water if boiling is to be prevented. Since there is no evidence for boiling in the massive ore, the water depth must have exceeded 280 m. The moderate water depths indicated suggest that the direct measurements of homogenisation temperature (Th) may be confidently used without a pressure correction. With depths less than 1000 m the correction is unlikely to be substantially greater than the maximum analytical error of $\pm$ 5^{o}C.

Ore forming fluids are known to be largely NaCl brines (Helgeson, 1964; Roedder,1972). In such fluids the lowering of the freezing point is proportional to the solution concentration (Yermakov,1965). The

salinity of the fluid inclusions, in terms of equivalent NaCl, can thus be found by measuring the depression of the freezing point in the system NaCl - H_2O (Roedder,1962, Figure 4). The temperature at which the last ice crystal in an inclusion remains in equilibrium with the solution is equivalent to the freezing point of the solution.

Freezing experiments were performed on a stage developed in this department by F.W.Smith and described in detail by Smith (1973). Smith suggested the use of dry nitrogen, cooled by passing through a copper coil immersed in liquid nitrogen. Interruption in the supply of dry, cooled nitrogen was, however, found to take place. This resulted from condensation of nitrogen in the copper coil. This effect was avoided by cooling the dry nitrogen in a copper coil immersed in liquid air. Nitrogen cooled in this way was equally effective in quickly producing temperatures of -100°C. A rapid cooling rate was also found to be useful in overcoming metastability in some inclusions. Roedder (1962) had previously noted that many inclusions in sphalerite, with actual freezing temperatures of about -3°C, would not freeze even when held for an hour at -35°C.

Freezing temperatures were recorded as the point at which the last ice crystal disappears during heating of the supercooled inclusions (Rankin,1978). Freezing points were recorded on a 5000 series Comark thermometer, calibrated to 0.1°C and connected to a chromel-alumel thermocouple. The calibrations were made against compounds of known freezing temperatures, listed in Table 7.1., precision from duplicated runs was better than $\pm$ 0.5°C.

7.2.3 Results and discussion

Measurements on primary fluid inclusions from quartz, sphalerite and barite indicate that ore deposition took place over a wide range of temperatures, between 144°C and 298°C. The temperature measurements are

presented in Figure 7.1.

Homogenisation temperatures from the lowermost stockwork ore, composed of pyrite-quartz veins, fall within a narrow range, between 260°C and 298°C, with the mean value of 285°C. They have the highest values found within the ore-bodies. The overlying stockwork sphalerite, occurring beneath the massive black ore, has a mean temperature of 247°C, with a range from 230°C to 272°C. Sphalerite from the massive ore yields a mean temperature of 228°C although barite from the same zone usually has higher temperatures, averaging 249°C. This is a similar relationship to that obtained from inclusions in the Kuroko and Bulancak deposits. (Tokunaga and Honma ,1974; Akinci,1974). The baritic zone, overlying the massive black ore, has yielded the lowest temperatures with an overall average of 175°C.

The temperature data indicate a steep gradient of approximately 12°C/ 10 m from the lower, quartz-rich stockwork ore to the upper baritic zone.

Smith and Phillips (1975) have shown that in the Northern Pennine Orefield, although there is some decrease in temperature with depth, there was no overall relationship between temperature and depth, indeed some samples from the upper part of the veins showed higher temperatures than the same vein at depth. They suggested that the two parts of the veins had been filled laterally from different feeders.

An average temperature gradient of 3 to 5°C/10 m, occasionally rising to 7°C/10 m, has been observed in hydrothermal deposits by Miyazawa (1967). These values are substantially lower than those derived from the present study, although the variation in temperature resembles that in Kuroko ore fluids reported by Tokunaga and Honma (1974) and Urabe and Sato (1978).

A simple mechanism involving interaction of hydrothermal ore fluids with the wall rock cannot adequately explain the steepness of the observed gradient.

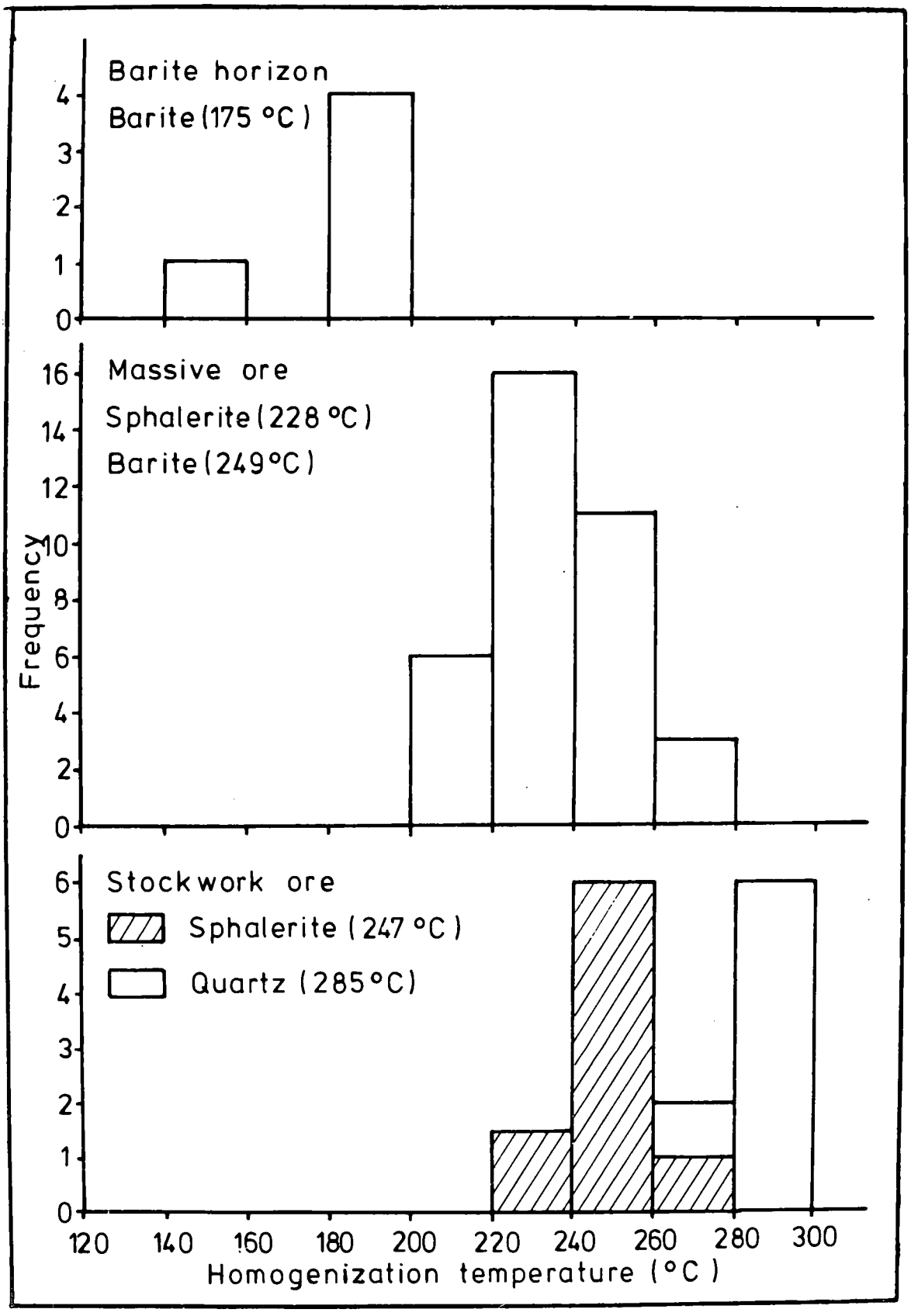

FIGURE 7.1: Homogenisation temperatures for massive sulphide deposits from the northern Harsit river area

Freezing point determinations vary between -1.2 and - 5.4°C, corresponding to salinities of 2.2 and 8.6 wt% equivalent NaCl respectively (Fig.7.2). The variation in salinity is irregular and does not correspond with any known factor such as temperature or depth. The data shown in Figure 7.2 indicate that although some results are similar to the salinity of present-day sea-water, most samples, particularly those from the stockwork sphalerite and uppermost barite zones, have values which are significantly higher. They exhibit similarities to Kuroko ore fluids whose salinities are reported to mostly fall in the range 2.1 and 8.4 wt% NaCl(Urabe and Sato,1978). They differ from the salinities for the hydrothermal fluid responsible for cupriferous Cyprus ore deposits, for which Spooner et al (1976) report the mean and standard deviation of 205 measurements of fluid inclusion freezing points to be -1.9 $\pm$ 0.4°C. This value is identical to the freezing point of -1.9°C for average sea-water and corresponds to a salinity of 3.5 wt% equivalent NaCl. Differences between values derived from the present study and those for the Providencia Pb-Zn deposit studied by Sawkins (1964), porphyry coppers (Roedder,1971) or Mississippi Valley Type ore deposits (White,1968) are more pronounced. In the two former cases, the ore fluids are of magmatic origin, characterised by high salinity and high temperature, whereas the Mississippi Valley Type deposits are of presumed connate origin and are characterised by fluids of high salinity and moderate to low temperature.

From the chemistry of the ore body and its associated hydrothermal alteration, a contribution by magmatic fluids is thought to play an important part in the formation of the ores. It is thus necessary to explain the low to moderate salinities and temperatures. Changes in salinity, and particularly Na/K ratios, have been attributed to various mechanisms. Hirst and Smith (1974) and Smith and Hirst (1974) favour

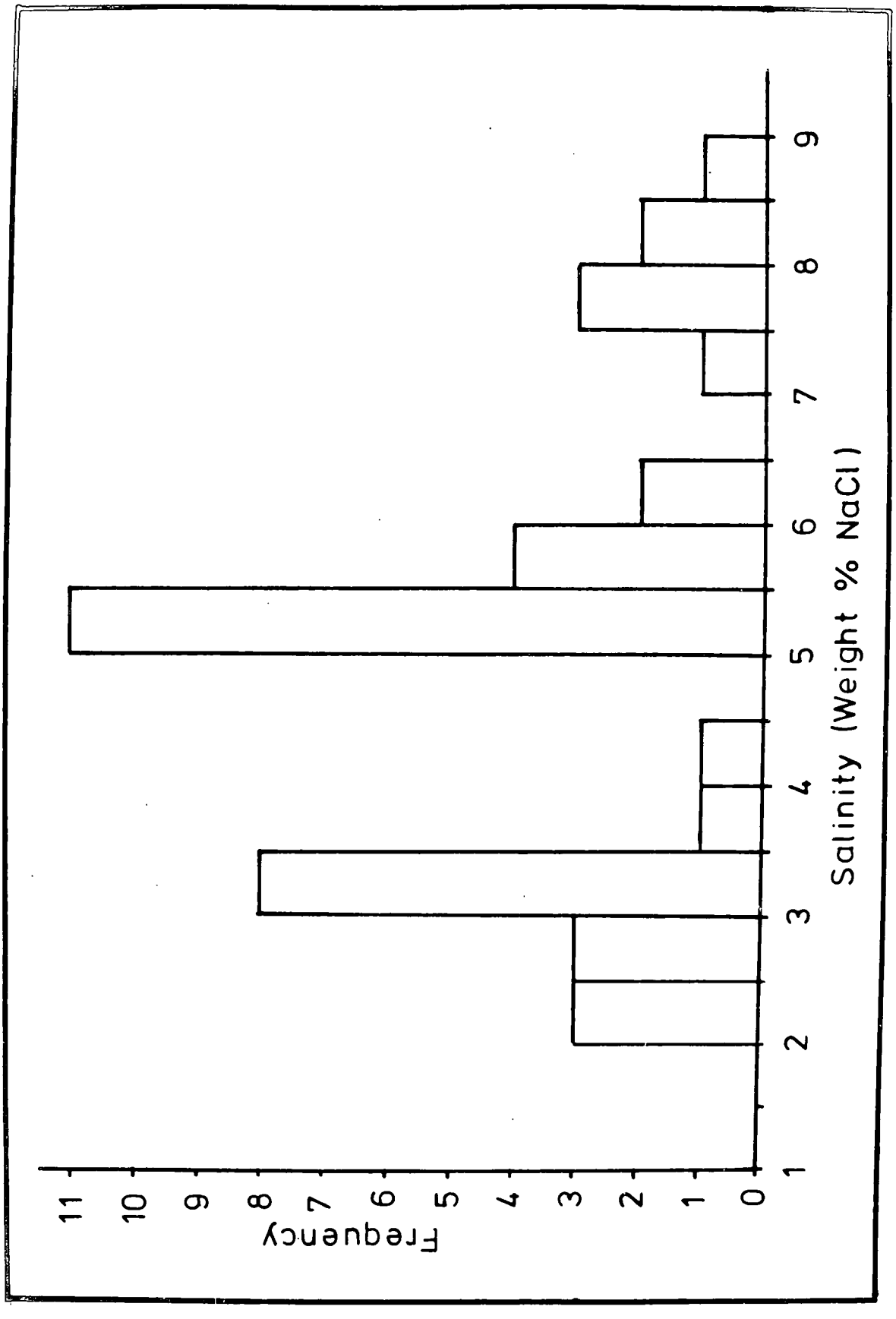

FIGURE 7.2: Salinity data for massive sulphide deposits from the northern Harsit river area

the involvement of connate water with the evaporites in the formation of Mississippi Valley Type deposits. Such mechanisms however, cannot be applied to the present discussion as neither evaporites nor suitable strata containing connate water are present in the region (Gattinger et al, 1962; Goksu et al, 1974).

In recent years geological information on massive sulphide deposits, combined with a study of hydraulics has demonstrated the importance of convective sub-surface flow (Ellis,1967; Corliss,1971; Solomon, 1976 and Solomon and Walshe, in print). Massive sulphide deposits appears to be formed mainly in marine environments (Anderson,1969) and thus the mechanism suggested by Corliss (1971) indicates that the ore-fluids may well be evolved sea-water. As this sea-water comes into contact with rocks and perhaps also mixes with residual magmatic components it gains heat. Corliss (1971, p.8134) states that "the temperature gradients so established drive a convective flow in the vertical fractures which brings fresh sea-water into contact with the rocks and allows these solutions to enter the deep marine environments as submarine hot springs". Kajiwara (1973) and Ohmoto and Rye (1974) have also demonstrated that sea-water is the most likely source for Kuroko ore fluids, as well as for the fluids responsible for the Cyprus ores (Spooner, et al, 1976).

With the information currently available the source of the ore fluids is somewhat speculative. The extensive argillization and the silicification of the host rock, immediately surrounding the ore body are not, in themselves, evidence for magmatic ore-fluids. The abundance of Pb, however, and particularly the Co/Ni ratios and Se contents of the stockwork ore (Chapter 6) do lend more credence to a magmatic contribution. Since the mineralisation is always associated with a thick, submarine pyroclastic pile, it is also important to consider the effects of sub-surface convective cells derived in part

at least, from the hot magmatic liquids which form the rhyolites and pyroclastics. Injection of hot magmatic liquids under the sea bed would establish convective circulation in sea-water trapped within the pyroclastics. The water would tend to be driven upwards and away from the hot rhyolites establishing convective circulation in the overlying and surrounding pyroclastics, the magmatic water mixing with the sea-water.

Barnes and Czamanski (1967), White (1968), Ridge (1973, 1974) have concluded that ascending solutions must essentially behave as a liquid if they are to form a major ore-body. Ridge (1973) has shown that above certain temperatures solutions cannot reach the sea-floor unless the depth of sea-water is sufficient to keep them in the liquid state. If not the solutions would boil at some appreciable depth beneath the sea-floor. Ridge states that "such boiling would result in the precipitation of all constituents of the ore fluids of significantly lower vapour pressure than water. The principal such constituent would be salt and no sulphide deposition". Geological and chemical data presented above suggest that the massive ore formed at or near the sea-floor implying minimum water depths of at least 280 m as discussed previously.

It is perhaps more important to consider the changes which would occur due to the interaction of the ascending hot magmatic fluids with the sea-water. A first consequence would be a steep temperature gradient, emphasised and stabilized by the convective cell. Mixing would also produce intermediate salinities, higher than those of sea-water, but lower than for typical magmatic ore fluids. The change in oxidation state of the ore fluids, necessary to form the colloform textures in the massive ore and supported by the presence of manganese oxides and hematitic beds overlying the latter, might also result from an increasing content of sea-water in the ore fluid within the rising column of the

convective cell. The involvement of sea-water during the formation of massive ore is further supported by the Se content and Co/Ni ratios of the colloform pyrite. The virtual absence of Se, whose affinity is strictly magmatic (Stanton,1972), and the decrease in the Co/Ni ratios towards the massive ore (Chaper 6), strongly support a contribution from sea-water.

As demonstrated above the temperature of the ore body increases downwards, reaching a maximum in the lower quartz-pyrite stockwork ore. Since the hydrostatic pressure of the overlying water column remains the same, the rise in the temperature might result in some boiling during formation of the stockwork ore. This is believed to happen for a short period of time because of the limited distribution of the CO_2 rich inclusions. According to Ridge (1973, p.348) the first minerals to precipitate during boiling would be those low vapour pressure constituents of the fluid, already near to their limit of solubility, mainly the sulphides. Ridge states that "such sulphides might sufficiently fill the openings in the rock through which the fluid was moving to raise the confining pressure above the solution pressure and thus to stop boiling of the ore fluid before it had become saturated with salt". The homogenisation temperatures of the stockwork ore would require a water column of approximately 750 m to prevent boiling (Ridge 1974). Faunal evidence, presented above, supports water depths of this magnitude but a further contribution would result from the lithostatic pressure of the pyroclastics. This would be equal to 2.7 times the hydrostatic pressure of an equivalent column of water (Rankin,1978). A significant degree of boiling would thus be unlikely even in the lowermost stockwork zone.

7.3 Wall rock alteration

7.3.1 Introduction

Wall rock alteration develops as a result of interaction between the

ore forming solutions and the host rock. Thus host rock composition, the initial composition of the ascending hydrothermal solutions, their mixing with the sea-water and their temperature and salinity are important factors controlling the nature of the hydrothermal alteration.

Wall rock alteration patterns are commonly used in ore prospecting. This is particularly exemplified in studies of porphyry-type deposits (e.g. Creasey,1959; Lowell and Guilbert,1970). Wall rock studies are scarce from the eastern Pontids. They are briefly described, for the Lahanos area, by Tugal (1969) and in more detail by Cagatay (1977) for the Madenkoy/Cayeli deposit. The results obtained in this study are closely similar to those reported by Tugal and Cagatay.

Mineral species resulting from hydrothermal alteration were determined by X-ray diffraction analyses, using a Phillips X-ray diffractometer. Minerals have been identified from their characteristic reflections (Tables 7.2, 7.3) following techniques outlined by Thorez (1975,1976), including examination after heat treatment and glycolation. Reflection intensities have been used as a semi-quantiative measure of relative abundances. Meyer and Hemley (1967) have shown that hydrothermal alteration is primarily a metasomatic process involving changes in rocks and mineral composition. Consequently the altered wall-rocks have been chemically analysed by X-ray fluorescence methods. The results of the typical alteration products are presented in Table 7.4.

7.3.2 Hydrothermal alteration patterns

The alteration patterns obtained from both the Harsit-Koprubasi and Harkkoy mines, and other mineral occurrences studied in less detail, exhibit similar characteristics. Individual occurrences therefore are not considered in the text.

Distinction between hydrothermal alteration and weathering must be made since the latter is widespread in the area. Generally, the co-existence of sulphide mineralisation and extensive alteration in many types of ore-

Kaolinite*		Dickite*		Kaolinite H24-133m		Dickite HRK 14-103m	
d°A	I	d°A	I	d°A	I	d°A	I
7.15	10	7.16	10	7.19	10	7.16	10
4.45	4	4.46	0.5	4.45	3	-	
-		4.44	4	-		4.44	3
4.35	6	4.37	4	4.37	5	4.36	2.5
4.17	6	4.27	3	4.17	4	4.29	0.5
4.12	3	4.13	7	-		4.11	3
3.84	4	3.95	2	3.86	3	3.96	1.5
3.73	2	3.795	6	3.71	3	3.79	5
3.56	10	3.587	10	3.58	10	3.58	9
3.36	4	3.427	3	3.35	6	3.43	1
3.138	2	3.272	2	-		-	
3.019	2	3.101	2	-		-	
-		2.938	2	-		2.95	1
2.748	2	2.794	2	2.74	2	2.83	2
2.553	8	2.560	4	2.55	6	2.56	5
2.521	4	2.51	5	2.52	1.5	2.507	5
2.486	9			2.49	7	2.458	1
2.374	7	2.40	1	2.38	6	2.395	3
2.331	10	2.322	9	2.34	9	2.324	7
2.284	9			2.29	7	2.243	0.5
2.182	3	2.122	2	2.20	4	2.194	1.5
2.127	2			-		2.038	0.5
1.985	7	1.975	5	1.98	4	1.973	3
1.935	4	1.937	1	-		-	
1.892	2	1.898	2	-		-	
1.835	4			1.82	4	-	
1.809	2	1.805	1	1.80	3	1.79	2
1.778	5	1.785	1	-		-	
1.682	2	1.686	1	-		-	
1.659	8	1.652	5	1.66	6	1.652	4
1.616	6	1.613	1	-			
1.581	4	1.586	1				
1.539	5	1.555	4	1.54	4		
1.486	9	1.489	5	1.49	8		

* Data from: Douillet and Nicolas (1969)

TABLE 7.2: Comparative data for the kaolinite group minerals

Montmorillonite				Mordenite				Siderite			
ASTM (13-135)		274 (Harsit mine)		ASTM (6-0239)		183 (Harsit mine)		ASTM (8-133) H24-133m; H41-129m			
$d^{o}A$	I	$d^{o}A$	I	$d^{o}A$	I	$d^{o}A$	I	$d^{o}A$	I	$d^{o}A$	I
15.00	10	15.50	10	13.70	5	14.25	4	2.79	10	2.78	10
5.01	6	5.05	3	9.10	9	9.11	7	1.73	8	1.72	5
4.50	8	4.49	8	6.61	9	6.60	6	3.59	6	3.58	8
3.77	2	4.00	2	6.10	5			1.96	3	1.96	3
3.50	1	3.59	3	5.79	5	5.79	4				
3.30	1	3.36	3	4.53	8	4.51	8				
3.02	6	3.01	7	3.76	2	3.77	5				
2.58) 2.50)	4	2.56	8	3.48	10	3.47	10				
				3.39	9	3.36	10				
2.26	1	2.34	3	3.22	10	3.20	10				
1.70	3	1.69	4	2.896	6	2.90	4				
1.50	5	1.50	6	2.560	4	2.57	3				
1.285	2	1.29	3								
1.243	2	1.24	2								

TABLE 7.3: Comparative characteristic reflections for montmorillonite, mordenite and siderite

Table 7.4. Analyses of typical alteration species from northern Harsit river area

Alteration Assemblage	-	-	-	I		II	III		IV	
	1	53	59	H24-134m	H47-27m	H31-138m	HI-66m	H.1	274A	183
SiO_2	70.62	69.61	77.65	34.62	52.51	54.10	57.77	58.75	59.10	71.43
Al_2O_3	14.81	15.07	12.12	26.59	36.05	29.50	26.54	17.25	23.28	11.69
Fe_2O_3	2.59	2.97	1.44	13.73	4.81	1.06	1.05	11.90	2.83	0.96
MgO	0.52	0.33	0.51	2.98	0.07	1.89	2.72	2.54	5.10	0.35
CaO	2.22	3.00	1.61	12.14	0.00	0.06	0.30	1.60	1.47	1.97
Na_2O	2.62	3.96	1.69	0.19	0.00	0.19	1.34	0.01	0.02	1.29
K_2O	3.58	1.22	3.30	0.22	0.00	6.98	6.42	1.67	0.07	1.99
TiO_2	0.32	0.12	0.24	0.83	0.42	0.38	0.29	1.05	0.21	0.20
MnO	0.06	0.11	0.03	0.27	0.10	0.02	0.08	0.29	0.03	0.02
S	0.05	0.03	0.03	0.25	0.08	0.60	0.44	0.01	0.01	0.13
P_2O_5	0.10	0.22	0.09	0.62	0.00	0.03	0.04	0.04	0.02	0.03

1 = Average dacite-rhyodacite (Egin et al., in print); 53,59 = unaltered rhyolites; H24-134m = kaolinite, ferroan dolomite, dolomite; H47-27m = kaolinised tuff; H31-138m = sericitised tuff; HI-66m = Illite, sericite tuff; H.1 = chlorite, illite tuff; 274 = montmorillonite; 183 = mordenite tuff.

deposits has long been sufficient in itself to suggest a possible genetic connection (cf. Meyer and Hemley,1967). In the Harsit-Koprubasi mine, for example, the occurrence of extensively altered host-rock alongside virtually fresh rhyodacite suggests that the alteration is hypogene. The presence of minerals such as dickite is also now established as indicative of a hypogene origin (Deer et al,1962), while it is also believed that montmorillonite cannot form by further weathering of rocks which have already been kaolinised or sericitised during weathering since its formation requires some Mg.

Meyer and Hemley (1967) have proposed a classification of wall rock alteration in order of roughly decreasing hydrogen metasomotism. Their data is based on examples from worked ore-deposits. It is evident that the most important chemical change taking place in the hydrothermal solution relates to the H^+/OH^- balance (Ibid,p.171). Their classification is as follows:

a. Advanced argillic
b. Sericitic
c. Intermediate argillic
d. Propylitic
e. Potassium silicate alteration

Adopting the above framework, the wall rock alteration shown by the ore deposits of the northern Harsit river area may be subdivided into the following assemblages:

I. Advanced argillic alteration: Dickite+kaolinite+ferroan dolomite+ siderite + sericite $\mp$ quartz

II. Sericitic alteration and silicification: Sericite+quartz+illite $\mp$ kaolinite

III. Intermediate argillic alteration: Illite+ montmorillonite$\mp$ chlorite $\mp$ quartz $\mp$ kaolinite

IV. Montmorillonite - zeolite alteration: montmorillonite+mordenite $\mp$ chlorite

The term "assemblage" is used in the sense of Meyer and Hemley (1967), referring to a specific and usually characteristic observed mineral association;

equilibrium between the species is not necessarily implied. As seen from the above classification, kaolinite is present in assemblages I, II and III. Since it can only form in acid conditions, compared to montmorillonite which requires an alkaline environment (Deer et al,1962), equilibrium between the two minerals cannot be attained from the same fluids under the same physico-chemical conditions. Some of the kaolinite is undoubtedly a supergene weathering product, the common weathering of the acid volcanic rocks in the regions being superimposed on the hydrothermal alteration pattern.

Figure 7.3 shows the surface expression of the alteration halos, based on study of Harsit-Koprubasi mine area. The inner zone, in the immediate vicinity of the ore body, is characterised by dominance of sericite* and quartz. This is succeeded outwards by a zone in which illite* becomes the dominant species, usually accompanied by montmorillonite, quartz; chlorite and/or kaolinite may also be present. Montmorillonite and mordenite characterise the inner and outer parts of zone IV respectively, together consituting the outermost part of the alteration halo. Mordenite in particular only occurs some 500 m SWW of the ore-body as shown in the inset on Figure 7.3.

Figure 7.4 shows the vertical change in the alteration products, based on the borehole-core data and available surface samples. Assemblages II and III are essentially the same as those observed in surface samples shown in Figure 7.3. Assemblage I is intercepted in some of the deeper levels of the borehole cores. It is characterised by the occurrence of substantial dickite, ferroan dolomite and siderite. Assemblage IV, as shown in Figure 7.4. is only represented by the montmorillonite-rich assemblage.

---

*Sericite is used here to indicate clay minerals with sharp basal reflections at about $10^{o}A$, $5^{o}A$, $3.33^{o}A$, $2.50^{o}A$ and $2^{o}A$. Illite, however, gives asymmetric basal reflections notably broadened and/or displaced compared to sericite and suggesting the presence of expandable mixed layering according to Suda et al (1962), Kodama (1962) and Shirozu and Higashi (1972).

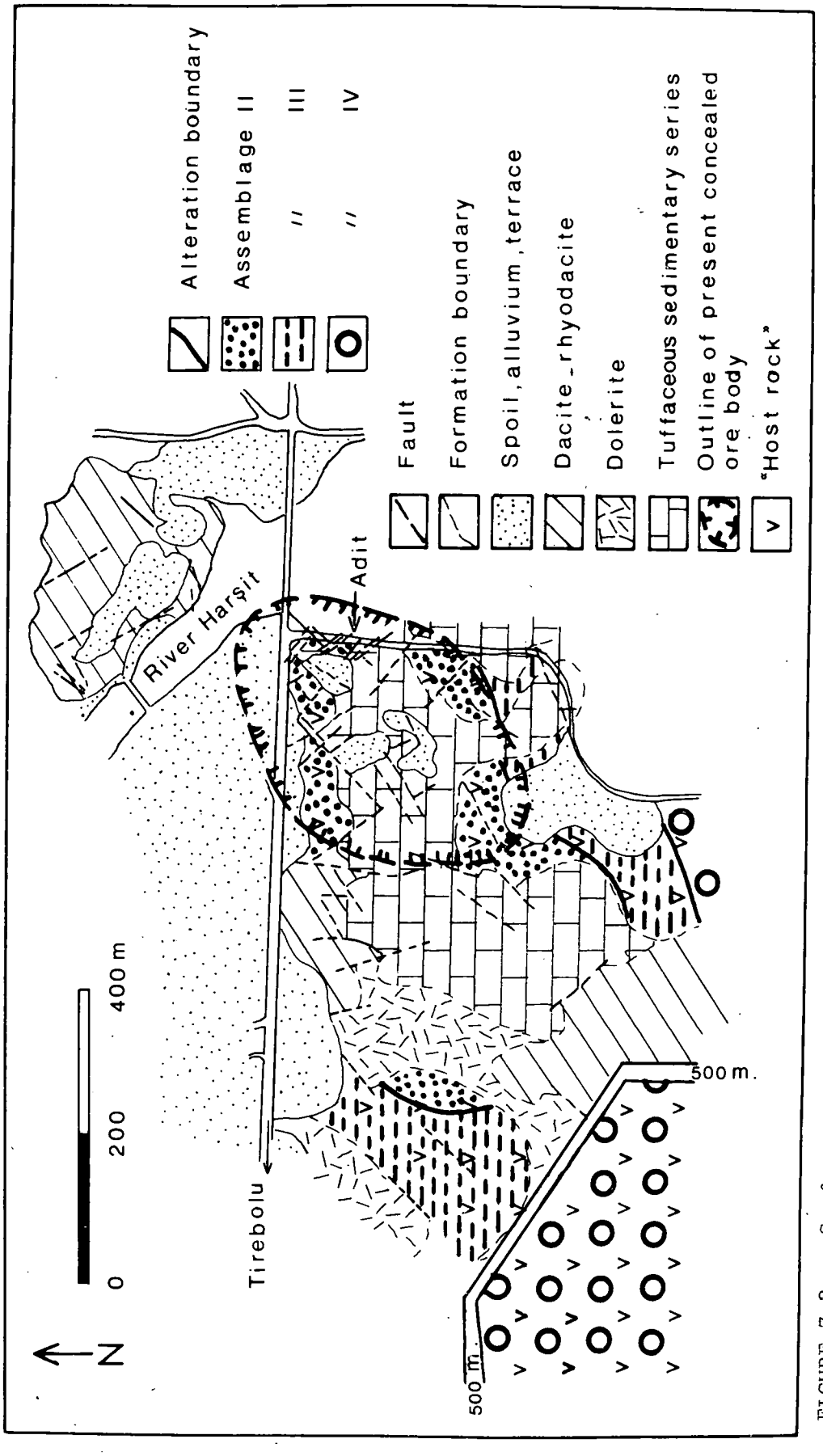

FIGURE 7.3: Surface expression of the alteration halo in the Harsit-Koprubasi mine area

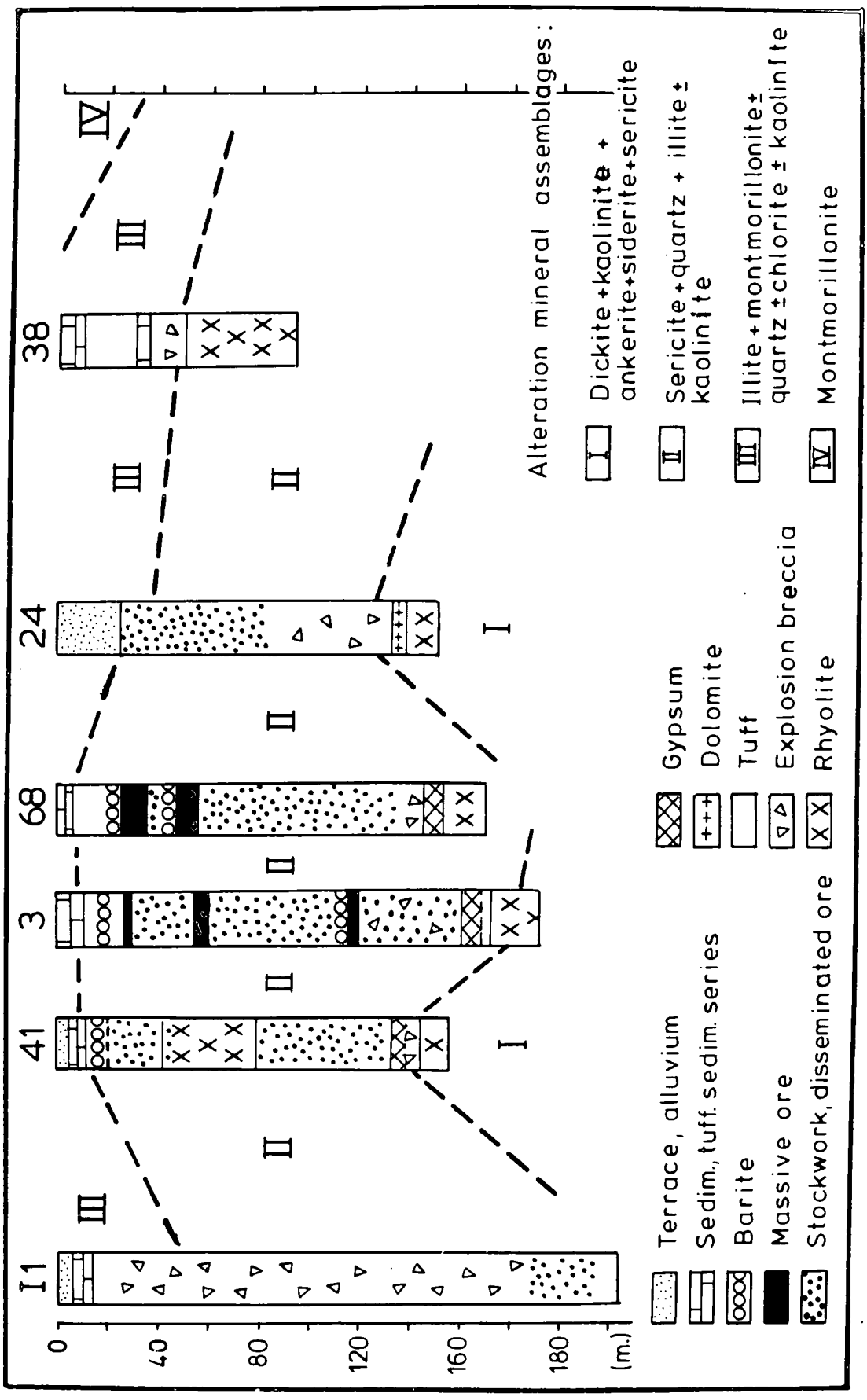

FIGURE 7.4: Vertical expression of the alteration mineral assemblages in the Harsit-Koprubasi mine

The alteration halos described above are present, in part, in the vicinity of the Harkkoy mine and Ketencukuru. Only assemblages I, II and III are present. The absence of assemblage IV may be due to the limited surface outcrops resulting in failure to identify its presence.

7.3.3 Discussion

A distinctive feature of massive sulphide deposits is their association with submarine volcanics. Wall rock alteration from separate deposits show common charactertistics. Rocks above the ore bodies show little or no alteration, whereas rocks underlying and enclosing the deposits are exensively altered, usually forming well developed halos. The size of such halos may extend to 1200 m laterally at the same stratigraphic horizon, and up to 450 m below the ore, as observed in the Brunswick No:12 deposit, in Canada (Goodfellow,1975; Govett and Goodfellow, 1975). Similar results have been obtained from the Japanese Kuroko deposits with 2000 m of lateral alteration being accompanied by approximately 600 m in the vertical sense, (Utada et al,1974). Data obtained from the Pontid deposits, for example at Cayeli (Cagatay,1977), and in the study area, have yielded halos of smaller dimensions. This may be due, in part, to the lack of widespread drilling and perhaps more significantly to the limited exposures of the host rock.

Although the size of the alteration halos of the Canadian and Japanese deposits are similar. Sangster (1962) first noted the difference between the alteration products of the respective deposits. Footwall alteration in the Canadian deposits is predominantly characterised by Mg metasomatism (Chloritisation), whereas in most Kuroko deposits the footwall is silicified and sericitized (Lambert and Sato,1974). In this respect the Kuroko deposits are similar to the deposits from the eastern Pontids. Because the rocks and ore in the two types of deposits are separated by about 300 b.y., Sangster (1972) suggested that the

difference was related to "fundamental and long term changes in earth chemistry whereby volcanic related hydrothermal solutions may have changed in time". Large (1977,p.570), however, proposed an alternative explanation, that the observed differences are a function of differences in evolved sea-water chemistry during recycling in basic and felsic volcanic rocks. The former would probably generate evolved sea-water solutions enriched in Mg^{++}, Fe^{++} and Ca^{++} with lesser amounts of K^{+} and Si^{4+}, whereas recyling in felsic volcanic rocks would probably generate evolved sea-water solutions enriched in K^{+} and Si^{4+} but generally depleted in Mg^{++} and Ca^{++}. Although such a difference would probably arise from sea-water recycled in mafic and felsic volcanic rocks, there is no appreciable difference between the host rocks in Canada and Japan. Sinclair (1971) noted that "the massive sulphide deposits characteristic of the Noranda area occur predominantly in the felsic volcanics", this being analogous to their Japanese and Pontid counterparts.

The data shown in Table 7.4, and presented by Egin et al (in print), clearly demonstrate that neither the volcanic rocks in general, nor those in the alteration halo in particular, are depleted in Mg^{++}, in fact there is an increase in the MgO content of the pyroclastics in the halo zone, particularly in the illite and montmorillonite dominated assemblages III and IV. During evolution of the hydrothermal system Mg^{++} leaching of the volcanic rocks thus does not seem to have been an operative mechanism. Table 7.4 suggests that Ca^{++} and Na^{+} are strongly depleted in the halo zone while K^{+}, Mg^{++} and probably Al^{3+} are enriched relative to surrounding rocks of the same bulk petrography. Table 7.4 also shows that Mg^{++}, Ca^{++} and possibly Na^{+} increase, while K^{+} decreases outwards from the ore body, in assemblages I to IV. It is thus evident that fixation of Mg^{++} into montmorillonite, illite (and chlorite) took place in the outermost

part of the halo where sea-water was probably the dominant mineralising agent. The Mg^{++} was probably thus derived from circulating sea-water, under favourable pH conditions. In contrast the deficiency of K^{+} in these assemblages and its enrichment in the inner sericite zone implies that K was supplied from the ascending magmatic hydrothermal solutions. Na^{+} and Ca^{++} were leached by the circulating sea-water and/or ascending hydrothermal solutions, and fixed into mordenite and Na-montmorillonite, and gypsum, dolomite(and ankerite) respectively. The occurrence of gypsum towards the base of the stockwork zone is interesting. This occurrence could result from a decrease in $CaSO_4$ solubility resulting from increase in temperature in the descending part of a convective cell. $CaSO_4$ solubility has been shown to decrease with increase in temperature of the solution, by Blount and Dickson (1973).

Fields of formation of the alteration products, together with various sulphide assemblages, are given by Meyer and Hemley (1967, p.220). The stability fields of the observed alteration products are well within the temperature ranges obtained by the fluid inclusion study. The stability fields are, however, strongly dependant on the pH of the solution from which they formed, thus assemblages should yield valuable information on the pH of the depositional environment.

The formation of kaolinite and illite/sericite in the same assemblage generally requires moderately high temperatures of 250°C to 350°C and acid conditions with a pH of 3 to 5 (Cagatay,1977). Utada et al (1974) suggest that sericite can form under less acid conditions, between pH 5.2 and 6.1, but that slightly alkaline to alkaline conditions, coupled with a low temperature are required for the formation of montmorillonite (pH 8.8 to 8.9) and mordenite (pH 8.3 to 9.5). It is also necessary to have sufficient Mg^{++} and a low K^{+} content to form montmorillonites (Deer et al,1972).

The alteration halos shown in Figure 7.4 clearly demonstrate the outwards progression from assemblage I through to assemblage IV. Figure 7.1 shows a decrease in temperature in the same direction. A combination of this data and the chemical variation given above suggest that assemblages I and II were formed by the interaction of hydrothermal solutions with the volcanics in the lowermost part of the pyroclastic pile, where the circulation of sea-water was limited. Upwards and outwards however, the pH of the solutions increased and the temperature decreased through interaction with sea-water. These conditions favoured the formation of illite, montmorillonite and mordenite, the process being accompanied by an increase in Mg^{++} and decrease in K^{+}. Figure 7.5 attempts to summarise the variation in diagrammatic form.

The ore fluids responsible for mineralisation in the study area are thought to be a mixture of magmatic water and sea-water. The magmatic fluids are epigenetic relative to the host rock pyroclastics although both were possibly derived from the same source and are closely related to the rhyolites.

The major physico-chemical changes occurring during the ore deposition are a decrease in temperature and an increase in the pH and in the oxidation state of the ore forming solutions.

Thus, once again, support is given to the statement made by White (1968,p.701); "Most ore deposits are formed by complex rather than by simple end-member processes; the water, the dissolved salts, metals, sulphides and other critical constituents of each deposit may be derived from two or more sources".

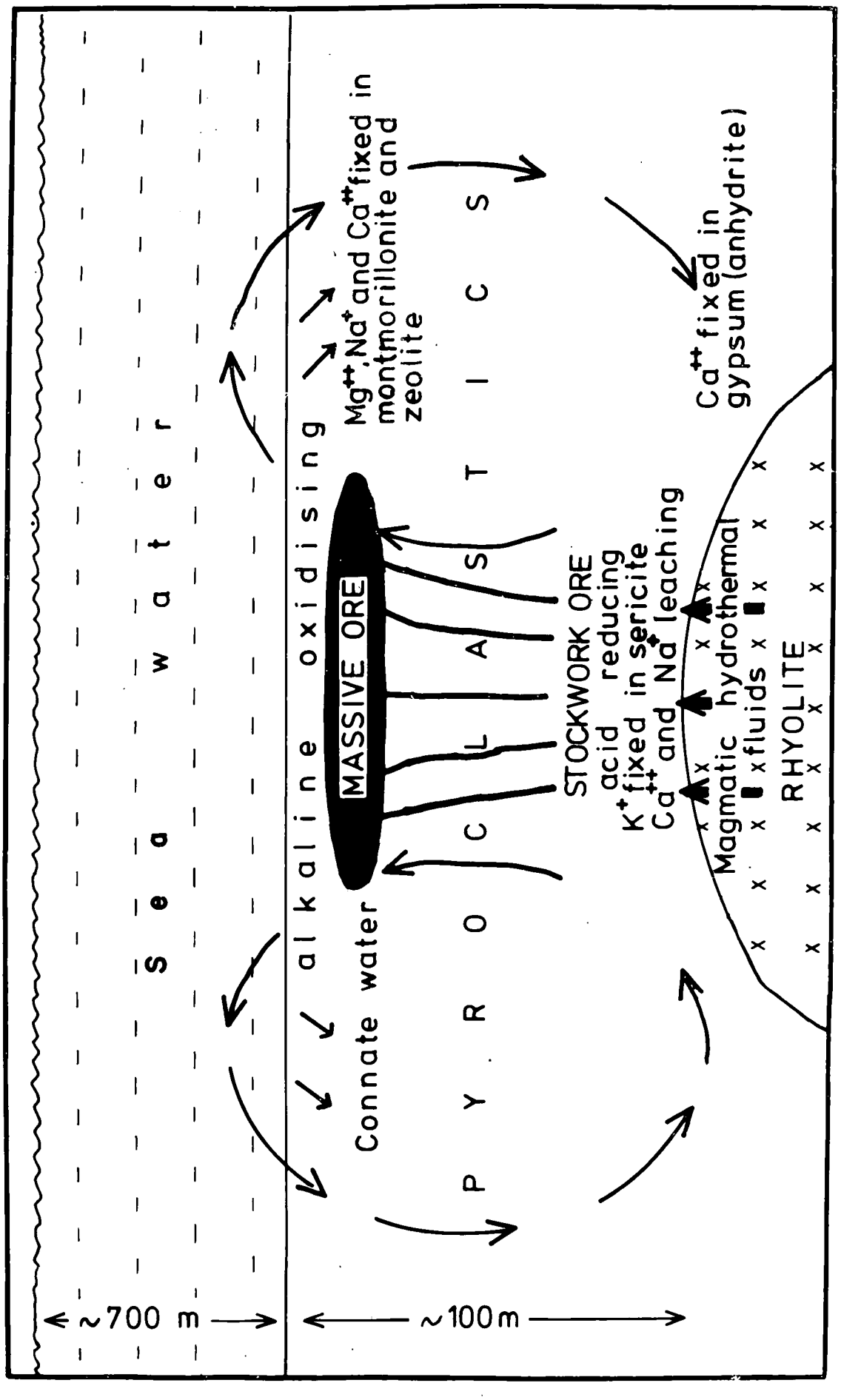

FIGURE: 7.5: Idealised diagram showing the physico-chemical changes occurring during ore deposition

CHAPTER EIGHT

LITHOGEOCHEMICAL EXPLORATION

8.1 Introduction

Volcanogenic sulphide deposits may be simply defined as a genetic class closely related to volcanism and volcanic processes. A pronounced characteristic of the strata-bound, massive ore bodies is their association with specific horizons of the volcanic cycle. As a consequence of this, and the shallow dip of the volcanics, the ore bodies usually do not have a surface outcrop and may be termed "blind ores".

Deposits of this kind, which occur in both the older and recent volcanic terrains of the world, are important producers of base and precious metals. For example, of the total Canadian metal production in 1971, 80% of the Zn, 39% of the Cu, 68% of the Pb and 62% of the Ag together with significant amounts of Au, came from this type of mineralisation (Sangster and Scott,1976). Vokes (1976) reported that the Caledonian massive sulphide deposits play an important part in the Norwegian metal mining industry. The younger volcanogenic deposits which occur in Turkey and Japan also supply substantial amounts of the total domestic metals production of these countries. In Turkey most of the Cu, Pb, Zn, Ag and Au come from the Murgul, Ergani, Kure and Lahanos deposits, whereas in Japan, in 1972, Kuroko deposits supplied approximately 45% of Japan's domestic production of Cu, 26% of its Zn, 33% of its Pb, 31% of its Ag and 20% of its Au (Lambert and Sato,1974).

Despite the importance of the deposits, applied geochemistry has played only a relatively minor role in exploration. Cameron (1975) considers that there are two reasons for this. The first is that the ore bodies are small and dispersed mineralisation of the host rock is not extensive. Thus the exploration target is relatively small. Secondly, in the area of Canada considered by Cameron, the volcanics are covered, in

many places, by thick, impermeable glacial sediments. In Turkey and Japan the ore bodies and the productive horizons, are overlain by thick volcano-sedimentary formations.

8.2 Geochemical exploration for massive sulphide deposits

Until recently exploration for this type of deposit was mostly based on "the tracing of the horizon bed" (Maruyama,1967), in conjunction with advanced drilling methods. In Japan, mining companies have drilled a total of 125 miles of exploration holes per year in the Hokuroko district, with another 20,000 metres being drilled by the Geological Survey of Japan for the purpose of clarifying geological structures (Maruyama,1967).

In the last one or two decades, as a result of detailed studies of primary geochemical halos, certain elements have been found to be useful pathfinders or geochemical indicators of blind, massive sulphide deposits.

Ovchinnikov and Baranov (1971) have shown that the polymetallic Rudnyy Altay and northern Armenia deposits are characterised by the presence of Zn, Pb, Ba and Ag as typical indicators in the overburden. Co, Mo and Bi are conversely found to be typically enriched in zones underlying the ores.

A lithogeochemical survey of the acid, porphyry rocks of the Proterozoic Bear Province, Canada, undertaken by Garrett (1975), showed that the distribution pattern of Cu and Zn was related to known mineral occurrences. Additional areas of anomalous metal concentrations are possibly related to as yet undiscovered mineral occurrences. The study of Cameron (1975), in the Canadian Shield, revealed that the S content of intermediate and acidic volcanic rocks associated with massive sulphides is significantly higher than for barren sequences. There is also a slight to moderate increase in the Zn content of volcanic rocks hosting the Zn-Cu type of massive sulphide ore deposit. Goodfellow (1975) has studied the Brunswick No.12 deposit in Canada and demonstrated that Mn,

Mg and Fe markedly increase, while Ca and Na decrease, in the intensely altered zone immediately adjacent to the mineralisation. Mg and Fe were, further, found to increase and Ca to decrease in the geochemical halo zone which extends some 1500 ft below the deposit and 1500 ft laterally, both to the north and south.

The distribution of minor elements in some altered zones of Japanese Kuroko deposits, has led Ishikawa et al (1962) to conclude that Ag, Cu, Ni, Ba, Cr, V, Co and Pb decrease regularly with distance from the ore body and may efficiently be used as geochemical indicator elements. The primary dispersion of Mn, Zn, Pb, Ag, V, Co, Ba, Bi, Mo and Ni in the tuffs and of Mn, Ni, Zn, V, Mo and Co in dolerite overlying the Shakanai massive ore is also well established by Shiikawa and Tono (1972). Data from the Matsumine and Fukuzawa mines in Akita prefecture has revealed that Ag and Mo decrease gradually with distance from the ore zone. Ba is not only high in the main ore zone but also in the overlying lithic tuff where it is accompanied by Fe. The Fe enrichment was assumed to be due to pyrite mineralisation (Shiikawa et al,1975, Figure 8). Enrichment of Zn, Cu and Pb is also pronounced in the host rock immediately overlying the massive ore.

An early, applied geochemical study in the eastern Pontids was the geobotanical survey conducted by Pollak (1962 , cited in Tugal , 1969). Pollak was able to demonstrate the presence of a secondary Cu anomaly over the Lahanos pyritic, massive, ore body. Lithogeochemical investigation of the dispersion of 25 elements, however, showed that in the same area ".....primary geochemical anomalies are of doubtful value as indicators of the exact location of economic mineralisation" (Tugal,1969, p.130). Cagatay (1977) investigated the Cayeli area and showed that F, As, Pb, Zn and Cu have primary halos, with high anomaly contrasts, in the host rock around the mineralisation. Cagatay suggested that the

concentrations of the geochemical indicators increased significantly in the direction of massive sulphide mineralisation and thus could be used as directional vectors during drilling programmes.

8.3. A lithogeochemical survey in the Harsit-Koprubasi mine area

8.3.1 Method of Study

115 surface samples and 17 near surface samples from borehole cores, located within an area of 1000 m x 800 m were chemically analysed by X-ray fluorescence methods for Si, Al, Fe (total), Mg, Ca, Na, K, Ti Mn, S, P, Ba, Nb, Zr, Y, Sr, Rb, Zn, Cu, Ni and Cr. The analytical techniques and data are presented in Appendix 1.

The object of this study was to establish the chemical variation in the lithological units hosting, and overlying, the ore body, thus providing information which would allow localisation of the mineralisation within the altered halo. In chapter 7.3. the general features of the alteration halo have been described with Mg, Ca and possibly Na increasing while K decreases outwards from the ore body.

Beus and Grigorian (1977) have suggested that primary geochemical halos are detected and delineated with the help of conventional techniques which are based on comparisons between the areas being studied and the background distribution parameters of the element. In order to calculate these parameters, and to determine the minimum anomalous content of a given element, selected background areas were chosen for every lithological unit mapped in the area. To avoid possible contamination from the mineralisation, these background areas were chosen remote from known mineralisation, care being taken to ensure that they were indeed free from mineralisation.

Hawkes and Webb (1962) have indicated that values greater than $\bar{x}$ + 2 s.d.(mean + 2 standard deviations) but less than $\bar{x}$ + 3 s.d. may be regarded as the lower limits of anomalous concentration. Siegel (1974, p.210) also pointed out that although a figure of $\bar{x}$ + 1 s.d. could be taken as the background value, the value of $\bar{x}$ + 2 s.d. more accurately

reflected the limit of regional and local fluctuations, the threshold. Values corresponding to $\bar{x}$ and 2 s.d or values above this, must thus be considered as anomalous. The threshold values ($\bar{x}$+2 s.d) of each lithological unit are shown in table 8.1 and, in order to emphasise the magnitude of the anomalous values, arbitrary levels of $\bar{x}$ + 5 s.d and $\bar{x}$ + 20 s.d. are also shown. Siegel (1974) has suggested that too few intervals can hide important charactertistics in the distribution while too many intervals can also obscure the true details of a distribution. Choice of optimum interval is difficult.

8.3.2 Primary halos in units overlying massive ore bodies

Ovchinnikov and Baranov (1971) have noted that the relative size of the halo produced by a particular element depends significantly upon the concentration of that element in the ore. The distribution of the elements S, Ba, Cu and Zn and of Fe and Mn are plotted in Figures 8.1 to 8.6. The former group are the most abundant elements of the polymetallic ore bodies while Mn (and Fe) represent the last exhalates of volcanogenic activity in a marine environment (c f. Whitehead,1973; Russell,1974).

Figures 8.1 to 8.6 show that two conspicuous geochemical halos are present. Anomaly A occurs over the known Harsit-Koprubasi deposit, described in Chapter 5. A second halo, anomaly B, is present however, for all elements, situated approximately 400 m S.W. of the adit and beyond the outline of the concealed deposit. It is important to note that, although both occur in the same stratigraphical unit, data for individual samples indicate that the two anomalies are not connected but are separate and dicrete. Evaluation of these halos is based on the abundance of the anomalous samples for most of the studied elements. The occurrence of anomalous samples for a single element is disregarded and may be due to possible contamination. This is well exemplified near Kaan T. where the Upper Volcanic Cycle rhyodacites (RYD), Figures 8.3. and

Table 8.1: Background (threshold) and anomalous concentrations for each lithological unit from northern Harsit river area

	S(%)				Ba(ppm)				Cu(ppm)				Zn(ppm)				Fe_2O_3* (%)				Mn(ppm)			
Lithological unit	1	2	3	4	1	2	3	4	1	2	3	4	1	2	3	4	1	2	3	4	1	2	3	4
Sedimentary Series (Radiolarian cherts and mudstone)	0.09	0.39	0.84	3.09	91	231	441	1491	8	32	68	248	18	64	133	478	1.63	3.47	6.23	20.03	228	684	1368	4788
Rhyolite and rhyolitic pyroclastics (Host rock)	0.05	0.09	0.15	0.45	209	481	889	2929	7	31	67	247	30	64	115	370	1.82	2.36	3.17	7.22	251	575	1061	3491
Dacite (Lower Volcanic Series)***	0.05	0.11	0.20	0.65	559	843	1269	3399	1	7	16	61	30	50	80	230	2.59	3.83	5.69	14.99	464	924	1614	5064
Rhyodacite (Upper Volcanic Series)***	0.06	0.14	0.26	0.86	1227	1735	2497	6307	0	7**	16**	61**	23	75	153	543	1.74	3.26	5.54	16.94	230	370	580	1630
Andesites (Lower Basic Series)***	0.07	0.19	0.37	1.27	366	520	751	1906	15	55	115	415	82	132	207	582	7.23	10.77	16.08	42.63	1161	2245	3871	12001
Dolerites (Upper Basic Series)	0.14	0.30	0.54	1.74	1217	1651	2302	5557	95	205	370	1195	65	101	155	425	8.55	11.93	17.00	42.35	1161	1621	2311	5761

* Total Fe expressed as Fe_2O_3

** Arbitrary limits of dacite are used

*** Data from Egin et al. (in press)

1: Mean value ($\bar{x}$)

2: Mean + 2 standard deviations ($\bar{x}$ + 2 s.d.)

3: $\bar{x}$ + 5 s.d.

4: $\bar{x}$ + 20 s.d.

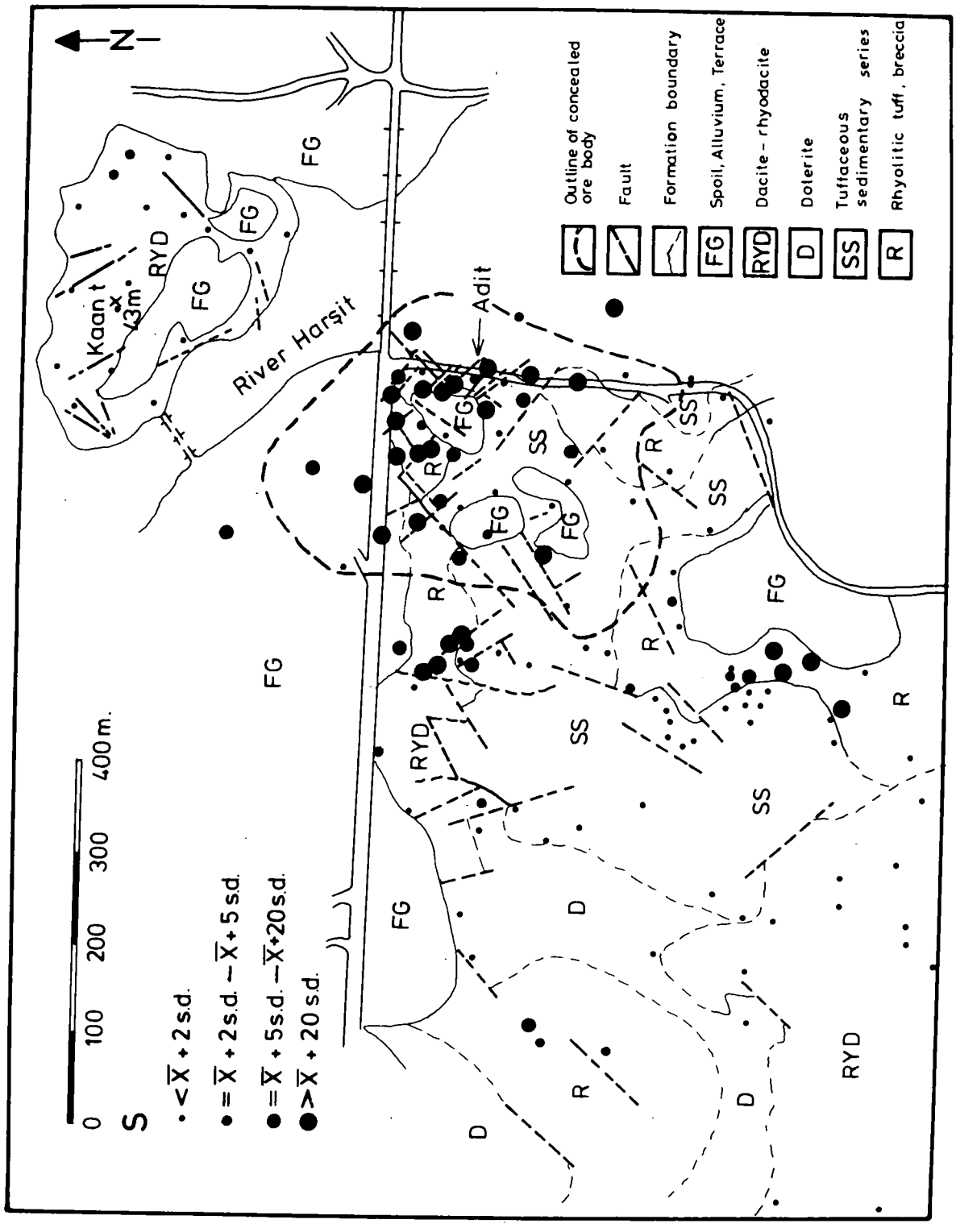

FIGURE 8.1: Distribution of S in the cover rocks in the Harsit-Koprubasi mine area

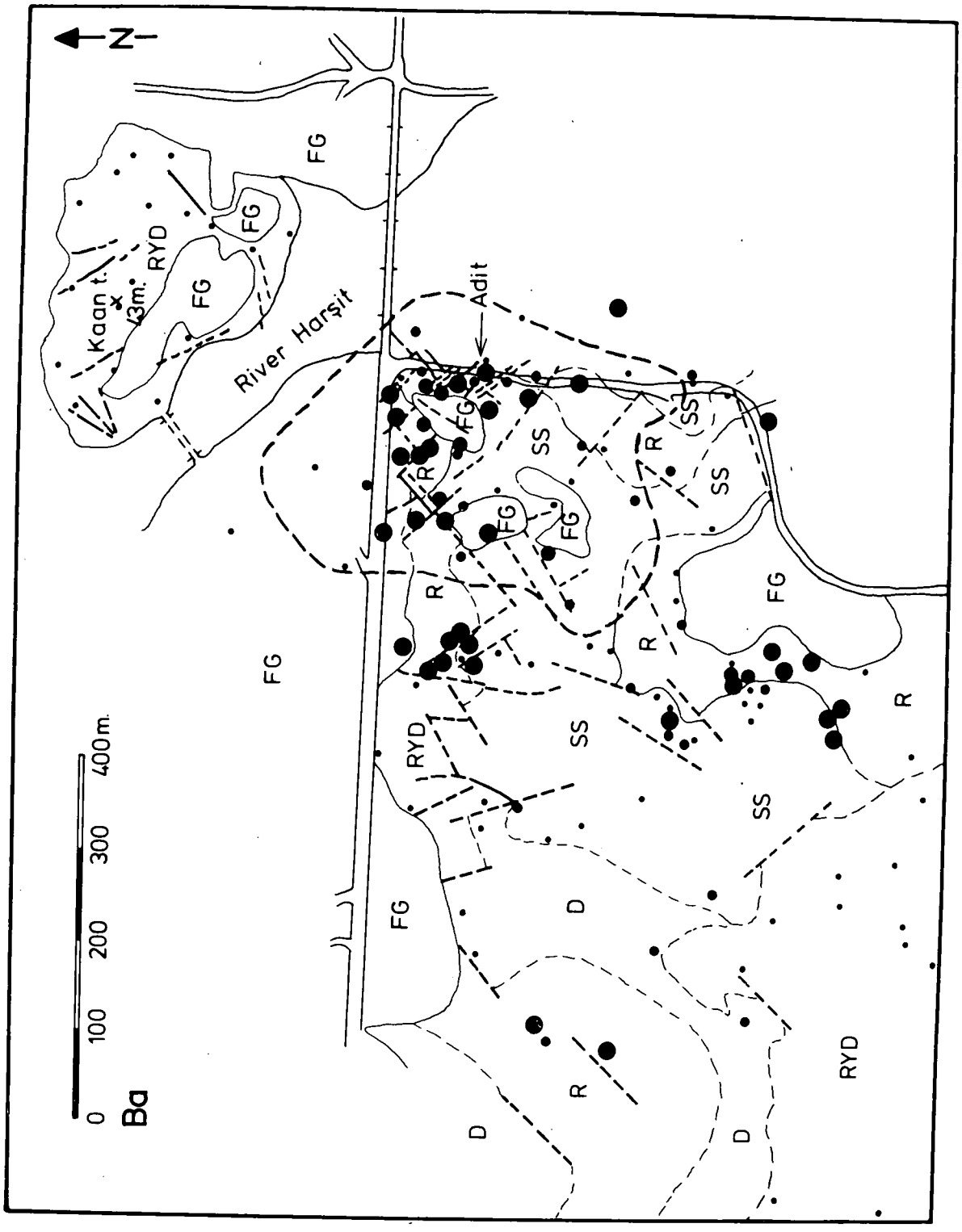

FIGURE 8.2: Distribution of Ba in the cover rocks in the Harsit-Koprubasi mine area (Symbols as in Figure 8.1)

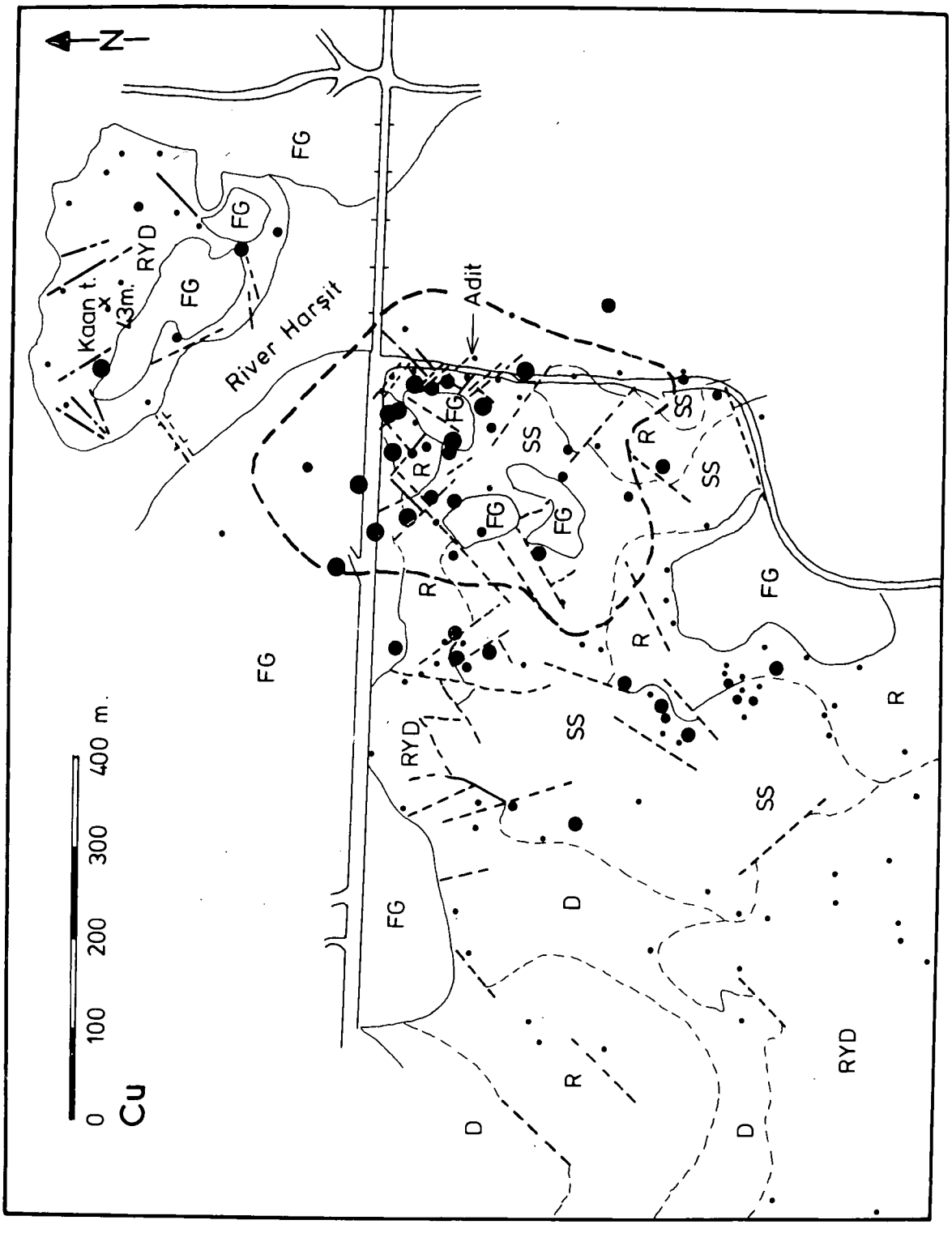

FIGURE 8.3: Distribution of Cu in the cover rocks in the Harsit-Koprubasi mine area (Symbols as in Figure 8.1)

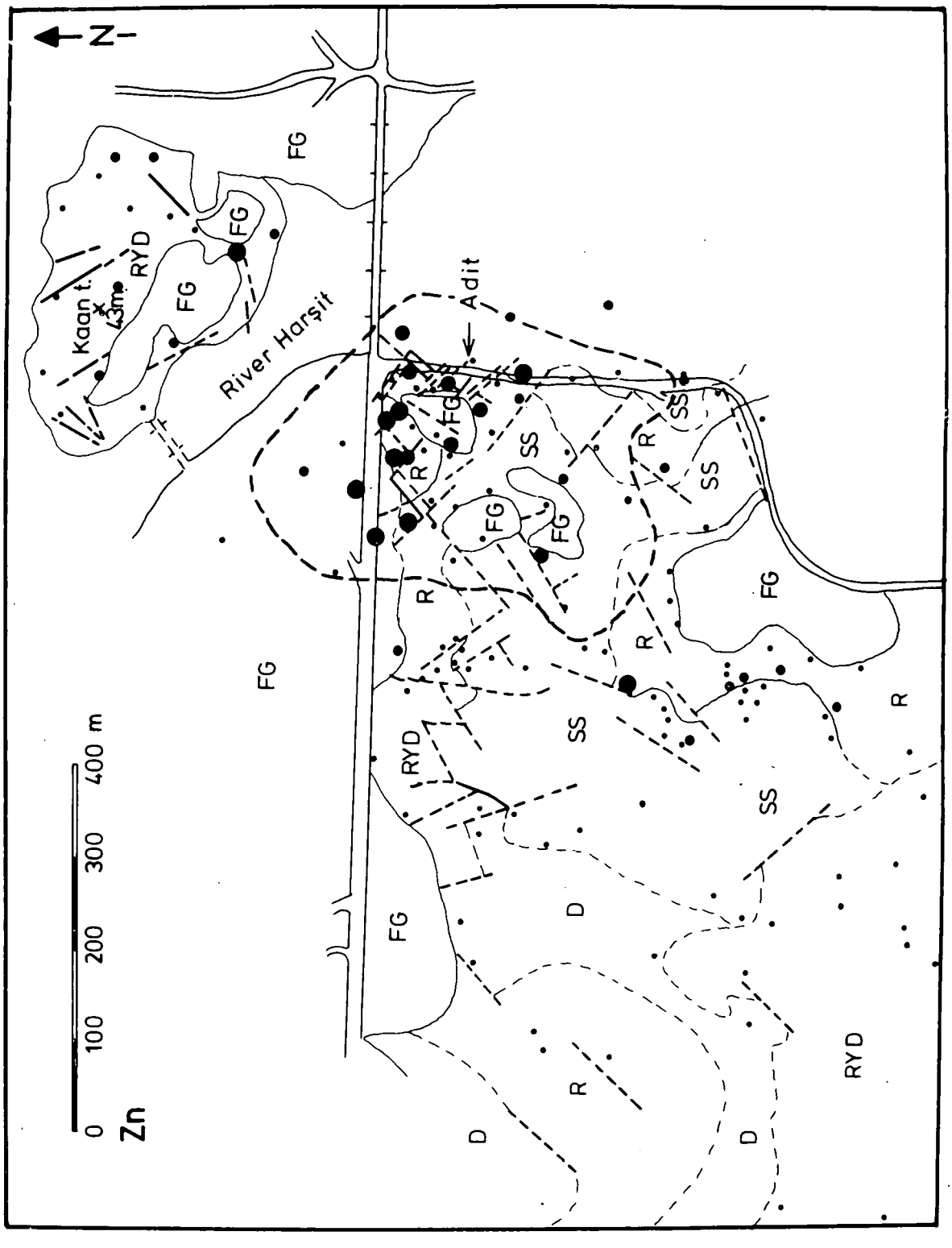

FIGURE 8.4: Distribution of Zn in the cover rocks in the Harsit-Koprubasi mine area (Symbols as in Figure 8.1)

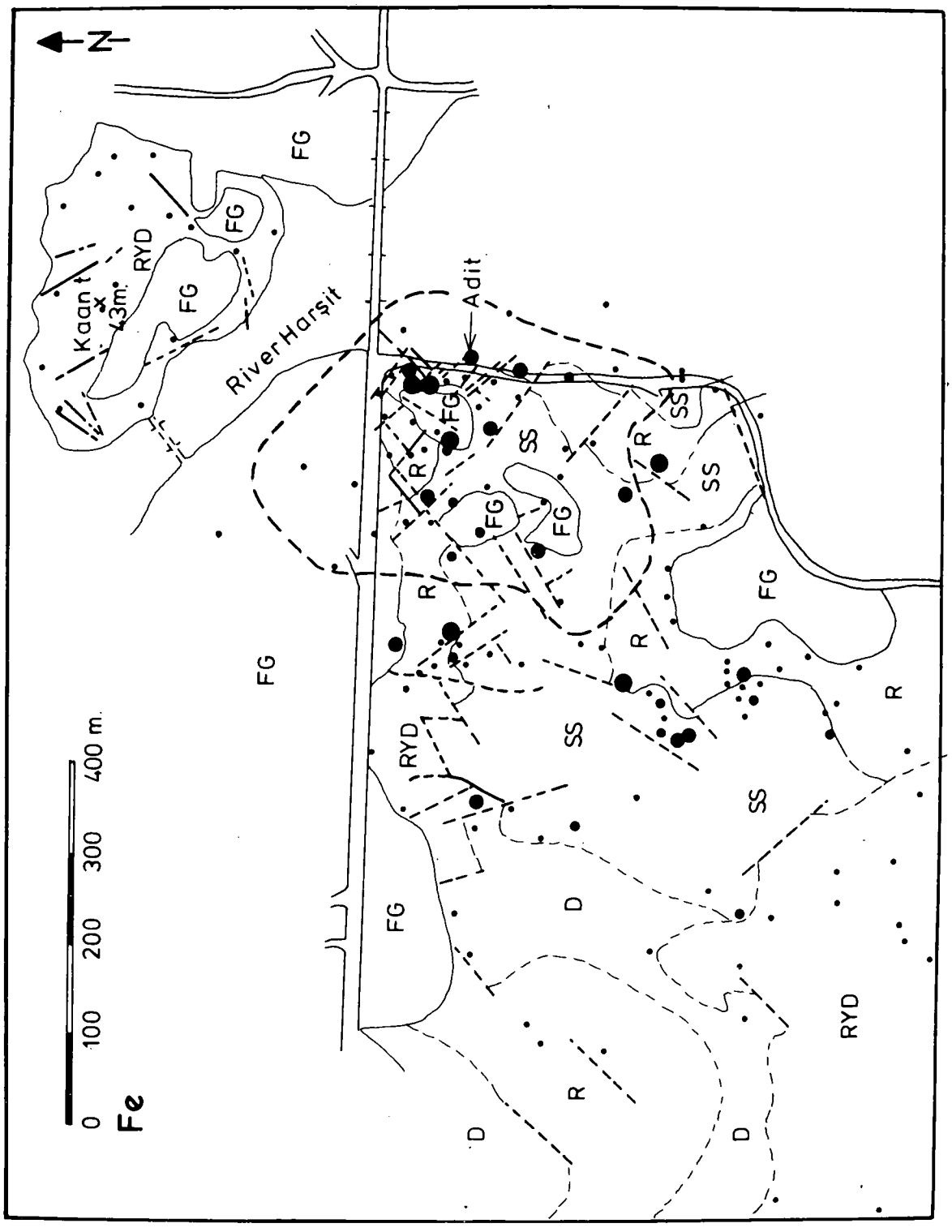

FIGURE 8.5: Distribution of Fe in the cover rocks in the Harsit-Koprubasi mine area (Symbols as in Figure 8.1)

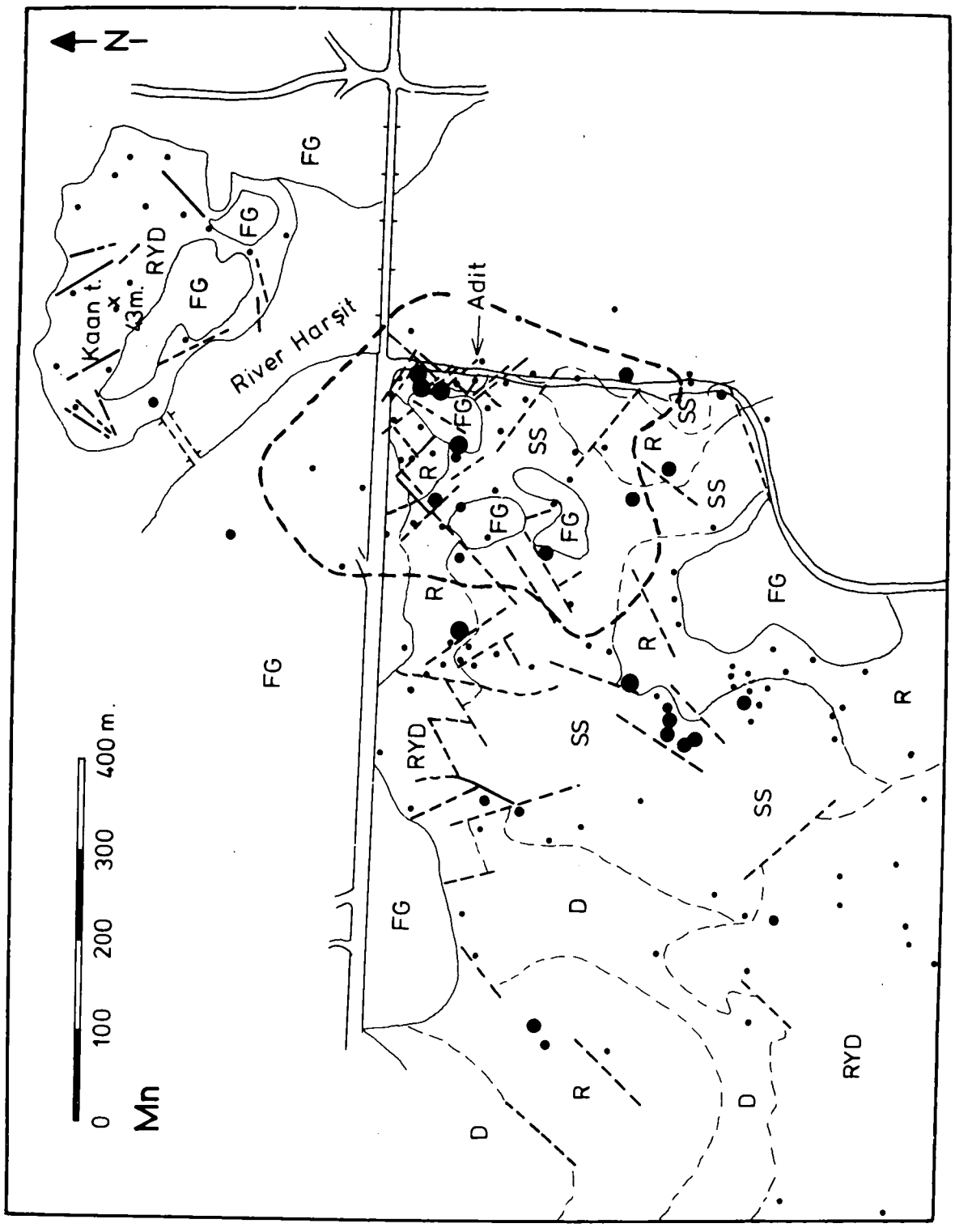

FIGURE 8.6: Distribution of Mn in the cover rocks in the Harsit-Koprubasi mine area (Symbols as in Figure 8.1)

8.4, show anomalous Cu and Zn values. These are undoubtedly related to secondary dispersion from a nearby spoil (F.G.), shown in Figure 5.1.

Both halos A and B fall substantially within a single horizon, the tuffs and tuffaceous sedimentary series. Younger volcanic units, such as the intrusive dolerites and rhyodacites of the Upper Volcanic Cycle previously considered to be unrelated to mineralisation, contain no dispersion patterns which can be related to the mineralisation. This further emphasises the co-eval nature of the mineralisation and the host rock.

Various applied geochemical studies in the search for ore deposits show that there is no reliable method to relate the intensity of an anomaly to the tenor of mineralisation although Beus and Grigorian (1977) have shown that wider and more extensive halos usually form around thick ore bodies. In order to test the validity of this assumption and to explain the irregular shape of halo A, which occurs over the Harsit-Koprubasi deposit, the important charactertistics of the concealed massive ore, such as thickness and depth to the ore body, are shown in Figures 8.7(a) and 8.7(b) respectively. Although the magnitude and distribution of the halo is closely related to the thickness of the massive ore, as shown for example approximately 100 m NW of the adit, the absence or weakness of the anomaly over the 10 m thick massive ore to the WSW of the adit suggests that the thickness of the overburden may also influence the distribution of the anomalous samples. Figure 8.8 shows the thickness of the tuffaceous sedimentary series. Although a separation between the tuffs and the sediments was not established, it is clear that the proportion of tuffaceous material decreases gradually upwards. Figure 8.8 shows clearly that to the west of the adit the normal or weakly anomalous samples occur in the thicker parts of the unit. This, in turn, suggests that the mineralisation and subsequent dispersion of the elements

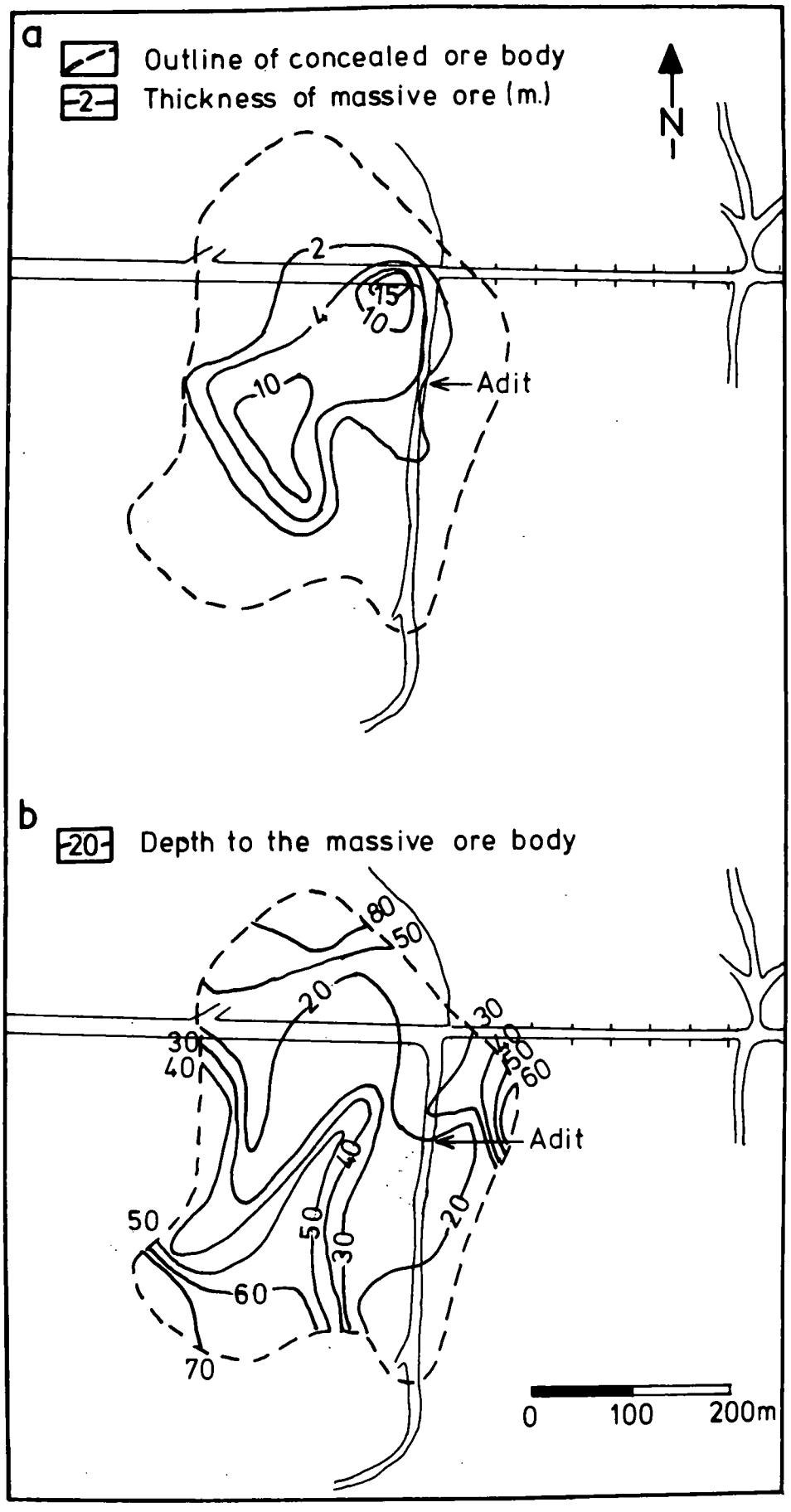

FIGURE 8.7(a): Thickness of the massive ore in the Harsit-Koprubasi mine
FIGURE 8.7(b): Depth to the massive ore in the Harsit-Koprubasi mine

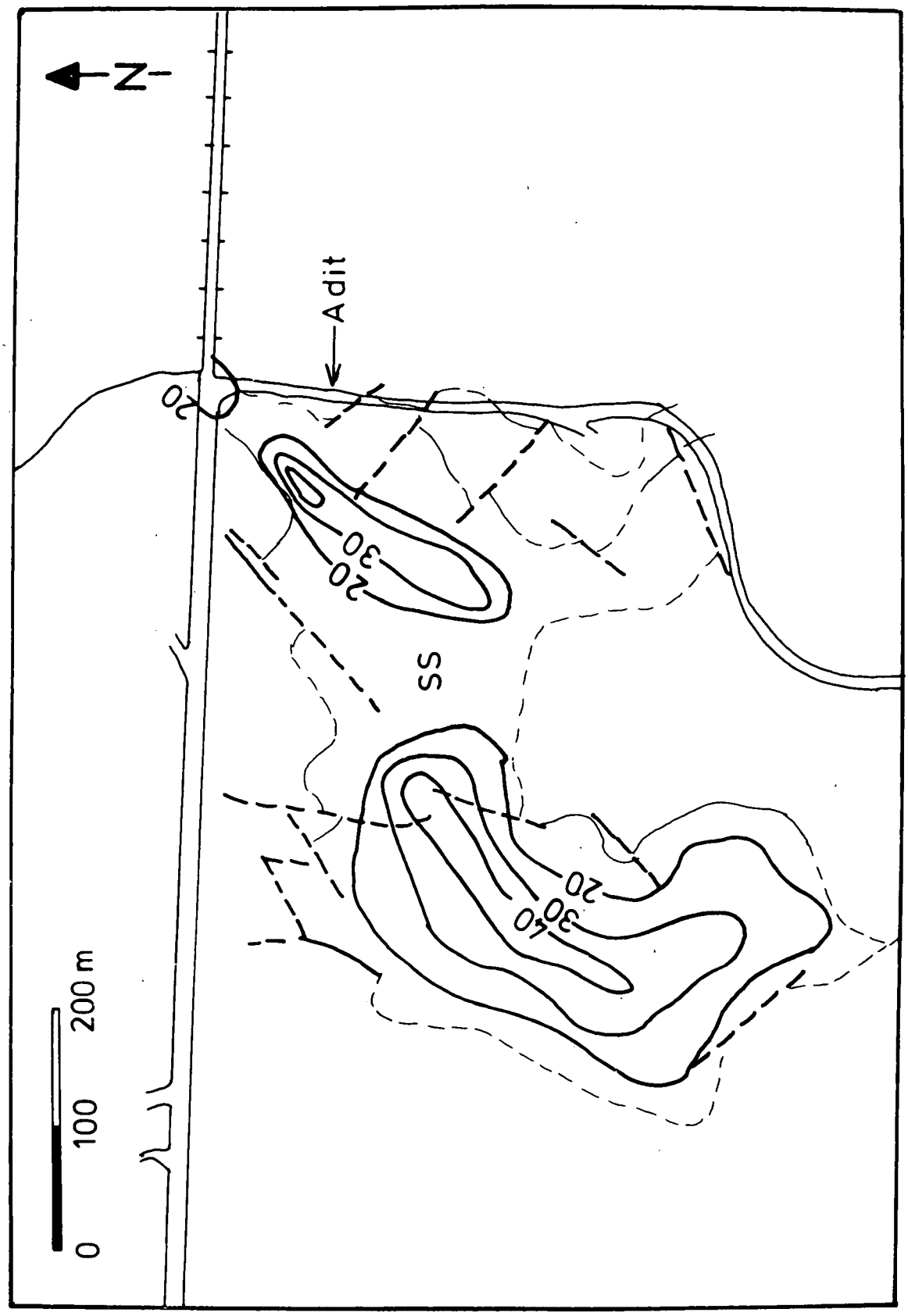

FIGURE 8.8: Thickness of the tuffaceous sedimentary series (SS) in the Harsit-Koprubasi mine area

may predate the deposition of the true sedimentary series (e.g.the marls).

Individual halos in the host rock (R), in general exhibit the following width of dispersion: In decreasing order, Ba, S > Cu > Zn > Fe > Mn (Figures 8.1 to 8.6). The relative abundance of the various elements in the halo however differs markedly between the host rock (R) and the overlying tuffaceous sedimentary series. Ba, S, Zn, and to a lesser extent Cu, occur dominantly in the host rock unit (R) (Figures 8.1 to 8.4), whereas Fe and Mn are relatively more abundant in the tuffaceous sedimentary series (SS) (Figures 8.5 and 8.6) thus giving a crude vertical zonation. In chapter 5 evidence was given to show that there is a pronounced enrichment of Ba, Mn, Fe (and As) in the hanging wall tuffs and tuffaceous sedimentary series. Due to the scarcity of bore-hole core samples from that horizon the data failed to show any useful pattern. The flat-lying nature of the tuffaceous sedimentary series and hanging wall tuffs suggest that sampling across the topography can be used to investigate vertical compositional variation within the halo. Figure 8.9 shows that in halo B, anomalous levels of Mn and Fe occur at a higher topographical, and hence stratigraphical, level than Ba. Co-variance between Ba and S (in barite) rather than between Fe and S confirm that this Fe is not in a sulphide phase but more likely occuring as an oxide, together with Mn.

8.4 A lithogeochemical survey in the Harkkoy mine area

32 surface samples and 3 samples from near-surface from borehole cores in a 1 km x 1 km area have been investigated for Ba, Cu, Zn, Fe and Mn. The data are plotted in Figures 8.10 to 8.14. All these elements show enrichments relative to the background values in the host rock (R and RD) and the tuffaceous sedimentary series (SS). The absence of anomalous values in the Lower Basic Series (LBS) and dacite (D) of the Lower Volcanic Cycle is particularly important in that it imposes a limit to the mineralising episode.

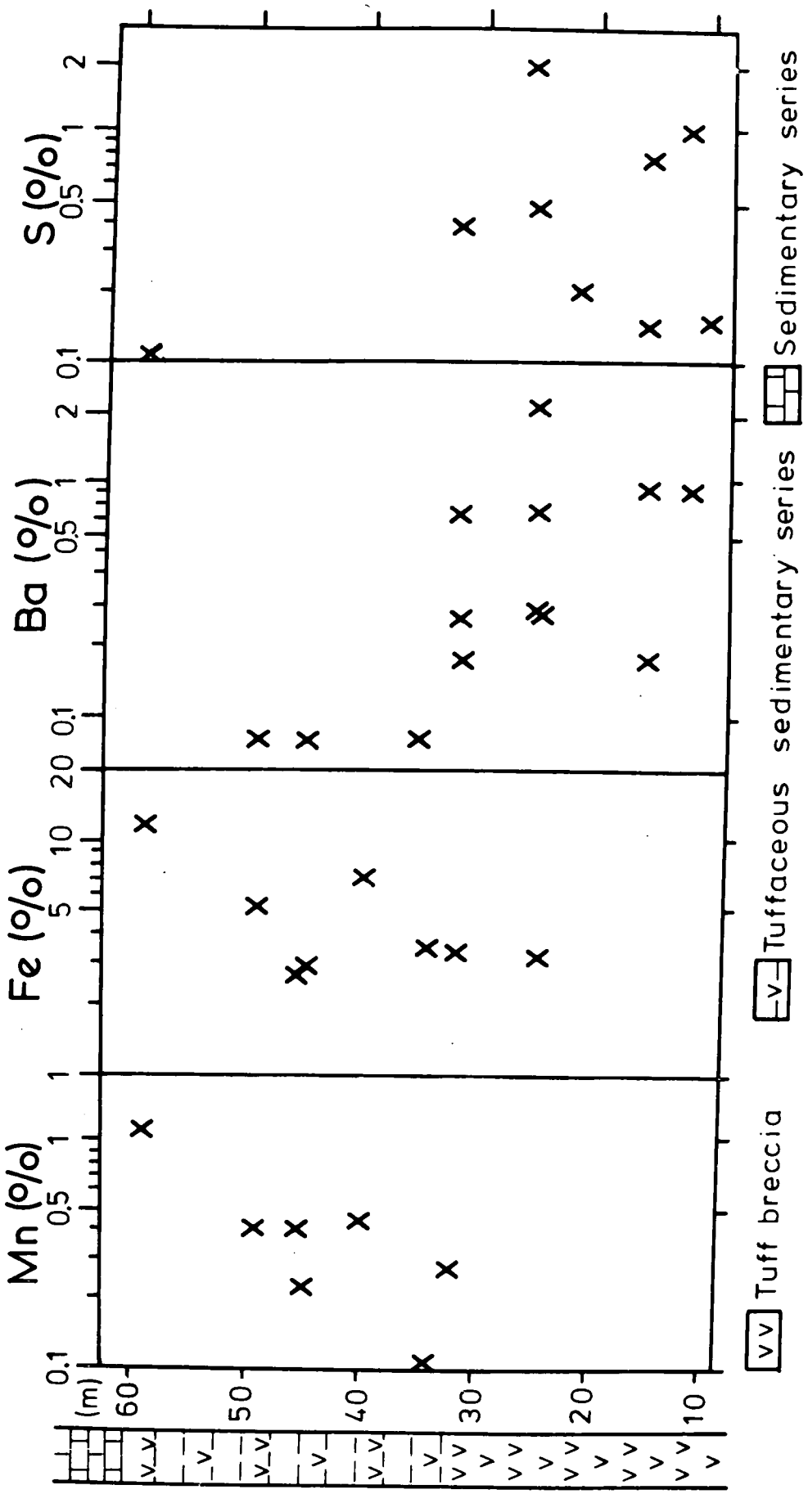

FIGURE 8.9: Distribution of Mn, Fe, Ba and S within a vertical section in the host-rock from the Harsit-Koprubasi mine

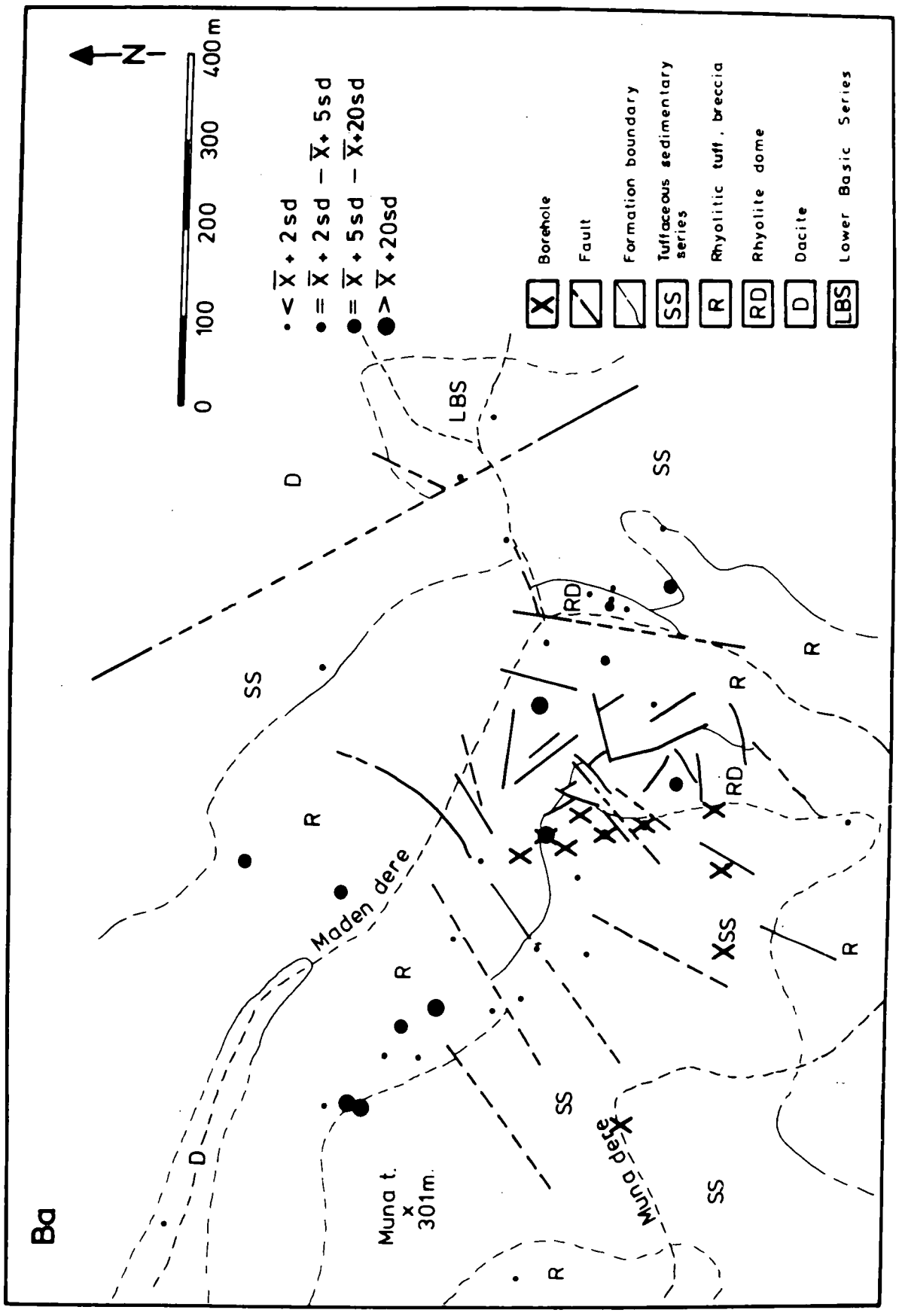

FIGURE 8.10: Distribution of Ba in the host-rock and underlying volcanic rocks in the Harkkoy mine area

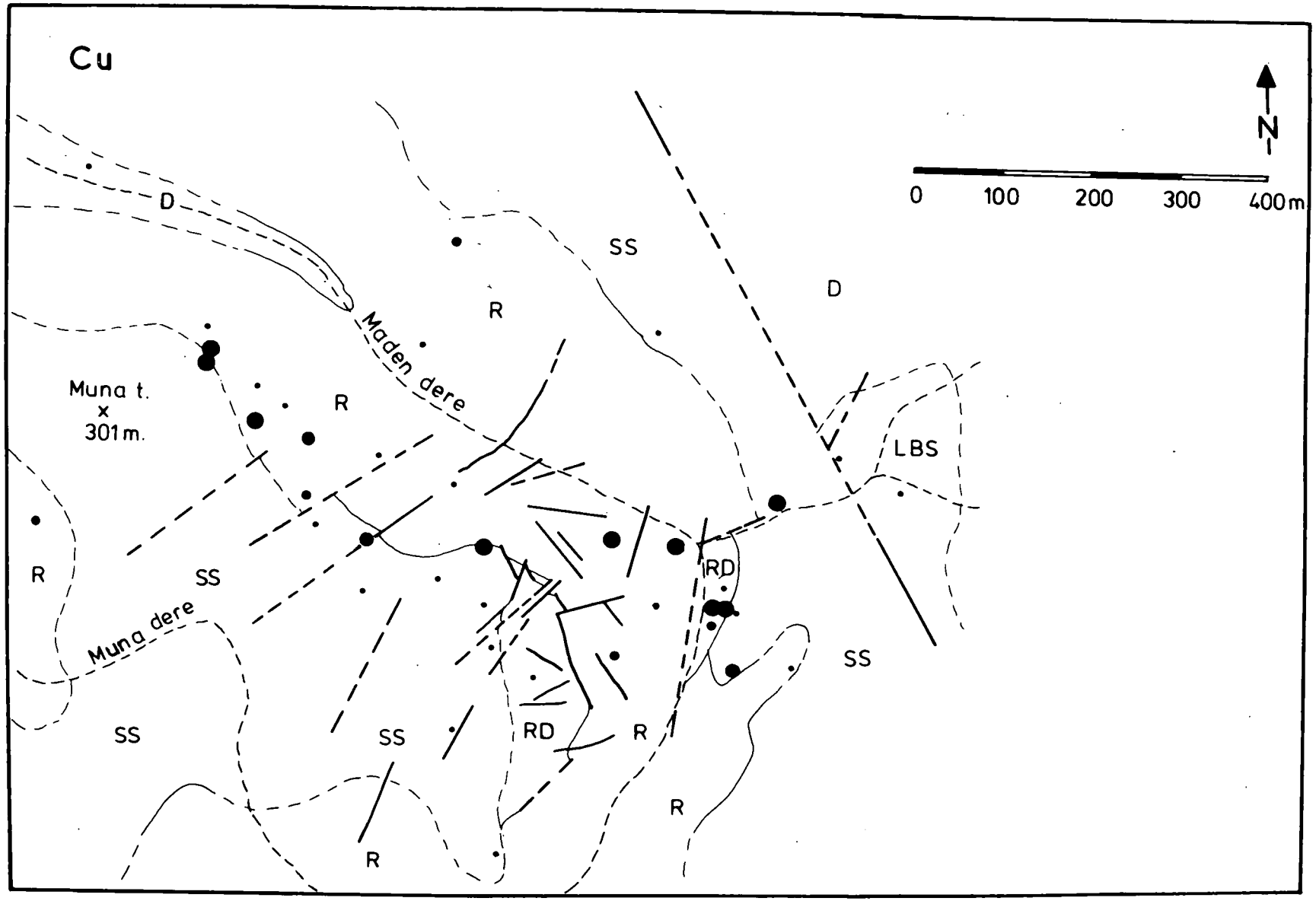

Figure 8.11: Distribution of Cu in the host-rock and underlying volcanic rocks in the Harkkoy mine area (Symbols as in Figure 8.10)

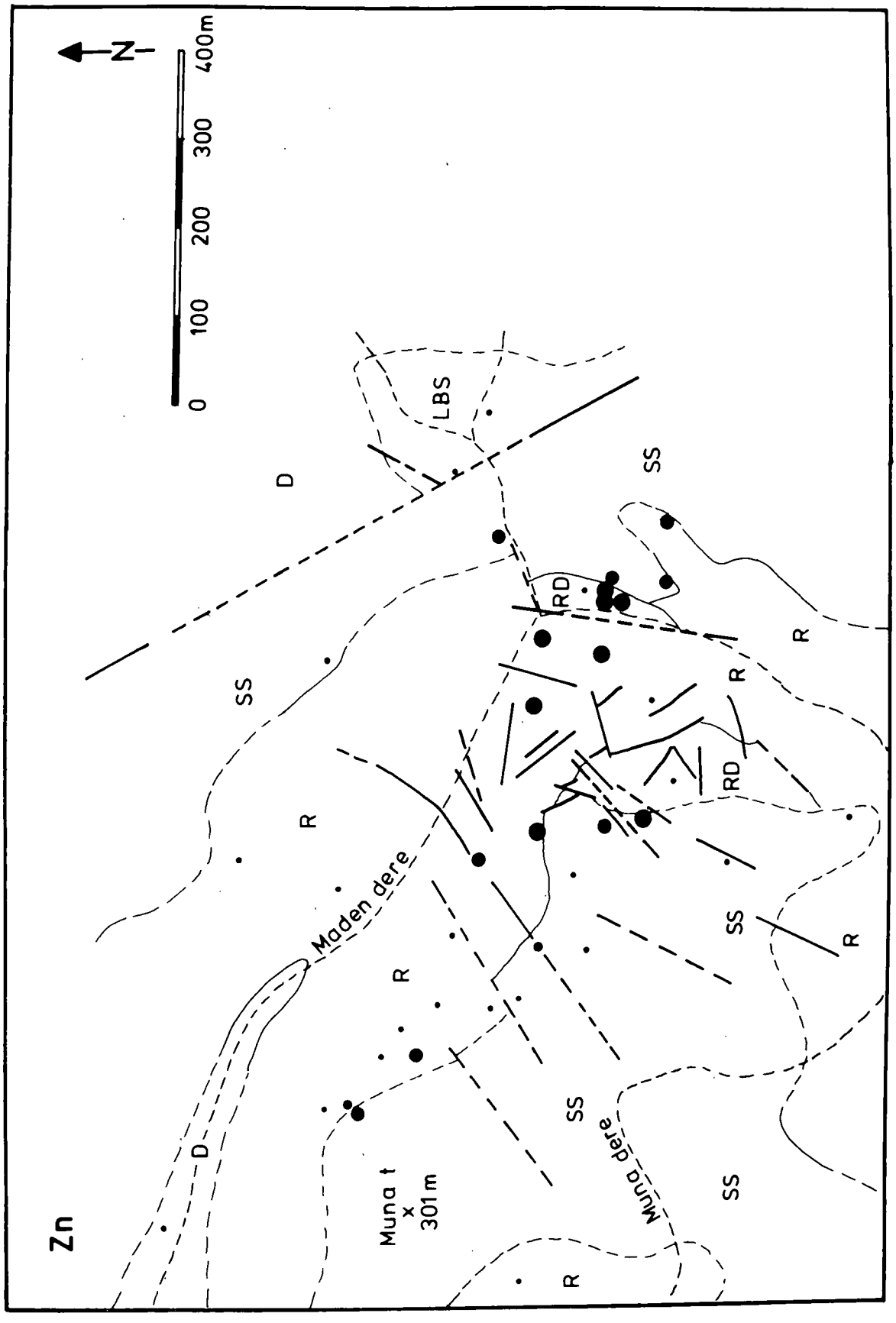

FIGURE 8.12: Distribution of Zn in the host-rock and underlying volcanic rocks in the Harkkoy mine area (Symbols as in Figure 8.10)

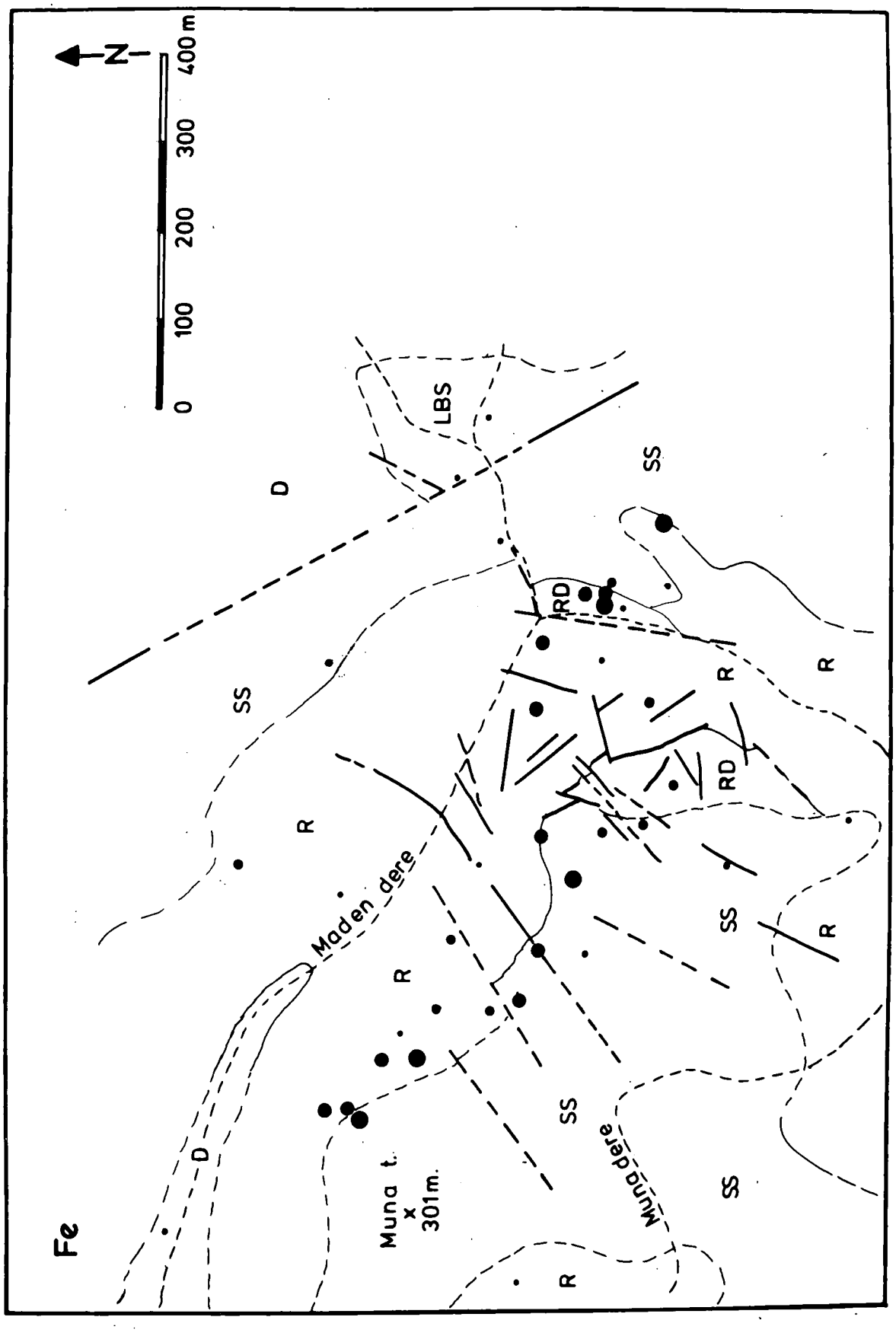

FIGURE 8.13: Distribution of Fe in the host-rock and underlying volcanic rocks in the Harkkoy mine area (Symbols as in Figure 8.10)

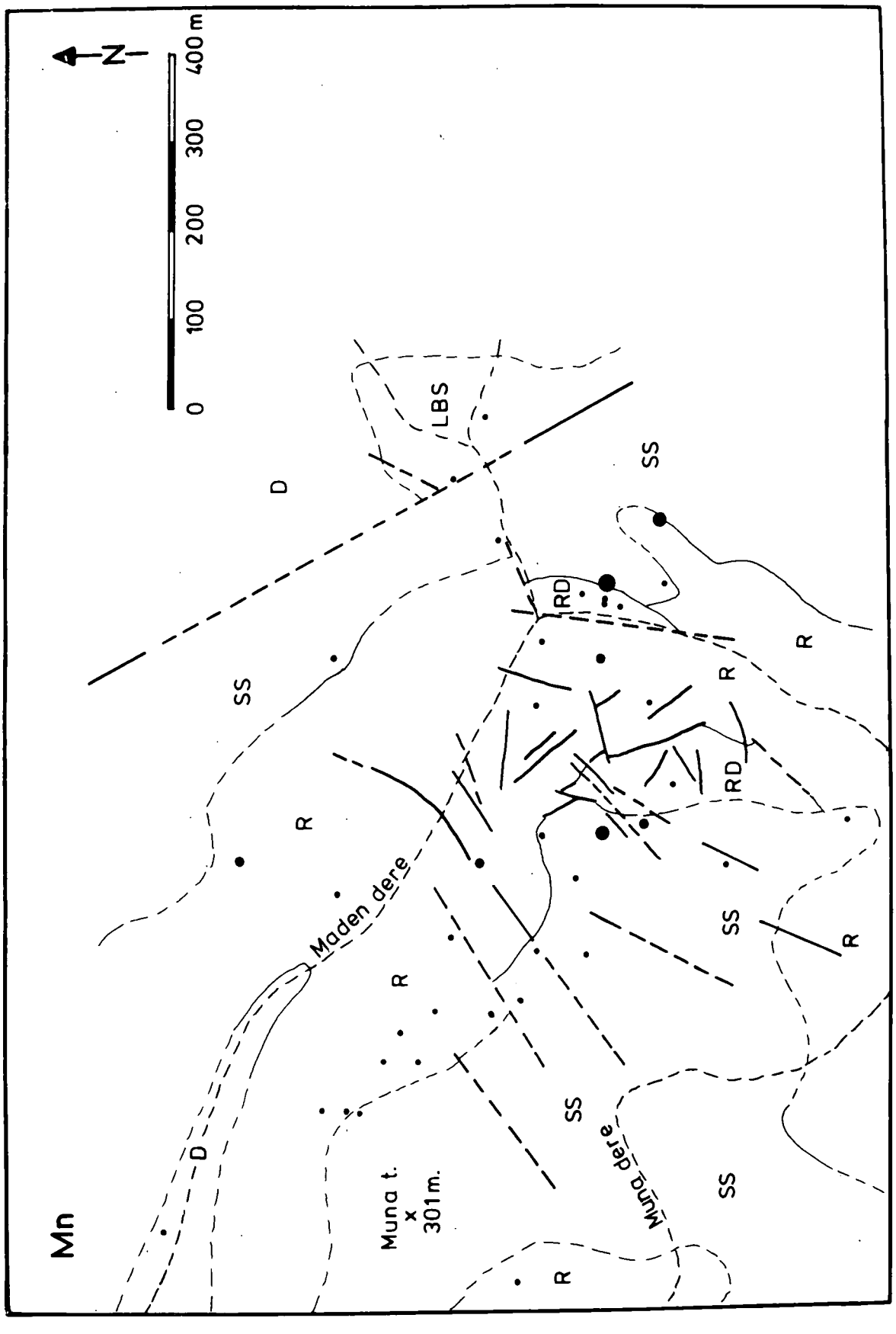

FIGURE 8.14: Distribution of Mn in the host-rock and underlying volcanic rocks in the Harkkoy mine area (Symbols as in Figure 8.10)

Assessment of the dispersion patterns is difficult owing to the limited knowledge of this ore body. Figure 5.9 indicates that exploration of the area by M.T.A. has been confined to the east of Muna dere, near to the rhyolitic dome. To the east of the present borehole locations (Figure 8.10) and east and northeast of Muna Tepe, however, significant anomalies occur (Figures 8.10 to 8.14). This geochemical data, combined with the geological information presented in Chapter 5.2.3, suggests that these may be promising areas in which to search for extensions of the Harkkoy ore body.

Although a vertical zonation of the anomalous samples has not been established in the area, due to limited surface outcrops, Mn does appear to concentrate at a higher stratigraphical level than Ba (Figures 5.11.a and 5.11.c). In this respect the anomalies show similarity to anomaly B of the Harsit-Koprubasi mine area.

8.5 Summary and discussion

The lithological units most affected by the mineralising fluids are the host rock dacitic, rhyolitic lava tuff and breccia (R) and the lowermost part of the overlying tuffaceous sedimentary series (SS). Both units, particularly unit (R), contain much greater abundances of the elements involved in formation of the dispersion halos than do other units found in the vicinity of the ore bodies which are considered to be unrelated to the mineralisation. These latter would include other units of the Lower Volcanic Cycle as seen at Harkkoy, and units of the Upper Volcanic Cycle at Harsit-Koprubasi.

The size and magnitude of the dispersion halo is related to the thickness of the ore body, as proposed in general by Beus and Grigorian (1977). The magnitude of the anomaly however is also affected by the thickness of the overburden, particularly the thickness of the hanging wall tuffaceous sedimentary series. The upwards decay of the anomaly within

the latter is further related to the upwards increase in the sediment/ tuff ratio away from the ore bodies.

Within the lower levels of the tuffaceous sedimentary series a Ba anomaly is succeeded upwards by anomalies in the levels of Fe and Mn , thus defining a vertical chemical zonation.

Dispersion of a given element is directly related to changes in the internal equilibrium of the ore-forming solutions (Ovchinnikov and Grigorian,1971). The mobility of the ore metals in a fluid transporting medium generally follows a sequence in decreasing order; Ba > Cu > Zn > Fe > Mn (Siegel,1974; Beus and Grigorian,1977). This is closely similar to the stabilities of these elements in the complexes described by Barnes and Czamanski (1967). Lateral dispersion of Ba would thus be more extensive than Mn, which yields the smallest halo (Figures 8.2 and 8.6). In the vertical sense, however, the presence of Mn, with Fe, at higher stratigraphical levels than Ba, Cu or Zn is believed to be due to changes in temperature, pH and oxidation state of the ascending ore fluids. In the immediate vicinity of the sulphide deposition, in the high temperature reducing environment, the pH is low, while away from the sulphide zone conditions become more oxidising, weakly acid-alkaline and temperatures are lower (Chapter 7). This enhances the precipitation of Fe and Mn (Barnes and Czamanski,1967,p.366; Stanton,1972, p.463). The solubility of barite is only temperature dependant. Precipitation of barite will therefore take place on cooling from any temperature (Holland, 1967). Such cooling is achieved as solutions move from the lower stockwork ore to the upper massive and barite ores (Figure 7.1) and barite will therefore be found near to the main ore body. The presence of Fe and Mn in tuffaceous sediments above the Ba halo may be indicative of precipitation on the sea floor. This would produce the most effective mixing of ascending ore-fluids with sea-water. The co-existence of the two

elements suggests that they may have been contained in the same solution, probably the ascending hydrothermal solutions, since according to Stanton (1972,p.463) "...it appears virtually impossible to precipitate manganese without precipitation of iron, and vice versa".

In the eastern Pontids typical exhalative deposits associated with the sulphide ore deposits, such as jasper, ferruginous chert and iron formations, are not common. The detection of Mn and Fe anomalies may thus yield information on the location of palaeo-hot-springs and underlying associated ore bodies, as exemplified from the Harsit-Koprubasi and Harkkoy mines. The establishment of vertical zonation would further provide way-up criteria in regions where other indications are lacking or where the massive ores have a steep dip, as seen, for example, at Cayeli.

This study has revealed two anomalous regions, halos A and B, in the Harsit-Koprubasi area. They may be considered to have originated by closely similar processes as both occur in the same lithological unit in an identical structural setting. Halo B thus deserves special attention in the search for extensions of the massive, concealed ore bodies of the Harsit-Koprubasi mine area. The form of the anomaly and the topography suggests that drilling above and to the west of the presently outcropping anomaly may be rewarding.

On a somewhat more speculative basis further investigation of the Mn occurrences shown in Figure 2.1 may be worthwhile. These may be reflections of the uppermost zone of dispersion halos related to concealed ore bodies. This would particularly apply to Mn occurrences which show close spatial association to the dominant fault pattern with which the host rock horizon (unit R) also shows association, as explained in Chapter 4.

CHAPTER NINE

CONCLUSIONS

9.1 Geological Conclusions

The following conclusions, worthy of particular attention, may be drawn:

1. Both petrographically and chemically two volcanic cycles can be clearly distinguished. An Upper Cretaceous, tholeiitic suite (the Lower Volcanic Cycle) is overlain by an early Tertiary, calc-alkaline, Upper Volcanic Cycle. This result, in part, confirms observations in the Cayeli area by De Geoffroy (1960) that the Lower Basic Series are tholeiitic.

2. Palaeontological and field relationships suggest that the Upper Cretaceous volcanism started in a deep, marine environment which persisted throughout formation of the Lower Volcanic Cycle and most of the overlying Sedimentary Series. This was followed by a rapid shallowing of the water and the volcanism probably terminated under shallow water to subaerial conditions in the early Tertiary.

3. The massive-type, polymetallic mineralisation of the study area in particular, and in the Pontids as a whole, is associated with the final phase of the Lower Volcanic Cycle, the dacitic-rhyolitic lava, tuff and breccia. The host rock contains abundant pyroclastic material in contrast to other rocks of similar composition in the area, such as the dacites and the rhyodacites.

4. The host rock, and associated mineralisation, show a strong spatial association with the dominant fault pattern in the region. The implication from such association is that the fracture system provided a channelway for magmatic activity and mineralising fluids.

5. Evidence presented above suggests that the mineralisation predates the overlying sediments and that erosion of the underlying mineralised

volcanics was taking place simultaneous with sedimentation. There is no evidence for derivation of ore-fluids from igneous activity during the Tertiary era. Equally, the unmineralised nature of the early differentiated members of the Lower Volcanic Cycle, the Lower Basic Series and the dacites, together with associated limestones, restricts the mineralising episode to a short period of the felsic, Upper Cretaceous volcanism. It may be concluded that deposition of massive ore in the Pontids is co-eval with the late dacitic-rhyolitic volcanism of the Lower Volcanic tholeiitic cycle.

6. The mineralisation is characterised by a sequence in which a predominantly quartz-pyrite stockwork ore is overlain by massive ore containing galena, sphalerite, chalcopyrite, barite and sulphosalts. This is, in turn, overlain by a horizon in which barite is dominant, followed by hematitic and manganiferous tuffs and sediments. The sequence bears close resemblance to the Kuroko deposits found in the Miocene of Japan.

7. In the Harsit-Koprubasi mine area three separate massive ore horizons have been elucidated from study of borehole cores. One such horizon occurs at the Harkkoy mine, although drilling in that vicinity is much more limited. The evidence from the Harsit-Koprubasi mine clearly points to more than one pulse of mineralisation.

8. Volcanism and/or volcanic processes are thought to be responsible for the generation of the ore fluids. Holland (1972) has re-emphasised the classical theory that metal-rich fluids are separated during the final stage of fractionation and solidification of silicate magmas. Holland has demonstrated that ore metals are strongly partitioned into the aqueous phase in equilibrium with silicate melts of granitic composition. Under favourable conditions such metals "can be extracted

virtually quantitatively from granitic magmas". Such a granitic melt can be the final product of a suite that has evolved by fractional crystallisation and may carry enough base metals to yield a potential ore deposit.

9. Various lines of evidence suggest that the ascending magmatic ore solutions interacted with the sea-water. This process resulted in the exchange of various ions, in a decrease in temperature and salinity, and in an increase in the oxidation state and pH relative to the initial composition of the magmatic fluids. Changes in temperature, pH and oxidation state are effective causes of ore deposition from solutions carrying metals in the various sulphide, bisulphide and/or chloride complexes which might have been stable within the limited conditions of the initial solutions (Helgeson,1964, 1969; Barnes and Czamanski,1967).

9.2 Exploration guides

The following guidelines may lead to discovery and/or extension of ore bodies in the region.

1. Exploration must be aimed at rocks comprising the terminal phase of the Lower Volcanic Cycle. Since there is no discipline in terminology in the area, for practical purposes attention should be focused on acidic volcanic rocks which are characterised by abundant pyroclastic material and are closely related to the dominant faults directions.

2. Localisation of the host-rock can be achieved through careful stratigraphical correlation, in conjunction with a study of the major lineaments. Conventional aerial photographs may effectively be used to detect the major faults. The fault controlled nature of the Black Sea coastline (Figure 1.3) suggests that extension of these coastal lineaments may provide useful information.

3. The detection of volcanic centres may be achieved through careful lithological analyses of the pyroclastic pile. The element pairs Nb-Zr and Mn-Fe would appear to be useful lithological indicators of such centres.

4. Host rock horizons, outlined in Figure 2.1, require detailed lithogeochemical exploration for Mg, Na, K, Ca, S, Ba, Zn, Cu, Fe and Mn. Owing to the small size of the orebodies, the survey must be made on a local scale. Reconnaissance surveys, on a regional scale, may overlook such small ore bodies (c.f.Colley, 1976).

5. The ore-bodies usually exhibit a well-zoned alteration halo. Identification of mineral species together with bulk chemical variations within the pyroclastics can be used as directional vectors. Within the K^+ abundant, Mg^{++}, Ca^{++} and Na^+ deficient, sericitic assemblage (Assemblage II, Chapter 7) the following sequence of elements can be used to determine the proximity of the ore-bodies. In the host rock horizon, including the hanging wall tuffs and tuffaceous sedimentary series, the dispersion of the elements is such that S, Ba > Cu,Zn > Mn, Fe.

6. Arising from this study, the following regions are considered to be potential targets for the discovery of blind ore-deposits in the northern Harsit river area:

a. "Anomaly B", 400 m S.W. of the adit in the Harsit-Koprubasi mine area(p.177) seems to be the most promising initial target for drilling. This anomaly may well represent a further discrete massive sulphide horizon, in addition to the three horizons discovered so far by the drilling programme.

b. The anomaly pattern at Harkkoy, although limited, suggests that further drilling to the north and northeast of the presently drilled area could extend the known limits of mineralisation.

c. The Mn occurrences in the area also call for special attention as they mark the last exhalates from palaeo-hot-springs and may thus be related to underlying sulphide mineralisation.

REFERENCES

Acar, E. C., 1974. Dogu Karadeniz bolgesi ili dahilindeki bazi bakir-kursun-cinku madenlerinin iz element ler yonunden onemi. M.T.A. Dergisi, 82 : 136-146 (in Turkish).

Acar, E. C., 1976. Dogu Karadeniz bolgesi, Tirebolu, Harsit vadisi ve civarinin jeolojisi, petrografik etudu ve ekonomik jeolojisi hakkinda. Yuk. Muhendislik tezi, Ege Universitesi (unpublished, in Turkish).

Acar, E. C. and Akinci O. T., 1975. statistical determination of the Zn/Cd relation for the Harsit-Koprubasi Cu-Pb-Zn mine. Bull. Geol.Soc. Turkey, 18 : 85-86.

Adamia Sh. A., 1975. Discussion on: Plate tectonics and the evolution of the Alpine system. Geol.Soc. Am. Bull., 86 : 719-720.

Adamia, Sh. A., Lordkipanidze, M. B. and Zakariadze, G. S., 1977. Evolution of an active continental margin as exemplified by the Alpine history of Caucasus. Tectonophysics, 40 : 183-199.

Akinci, O. T., 1974. The geology and mineralogy of copper lead zinc sulphide veins from Bulancak, Turkey, Ph.D. thesis, University of Durham (unpublished).

Anderson, C. A., 1969, Massive sulphide deposits and volcanism. Econ. Geol. 64 : 129-146.

Anderson, A. T. and Greenland, L. P., 1969. Phosphorus fractionation diagram as a quantitative indicator of crystallisation differentiation of basaltic liquids. Geochem. Cosmochim. Acta, 33 : 493-505.

Andrews, P. and Tobien, H., 1977, New Miocene locality in Turkey with evidence on the origin of Ramapithecus and Sivapithecus. Nature (London), 268 : 699-701.

Aoki, K. and Oji, Y., 1966. Calc-alkaline volcanic rock series derived from alkali olivine basalt magma. J. Geophys. Res., 71: 6127-6135.

Arni, P., 1939. Dogu Anadolu ve mucavir mintikalarnin tektonik ana hatlari M.T.A. yayinl. 5., Seri B (in Turkish).

Ataman, G., Buket, E. and Capan, U.Z., 1975. Kuzey Anadolu fay sonu bir Paleo-Benioff zonu Olabilirmi? M.T.A. Dergisi, 84: 112-118 (in Turkish).

Bailey, E. B. and McCallien, W. J., 1953. Serpentine Lavas, the Ankara Melange and the Anatolian Thrust. Trans. Roy. Soc. Edin., 62: 403-442.

Baker, P. E., 1968. Comparative volcanology and petrology of the Atlantic island-arcs. Bull. Volcanol., 32: 189-206.

Baragar, W. R. A. and Goodwin, A. H., 1969. Andesites and Archaen volcanism of the Canadian Shield. In: A. R. McBirney (Editor), Proc. Andesite Conf., Oregon Dept. Geol. Mineral Ind. Bull., 65: 121-142.

Barnard, J. H., 1970. Mineralogy of the polymetallic ore deposits of Piraziz, Vilayet Giresun, north eastern Turkey. M.T.A. Bull., 75: 16-27.

Barnes, H. L. and Czamanski, G. K., 1967. Solubilities and transport of ore minerals. In: H. L. Barnes (Editor), Geochemistry of hydrothermal ore deposits, Holt, Rinehart and Winston Inc., New York, 334-381.

Barton, P. B. and Skinner, B. J., 1967. Sulphide minderal stabilities. In: H. L. Barnes (Editor), Geochemistry of hydrothermal ore deposits, Holt, Rinehart and Winston Inc., New York, 236-326.

Barton P. B. and Toulmin III. P., 1966. Phase relations involving sphalerite in the Fe-Zn-S system. Econ. Geol., 61: 815-849.

Bastin, E. S., 1950. Interpretation of ore textures. Geol. Soc. Am. Memoir, 45, 191 pp.

Bethke, P. M. and Barton, P. B., 1971. Distribution of some minor elements between co-existing sulphide minerals. Econ. Geol., 66: 140-163.

Beus, A. A. and Grigorian, S. V., 1977. Geochemical exploration methods for mineral deposits. Applied Publ. Ltd., Wimette, Illinois, 287pp.

Blount, C. W. and Dickson, F. W., 1973. Gypsum-anhydrite equilibria in systems $CaSO_4$-H_2O and $CaSO_4$-NaCl-H_2O. Am. Mineral., 58: 323-331.

Boccaletti, M., Bortolotti, V., Malesani, P. G., Manetti, P., Papani, G. and Sasti, F. P., 1968. Preliminary report on the geological and petrographic mission in the Pontic ranges (Turkey, Summer, 1968), Bull. Geol. Soc. It., 87: 667-676.

Boettcher, A. L. 1973. Volcanism and orogenic belts - the origin of

andesites. Tectonophysics, 17: 223-240.

Bogdanova, B. and Boganov, B., 1974. Asseral porphyry copper in Strednegore (Bulgaria). Intn. Ass. Genesis Ore Deposits, IAGOD 1974 Chetverty Symp. Handbook, Varna, 296.

Brinkmann, R., 1972. Mesozoic troughs and crustal structure in Anatolia. Geol. Soc. Am. Bull., 83: 819-826.

Brinkmann, R., 1974. Geologic relations between Black Sea and Anatolia. In: E. T. Degens and D. A. Ross (Editors), The Black Sea - Geology, Chemistry, and Biology. Am. Assoc. Petroleum Geologists, Memoir 20: 63-76.

Brinkmann, R., 1976. Geology of Turkey. Elsevier, 158pp.

Brown, G. M., Emeleus, C. H., Holland, J. G. and Phillips R., 1970. Petrographic, mineralogic and X-ray fluorescence analysis of lunar igneous type rocks and spherules. Science 167: 599-601.

Brown, G. M., Holland, J. G., Sigirdsson, H., Tomblin, J. F. and Arculus, R. J. 1977. Geochemistry of the Lesser Antilles volcanic island arc. Geochim. Cosmochim. Acta. 41: 785-801.

Burns, R. G., 1969. Site preferences of transition metal ions in silicate crystal structure. Chem. Geol., 5: 275-283.

Cagatay, M. N., 1977. Development of geochemical exploration techniques for massive sulphide ore deposits, Eastern Black Sea region, Turkey. Ph.D. Thesis, University of London (unpublished).

Cameron, E. M., 1975. Geochemical methods of exploration for massive sulphide mineralisation in the Canadian Shield In: I. L. Elliot and W. K. Fletcher (Editors), Geochemical exploration 1974, Elsevier, 21-50.

Cann, J. R. 1970a. Rb, Sr, Y, Zr and Nb in some ocean floor basaltic rocks. Earth Planet Sci. Lett., 10: 7-11.

Cann J. R., 1970b, New Model for the structure of the ocean crust. Nature (London), 226: 928.

Carmichael, I. S. E., Turner, F. J. and Verhoogen, J., 1974. Igneous Petrology. McGraw-Hill, 739pp.

Chao, E. C. T. and Fleischer, M., 1960. Abundance of Zirconium in igneous rocks. Intn, Geol. Congr., 21st Session (Norden) 1: 106-131.

Coats, R. R., 1968. Basaltic andesites. In: H. H. Hess and A. Poldervaart (Editors), Basalts, V.2. Interscience, New York, 689-736.

Colley, H., 1976. Classification and exploration guides for Kuroko-type deposits based on occurrences in Fiji. Trans. Instn. Min. Metall. (Section B) 85: B190-B200.

Corliss, J. B., 1971. The origin of metal-bearing submarine hydrothermal solutions. J. Geophys. Res. 76: 8128-8138.

Creasey, S. C., 1959. Some phase relations in hydrothermally altered porphyry copper deposits. Econ. Geol., 54: 351-373.

Davidson, C. F., 1962. On the Co/Ni ratio in ore deposits. Mining Mag. (London), 106: 78-85.

Deer, W. A., Howie, R. A. and Zussman, J., 1962. Rock forming minerals. Sheet silicates, V.3, Longmans, London., 270pp.

Dermirtasli, E., 1975. Iran, Pakistan ve Turkiyedeki paleyo zoik yash kayaclarin stratigrafik korelasyonu. In: Cumhuriyetin 50. Yili Yerbilimleri Kongresi Tebligler. M.T.A., Ankara 204-222 (in Turkish).

Dewey, J. F. and Bird, J. M., 1970. Mountain Belts and the new global tectonics. J. Geophys. Res., 75: 2625-2647.

Dewey, J. F., Pitman, W., Ryan W., and Bonnin, J., 1973. Plate tectonics and the evolution of the Alpine System. Geol. Soc. Am. Bull., 84: 3137-3180.

De Geoffroy, J., 1960. Cayeli, Pazar ve Ardesen Bolgesinin jeolojisi ve Maden yataklari. M. T. A. Raporu, 3073 (unpublished, in Turkish).

Dixon, C. J. and Pereira J., 1974. Plate tectonics and mineralisation in the Tethyan region. Mineral. Dep. (Berl). 9: 185-198.

Dickinson, W. R. and Hatherton, T. 1967. Andesitic volcanism and seismicity around the Pacific. Science, 157: 801-803.

Dostal, J., Zentilli, M., Caelles, J. C. and Clark, A. H., 1977. Geochemistry and origin of volcanic rocks of the Andes

(26^{o}-28^{o}S). Contrib. Mineral, Petrol., 63: 113-128.

Douillet, Ph. and Nicols, J., 1969. Les mineraux du kaolin-historique-reflexions concernant les diverses classifications et nomenclatures-proposition dune nomenclature nouvelle. Bull. Soc. Fr. Ceramique, 83: 87-114 (in French).

Durukal, S., 1969. Tirebolu-Gorele guneyi jeoloji ve prospeksiyonu raporu. M.T.A. Raporu, 1150 (Unpublished, in Turkish).

Edwards, A. B., 1965. Textures of the ore minerals and their significance. Austr. Inst. Min. Metall. publ. 242pp.

Egeran, E. N., 1947. Tectonique de la Turquie et relations etc., University of Nancy, (Unpublished, in French).

Egin, D., Hirst, D. M. and Phillips, R., in print. The petrology and geochemistry of volcanic rocks from the northern Harsit river area Pontid volcanic province, northeast Turkey. J. Volcanol. Geothermal Res.

Ellis, A. J., 1967. The chemistry of some explored geothermal systems. In: H. L. Barnes (Editor), Geochemistry of hydrothermal ore deposits, Holt, Rinehart and Winston Inc., New York, 465-514.

Enjoji, M., 1972. Studies on Fluid inclusions as the media of the ore formation. Sci. Rp. Tokyo Kyoiku Daigaku, Sec. C, 11: 79-126.

Ewart, A. and Stipp, J. J. 1968. Petrogenesis of the volcanic rocks of the central North Island, New Zealand, as indicated by a study of $^{87}Sr/^{86}Sr$ ratios, and Sr, Rb, K. U. and Th abundances. Geochim. Cosmochim. Acta, 32: 699-736.

Ewart, A., Brothers, R. N. and Mateen, A., 1977. An outline of the geology and geochemistry and the possible petrogenic evolution of the volcanic rocks of the Tonga-Kermadec - New Zealand Island arc. J. Volcanol. Geothermal Res., 2: 205-250.

Fitton, J. G., 1971a. The petrogenesis of the of the calc-alkaline Borrowdale volcanic group Northern England. Ph.D. Thesis, University of Durham. (unpublished).

Fitton, J. G., 1971b. The generation of magmas in island arcs. Earth Planet. Sci. Lett., 63-67.

Fitton, J. G., and Gill, R. C. O., 1970. The oxidation of ferrous iron in rocks during mechanical grinding. Geochim. Cosmochim. Acta, 34: 518-524.

Fleisher, M., 1955. Minor elements in some sulphide minerals. Econ. Geol., 50th. Ann. Vol., 970-1024.

Floyd, P. A. and Winchester, J. A., 1975. Magma type and tectonic setting discrimination using immobile elements. Earth Planet. Sci. Lett., 27: 211-218.

Floyd, P. A. and Winchester, J. A., 1978. Identification and discrimination of altered and metamorphosed volcanic rocks using immobile elements. Chem. Geol., 21: 291-306.

Garrett, R. G., 1975. Copper and Zinc in Proterozoic acid volcanics as a guide to exploration in the Bear province. In: I. L. Elliot and W. K. Fletcher (Editors), Geochemical exploration 1974, Elsevier, 371-388.

Gass, I. G., 1977. Origin and emplacement of ophiolites. In: volcanic processes in ore genesis, Geol. Soc. London Spec. Publn., 7: 72-76.

Gast, P. W., 1968. Trace element fractionation and the origin of tholeiitic and alkaline magma types. Ceochim. Cosmochim, Acta, 32: 1057-1086.

Gattinger, T. E., Erentoz, C. and Ketin, I. 1962. Explanatory text of the geological map of Turkey. Trabzon sheet, 1:500,00 scale. M.T.A. Institue, Ankara.

Gill J. B., 1970. Geochemistry of Viti Levu and its evolution as an island arc. ContribMineral. Petrol., 27: 179-203.

Gill, R. C. O., 1972. The geochemistry of the Gronnedal ÷ Ika alkaline complex South Greenland. Ph.D. thesis, University of Durham (unpublished).

Goksu, E., Pamir, N. H. and Erentoz, C., 1974. Explantory text of the geological map of Turkey, Samsun sheet, 1:500,000 scale. M. T. A. Institute, Ankara.

Goldschmidt, V. M., 1954. Geochemistry, Oxford University press, 730pp.

Goodfellow, W. D., 1975. Major and minor element halos in volcanic rocks

Brunswick No: 12 sulphide deposit. N. B., Canada. In: I. L. Elliot and W. K. Fletcher (Editors), Geochemical exploration. 1974, Elsevier 279-296.

Goossens, P. J., 1972. An exhalative volcanic iron sulphide stratabound deposit, near San Ferrando, Azuay province, Ecuador, Econ. Geol., 67: 469-480.

Gorshkov, G. S., 1969. Geophysics and petrochemistry of andesite volcanism of the circum-Pacific belt. Intn. Upper Mantle Prog. Sci. Rp. 16: 91.

Govett, G. J. S. and Goodfellow, W. D., 1975. Use of rock geochemistry in detecting blind sulphide deposits: a discussion. Trans. Instn. Min. Metall. (Section B), 84: B134-B140.

Graeser, S., 1969. Minor elements in sphalerite and galena from Binnatel. Contrib. Mineral. Petrol., 24: 156-163.

Grant, J. M. N., 1974. Some aspects of tectonics, magmatism and mineralisation in the Tethyan region. M.Sc. dissertation, University of London (unpublished).

Green, D. H., and Ringwood, A. E., 1967. The genesis of basaltic magmas. Contrib. Mineral. Petrol., 15: 103-190.

Guild, P. W., 1972a. Massive sulphides vs. porphyry deposits in their global tectonic settings. Publn. MMIJ and AIME Joint Mtg., Tokyo, 1-12.

Guild, P. W., 1972b. Metallogeny and the new global tectonics. Intn. Geol. Congr., 24th session, 4: 17-24.

Gumus A., 1970. Turkiye metalojenezi, 1:2,500000 olcekli Turkiye metalojenik haritasinin izahi. M.T.A. yayinlari, 144, Ankara (in Turkish).

Hall, A. J., 1972. Substitution of Cu by Zn, Fe and Ag in synthetic tetrahedrite (Cu_{12} Sb_4S_{13}). Bull. Soc. Fr. Mineral. Cristall., 95: 583-594.

Hamacioglu, A. and Sawa, T., 1971. Yeni goruslerin isigi altinda Karadeniz bakir-kursun-cinko yataklari. Turkiye Mad. Bilim. Tekn. Kong II: 64-73.

Hamilton. W., 1969. Mesozoic California and the underflow of Pacific mantle. Geol. Soc. Am. Bull., 80: 2409-2430.

Hawkes, H. E. and Webb, J. S., 1962. Geochemistry in mineral exploration. Harper and Row. New York, 415pp.

Hawley, J. E., 1952. Spectrographic studies of pyrite in some eastern Canadian gold mines. Econ. Geol., 47: 260-304.

Helgeson, H. C., 1964. Complexing and hydrothermal ore deposition. Pergamon press, New York. 128pp.

Helgeson, H. C., 1969. Thermodynamics of hydrothermal systems at elevated temperatures and pressures, Am. J. Sci., 267: 729-804.

Hirabayashi, T., 1974. On the Kuroko-type ore bodies in the Yokoto mine area, Nishi-Aizu district, Fukushima prefecture. In: S.Ishihara (Editor), Geology of Kuroko deposits. Min. Geol. Spec. Issue, Tokyo, 6: 195-201.

Hirst, D. M. and Smith, F. W., 1974. Controls of barite mineralisation in the lower magnesian limestone of the Ferryhill area, County Durham. TRans. Instn. Min. Metall. (Section B), 83: B49-B56.

Holland, H. D., 1967. Gangue minerals in hydrothermal deposits. In: H. L. Barnes (Editor), Geochemistry of hydrothermal ore deposits. Holt, Rinehart and Winston Inc., New York, 382-436.

Holland, H. D., 1972. Granites, solutions and base metal deposits. Econ. Geol., 67: 281-301.

Holland J. G., and Brindle, D. W., 1966. A self-consistent mass absorption correction for silicate analysis by X-ray fluorescence. Spectrochim. Acta, 22: 2083-2093.

*

Horikoshi, E., 1969. Volcanic activity related to the formation of the Kuroko-type deposits, Japan. Mineral. Dept., (Berl). 4: 321-345.

Howard, J. H. III., 1977. Geochemistry of selenium: formation of ferroselite and seleniumbehaviour in the vicinity of oxidising sulphide and uranium deposits. Geochim. Cosmochim, Acta, 41: 1665-1678.

Ilhan, E., 1964. The green rocks of Turkey : their importance for the tectonic pattern of the eastern part of the Mediterranean-Alpine orogenic belt. Intn. Geol. Congr., 22nd session, 4: 608-618.

Ilhan, E., 1971. The structural features of Turkey. In: A. S. Campbell (Editor), Geology and history of Turkey. Petroleum Expl. Soc. Libya.

* Holmes, A., 1965. Principles of physical geology, 2nd Edition. Nelson.

159-170.

Ilhan, E., 1974. Eastern Turkey. In: A. M. Spencer (Editor), Mesozoic-Cenozoic Orogenic Belts. Scottish Academic Press, 187-197.

Irvine, T. N. and Baragar, W. R. A., 1971. A guide to the chemical classification of the common volcanic rocks. Can. J. Earth Sci., 8: 523-548.

Ishihara, S., 1974. (Editor) Geology of Kuroko deposits. Min. Geol. Spec. Issue, Tokyo. 6, 435pp.

Ishikawa, H., Kurada, R. and Sudo, T., 1962. Minor elements in some altered zones of Kuroko (Black ore) deposits in Japan. Econ. Geol., 57: 785-789.

Jakes, P. and Gill, J. B., 1970. Rare earth elements and the island are tholeiite series. Earth Planet. Sci. Lett., 9: 17-28.

Jakes, P. and White A. J. R., 1970. K/Rb ratios of rocks from island arcs. Geochim, Cosmochim, Acta, 34: 849-856.

Jakes, P. and White, A. J. R., 1972a. Major and trace element abundances in volcanic rocks of orogenic areas. Geol. Soc. Am. Bull., 83: 29-40.

Jakes, P. and White, A. J. R., 1972b. Hornblendes from calc-alkaline volcanic rocks of island arcs and continental margins. Am. Mineral., 57: 887-902.

Jakobsen, J. B. E., 1975. Copper deposits in time and space. Minerals Sci. Engng., 7: 337-371.

Jankovic, S., 1977. The copper deposits and geotectonic setting of the Tethyan-Eurasian metallogenic belt. Mineral. Dep., (Berl.), 12: 37-47.

Johannesson, H., 1975. Structure and petrochemistry of the Reykjadalur central volcanoe and the surrounding areas, midwest Iceland. Ph.D Thesis, University of Durham (unpublished).

Kajiwara, Y., 1973. Chemical composition of ore forming solutions responsible for the Kuroko-type mineralisation in Japan. Geochem. J. (Japan), 6: 141-149.

Kamen-Kaye, M., 1971. A review of depositional history and geological structure in Turkey. In: A. S. Campbell (Editor), Geology and history of Turkey. Petroleum Expl. Soc. Libya, 111-137.

Kennedy, G. C., 1955. Some aspects of the role of water in rock melts.

Geol. Soc. Am. Spec. paper, 62: 489-504.

Ketin, I., 1966. Tectonic units of Anatolia (Asia Minor) M.T.A. Bull., 66: 23-33

Kieft, C., 1955. Tirebolu bolgesindeki bazi bakir cevher yataklarinin etudu. M.T.A. raporu. 52 (unpublished, in Turkish).

Kieft, C., 1956. Giresun ili dahilindeki bazi piritic bakir zuhurlari etudleri M.T.A. Raporu, 531 (unpublished, in Turkish).

Kodama, H., 1962. Interpretation of X-ray powder patterns of some hydro-muscovite from Japan with reference to their alkali contents. Clay. Sci. (Japan), 1:89-99.

Koprivica, D., 1976. Hopa-Arhavi bolgesinin jeolojisi, yapisal ozellikleri ile sulfit ve manganez zuhuralari (N.E. Turkiye). M.T.A. Dergisi, 87: 1-20. (In Turkish).

Kraeff, A., 1963. Geology and mineral deposits of the Hopa-Murgul Region (western part of the Province of Artvin, N.E. Turkey). M.T.A. Bull. 60: 45-60.

Kribek, B., 1975. The origin of framboidal pyrite as a surface effect of sulphur grains. Mineral Dep., (Berl)., 10: 389-396.

Kronberg, P., 1970. Dogu Karadeniz daglarinin (Kuzeydogu Turkiye) tektonigi uzerine fotojeolojik veriler. M.T.A. Dergisi, 74: 57-65 (in Turkish).

Kuno, H., 1950. Petrology of Hakone Volcano and the adjacent areas. Geol. Soc. Am. Bull., 61: 957-1020.

Kuno, H., 1960. High-alumina basalt, J. Petrol., 1: 121-145.

Kuno, H., 1966, Lateral varation of basalt magma type across continental margins and islands arcs. Bull. Volcanol., 29: 195-222.

Kuno, H., 1968a. Differentation of basaltic magmas. In: H. H. Hess and A. Poldervaart (Editors). Basalts v 2, Interscience, New York, 623-688.

Kuno, H., 1968b. Origin of Andesite and its bearing on the island arc structure. Bull. Volcanol., 32: 141-176.

Kushiro, I., 1973. Origin of some magmas in oceanic and circum-oceanic regions. Tectonophysics, 17: 211-222.

Lambert, I. B. and Sato, T., 1974. The Kuroko and associated ore deposits of Japan. a review of their features and metallogenesis. Econ. Geol.

69: 1215-1236.

Large, R. R., 1977. Chemical evolution and zonation of massive sulphide deposits in volcanic terrains. Econ. Geol., 72: 549-572.

Lob, F., 1960. Komplexe erze der Turkischen lagerlstaette Harkkoy und deren aufbereitung. Montan-Rundschau. 9: 259-260 (in German).

Loftus-Hills, G. and Solomon, M., 1967. Co-Ni and Se in sulphides as indicators of ore deposits. Mineral. Dep. (Berl.) 2: 228-242.

Lowell, J. D. and Guilbert. J. M., 1970. Lateral and vertical alteration-mineralisation and zoning in porphyry ore deposits. Econ. Geol., 65: 373-408.

Malakhov, A. A., Malakhov, D. O., and Bobrova, M.S., 1974. Se, Te, As and Thallium content in pyrites and chalcopyrites of the Makansky copper sulphide deposits, Southern Urals. Geochem. Intn. 11: 92-111.

Maruyama, S., 1967. Kuroko geology. World Min. 47-49.

Maucher, A., 1958. Tirebolu bolgesindeki jeolojik calismalar M.T.A. Raporu, 2528 (unpublished, in Turkish).

McBirney, A. R., 1963. Factors governing the nature of submarine volcanism Bull. Volcanol. 26: 455-469.

McBirney. A.R., 1969. Compositional variations in Cenozoic calc-alkaline suites Oregon Dept. Geol. Mineral. Ind. Bull., 65: 185-189.

McKenzie, D. P., 1972. Active tectonics of the Mediterranean region. Geophys. J. Astr. Soc., 30: 109-185.

Meyer, C. and Hemley, J., 1967. Wall rock alteration. In: H. L. Barnes (Editor) Geochmistry of Hydrothermal ore deposits, Holt, Rinehart, and Winston Inc., New York, 167-235.

Mitchell, A. H. G. and Garson, M. S., 1976. Mineralisation at plate boundaries. Minerals Sci. Engng., 8: 129-169.

Miyashiro, A., 1974. Volcanic rock series in island arcs and active continental margins. Am. J. Sci., 274: 321-355.

Miyazawa, T., 1967. Lowest limit and depth of formation of hydrothermal

veins, Sci. Rp. Tokyo Kyoiku Daigaku, Sect. C, 9: 257-261.

Moore J. G., 1962. K/Na ratio of Cenozoic igneous rocks of the Western United States. Geochim. Cosmochim. Acta. 26: 101-130.

M.T.A. Enstitusu Publn. 1972. Lead, copper and zinc deposits of Turkey. 119pp., Ankara.

M.T.A. Enstitusu Publn. 1977, Dunya maden haberleri (1974). 125pp. Ankara (in Turkish).

M.T.A. Estitusu Publn. 1978. M.T.A. Haberleri (news letter) April 1978. Ankara (in Turkish).

Nash J. T., 1975, Geochemical studies in the Park City district II. Sulphide minerology and minor element chemistry, Mayflower mine, Econ. Geol., 70: 1038-1049.

Neprochnov, Yu. P., 1959. Deep structure of earth's crust underneath Black Sea, southwest of Crimea, from seismic data. Akad. Nauk. S.S.S.R. Doklady, 125 (5) 1119-1122.

Neprochnov, Yu. P., Neprochnov, A. F. and Mirlin, Ye. G., 1974. Deep strucuture of Black Sea Basin. In: E. T. Degens and D. A. Ross (Editors), the Black Sea - Geology, Chemistry and Biology. Am. Assoc. Petroleum Geologists, Memoir 20: 35-49.

Nishiyama, T., 1974. Minor elements in some sulphide minerals from the Kuroko deposits of the Shakani mine. In: S. Ishihara (Editor). Geology of Kuroko deposits. Min. Geol. Spec. Issue, Tokyo, 6: 371-376.

Ohmoto, H. and Rye, R. O., 1974. Hydrogen and oxygen isotopic composition of fluid inclusions in the Kuroko deposits, Japan, Econ. Geol. 69: 947-953.

Oner. O. and Iwao, S., 1974. Report on geological survey of Trabzon area, north eastern Turkey. Joint survey report by M.T.A., Metal Mining Agency of Japan, Japan. International Co-operation Agency, Government of Japan (limited circulation).

Osborn. E. F., 1959. Role of oxygen pressure in the crystallisation and differentitation of basaltic magma. Am. J. Sci., 257: 609-647.

Osborn. E. F., 1962. Reaction series for subalkaline igneous rocks based

on different oxygen pressure conditions. Am. Mineral., 47: 211-226.

Oswald, F., 1912. Armenian handbuck der regional geologie. 3(10), Heidelberg (in German).

Ovalioglu, R., 1969. Turkiye bakir-kursun-cinko madenleri ve bunlarin arama-degerlendirme problemleri. Turkiye Mad. Bilim Tekn. Kong. I: 101-118 (in Turkish).

Ovchinnikov, L. N. and Baranov, E. N. 1971. Endogenic geochemical halos of pyritic ore deposits. Intn. Geology Rev., 14: 419-429.

Palache, C., Berman, H. and Frondel, C., 1944. The system of mineralogy v.1., John Wiley and Sons, London, 834pp.

Papazochos, B. C., 1976. Seismotectonics of the northern Aegean area. Tectonophysics, 33: 199-209.

Peacock, M. A., 1931. Classification of igneous rocks. J. Geol., 39: 54-67.

Pearce, J. A. and Cann, J. R., 1973. Tectonic setting of basic volcanic rocks determined using trace element analysis. Earth Planet Sci. Lett., 19: 290-300.

Pearce, J. A. and Gale, G. H., 1977. Identification of ore deposition environment from trace element geochemistry of associated igneous host rocks. In: Volcanic processes in ore genesis. Geol. Soc. London. Spec. Publn., 7: 14-24.

Peccerillo, A. and Taylor, S. R., 1976. Geochmistry of Eocene calc-alkaline volcanic rocks from the Kastamonu area, N.E. Turkey. Contrib. Mineral. Petrol., 58: 63-81.

Peccerillo, A. and Taylor, S. R., 1977. Geochemistry of Upper Cretaceous volcanic rocks from the Pontic chain. Northern Turkey. Bull. Volcanol., 39: 557-569.

Pollak, A., 1961. Karadeniz sahilinde, Giresun vilayeti dahilinde Lahanos cevhar yataklari M.T.A. Dergisi, 56 (in Turkish).

Pollak, A., 1962. M.T.A. Raporu, 14944 (unpublished, in Turkish).

Pollak, A., 1968, Kuzey Anadolu, Cevher bolgesi. M.T.A. Dergisi, 70:

122-128 (in Turkish).

Popovic, R., 1975. Dogu Pontidlerdeki demirsiz metallerin zonal dagilimi ile yapisal ve jenetik ozellikleri. M.T.A. Dergisi, 85: 1-16 (in Turkish).

Prinz, M., 1968. Geochemistry of basaltic rocks: Trace elements. In: H.H. Hess and A. Poldervaart (Editors), Basalts, V.1., Interscience, New York. 271-323.

Ramdohr, P., 1969. The ore minerals and their intergrowths. Pergamon Press, Oxford. 1174pp.

Rankin, A. H., 1978. User school on fluid inclusion equipment and methods, course notes, Imperial College, London 30 March-1 April 1978. (limited circulation).

Rezanov, I. A. and Chamao, S. S., 1969. Reasons for absence of a "granitic" layer in basins of the South Caspian and Black Sea, Can. J. Earth. Sci. 5: 671-678.

Rickard, D. T., 1970 The origin of framboids. Lithos 3: 269-293.

Ridge, J. D., 1973. Volcanic exhalations and ore deposition in the vicinity of the sea floor. Mineral Dep. (Berl.), 8: 332-348.

Ridge, J. D., 1974 Note on boiling of ascending ore fluids and the position of volcanic-exhalative deposits in the modified Lindgren classification. Geology, 2: 287-288.

Ringwood, A. E., 1969. Composition of the crust and upper mantle. In: P. J. Hart (editor), The earth's crust and upper mantle. Am.Geohpys. Monogr. 13: 1-17.

Roedder, E., 1964. Studies of fluids inclusions: low temperature application of a dual purpose freezing and heating stage. Econ. Geol. 57: 1045-1061.

Roedder, E., 1965. Evidence from fluid inclusions as to the nature of the ore forming fluids. Sym. Problems of post magmatic ore deposition. Prague, 2: 375-384.

Roedder, E., 1967. Fluid inclusions as samples of ore fluids. In: H. L. Barnes, Geochmistry of Hydrothermal ore-deposits, Holt, Rinehart and Winston Inc., New York, 515-576.

Roedder, E., 1971. Fluid inclusion studies on the porphyry-type ore-deposits at Bingham, Utah; Butle, Montana and Climax, Colorado, Econ. Geol. 66: 98-120.

Roedder, E., 1972. Composition of fluid inclusions. In: Data of Geochemistry. chapter JJ. U.S. Geol. Surv. Prof. Paper. 440JJ., 164pp.

Russell, M. J. 1974. Manganese halo surrounding the Tynagh ore deposit Ireland: a preliminary note, Trans. Instn. Min. Metall. (Section B); 83: B65-B66.

Ryan, C. W., 1960. A guide to the know minerals of Turkey. M.T.A. Publn.

Sangster, D. F., 1972. Precambrian volcanogenic massive sulphide deposits in Canada, a review. Geol. Surv. Canada, paper 72-73, 44pp.

Sangster, D. F. and Scott, S. D., 1976. Precambrian, strata-bound, massive Cu-Zn-Pb sulphide ores of north America. In: K. H. Wolf, (Editor) Handbook of strata-bound and stratiform ore deposits, v.6, Elsevier, Amsterdam. 129-222.

Sawa, T. and Altun, Y., 1977. Dogu Karadeniz bolgesindeki tabakali ve stockvork tip Bakir, Kursun, Cinko, Yataklari, M.T.A. Raporu, 1510, (unpublished, in Turkish).

Sawkins, F. J., 1964. Lead-zinc ore deposition in the light of fluid inclusion studies, Providencia mine, Zacatecas, Mexico, Econ. Geol. 59: 893-919.

Sawkins, F. J., 1966. Ore genesis in the north Penine ore-field in the light of fluid inclusions studies. Econ. Geol., 61:385-401.

Sawkins, F. J., 1972. Sulphide ore deposits in relation to plate tectonics. J. Geol., 80: 377-397.

Schuiling, R. D., 1962. On petrology, age and structure of Menderes migmatite complex, S.W. Turkey, M.T.A. Bull. 58: 71-84.

Schutze-Westrum. H. H. 1961. Das geologische profil des Aksudere bei Giresun ein beitrag zur geologic und lagerstattenkunde der Ostpontischen erz und mineralprovinz. N.E. Anatolien. M.T.A. Dergisi, 57: 65-74 (in German).

Shatskiy, N.S. 1966. On manganiferous formations and the metallogeny of

manganese, paper 1. Volcanogenic-sedimentary manganiferous formations. Intn. Geol. Rev. 6: 1030-1056.

Shiikawa, M., Wakasa, K. and Tono, N., 1975. Geochemical exploration for Kuroko deposits in north-east Honshu, Japan. In: I. L. Elliot and W. K. Fletcher (Editors), Geochemical exploration ,1974. Elsevier 65-76.

Shiikawa, M. and Tono, N., 1972. Geochemical exploration in the region of Kuroko deposits. Joint Mtg., MMIJ-AIME 1972, preprint. T1 c3, 10pp.

Shimazaki, Y., 1974. Ore minerals of the Kuroko-type deposits. In: S. Ishihara (Editor), Geology of Kuroko deposits. Min. Geol. Spec. Issue, Tokyo, 6: 311-322.

Shirozu, H. and Higashi, S., 1972. X-ray examination of sericite minerals associated with the Kuroko deposits. Clay. Sci. (Japan) 4: 137-142.

Siegel, F. R., 1974. Applied Geochemistry. A. Wiley - Interscience Publn., New York, 353pp.

Siegers, A., Pichler, H. and Zeil, W., 1969. Trace element abundances in the "Andesite" formation of north-eastern Chile. Geochim, Cosmochim. Acta, 33: 882-887.

Sillitoe, R. H., 1977. Metallic mineralisation affiliated to subaerial volcanism: a review. In: Volcanic processes in ore genesis. Geol. Soc. London. Spec. Publn. 7: 99-116.

Sinclair, W. D., 1971. A volcanic origin for the No. 5 zone of the Horne mine. Econ. Geol., 66: 1225-1231.

Smith, A. G. 1973. The so-called Tehyan ophiolites. In: D. H. Tarling and S. K. Runcorn (Editors), Implication of continental drift to the earth sciences, v.2. Nato. Adv. Study Inst., 1972, Academic Press, London. 977-986.

Smith, F. W., 1973. A simple microscope freezing stage. Mineral. Mag., London., 39: 366-367.

Smith, F. W., 1974. Factors governing the development of fluorspar orebodies in the north penine ore field. Ph.D. thesis, University of Durham. (unpublished).

Smith F. W., and Hirst D. M., 1974. Analysis of trace elements and fluid inclusions in fluorite from the Ardennes massif. Ann. Soc. Geol. Belgique, T.97: 281-285.

Smith, F. W., and Phillips R., 1975. Temperature gradient and ore deposition in the north Penine ore-field. Fortschr. Miner., 52: 491-494.

Smith, R. L. and Bailey, R. A., 1966. The Bandelier tuff: A study of ash-flow eruption cycles, zoned magma chambers. Bull. Volcanol., 29: 83-104.

Snelgrove, A. K., 1971. Metolojeni ve yeni kuresel tektonik. M.T.A. Dergisi, 76: 135-153 (in Turkish).

Solomon, M., 1976 "Volcanic" massive sulphide deposits and their host rocks. a review and explanation. In: K. H. Wolf (Editor), Handbook of strata-bound and stratiform ore deposits. v.6., Elsevier, Amsterdam. 21-54.

Solomon, M. and Walshe, J. L., in print. The formation of massive-sulphide deposits on the sea-floor. Econ. Geol.

Spence, C. D. and De Rosen-Spence, A. F., 1975. The place of sulphide mineralisation in the volcanic sequence at Noranda, Quebec, Econ. Geol., 70: 90-101.

Spooner, E. T. C., Bray, C. J., and Chapman, H. J., 1977. Sea-water source for hydrothermal fluids which formed the ophiolitic cupriferous pyrite ore deposits of the Troodos massif, Cyprus. (Abstract), Trans. Instn. Min. Metall. (Section B), 86: B159.

Springer. G., 1969 Electron probe analysis of tetrahedrite. Neues. Jahrb. Mineral. Monatsh., HF1: 24-33.

Stanton, R. L. 1972. Ore petrology. McGraw-Hill, New York, 713pp.

Stojanov, R., 1975. Pontidlerde, Harsit nehri sahasindaki volkanik taslarin petrolojisi. In: Cumhuriyetin 50 yili Yerbilimleri Kongresi, Tebligleri. M.T.A., Ankara 490-517. (in Turkish).

Sudo, T., Hayashi, H. and Shimoda, S., 1962. Mineralogical problems of intermediate clay material. Clays and Clay Miner., 8: 378-392.

Sugimura, A., 1960. Zonal arrangement of some geophysical and petrological features in Japan and its environments. Jour. Fac. Sci. Univ. Tokyo. sect. 2,12: 133-153.

Sugimara, A., 1968. Spatial relations of basaltic magmas in island arcs. In: H.H. Hess and A. Poldervaart (Editors), Basalts. v.2, Interscience, New York. 537-571.

Supercanu, C. I. 1971. The Mediterranean-Iranian Alpine copper-molybdenum belt. In: Y. Takeuchi (Editor). Proc. IMA-IAGOD Mtg. 1970, IAGOD vol., Soc. Min. Geol. Japan, Spec. Issue, 3: 393-398.

Takin, M., 1972. Iranian geology and continental drift in the Middle-East. Nature (London) 235: 147-150.

Talluri, A., 1951., Dasatura spettrografica dell' arsenico in piriti Italiane. Soc. Toscana. Sci. Nat. Atti. Mem., 58: 3-19 (in Italian).

Tatsumi, T. and Clark, L. A., 1972. Chemical compositions of acid volcanic rocks genetically related to the formation of the Kuroko deposits. J. Geol. Soc. Japan, 78: 191-201.

Taylor, R. P., 1977. The geology of the Bakircay and Ulutas porphyry copper prospects. (Abstract). Geol. Soc. London Newsletter. 6 (2).

Taylor. S. R., 1965. The application of trace element data to problems in petrology. Phys. Chem. Earth, 6: 133-213.

Taylor S. R., 1968. Geochemistry of andesites. In: L. H, Ahrens (Editor), Origin and distribution of the elements. Pergamon Press. Oxford. 559-583.

Taylor, S. R., 1969. Trace element chemistry of andesite and associated calc-alkaline rocks. In: A. R. McBirney (Editor), Proc. Andesite Conf. Oregon Dept. Geol. Mineral Ind. Bull., 65, 43-64.

Taylor S. R. and White A. J. R., 1966. Trace element abundances in andesites. Bull. Volcanol., 29: 177-194.

Thorez, J., 1975. Phyllosilicates and clay minerals: A. laboratory handbook for their X-ray diffraction analysis. G. Lelotte, Belgique. 579pp.

Thorez, J., 1976. Practical identification of clay minerals: A handbook

for teachers and students in clay mineralogy. G. Lelotte, Belgique. 90pp.

Thorton, C. P., and Tutle, O. F., 1960. Chemistry of igneous rocks, I. Differentation Index. Am. J. Sci. 258: 664-684.

Thurlow. J. G., Swanson, E. A., and Strong, D. F., 1975. Geology and lithogeochemistry of the Burchans polymetallic sulphide deposits. Newfoundland. Econ. Geol., 70: 130-144.

Tilley, C. E., 1950. Some aspects of magmatic evolution. Quart. J. Geol. Soc. London, 106: 37-61.

Titley, S. R., 1975. Geological characteristics and environment of some porphyry copperr occurrences in the SW Pacific. Econ. Geol., 70: 499-514.

Tokel. S., 1973. The stratigraphical and volcanic history of the Gumushane area North-east Anatolia. Ph.D. Thesis University of London, (unpublished).

Tokunaga, M., and Homma, H., 1974. Fluid inclusions in the minerals from some Kuroko deposits. In: S. Ishihara (Editor), Geology of Kuroko deposits. Min. Geol. Sepc. Issue, Tokyo, 6: 385-388.

Tono, N., 1974 Minor element distrubtion around Kuroko deposits in northern Akita, Japan. In: S. Ishihara (Editor), Geology of Kuroko deposits. Min Geol. Spec. Issue, Tokyo, 6: 399-420.

Tugal, H. T., 1969. The pyritic sulphide deposits of the Lahanos Mina area, Eastern Black Sea region, Turkey. Ph.D. Thesis, University of Durham, (unpublished).

Urabe, T. and Sato, T., 1978. Kuroko deposits of the Kosaka mine, north-east Honshu, Japan. Products of submarine hot springs on Miocene sea-floor. Econ. Geol., 73: 161-179.

Utada, M., Minato, H., Ishiikawa, T. and Yoshizaki, Y., 1974. The alteration zones surrounding Kuroko-type deposits in Nishi-Aizu district Fukushima prefecture, with emphasis on the analcime zone as an indicator in exploration for ore deposits. In: S. Ishihara (Editor), Geology of Kuroko deposits. Min. Geol. Spec. Issue, Tokyo, 6: 291-302.

Van Der Voo, R., 1968. Jurassic, Cretaceous and Eocene pole positions from north-eastern Turkey. Tectonophysics, 6: 251-269.

Vokes, F. M., 1976. Caledonian massive sulphide deposits in Scandinavia: a comparative review. In: K. H. Wolf (Editor), Handbook of strata-bound and stratiform ore-deposits; v.6, Elsevier, Amsterdam, 79-127.

Vujanovic, V., 1972. The Koprubasi ore occurrence (NE Turkey). M.T.A. Bull., 79: 17-21.

Vujanovic, V., 1974. The basic mineralogic paragenetic and genetic characteristics of the sulphide deposits exposed in the eastern Black Sea coastal region (Turkey). M.T.A. Bull., 82: 21-26.

Watanabe, M., 1974. Ores and ore minerals from the Shakanai mine, Akita prefecture, Japan. In: S. Ishihara (Editor), Geology of Kuroko deposits. Min. Geol. Spec. Issue, Tokyo, 6: 337-348.

White, D. E., 1968. Environments of generation of some base-metal ore deposits. Econ. Geol., 63: 301-335.

Whitehead, R. E., 1973. Environment of stratiform sulphide deposition: Variation in the Mn: Fe ratio in host-rocks at Heath Steel mine, New Brunswick, Canada. Mineral. Dep. (Berl.), 8: 148-160.

Whitehead, R. E. S., and Goodfellow, W. D., 1978. Geochemistry of volcanic rocks from the Tetagouche Group, Bathhurst, New Brunswick, Canada. Can. J. Earth Sci., 15: 207-219.

Wilcoxon, F. and Wilcox, R. A., 1964. Some rapid approximate statistical procedure Lederle Laboratories, New York, 60pp.

Wilkinson J. F. G., 1968. The petrography of basaltic rocks. In: H. H. Hess and A. Poldervaart (Editors), Basalts, v.1. Interscience. New York. 163-214.

Wilson, A. D., 1955. A new method for the determination of ferrous iron in rocks and minerals. Bull. Geol. Soc. Great Britain, 9: 56-58.

Winchester, J. A. and Floyd, P. A., 1977. Geochemcial discrimination of different magma series and their differentation products using immobile elements. Chem. Geol., 20:325-343.

Wright. A. E., abd Bowes, D. R., 1968. Formation of explosion-breccias, Bull. Volcanol, 32: 15-32.

Wyllie, J. P., 1973. (Editor). The experimental petrology and global tectonics. Tectonophysics, 17: 187-297.

Yermakov, N. P., 1965. Research on the nature of mineral forming solutions with special reference to data from fluid inclusions. Intn. Ser. Monog. Earth Sci., v.22. Pergamon Press, Oxford, 743pp.

Yilmaz, Y., 1973. The petrology and structure of the Gumushane granite and surrounding rocks, north-east Anatolia. Ph.D. Thesis University of London, (unpublished).

Yoder, H. S. Jr., 1969. Calc-alkalic andesites:experimental data bearing on the origin of their assumed characteristics. In: A. R. McBirney (Editor). Proc. Andesite Conf., Oregon Dept. Geol. Mineral. Ind. Bull., 65: 77-89.

Yoder, H. S. Jr., and Tilley, C. E., 1962. Origin of basalt magmas: an experimental study of natural and synthetic rock systems. J. Petrol., 3: 342-532.

Yui, S., 1971. Heterogeny within a single grain of minerals of the tennantite-tetrahedrite series In: Y. Takeuchi (Editor). Proc. IMA-IAGOD Mtg., 1970. Joint Symp. Vol., Soc., Min. Geol. Japan. Spec. Issue, 2: 22-29.

Yui, S. and Czamanski, G. K., 1971. Iron content of sphalerite from the Iimori mine, Japan. In: Y. Takeuchi (Editor). Proc. IMA-IAGOD Mtg., 1970. IAGOD, vol., Soc. Min. Geol. Japan, Spec. Issue 3: 277-279.

Zankl, H., 1959. Harsit vadisi, Giresun Hakkinda rapor M.T.A. Raporu, 2689 (unpublished in Turkish).

Zankl, H., 1961. Magmatismus und hauplat des Ostpontischen gebirges in querprofil des Harsit-Tales, N.E. Anatolia, Geol. Rundschau, 51: 218-239 (in German).

APPENDIX ONE

ROCK ANALYSES

A.1.1 Sample preparation

Hand specimens of volcanic rocks were cleaned of all foreign materials prior to crushing, and split into coarse fragments of less than 5cm. diameter. Using a hydraulic rock splitter. The fragments were then reduced to gravel size using a Sturtevant Roll Jaw Crusher. The crushed sample was quartered and approximately 100 grams of the sample were ground in a Tema Laboratory Disc Mill, Model T.100 with a tungsten-carbide widia grinding barrel.

The powders were stored in sealed polythene bags. Bricquettes of the sample to be analysed were prepared by using a hydraulic ram operated at 8 tons/sq. in. Three to six drops of an inert organic binding agent, Mowiol, were added to the powder prior to compression.

A.1.2 Analysis

The bricquette samples were analysed on a Philips PW1212 automatic X-ray fluorescence spectrometer. A Cr tube in vacuum was employed for all major elements except Mn. Trace elements and Mn were determined using W radiation. The accumulation of counts for the unknowns was based on a 'fixed count' time for a monitor. This minimizes instrumental drift due to electronic instability. Data handling was performed using a procedure described by Holland and Brindle (1966).

H_2O and FeO were analysed wet chemically by Mr. R. Lambert of this Department. Water is driven off the specimen by heating to 1100-1200^{o}C and flushed by nitrogen through an absoprtion tube filled with Ca Cl_2. The tube is weighed before and after water absorption. FeO was determined for selected samples using the ammonium metavanadate method (Wilson, 1955).

Of the trace elements, lead was determined differently owing to the very strong interference of ASKα on PbKα in the presence of both elements in a sample. Standards used in this procedure were made by spiking a series fo As-free lead standards and a series of Pb-free arsenic standards, the

matrix being uncontaminated rhyolitic tuff (Sample 284). Real Pb values were thus calculated by reading the As value and its subsequent Pb equivalent Subtraction of this level from the apparent Pb figure yields the real Pb levels.

Routine operating conditions for the X-ray spectrometer are given in Table A.1.1. Lower limits of detection (LLD) for trace elements are also presented in Table A.1.1 together with the upper limits of calibration (ULC), determined using a rhyolitic tuff matrix (sample 284) spiked with certain trace elements.

The major and trace element analyses and available norm calculations are presented in Tables A.1.2 and A.1.3, respectively.

Explanation for Tables A.1.2

* In percent (inlcuding the major oxides), otherwise in ppm.

** Above the upper limits of calibration (ULC, see table A.1.1.)

0 below the lower limit of detection.

\- Not determined.

H and HK, borehole core data for Harsit-Koprubasi and Harkkoy mines, respectively (e.g. H4,10 : Harsit-Koprubasi mine, borehole 4, 10 meters).

Element	2θ	Crystal	Counter	kV	mA	Collimator	LLD	ULC
Si	109°15'	P.E.T.	Flow	60	16	Course	-	-
Al	145°13'	"	"	50	40	"	-	-
Fe	25°59'	"	"	40	8	"	-	-
Mg,p.	44°60'	ThAP	"	50	40	"	-	-
Mg,b.	47°00'	"	"	50	40	"	-	-
Ca	45°07'	P.E.T.	"	20	8	"	-	-
Na,p.	54°50'	ThAP	"	50	40	"	-	-
Na,b.	58°00'	"	"	50	40	"	-	-
K	50°58'	P.E.T.	"	60	8	"	-	-
Ti	36°58'	"	"	60	8	"	-	-
Mn,p.	95°25'	LiF110	Flow+Scint.	60	24	"	-	-
Mn,b.	97°00'	"	"	60	24	"	-	-
S,p.	75°83'	P.E.T.	Flow	50	40	"	-	12,04*
S,b.	77°00'	"	"	50	40	"		
P,p.	89°50'	"	"	50	40	Fine	-	-
P,b.	91°83'	"	"	50	40	"	-	-
Ba,p.	15°46'	LiF110	Scint.	60	32	Coarse	7	20,00*
Ba,b.	16°54'	"	"	60	32	"		
Nb,p.	30°30'	"	"	60	32	"	2	250
Nb/Zr,b.	30°81'	"	"	60	32	"		
Zr,p.	32°00'	"	"	60	32	"	2	5000
Zr/Y,b.	32°89'	"	"	60	32	"		
Y,p.	33°75'	"	"	60	32	"	2	500
Y/Sr,b.	34°78'	"	"	60	32	"		
Sr,p.	35°76'	"	"	60	32	"	2	1006
Rb/Sr,b.	36°77'	"	"	60	32	"		
Rb,p.	37°89'	"	"	60	32	"	2	1000
Rb,b.	39°60'	"	"	60	32	"		

Element	2θ	Crystal	Counter	kV	mA	Collimator	LLD	ULC
Zn,p.	59°25'	LiF110	Scint.	60	32	Coarse	2	20,00*
Zn,b.	60°50'	"	"	60	32	"		
Pb,b.	48°00'	"	"	80	24	"		
Pb,p.	48°68'	"	"	80	24	"	7	20.00*
Pb,b.	50°20'	"	"	80	24	"		
Cu,b.	64°90'	"	"	80	24	"		
Cu,p.	65°50'	"	"	80	24	"	3	20.00*
Cu,b.	66°76'	"	"	80	24	"		
Ni,b.	69°92'	"	"	60	32	"		
Ni,p.	71°24'	"	"	60	32	"	2	1000
Ni,b.	73°13'	"	"	60	32	"		
Cr,b.	105°30'	"	Flow	80	24	"		
Cr,p.	107°09'	"	"	80	24	"	3	3471
Cr,b.	109°50'	"	"	80	24	"		
Mo,b.	27°60'	"	Scint.	80	24	"		
Mo,p.	28°85'	"	"	80	24	"	2	500
Mo,b.	29°80'	"	"	80	24	"		
Sb,b.	18°40'	"	"	80	24	"		
Sb,p.	18°98'	"	"	80	24	"	3	4.00*
Sb/Cd,b.	20°80'	"	"	80	24	"		
Cd,p.	21°60'	"	"	80	24	"	3	500
Cd/Ag,b.	22°20'	"	"	80	24	"		
Ag,p.	22°60'	"	"	80	24	"	1	500
Ag,b.	23°80'	"	"	80	24	"		
As,b.	41°60'	"	"	80	24	"		
As,p.	43°54'	"	"	80	24	"	14	4.00*
As,b.	44°50'	"	"	80	24	"		

TABLE A.1.1: Optimum analysing conditions for the X-ray fluorescence spectrometer. p and b are peak and background positions, respectively.
* indicates values in percent, otherwise LLD and ULC are in ppm .

TABLE,A.1.2:LOWER BASIC SERIES,BASALTS,LOWER VOLC.CYCLE

	86	224	242	245
PERCENT				
SIO2	54.18	52.86	53.47	52.02
AL2O3	18.30	17.30	15.08	14.82
FE2O3	10.11	10.12	10.26	10.76
MGO	2.81	3.66	6.44	8.34
CAO	10.06	10.90	8.91	9.95
NA2O	2.19	1.48	1.49	2.13
K2O	0.43	0.28	0.67	0.12
TIO2	0.82	1.21	1.00	1.02
MNO	0.20	0.07	0.18	0.31
S	0.02	0.07	0.13	0.38
P2O5	0.11	0.16	0.14	0.16
TOTAL	99.23	98.11	97.77	100.01
PPM				
BA	302	115	280	126
NB	2	2	2	2
ZR	66	69	51	63
Y	21	20	17	20
SR	256	306	271	287
RB	26	7	18	5
ZN	89	310	71	73
CU	37	60	20	122
NI	0	0	2	23
CR	20	130	137	130

TABLE,A.1.2:LOWER BASIC SERIES,ANDESITES,LOWER VOLC.CYCLE

	22	23	24	25	27	28	29	30	31	32
PERCENT										
SIO2	59.75	63.06	64.32	63.13	55.36	55.41	55.52	58.07	55.04	65.32
AL2O3	16.50	15.16	15.53	15.89	17.21	15.64	17.19	14.58	16.84	13.27
FE2O3	3.01	3.11	3.21	2.62	4.30	5.63	4.53	6.66	4.63	2.45
FEO	4.08	2.19	2.34	2.39	5.95	5.42	2.69	2.15	5.63	1.67
MGO	2.46	1.23	1.30	1.33	3.68	3.26	3.15	2.67	2.35	0.84
CAO	7.70	6.71	6.85	8.11	9.52	8.24	9.05	7.11	9.03	6.69
NA2O	2.59	2.30	2.12	2.46	2.08	2.39	1.78	2.60	2.66	2.92
K2O	1.23	2.18	1.47	1.47	0.62	0.89	1.76	1.05	0.76	2.78
TIO2	0.51	0.67	0.67	0.69	0.74	1.06	0.84	0.95	1.00	0.55
MNO	0.13	0.11	0.06	0.13	0.17	0.20	0.07	0.35	0.19	0.30
S	0.03	0.03	0.03	0.03	0.03	0.03	0.03	0.04	0.03	0.04
P2O5	0.16	0.18	0.16	0.18	0.12	0.19	0.16	0.17	0.16	0.20
H2O	3.64	1.33	1.03	1.83	2.23	3.10	2.82	3.04	2.83	1.71
TOTAL	101.79	98.26	99.09	100.26	102.01	101.46	99.59	99.44	101.15	98.74
PPM										
BA	442	458	491	316	302	322	309	404	313	396
NB	4	4	2	4	3	5	3	4	4	4
ZR	87	91	91	98	79	77	72	93	73	102
Y	21	45	24	25	20	29	22	45	28	37
SR	260	230	251	239	253	258	268	270	278	200
RB	67	93	51	56	38	34	43	34	22	87
ZN	58	71	43	71	104	95	79	107	93	64
CU	3	7	5	20	27	32	55	0	32	0
NI	25	45	0	0	23	0	0	0	0	0
CR	19	25	21	26	28	19	34	13	13	0

TABLE,A.1.2:LOWER BASIC SERIES,ANDESITES,LOWER VOLC.CYCLE

	33	34	35	36	47	49	55	56	130	137
PERCENT										
SIO2	59.71	55.84	56.18	60.08	60.65	55.31	60.98	60.40	60.26	60.11
AL2O3	16.56	15.54	17.33	15.56	15.64	14.31	14.69	15.51	16.52	16.92
FE2O3	3.54	4.19	2.95	5.93	2.61	4.12	3.54	3.99	1.36	3.06
FEO	2.57	3.34	5.52	2.54	3.04	5.29	3.59	3.10	5.64	3.79
MGO	1.41	3.20	2.54	1.38	1.96	4.99	2.06	2.22	1.73	3.50
CAO	8.12	10.48	8.93	6.77	7.52	4.51	6.23	7.69	6.48	7.31
NA2O	2.23	2.35	2.89	2.64	2.91	2.56	3.17	2.91	2.35	2.23
K2O	0.99	0.52	0.56	1.73	2.17	1.70	0.85	0.79	1.28	1.23
TIO2	0.86	0.76	0.71	0.79	0.85	0.90	0.76	0.82	0.85	0.55
MNO	0.12	0.18	0.19	0.10	0.30	0.12	0.16	0.12	0.13	0.13
S	0.02	0.03	0.03	0.03	0.04	0.04	0.03	0.04	0.12	0.06
P2O5	0.19	0.25	0.10	0.15	0.14	0.13	0.21	0.18	0.19	0.15
H2O	2.32	4.37	4.28	3.15	0.83	2.91	3.83	3.44	2.12	1.96
TOTAL	98.64	101.05	102.21	100.85	98.66	96.89	100.10	101.21	99.03	101.00
PPM										
BA	276	347	354	390	523	269	367	317	446	379
NB	4	4	3	2	3	2	2	2	0	2
ZR	67	83	87	101	81	78	107	103	90	73
Y	24	31	26	33	29	26	35	33	25	40
SR	276	257	259	226	244	145	298	297	174	313
RB	34	19	29	68	34	34	74	57	32	0
ZN	83	98	78	91	97	105	101	101	82	0
CU	68	28	6	3	0	0	0	0	0	17
NI	21	24	21	0	0	0	0	32	0	0
CR	30	20	20	12	14	0	11	0	68	19

TABLE,A.1.2:LOWER BASIC SERIES,ANDESITES,LOWER VOLC.CYCLE

	200	226	230	231	232	236	237
PERCENT							
SIO2	56.13	60.89	63.80	70.75	56.43	62.18	59.31
AL203	16.17	16.70	14.99	13.36	16.27	14.98	17.43
FE203	9.40	9.08	7.94	5.47	9.51	7.44	5.88
FEO	—	—	—	—	—	—	—
MGO	5.37	3.06	2.72	0.93	5.86	3.03	1.42
CAO	9.30	7.23	6.77	5.01	7.89	7.32	6.58
NA2O	1.64	1.74	1.76	2.43	1.73	2.58	3.32
K2O	0.86	0.47	0.87	2.22	1.09	1.08	1.42
TIO2	0.88	0.95	0.71	0.58	0.96	1.02	0.82
MNO	0.11	0.17	0.16	0.03	0.12	0.17	0.10
S	0.10	0.18	0.20	0.11	0.06	0.16	0.25
P2O5	0.14	0.16	0.09	0.13	0.16	0.14	0.22
H2O	—	—	—	—	—	—	—
TOTAL	98.64	101.05	102.21	100.85	98.66	96.89	100.10
PPM							
BA	345	266	519	457	303	272	307
NB	3	4	3	2	0	4	5
ZR	49	99	92	75	67	54	95
Y	21	54	36	21	20	23	32
SR	242	314	281	237	275	269	195
RB	27	37	50	70	35	12	31
ZN	117	99	76	38	77	91	99
CU	53	0	0	1	30	10	0
NI	7	0	0	1	0	0	0
CR	38	5	3	8	153	5	7

TABLE,A.1.2:LOWER BASIC SERIES,A L T E R E D ,LOWER VOLC.CYCLE

	26	87	135	179	235	248	262	263A	H2
PERCENT									
SIO2	59.64	53.64	56.56	54.27	52.59	53.69	53.91	60.51	54.90
AL2O3	15.96	17.15	19.01	15.42	16.47	14.97	19.18	22.35	15.32
FE2O3	3.84	9.26	8.20	10.87	11.58	8.79	8.17	3.57	11.92
FEO	2.10	—	0.92	2.27	—	—	—	—	—
MGO	1.74	4.74	6.20	8.44	6.93	6.66	1.80	0.23	5.90
CAO	6.61	5.31	0.22	2.44	4.63	5.50	3.95	9.74	9.22
NA2O	2.04	4.12	0.00	0.01	4.30	3.59	2.33	0.08	1.49
K2O	3.32	2.30	5.00	5.66	0.76	1.18	2.36	0.04	0.90
TIO2	0.65	0.98	0.60	0.69	0.94	0.85	1.00	0.37	0.92
MNO	0.32	0.09	0.12	0.12	0.21	0.12	0.49	0.05	0.22
S	0.02	0.04	0.05	0.03	0.15	0.88	0.13	0.23	0.08
P2O5	2.02	0.12	0.00	0.01	0.13	0.08	0.20	0.08	0.13
H2O	2.36	—	2.42	—	—	—	—	—	—
TOTAL	100.62	97.75	99.30	100.23	98.69	96.51	93.52	97.25	101.00
PPM									
BA	444	402	27	390	309	287	93	93	197
NB	5	5	1	0	1	0	4	2	0
ZR	99	93	57	27	72	60	59	109	79
Y	48	31	15	3	23	19	116	22	22
SR	216	232	5	74	223	151	192	97	241
RB	117	51	258	169	14	12	28	0	16
ZN	60	104	47	59	71	70	293	49	63
CU	10	10	26	11	49	75	38	0	28
NI	12	0	3	12	0	0	7	0	0
CR	21	17	57	28	148	5	40	0	99

TABLE A.1.2: DACITES, LOWER VOLC. CYCLE

	1	2	5	6	11	15	16	17	18	19
PERCENT										
SIO2	69.12	71.06	73.95	64.11	68.22	65.93	70.17	67.77	68.03	68.83
AL2O3	15.22	15.61	12.71	15.37	15.64	14.81	16.41	15.20	15.54	14.51
FE2O3	3.19	3.16	0.91	1.75	2.32	0.99	0.57	0.98	1.07	1.03
FEO	—	—	2.09	2.13	1.01	1.67	1.36	2.07	1.61	1.39
MGO	1.27	0.27	0.88	1.33	0.43	1.02	0.29	0.59	0.67	0.66
CAO	3.10	2.24	3.19	4.68	2.36	3.92	0.91	1.98	2.62	3.61
NA2O	2.34	2.44	2.87	2.24	2.77	2.44	2.93	2.32	3.39	3.13
K2O	2.25	3.34	1.65	3.36	3.90	4.60	3.01	4.03	3.56	2.43
TIO2	0.38	0.42	0.34	0.40	0.41	0.34	0.32	0.29	0.39	0.37
MNO	0.10	0.04	0.05	0.07	0.05	0.05	0.06	0.03	0.07	0.08
S	0.04	0.03	0.02	0.04	0.03	0.03	0.03	0.04	0.02	0.03
P2O5	0.13	0.04	0.13	0.09	0.17	0.15	0.10	0.13	0.13	0.14
H2O	—	—	2.64	3.84	1.56	1.58	4.84	3.28	2.38	2.87
TOTAL	97.14	98.65	101.43	99.41	98.87	97.53	101.00	98.71	99.48	99.08
PPM										
BA	796	732	595	613	631	645	369	559	587	591
NB	4	3	3	5	3	2	6	6	4	4
ZR	108	119	94	115	98	105	120	122	98	98
Y	25	16	21	19	45	20	16	25	17	15
SR	151	142	164	257	154	150	126	134	150	167
RB	83	94	88	90	125	113	65	108	132	103
ZN	35	34	37	41	20	32	20	46	36	29
CU	12	0	7	0	0	7	0	0	0	0
NI	0	0	5	0	0	0	6	0	0	0
CR	20	16	10	10	5	12	10	12	6	14

TABLE A.1.2:DACITES,LOWER VOLC.CYCLE

	20	38	39	43	44	57	62	64	65
PERCENT									
SIO2	69.82	66.60	67.98	68.92	70.01	71.26	73.43	76.97	77.72
AL2O3	15.40	15.61	16.65	14.57	14.62	16.62	13.91	11.77	12.37
FE2O3	0.60	1.93	1.46	2.60	0.49	0.99	2.13	1.37	1.82
FEO	1.22	1.16	1.30	1.60	1.38	1.20	—	—	—
MGO	0.44	0.49	0.52	0.90	0.61	0.38	0.35	0.30	0.04
CAO	2.34	2.16	1.23	1.58	1.93	0.58	0.78	1.02	1.17
NA2O	2.98	2.94	1.84	1.75	2.66	1.46	3.67	2.62	2.56
K2O	3.01	4.51	5.79	2.46	4.38	3.54	3.70	4.18	3.85
TIO2	0.32	0.32	0.28	0.41	0.26	0.31	0.22	0.18	0.23
MNO	0.05	0.08	0.10	0.04	0.08	0.04	0.03	0.03	0.05
S	0.03	0.03	0.03	0.04	0.02	0.02	0.03	0.03	0.02
P2O5	0.13	0.13	0.12	0.10	0.12	0.10	0.03	0.03	0.05
H2O	3.05	1.72	3.01	4.49	1.37	3.14	—	—	—
TOTAL	97.14	98.65	101.43	99.41	98.87	97.53	101.00	98.71	99.48
PPM									
BA	594	622	509	543	507	530	316	174	472
NB	4	2	6	2	5	4	5	4	2
ZR	99	110	99	81	97	131	118	101	119
Y	16	14	18	37	15	19	18	17	22
SR	151	142	101	89	120	125	65	67	150
RB	101	108	111	117	112	86	73	95	98
ZN	41	28	41	30	20	17	43	34	35
CU	0	0	0	0	0	0	0	0	0
NI	0	0	0	0	0	0	0	0	0
CR	10	11	10	10	0	0	8	5	0

TABLE A.1.2:DACITES,LOWER VOLC.CYCLE

	136	139	164	220	221	226
PERCENT						
SIO2	69.90	73.48	73.04	73.71	74.33	72.26
AL2O3	17.21	14.73	13.73	14.21	14.18	13.86
FE2O3	2.96	2.34	2.03	2.68	2.68	3.09
FEO	0.35	0.11	0.71	—	—	—
MGO	0.18	0.11	0.76	0.15	0.24	0.12
CAO	1.89	1.60	3.57	2.14	2.31	2.70
NA2O	2.29	2.22	3.19	2.64	2.74	3.14
K2O	3.34	4.91	2.31	4.18	4.14	3.37
TIO2	0.40	0.30	0.28	0.29	0.29	0.32
MNO	0.01	0.07	0.08	0.06	0.05	0.12
S	0.04	0.07	0.16	0.11	0.10	0.12
P2O5	0.07	0.06	0.06	0.04	0.07	0.09
H2O	—	—	—	—	—	—
TOTAL	98.64	100.00	99.92	99.91	101.13	99.19
PPM						
BA	728	613	329	555	687	702
NB	2	1	4	1	2	3
ZR	100	92	140	104	96	102
Y	19	53	23	11	11	16
SR	116	140	280	163	166	171
RB	104	90	64	102	107	112
ZN	33	0	40	22	26	25
PB	19	20	17	—	—	—
CU	0	0	0	0	0	0
NI	0	0	0	0	0	0
CR	25	4	0	9	0	0
MO	0	0	0	—	—	—

TABLE A.1.2:DACITES,A L T E R E D ,LOWER VOLC.CYCLE

	3	4	10	37	40	42	45	46	48	50
PERCENT										
SIO2	80.18	75.32	66.51	65.02	67.65	66.75	68.81	74.33	56.93	68.91
AL2O3	10.08	12.87	19.07	17.33	17.31	17.89	14.31	12.61	14.12	12.69
FE2O3	1.64	0.40	2.36	1.78	2.89	0.59	1.09	0.01	7.63	2.95
FEO	—	—	0.99	1.36	—	1.50	1.14	2.00	—	1.79
MGO	0.31	0.06	0.45	0.60	0.24	0.70	0.83	0.61	3.61	0.72
CAO	1.21	0.61	0.35	1.78	0.79	1.73	1.43	1.62	8.87	0.85
NA2O	1.67	2.15	0.62	2.00	1.13	2.19	2.89	2.79	2.05	1.71
K2O	3.32	5.14	6.43	4.97	7.04	3.23	3.58	2.39	2.76	5.22
TIO2	0.15	0.16	0.40	0.31	0.31	0.26	0.29	0.29	0.98	0.27
MNO	0.03	0.02	0.10	0.04	0.05	0.05	0.16	0.02	0.19	0.11
S	0.05	0.02	0.03	0.03	0.03	0.03	0.02	0.03	0.04	0.03
P2O5	0.04	0.03	0.10	0.12	0.03	0.09	0.44	0.10	0.23	0.11
H2O	—	—	3.02	4.11	—	3.92	3.69	2.45	—	0.86
TOTAL	98.68	96.78	100.43	99.45	97.47	98.93	98.68	99.25	97.41	96.22
PPM										
BA	1294	1297	851	615	427	591	470	475	383	1161
NB	7	7	4	2	5	4	6	1	1	5
ZR	86	106	105	106	115	108	141	124	71	121
Y	19	15	20	19	15	15	23	52	42	23
SR	132	124	60	113	59	112	108	114	215	53
RB	112	179	149	112	120	124	65	68	48	115
ZN	24	16	32	32	31	17	36	23	96	45
CU	0	0	0	0	0	0	0	0	0	0
NI	0	11	0	0	0	0	0	0	0	0
CR	0	0	9	10	8	9	6	0	0	0

TABLE A.1.2:DACITES,A L T E R E D ,LOWER VOLC.CYCLE

	58	85	129	129A	160	162	163	203	212	218
PERCENT										
SIO2	65.64	65.43	54.32	75.14	71.58	77.02	73.59	79.95	66.16	73.02
AL2O3	16.06	14.56	20.65	13.20	16.71	11.64	13.44	12.54	16.95	20.43
FE2O3	2.28	2.25	14.55	0.01	1.65	1.24	1.65	1.26	3.04	1.67
FEO	1.12	—	—	3.00	0.13	0.73	0.46	—	0.37	—
MGO	1.64	0.32	3.12	0.34	2.32	0.51	0.12	0.20	3.48	0.50
CAO	0.84	5.67	0.38	2.33	1.31	2.64	1.08	0.31	1.96	0.24
NA2O	0.00	4.37	0.05	2.77	0.36	2.80	3.22	0.88	1.22	0.01
K2O	0.24	2.65	2.46	2.18	1.37	2.80	4.79	1.63	3.67	2.12
TIO2	0.34	0.42	0.90	0.28	0.28	0.20	0.24	0.16	0.40	0.32
MNO	0.05	0.07	0.06	0.06	0.20	0.07	0.05	0.01	0.07	0.01
S	0.02	0.05	0.10	0.02	0.05	0.10	0.06	0.05	0.04	1.78
P2O5	0.07	0.12	0.04	0.07	0.01	0.18	0.04	0.03	0.03	0.01
H2O	14.36	—	—	—	5.00	—	—	—	3.92	—
TOTAL	102.66	95.91	96.63	99.40	100.97	99.93	98.74	97.02	101.31	100.11
PPM										
BA	176	179	114	599	1244	395	464	285	1038	405
NB	6	4	1	3	9	5	4	2	6	3
ZR	159	106	56	92	126	100	131	114	163	107
Y	24	25	27	17	27	22	24	10	66	14
SR	58	122	3	134	197	98	68	244	309	18
RB	10	50	130	80	83	63	94	111	175	62
ZN	60	34	87	18	55	30	41	3	56	8
PB	—	—	26	31	59	19	26	—	—	—
CU	0	0	31	0	0	0	0	6	0	0
NI	0	0	0	0	0	0	0	0	0	0
CR	14	13	25	0	0	0	0	0	347	0
MO	—	—	0	0	0	0	0	—	—	—

TABLE A.1.2: DACITES, A L T E R E D , LOWER VULC. CYCLE

	227	241	249	255	256	257	259	260
PERCENT								
SIO2	76.58	74.17	71.08	59.44	88.10	77.41	84.29	77.22
AL2O3	15.28	14.29	14.44	24.02	6.55	13.51	9.02	14.05
FE2O3	2.54	2.87	2.85	4.22	2.88	0.63	0.53	0.24
MGO	0.11	0.08	0.26	3.95	0.32	0.00	0.02	0.09
CAO	1.18	0.64	0.22	1.15	0.00	0.17	0.28	0.28
NA2O	1.63	5.87	8.37	0.03	0.48	1.61	1.44	0.62
K2O	2.65	0.40	0.67	0.32	0.53	4.99	3.56	8.42
TIO2	0.28	0.32	0.14	0.52	0.15	0.12	0.09	0.24
MNO	0.07	0.16	0.02	0.12	0.89	0.02	0.03	0.01
S	0.15	0.25	0.04	0.02	0.08	0.03	0.02	0.03
P2O5	0.03	0.06	0.02	0.03	0.01	0.01	0.01	0.02
TOTAL	100.50	99.11	98.11	93.85	99.99	98.50	99.29	101.22
PPM								
BA	493	158	76	439	277	1135	913	280
NB	2	2	7	7	2	5	3	8
ZR	95	98	217	138	19	72	60	125
Y	9	31	68	31	4	10	12	8
SR	86	174	54	120	18	70	81	64
RB	94	13	10	48	18	163	109	232
ZN	35	58	80	70	18	5	8	3
CU	0	0	0	0	42	0	0	0
NI	0	0	0	1	2	0	0	0
CR	0	10	0	30	8	0	0	0

TABLE A.1.2:QUARTZ-FELDSPAR PORPHYRY,LOWER VOLC.CYCLE

	54	234	243	246	247
PERCENT					
SIO2	65.27	75.82	71.32	68.80	74.76
AL2O3	15.02	14.36	16.81	16.87	15.89
FE2O3	1.74	1.10	1.50	1.30	1.30
FEO	1.90	0.88	—	0.90	0.90
MGO	1.33	0.10	0.43	2.09	2.07
CAO	3.32	1.26	1.39	1.89	0.63
NA2O	2.70	2.46	3.29	2.91	4.34
K2O	3.24	3.40	5.50	2.81	2.68
TIO2	0.36	0.29	0.20	0.24	0.28
MNO	0.03	0.03	0.02	0.10	0.06
S	0.05	0.05	0.08	0.21	0.15
P2O5	0.14	0.05	0.05	0.05	0.06
H2O	1.67	—	—	—	—
TOTAL	96.77	99.80	100.59	98.17	103.12
PPM					
BA	487	492	147	418	510
NB	4	5	1	3	3
ZR	115	121	112	116	130
Y	28	18	21	22	27
SR	87	110	35	37	80
RB	94	110	100	68	65
ZN	33	16	18	27	36
CU	0	0	0	0	0
NI	0	0	1	1	0
CR	0	3	22	0	11

TABLE A.1.2: DACITIC-RHYOLITIC HOST ROCK, LOWER VOLC. CYCLE

	53	59	60	61	83	84	140	233
PERCENT								
SIO2	69.61	77.65	71.85	74.61	71.94	76.18	70.97	75.44
AL2O3	15.07	12.12	16.11	15.64	16.50	12.47	15.13	13.71
FE2O3	2.04	0.01	0.72	1.90	2.31	1.76	1.95	1.59
FEO	1.14	1.44	1.12	—	—	—	0.22	—
MGO	0.33	0.51	0.37	0.18	0.65	0.16	0.56	0.28
CAO	3.00	1.61	0.13	0.10	0.55	0.57	1.33	1.17
NA2O	3.96	1.69	2.95	1.85	4.16	2.71	3.65	3.97
K2O	1.22	3.30	3.06	4.01	1.72	3.21	2.57	3.50
TIO2	0.12	0.24	0.20	0.10	0.19	0.15	0.22	0.13
MNO	0.11	0.03	0.03	0.04	0.01	0.01	0.07	0.04
S	0.03	0.03	0.03	0.03	0.06	0.03	0.06	0.09
P2O5	0.22	0.09	0.08	0.02	0.03	0.03	0.05	0.01
H2O	0.76	1.19	2.18	—	—	—	—	—
TOTAL	96.61	99.91	98.83	98.48	98.52	97.26	96.78	99.93
PPM								
BA	405	401	80	174	93	194	396	125
NB	4	4	8	10	8	5	4	7
ZR	116	113	207	231	246	104	127	203
Y	46	22	63	68	60	25	58	46
SR	197	121	15	17	28	188	130	97
RB	29	91	39	64	26	57	0	50
ZN	95	21	32	29	28	50	0	51
CU	0	0	17	0	0	31	0	0
NI	0	0	0	0	0	0	0	0
CR	0	0	5	6	10	0	0	0

TABLE A.1.2:DACITIC-RHYOLITIC HOST ROCK,A L T E R E D ,LOWER VOLC.CYCLE

	12	13	52	63	66	68	69	74	75A	75B
PERCENT										
SIO2	67.71	65.60	69.33	61.69	60.43	80.76	58.75	69.20	84.00	51.40
AL2O3	21.64	20.69	15.78	14.89	13.34	10.88	11.80	13.53	5.61	18.94
FE2O3	1.33	0.00	0.41	2.23	3.40	2.06	1.55	2.09	4.04	10.52
FEO	1.05	2.99	0.85	—	—	—	—	—	—	—
MGO	0.58	0.92	0.32	1.63	0.62	0.41	7.56	1.49	0.30	7.51
CAO	0.08	0.16	0.25	9.30	11.00	0.09	11.78	0.27	0.40	0.87
NA2O	0.03	0.04	5.10	0.34	3.64	0.28	0.01	1.80	1.74	2.83
K2O	4.25	4.42	5.50	5.10	1.44	2.98	2.07	8.09	1.14	1.41
TIO2	0.44	0.39	0.30	0.18	0.33	0.05	0.11	0.24	0.08	1.00
MNO	0.01	0.01	0.36	0.04	0.17	0.02	0.10	0.04	0.02	0.48
S	0.02	0.20	0.02	0.03	0.05	0.10	0.03	0.02	1.15	1.31
P2O5	0.08	0.08	0.07	0.06	0.07	0.01	0.02	0.02	0.02	0.09
H2O	3.91	2.70	0.03	—	—	—	—	—	—	—
TOTAL	101.13	98.20	98.32	95.49	94.49	97.64	93.78	96.79	98.50	96.36
PPM										
BA	644	734	427	179	208	287	102	453	526	147
NB	2	4	8	5	9	5	4	6	1	2
ZR	106	115	194	143	144	97	98	177	56	41
Y	15	22	25	23	37	53	24	27	15	22
SR	18	8	51	246	106	8	40	39	48	26
RB	134	167	72	64	39	44	41	81	6	36
ZN	10	17	18	40	91	66	74	109	0	449
CU	0	0	0	0	72	2559	33	96	1225	176
NI	0	0	0	0	2	0	0	0	0	0
CR	16	90	0	0	13	0	6	6	0	41

TABLE A.1.2: DACITIC-RHYOLITIC HOST ROCK, A L T E R E D , LOWER VOLC. CYCLE

	77	79	82	100	101	103	106	107	107A	108
PERCENT										
SIO2	72.02	85.77	76.27	84.36	55.05	91.85	84.85	80.42	70.11	87.10
AL2O3	15.70	8.22	14.57	12.42	34.62	5.71	11.21	3.24	5.82	4.56
FE2O3	0.55	2.51	1.69	3.26	4.60	2.90	3.20	3.68	18.08	3.64
MGO	0.29	0.20	1.63	0.32	0.00	0.15	0.10	0.06	0.12	0.09
CAO	1.09	0.01	0.08	0.04	0.39	0.06	0.02	0.36	0.01	0.11
NA2O	0.37	0.00	0.06	0.58	0.20	0.47	0.53	0.01	0.49	0.01
K2O	6.64	1.87	2.39	0.21	0.01	1.00	0.64	0.58	1.02	0.93
TIO2	0.16	0.05	0.06	0.23	0.86	0.08	0.20	0.33	0.35	0.20
MNO	0.06	0.01	0.02	0.01	0.05	0.01	0.01	0.01	0.01	0.01
S	0.03	0.04	0.05	0.02	0.04	0.22	0.02	8.00	0.60	1.66
P2O5	0.04	0.01	0.01	0.01	0.06	0.01	0.03	0.01	0.01	0.01
TOTAL	96.95	98.69	96.83	101.46	95.88	102.46	100.81	96.70	96.62	98.32
PPM										
BA	1214	363	686	61	82	313	108	2.28*	6932	1.46*
NB	10	1	7	1	7	1	5	0	0	2
ZR	117	61	146	122	149	56	132	54	21	65
Y	26	22	36	11	18	10	21	4	1	7
SR	31	9	9	10	328	4	198	815	2	3
RB	175	15	27	5	0	4	17	0	6	0
ZN	15	25	237	22	14	43	7	82	454	421
PB	—	—	—	60	585	1239	10	3861	712	3399
CU	0	259	2	0	21	39	8	278	1414	634
NI	0	0	0	0	0	0	0	0	0	0
CR	0	0	34	0	120	16	0	0	0	0
MO	—	—	—	0	0	0	0	19	89	27

TABLE A.1.2:DACITIC-RHYOLITIC HOST ROCK,A L T E R E D ,LOWER VOLC.CYCLE

	110	111	112	113M	113WR	115	116	117	119	120
PERCENT										
SIO2	71.25	81.28	79.95	56.30	86.55	90.01	91.35	41.13	91.07	93.96
AL2O3	20.92	11.98	3.02	1.88	5.03	5.49	4.81	4.84	6.04	2.41
FE2O3	0.92	3.96	7.08	10.62	5.99	1.16	2.92	40.41	0.28	4.20
MGO	0.08	0.40	0.20	0.09	0.35	0.20	0.17	0.08	0.20	0.12
CAO	0.18	0.02	0.16	0.16	0.18	0.02	0.02	0.45	0.09	0.01
NA2O	0.61	0.49	0.00	1.12	0.01	0.52	0.47	0.09	0.46	0.48
K2O	6.19	2.44	0.81	0.74	1.21	0.26	0.86	0.41	0.80	0.16
TIO2	0.28	0.16	0.02	0.04	0.09	0.37	0.09	0.06	0.14	0.02
MNO	0.07	0.01	0.00	0.01	0.01	0.00	0.01	0.00	0.03	0.01
S	0.03	0.43	4.13	17.33	2.40	0.05	0.05	1.04	0.19	0.10
P2O5	0.03	0.01	0.00	0.00	0.01	0.01	0.01	0.02	0.00	0.02
TOTAL	100.56	101.18	95.37	88.29	101.83	98.11	100.76	88.53	99.30	101.49
PPM										
BA	31	104	16	549	144	4	1158	360	2280	111
NB	2	3	0	0	3	4	2	0	1	0
ZR	129	79	34	25	43	220	62	34	34	6
Y	14	14	21	9	9	24	27	16	4	4
SR	75	14	1	0	3	15	3	14	40	60
RB	105	34	0	0	6	8	0	0	10	0
ZN	157	58	1828	5.16*	1033	49	35	251	10	2
PB	87	403	1.20*	6307	2016	42	3203	9172	854	172
CU	13	23	2659	2.87*	332	31	19	1344	13	27
NI	0	0	0	0	0	0	0	0	0	0
CR	0	26	22	52	36	0	45	6	0	0
MO	0	0	20	187	11	0	0	100	0	13

TABLE A.1.2:DACITIC-RHYOLITIC HOST ROCK,A L T E R E D ,LOWER VOLC.CYCLE

	123	134	142	143	145	146	147	147A	149	150
PERCENT										
SIO2	88.39	77.96	63.87	82.67	76.99	74.03	72.60	86.22	81.75	80.02
AL2O3	5.47	12.45	16.75	10.29	14.41	13.65	9.24	3.08	13.73	13.68
FE2O3	1.70	0.87	2.02	0.69	0.57	3.32	6.99	1.20	0.63	1.26
FEO	1.92	0.29	1.11	0.31	1.27	—	—	—	0.28	0.36
MGO	0.12	3.19	3.94	0.01	0.75	0.62	0.84	1.73	0.59	0.55
CAO	0.13	0.82	7.72	0.11	0.23	0.28	0.65	2.59	0.09	0.03
NA2O	0.52	0.31	1.90	5.61	1.49	2.66	0.01	0.50	0.55	0.55
K2O	1.05	0.58	2.05	0.13	2.71	2.46	2.87	0.36	2.15	3.34
TIO2	0.14	0.19	0.26	0.05	0.15	0.15	0.07	0.02	0.07	0.12
MNO	0.20	0.03	0.12	0.01	0.02	0.01	0.03	0.08	0.02	0.01
S	0.07	0.02	0.09	0.07	0.43	3.05	3.50	0.26	0.10	0.05
P2O5	0.06	0.00	0.04	0.01	0.02	0.00	0.00	0.04	0.01	0.01
H2O	—	4.60	—	—	—	—	—	—	—	—
TOTAL	99.77	101.31	99.87	99.96	99.04	100.63	98.80	96.08	99.97	99.98
PPM										
BA	141	804	141	70	261	311	317	4	176	844
NB	1	6	7	7	3	4	3	3	7	6
ZR	73	99	125	175	126	127	136	8	125	153
Y	12	17	14	79	16	26	37	105	52	53
SR	307	92	72	41	20	33	2	47	8	5
RB	44	25	50	3	71	63	53	6	38	47
ZN	52	33	126	0	128	2	52	38	48	1
PB	17	63	0	20	840	81	94	2	0	10
CU	4	0	0	0	77	0	0	0	0	0
NI	0	0	28	0	2	0	0	0	0	0
CR	12	0	0	0	774	0	25	0	608	1130
MO	0	0	0	0	0	370	33	0	0	0

TABLE A.1.2:DACITIC-RHYOLITIC HOST ROCK,A L T E R E D ,LOWER VOLC.CYCLE

	151	152	153	154	156	169	169A	171	172	174
PERCENT										
SIO2	87.27	61.41	68.53	85.72	68.30	70.26	72.00	76.98	72.61	69.77
AL2O3	9.45	21.33	19.45	10.09	18.31	15.31	14.08	12.70	13.60	6.04
FE2O3	0.41	4.22	1.97	0.28	1.27	1.27	1.35	0.18	0.98	2.03
FEO	0.31	—	0.44	0.44	0.85	0.23	0.13	0.66	0.16	—
MGO	0.45	2.20	2.53	0.38	2.53	2.45	3.40	0.26	2.04	0.04
CAO	0.04	0.80	0.45	0.01	0.52	1.58	1.65	0.66	1.73	0.31
NA2O	0.56	0.09	0.99	0.52	1.29	1.27	0.47	2.15	1.36	0.01
K2O	1.32	5.62	3.77	2.42	3.33	2.04	0.60	5.95	2.63	0.05
TIO2	0.05	0.15	0.11	0.05	0.11	0.31	0.29	0.22	0.30	0.87
MNO	0.02	0.05	0.05	0.01	0.08	0.07	0.28	0.07	0.16	0.01
S	0.09	0.17	0.16	0.14	0.24	0.05	0.05	0.05	0.14	4.72
P2O5	0.00	0.02	0.01	0.01	0.01	0.01	0.01	0.03	0.03	0.00
H2O	2.91	—	—	—	—	6.05	5.90	—	6.41	—
TOTAL	102.88	96.06	98.46	100.07	96.84	100.90	100.21	99.91	102.15	83.85
PPM										
BA	47	408	219	97	222	1594	1627	1428	1822	13.20*
NB	5	11	10	4	6	15	11	12	12	0
ZR	98	226	215	107	174	162	132	126	136	48
Y	53	79	108	31	59	24	39	59	11	0
SR	3	27	19	1	11	191	202	98	307	1108
RB	37	102	81	63	90	161	91	134	121	0
ZN	57	153	99	0	95	57	79	16	48	25
PB	34	78	0	123	7	65	39	70	79	804
CU	0	11	0	0	0	0	0	0	8	46
NI	0	0	0	0	12	0	0	0	0	0
CR	183	101	147	0	1766	0	0	0	15	0
MO	0	0	0	0	0	0	0	0	0	3

TABLE A.1.2:DACITIC-RHYOLITIC HOST ROCK,A L T E R E D ,LOWER VOLC.CYCLE

	177	183	190A	192A	193	195	196	198	199	202
PERCENT										
SIO2	75.30	71.43	73.50	67.49	41.99	66.57	78.90	85.53	67.35	76.04
AL2O3	12.41	11.69	3.30	26.34	35.41	24.48	11.79	10.72	19.08	9.84
FE2O3	1.19	0.96	1.04	0.72	12.91	1.70	3.00	0.81	2.01	5.46
MGO	0.09	0.35	0.11	0.01	0.39	0.03	0.07	0.36	2.37	0.63
CAO	0.74	1.97	0.18	0.01	0.28	3.59	0.19	0.01	6.09	0.25
NA2O	1.71	1.29	0.00	0.01	0.00	0.27	0.00	0.50	0.01	0.00
K2O	4.10	1.99	0.80	0.03	0.00	0.18	0.25	2.16	1.91	2.42
TIO2	0.49	0.20	1.77	0.92	1.62	0.47	0.76	0.14	0.40	0.38
MNO	3.33	0.02	0.00	0.01	0.69	0.07	0.00	0.01	0.11	0.00
S	0.13	0.13	3.07	0.39	1.66	0.20	2.48	0.28	0.41	6.87
P2O5	0.02	0.03	0.00	0.02	0.05	0.06	0.05	0.01	0.09	0.00
TOTAL	99.51	90.06	83.77	95.95	95.00	97.62	97.49	100.53	99.83	101.89
PPM										
BA	5241	1049	12.73*	5700	2611	1356	7360	217	550	6571
NB	8	7	3	27	7	11	6	1	6	2
ZR	153	104	43	316	157	142	99	65	139	25
Y	49	10	3	20	30	21	14	11	25	6
SR	101	173	864	927	593	564	591	1	435	16
RB	104	57	5	0	0	0	9	3	36	40
ZN	75	34	3798	4	54	20	53	461	410	700
PB	59	40	1824	—	—	—	—	—	—	—
CU	1	0	2897	0	181	35	47	55	13	2236
NI	0	0	0	0	9	1	0	0	0	6
CR	0	0	0	25	43	11	0	4	144	0
MO	0	0	11	—	—	—	—	—	—	—

TABLE A.1.2:DACITIC-RHYOLITIC HOST ROCK,A L T E R E D ,LOWER VOLC.CYCLE

	204	206	215	216	217	219	225	229	238	239
PERCENT										
SIO2	81.66	65.21	77.87	71.03	83.22	64.24	75.08	71.89	74.84	72.52
AL2O3	16.48	17.16	17.00	18.57	12.70	22.68	16.38	17.66	17.64	18.36
FE2O3	0.90	4.21	0.43	5.33	0.29	4.59	1.39	1.43	2.97	2.20
MGO	0.01	1.38	0.10	0.11	0.48	2.89	0.29	0.13	0.06	0.04
CAO	0.01	2.80	0.03	0.20	0.03	1.28	0.27	0.04	0.13	0.28
NA2O	0.36	2.56	0.36	0.11	0.35	0.31	0.05	1.25	1.14	2.17
K2O	0.22	4.82	3.82	0.19	2.79	0.05	5.13	5.58	2.94	3.83
TIO2	0.23	0.74	0.29	0.22	0.34	0.39	0.31	0.20	0.30	0.35
MNO	0.01	0.17	0.03	0.01	0.01	0.02	0.01	0.03	0.14	0.06
S	0.10	0.11	0.09	5.21	0.10	0.03	1.47	0.06	0.06	0.09
P2O5	0.01	0.29	0.00	0.01	0.01	0.00	0.01	0.01	0.02	0.03
TOTAL	99.99	99.45	100.02	100.99	100.32	96.46	100.39	98.28	100.24	99.93
PPM										
BA	1345	2039	257	0	688	190	721	875	86	98
NB	4	8	3	1	3	6	2	11	10	11
ZR	157	176	98	78	86	135	76	140	213	229
Y	40	35	8	0	6	40	7	18	13	49
SR	120	375	0	42	9	95	39	41	73	262
RB	8	197	109	0	77	2	117	194	74	77
ZN	8	71	0	0	2	67	2	13	29	25
CU	0	0	0	11	0	0	0	0	0	0
NI	0	0	3	0	0	0	0	260	0	0
CR	0	0	945	20	25	109	40	0	0	0

TABLE A.1.2:DACITIC-RHYOLITIC HOST ROCK,A L T E R E D ,LOWER VOLC.CYCLE

	264	265	268	269	274A	278	279	280	281	281A
PERCENT										
SIO2	75.52	87.89	84.94	91.69	59.10	81.68	74.36	80.60	76.87	83.23
AL2O3	15.27	5.62	6.68	4.72	23.28	12.46	19.43	12.33	19.77	15.85
FE2O3	1.48	4.52	1.60	0.76	2.83	0.59	0.23	4.61	0.47	0.58
MGO	0.00	0.00	0.34	0.36	5.10	0.54	0.13	0.00	0.00	0.00
CAO	0.00	0.00	0.44	0.00	1.47	0.39	0.11	0.12	0.10	0.10
NA2O	0.62	0.40	0.20	0.39	0.02	0.00	0.27	0.32	0.31	0.31
K2O	4.98	0.07	0.99	0.94	0.07	2.15	0.51	0.02	0.03	0.05
TIO2	0.13	0.14	0.17	0.04	0.21	0.39	0.89	0.27	0.27	0.20
MNO	0.00	0.19	0.01	0.00	0.03	0.00	0.00	0.00	0.00	0.00
S	0.03	0.07	1.64	0.09	0.01	1.08	0.79	0.20	0.15	0.06
P2O5	0.01	0.10	0.00	0.00	0.02	0.00	0.00	0.01	0.01	0.01
TOTAL	98.04	99.00	97.01	98.99	92.14	99.28	96.72	98.48	97.98	100.39
PPM										
BA	26	196	3508	75	227	9785	9278	2613	1841	281
NB	1	2	3	3	9	5	10	8	11	12
ZR	107	91	46	34	110	69	154	89	113	123
Y	16	8	14	7	60	14	9	13	19	17
SR	43	865	67	0	88	362	159	34	44	35
RB	76	8	0	14	0	28	5	7	7	7
ZN	16	36	163	53	770	20	76	81	0	1
CU	0	0	147	24	72	12	2	8	0	0
NI	0	0	0	0	0	0	0	0	0	0
CR	0	3	0	0	0	4	0	0	1	0

TABLE A.1.2:DACITIC-RHYOLITIC HOST ROCK,A L T E R E D ,LOWER VOLC.CYCLE

	283	284	286	289	290	291	292	300	312	313
PERCENT										
SIO2	77.52	80.19	70.73	93.47	88.70	93.60	78.68	39.90	77.37	67.23
AL2O3	19.02	18.48	24.08	4.35	6.13	0.00	6.06	33.82	18.21	21.80
FE2O3	0.62	0.62	1.14	0.10	0.06	1.50	2.04	16.85	0.64	2.22
MGO	0.00	0.01	0.00	0.04	0.00	0.37	0.19	2.56	0.40	0.20
CAO	0.10	0.12	0.13	0.00	0.00	0.55	0.91	0.00	0.12	0.35
NA2O	0.28	0.33	0.30	0.35	0.40	0.00	0.15	0.65	0.27	0.00
K2O	0.00	0.27	0.00	0.56	0.00	1.12	0.06	0.19	1.02	0.00
TIO2	0.17	0.19	0.85	0.17	0.85	0.43	0.98	1.90	0.56	2.56
MNO	0.00	0.00	0.00	0.00	0.01	0.01	0.00	1.35	0.00	0.00
S	0.15	0.06	0.06	0.14	0.91	2.42	4.53	0.10	0.40	1.98
P2O5	0.01	0.03	0.12	0.00	0.00	0.00	0.00	0.07	0.01	0.05
TOTAL	97.87	100.30	97.41	99.18	97.06	100.00	93.60	97.39	99.00	96.39
PPM										
BA	402	238	57	2354	1.12*	5271	2.23*	267	6493	2.16*
NB	7	10	5	1	2	1	1	7	8	9
ZR	97	133	106	20	26	72	42	164	93	152
Y	14	25	5	1	6	25	2	22	28	12
SR	17	274	860	47	336	170	1023	617	80	912
RB	3	15	3	24	4	0	0	0	18	1
ZN	16	3	0	5	3	1852	161	597	72	78
CU	0	0	0	0	3	3768	50	187	37	71
NI	0	0	0	0	0	0	0	37	0	0
CR	0	0	42	0	1	0	0	56	5	0

TABLE A.1.2:DACITIC-RHYOLITIC HOST ROCK,A L T E R E D ,LOWER VOLC.CYCLE

	323	324	325	326	327	328	343	344	345	376
PERCENT										
SIO2	62.96	85.94	51.98	49.36	60.90	46.58	79.20	75.96	76.28	56.75
AL2O3	25.08	4.65	41.54	40.32	29.45	28.06	12.16	14.40	19.74	30.04
FE2O3	4.23	0.82	0.84	1.22	0.53	16.41	1.25	0.84	0.48	0.82
MGO	0.00	0.00	0.20	0.28	0.36	0.55	0.68	0.12	0.06	0.00
CAO	0.00	0.00	0.35	0.36	0.42	0.56	1.15	0.03	0.11	0.00
NA2O	0.00	0.38	0.00	0.00	0.06	0.19	0.77	1.73	0.36	0.00
K2O	0.00	1.10	0.00	0.00	0.94	0.00	4.46	6.82	0.17	0.00
TIO2	1.12	0.90	0.31	0.95	2.11	1.78	0.27	0.16	0.36	0.45
MNO	0.00	0.00	0.00	0.00	0.00	1.48	0.03	0.08	0.00	0.01
S	0.26	1.12	1.78	4.52	1.71	1.86	0.13	0.12	0.35	0.04
P2O5	0.07	0.01	0.00	0.00	0.00	0.11	0.04	0.03	0.00	0.00
TOTAL	93.72	94.92	97.00	97.01	96.48	97.58	100.14	100.29	97.91	88.11
PPM										
BA	4208	1.15*	2.62*	1.11*	2.06*	3167	1922	1023	4108	39
NB	9	0	17	22	14	6	11	9	7	23
ZR	181	16	297	337	226	148	143	85	95	337
Y	29	4	21	11	10	30	17	13	15	27
SR	1031	499	1028	135	454	932	242	58	98	17
RB	0	0	0	0	25	0	168	182	10	4
ZN	79	496	0	5	14	50	31	6	3	8
PB	1700	1920	55	234	70	33	19	18	18	72
CU	168	451	0	28	0	219	0	0	0	0
NI	0	0	0	0	0	7	0	0	0	0
CR	50	0	0	0	30	57	15	24	10	370
MO	0	3	1	39	3	0	0	0	0	0

TABLE A.1.2:DACITIC-RHYOLITIC HOST ROCK,A L T E R E D ,LOWER VOLC.CYCLE

	377	379	H1	H4
PERCENT				
SIO2	72.31	66.20	58.75	72.77
AL2O3	23.74	27.02	17.25	20.92
FE2O3	0.26	0.55	11.90	2.98
MGO	0.07	0.07	2.54	0.26
CAO	0.09	0.24	1.60	0.15
NA2O	0.31	0.28	0.01	0.00
K2O	1.27	0.34	1.67	1.40
TIO2	0.32	0.69	1.05	0.10
MNO	0.00	0.01	0.29	0.09
S	0.05	0.46	0.01	0.00
P2O5	0.01	0.00	0.04	0.03
TOTAL	93.72	94.92	97.00	97.01
PPM				
BA	242	6465	324	839
NB	9	11	3	2
ZR	168	200	91	121
Y	9	17	39	38
SR	25	100	113	72
RB	32	9	62	19
ZN	1	49	88	58
PB	120	32	—	—
CU	0	0	16	28
NI	0	0	0	0
CR	0	0	—	—
MO	0	0	—	—

TABLE A.1.2: SEDIMENTARY, TUFFACECLS SEDIMENTARY SERIES

	9	102	104	105	109	125	144A	173	191A	191B
PERCENT										
SIO2	94.27	95.73	45.03	76.17	24.91	47.19	58.46	78.05	75.63	81.34
AL2O3	3.03	2.78	39.85	19.38	3.56	11.91	15.62	14.48	18.34	16.86
FE2O3	0.02	0.59	8.86	2.48	70.44	2.91	2.73	1.94	4.70	0.17
MGO	0.03	0.00	0.00	0.00	0.08	4.06	9.30	0.02	0.01	0.01
CAO	0.00	0.06	0.34	0.21	0.34	14.98	0.62	0.03	0.01	0.01
NA2O	0.00	0.56	0.00	0.39	0.13	0.07	6.70	0.48	0.47	0.47
K2O	0.71	0.21	0.26	0.22	0.04	3.87	0.05	4.40	0.12	0.12
TIO2	0.00	0.04	1.35	0.29	0.09	0.73	0.12	0.61	0.57	0.76
MNO	0.01	0.01	0.00	0.00	0.02	0.08	0.31	0.01	0.01	0.02
S	0.02	0.02	0.03	0.04	0.10	0.37	0.05	0.05	0.10	0.19
P2O5	0.01	0.11	0.02	0.06	0.00	0.16	0.02	0.03	0.07	0.05
TOTAL	98.10	100.11	95.75	99.24	99.71	86.33	93.98	100.10	100.03	100.00
PPM										
BA	16	108	0	765	96	193	0	138	31	945
NB	1	1	5	6	0	9	8	6	2	3
ZR	0	34	96	124	57	106	282	101	57	58
Y	2	27	5	9	0	14	100	10	10	8
SR	2	600	22	243	2	273	95	333	892	801
RB	0	3	5	0	0	167	0	114	0	0
ZN	0	0	97	471	32	53	225	29	24	0
PB	—	0	149	185	70	8	0	300	—	—
CU	0	0	70	87	24	27	0	0	58	0
NI	0	0	0	13	0	132	0	0	0	0
CR	0	5	0	0	0	222	0	1	25	44
MO	—	0	0	0	31	0	0	0	—	—

TABLE A.1.2: SEDIMENTARY, TUFFACEOUS SEDIMENTARY SERIES

	192	194	197	201	222	240	240A	240B	263	265A
PERCENT										
SIO2	70.27	68.80	77.03	76.55	95.72	85.65	84.48	93.99	84.79	48.42
AL2O3	21.91	21.40	14.97	20.65	1.56	1.63	9.75	4.33	8.72	38.66
FE2O3	2.07	7.92	3.49	2.04	9.12	1.30	2.23	1.31	2.09	8.40
MGO	0.07	0.00	0.01	0.01	0.00	0.07	0.05	0.00	0.00	0.02
CAO	0.15	0.20	0.01	0.01	0.00	0.46	0.00	0.00	1.52	0.21
NA2O	0.00	0.34	0.52	0.36	0.35	0.20	0.40	0.45	0.41	0.08
K2O	0.01	0.16	0.37	0.01	0.00	0.12	0.16	0.00	0.00	0.09
TIO2	1.04	1.06	0.38	0.28	0.00	0.12	0.23	0.05	0.22	1.18
MNO	0.00	0.02	0.01	0.01	0.02	10.02	0.01	0.03	0.14	0.05
S	2.08	0.10	0.10	0.08	0.01	0.16	0.04	0.03	0.10	0.14
P2O5	0.02	0.19	0.04	0.03	0.02	0.01	0.13	0.01	0.09	0.04
TOTAL	97.62	100.19	96.93	100.03	106.80	99.94	97.48	100.20	98.08	97.29
PPM										
BA	2052	45	63	174	0	3175	79	75	205	0
NB	5	5	1	8	0	0	0	3	0	5
ZR	93	109	70	115	34	2	55	29	23	134
Y	11	13	6	10	0	4	34	40	33	8
SR	373	1727	263	144	0	50	1157	142	201	350
RB	5	0	7	0	0	0	14	3	2	5
ZN	49	44	29	173	32	13	5	0	6	20
CU	91	58	37	123	0	2	14	0	34	0
NI	15	0	0	10	0	5	0	0	0	0
CR	112	22	3	38	20	0	16	13	3	0

TABLE A.1.2:SEDIMENTARY,TUFFACECUS SEDIMENTARY SERIES

	266	267	270	271	272	273	274	275	282	282A
PERCENT										
SIO2	68.67	43.84	88.31	85.83	91.09	87.72	90.64	84.99	85.46	70.79
AL2O3	23.08	7.12	5.73	6.93	4.05	10.52	6.18	11.50	13.00	23.91
FE2O3	1.47	9.09	0.12	3.19	2.99	2.16	1.72	3.41	0.31	0.59
MGO	0.08	7.80	0.14	0.21	0.00	0.00	0.00	0.00	0.00	0.00
CAO	0.47	23.27	0.00	0.46	0.00	0.00	0.00	0.13	0.00	0.11
NA2O	0.21	0.00	0.35	0.00	0.37	0.41	0.38	0.35	0.42	0.30
K2O	0.02	0.03	1.75	0.03	0.08	0.02	0.03	0.02	0.41	0.16
TIO2	1.26	0.34	0.08	0.44	0.13	0.25	0.22	0.50	0.31	0.28
MNO	0.04	0.88	0.00	0.00	0.14	0.01	0.09	0.00	0.00	0.01
S	0.99	0.31	0.04	1.85	0.09	0.06	0.06	0.19	0.08	0.12
P2O5	0.22	0.26	0.00	0.05	0.06	0.01	0.07	0.02	0.02	0.02
TOTAL	96.51	92.94	100.52	98.99	99.00	101.16	101.39	101.11	100.01	96.29
PPM										
BA	39	375	261	9698	78	299	100	2999	723	1138
NB	6	3	5	8	2	4	3	4	7	11
ZR	193	31	54	108	65	56	63	54	108	125
Y	42	20	8	11	7	0	2	1	14	16
SR	3064	881	2	604	632	19	960	297	197	71
RB	8	4	16	11	11	10	6	10	20	9
ZN	0	277	22	95	26	15	13	4	15	41
CU	14	0	0	18	10	0	9	0	9	19
NI	3	2	0	0	0	0	0	0	0	0
CR	80	12	0	3	14	34	30	0	16	44

TABLE A.1.2:SEDIMENTARY,TUFFACECUS SEDIMENTARY SERIES

	285	287	288	293	294	295	296	297	298	299
PERCENT										
SIO2	83.99	77.82	73.94	63.19	81.67	74.56	70.71	77.22	44.03	69.18
AL2O3	11.35	20.62	18.25	23.76	14.28	16.61	19.08	18.53	39.70	23.65
FE2O3	2.92	0.52	4.04	7.15	1.03	3.67	6.16	2.50	3.16	1.53
MGO	0.00	0.07	0.26	0.21	0.10	0.31	0.17	0.00	0.02	0.00
CAO	0.00	0.10	0.53	0.18	0.00	0.55	0.22	0.12	2.82	0.20
NA2O	0.40	0.30	0.00	0.30	0.45	0.02	0.30	0.33	0.92	0.32
K2O	0.18	0.47	0.00	0.00	0.06	0.00	0.00	0.00	0.03	0.00
TIO2	0.21	0.43	0.65	1.27	0.70	0.60	1.08	0.86	2.93	1.14
MNO	0.00	0.01	0.08	0.27	0.00	0.13	0.10	0.00	0.03	0.00
S	0.03	0.06	1.94	0.90	0.20	1.01	0.16	0.09	0.07	0.28
P2O5	0.02	0.10	0.30	0.09	0.20	0.11	0.13	0.17	0.14	0.68
TOTAL	99.10	100.50	99.99	97.32	98.69	97.97	98.11	99.82	93.85	97.18
PPM										
BA	78	231	373	1313	1814	526	624	47	6	223
NB	4	11	3	8	4	3	4	5	11	4
ZR	91	177	91	129	114	70	81	75	246	222
Y	9	29	20	21	25	10	4	1	43	51
SR	263	1138	1860	925	2395	951	1209	1564	2310	2500
RB	14	23	2	0	5	4	4	4	0	0
ZN	12	19	24	18	0	14	27	0	0	0
CU	0	10	112	88	15	62	94	0	18	8
NI	4	0	12	1	0	10	0	0	30	0
CR	9	41	66	23	39	16	51	44	107	49

TABLE A.1.2: SEDIMENTARY, TUFFACEOUS SEDIMENTARY SERIES

	301	302	303	304	305	305A	306	307	308	309
PERCENT										
SIO2	71.50	40.65	69.98	88.93	88.10	69.42	81.54	88.88	90.05	85.11
AL2O3	22.28	8.12	20.84	3.75	4.09	18.15	15.33	7.71	9.41	11.15
FE2O3	2.94	2.67	5.15	4.11	7.28	10.57	2.56	2.00	0.23	3.94
MGO	0.17	1.03	0.04	0.00	0.02	0.00	0.05	0.00	0.00	0.00
CAO	0.18	31.02	0.21	0.00	0.00	0.16	0.09	0.00	0.00	0.00
NA2O	0.30	0.13	0.31	0.42	0.43	0.31	0.35	0.40	0.41	0.39
K2O	0.69	0.23	0.41	0.21	0.27	0.01	0.48	0.20	0.00	0.07
TIO2	1.04	0.31	0.84	0.08	0.10	0.63	0.33	0.27	0.07	0.23
MNO	0.00	0.36	0.10	0.32	0.50	0.55	0.01	0.50	0.00	0.05
S	0.06	0.17	0.09	0.09	0.08	0.17	0.06	0.16	0.02	0.06
P2O5	0.13	0.20	0.14	0.08	0.13	0.09	0.02	0.10	0.00	0.05
TOTAL	99.29	84.89	98.11	97.99	101.00	100.26	100.82	100.22	100.19	101.05
PPM										
BA	23	2691	188	387	404	129	48	65	24	98
NB	1	2	5	1	0	3	7	3	5	5
ZR	68	36	68	13	24	60	92	83	52	84
Y	0	14	10	14	8	19	20	6	8	12
SR	767	343	689	453	418	326	249	1084	19	491
RB	39	5	22	26	28	5	32	19	2	11
ZN	19	47	46	33	43	114	19	23	8	26
CU	10	57	137	7	2	72	0	64	17	35
NI	0	0	0	1	0	2	9	0	0	0
CR	35	0	45	6	0	51	15	30	25	47

TABLE A.1.2: SEDIMENTARY, TUFFACEOUS SEDIMENTARY SERIES

	310	311	314	315	316	317	329	330	331	333A
PERCENT										
SIO2	88.88	63.56	77.22	68.87	70.68	78.54	55.24	52.28	78.07	83.42
AL2O3	10.84	31.44	18.09	20.51	21.58	15.37	36.61	40.97	17.80	10.74
FE2O3	0.66	0.95	2.62	4.42	2.65	2.77	4.16	2.02	0.82	3.98
MGO	0.03	0.03	0.05	0.68	0.04	0.34	0.00	0.00	0.00	0.44
CAO	0.00	0.10	0.13	0.14	0.11	0.79	0.16	0.16	0.00	0.19
NA2O	0.41	0.30	0.31	0.31	0.35	0.31	0.00	0.01	0.42	0.55
K2O	0.41	0.01	0.01	1.10	0.88	0.60	0.00	0.01	0.00	1.35
TIO2	0.20	0.49	0.42	1.10	0.72	0.60	1.56	1.63	0.95	0.22
MNO	0.00	0.00	0.02	0.01	0.01	0.10	0.00	0.00	0.00	0.01
S	0.07	0.05	0.10	0.05	0.07	0.18	0.07	0.06	0.17	0.03
P2O5	0.02	0.02	0.07	0.12	0.09	0.08	0.03	0.04	0.22	0.03
TOTAL	101.52	96.95	99.04	97.31	97.18	99.68	97.83	97.18	98.45	100.96
PPM										
BA	394	0	771	125	222	306	50	0	80	366
NB	5	15	6	6	4	3	3	6	4	8
ZR	64	213	171	91	65	41	116	133	105	119
Y	5	23	17	7	6	14	31	34	6	21
SR	122	67	508	914	579	634	548	803	1509	175
RB	28	4	6	67	26	39	0	0	1	46
ZN	9	40	14	63	10	26	4	7	0	24
PB	—	—	—	—	—	—	10	17	10	80
CU	2	9	4	74	1	53	150	85	10	0
NI	0	6	0	0	0	0	0	8	0	1
CR	19	15	18	57	13	42	82	61	43	0
MO	—	—	—	—	—	—	0	0	0	0

TABLE A.1.2:SEDIMENTARY,TUFFACEOUS SEDIMENTARY SERIES

	378	380	381	H3	H5
PERCENT					
SIO2	73.20	94.61	94.61	83.47	89.66
AL2O3	17.74	5.02	4.66	12.23	4.81
FE2O3	4.80	0.17	0.10	0.92	2.53
MGO	0.06	0.00	0.03	0.10	0.06
CAO	0.00	0.00	0.00	0.00	0.00
NA2O	0.43	0.40	0.36	0.00	0.07
K2O	0.37	0.09	0.59	0.84	0.23
TIO2	0.38	0.23	0.11	0.23	0.14
MNO	0.01	0.00	0.00	0.00	0.02
S	0.15	0.17	0.45	0.00	0.00
P2O5	0.05	0.02	0.02	0.22	0.21
TOTAL	101.52	96.95	99.04	97.31	97.18
PPM					
BA	1758	2942	301	109	115
NB	10	2	11	2	1
ZR	127	40	99	138	142
Y	15	12	18	19	10
SR	479	237	36	584	979
RB	20	13	0	14	9
ZN	20	0	22	12	1
PB	384	43	3940	—	—
CU	0	0	13	0	12
NI	1	0	0	0	0
CR	285	36	18	—	—
MO	0	0	3	—	—

TABLE,A.1.2:UPPER BASIC SERIES,BASALTS,UPPER VOLC.CYCLE

	121	208	209	211	214
PERCENT					
SIO2	55.12	53.01	54.61	52.22	52.13
AL2O3	15.72	14.73	15.44	14.19	15.13
FE2O3	1.44	4.61	9.10	8.78	5.99
FEO	5.99	4.67	0.81	1.68	3.65
MGO	5.14	7.81	6.88	8.93	7.31
CAO	8.07	8.62	6.79	6.84	6.61
NA2O	3.08	2.53	1.63	3.12	4.61
K2O	3.30	2.18	3.30	2.77	2.66
TIO2	0.93	0.76	0.85	0.79	0.88
MNO	0.11	0.18	0.18	0.18	0.18
S	0.06	0.10	0.08	0.07	0.18
P2O5	0.36	0.29	0.25	0.23	0.26
H2O	—	—	—	—	—
TOTAL	99.32	99.49	99.92	99.80	99.59
PPM					
BA	544	362	376	305	407
NB	7	3	5	2	5
ZR	113	79	88	67	72
Y	19	21	25	21	18
SR	690	617	432	382	457
RB	74	66	67	46	58
ZN	82	70	75	71	76
CU	25	262	207	136	99
NI	32	77	70	71	117
CR	138	230	232	213	188

TABLE,A.1.2:UPPER BASIC SERIES,ANDESITES,UPPER VLLC.CYCLE

	124	178	210
PERCENT			
SIO2	58.79	55.43	57.69
AL2O3	15.52	16.56	15.78
FE2O3	1.32	5.34	3.95
FEO	4.96	3.54	3.04
MGO	3.40	5.65	3.88
CAO	9.30	9.22	6.95
NA2O	2.89	1.29	3.14
K2O	2.03	2.53	3.82
TIO2	0.86	1.03	0.91
MNO	0.13	0.14	0.10
S	0.03	0.14	0.11
P2O5	0.24	0.28	0.30
H2O	—	1.10	—
TOTAL	99.47	102.25	99.67
PPM			
BA	520	708	481
NB	5	1	5
ZR	105	58	121
Y	18	18	27
SR	687	570	646
RB	86	62	93
ZN	54	84	84
CU	44	58	107
NI	34	16	26
CR	146	69	118

TABLE,A.1.2:UPPER BASIC SERIES,DOLERITES,UPPER VOLC.CYCLE

	76	78	132	166	184	187	188	346	347
PERCENT									
SIO2	60.68	51.26	49.38	53.26	52.09	60.36	53.67	52.88	51.88
AL2O3	15.43	17.88	15.72	15.69	15.79	16.10	16.00	16.57	17.91
FE2O3	5.31	8.97	5.93	4.33	6.31	3.07	5.26	10.69	8.37
FEO	—	—	4.41	6.29	2.73	3.87	3.99	—	—
MGO	2.39	4.13	4.02	3.47	4.74	1.32	5.85	2.91	3.97
CAO	3.18	9.44	9.47	8.34	9.04	5.36	7.14	11.09	8.58
NA2O	3.36	1.79	1.28	1.49	1.26	3.00	1.68	1.48	1.56
K2O	4.84	2.40	2.81	3.23	2.63	4.79	3.27	2.49	2.34
TIO2	0.75	0.95	1.11	1.03	1.01	1.05	1.05	1.20	0.92
MNO	0.09	0.13	0.18	0.20	0.12	0.17	0.18	0.18	0.13
S	0.32	0.03	0.09	0.15	0.16	0.12	0.12	0.21	0.11
P2O5	0.37	0.29	0.29	0.30	0.27	0.39	0.30	0.29	0.28
H2O	—	—	3.76	3.12	2.89	—	1.99	—	—
TOTAL	96.72	97.27	98.45	100.90	98.97	99.58	100.50	99.99	96.05
PPM									
BA	1551	1078	1073	1013	1097	1557	1376	1064	1144
NB	7	3	2	3	4	7	3	4	3
ZR	162	85	67	79	69	141	89	67	72
Y	39	21	18	18	20	32	22	16	17
SR	341	488	474	420	525	364	488	507	505
RB	177	91	92	129	86	168	108	101	89
ZN	94	53	57	63	60	98	59	63	44
CU	14	126	117	88	112	3	184	110	106
NI	0	0	42	5	4	0	0	0	2
CR	13	27	42	55	12	2	8	27	30

TABLE,A.1.2:UPPER BASIC SERIES,A L T E R E D ,UPPER VOLC.CYCLE

	7	8	161	207	250	252	319	332	334
PERCENT									
SIO2	52.97	49.37	52.11	59.35	65.37	54.38	49.44	51.27	48.30
AL2O3	13.82	15.84	15.61	14.13	17.83	19.17	16.57	33.08	25.41
FE2O3	8.00	2.55	6.06	3.67	3.39	6.22	9.26	4.12	10.24
FEO	1.17	6.82	3.65	1.22	—	—	—	—	—
MGO	6.28	5.63	7.27	0.98	0.14	6.96	1.77	0.28	0.40
CAO	3.06	9.90	5.40	9.87	1.39	1.87	9.75	1.91	2.88
NA2O	2.09	2.28	3.45	2.47	3.40	0.51	0.88	0.57	0.79
K2O	5.47	2.42	1.55	4.16	6.36	6.40	2.27	2.77	2.34
TIO2	0.78	0.71	0.94	0.70	0.78	1.05	1.10	1.12	1.25
MNO	0.15	0.17	0.14	0.27	0.04	0.13	0.18	0.03	0.10
S	0.04	0.03	0.14	0.16	0.08	0.07	0.37	0.19	0.35
P2O5	0.09	0.33	0.13	0.32	0.17	0.30	0.26	0.33	0.27
H2O	4.27	3.28	2.95	—	—	—	—	—	—
TOTAL	98.19	99.33	99.40	97.30	98.95	97.06	91.85	95.67	92.33
PPM									
BA	332	567	271	1689	2019	1497	1059	1787	2336
NB	4	4	1	6	9	5	4	3	4
ZR	36	68	61	165	186	115	67	91	82
Y	15	23	19	35	34	23	17	15	20
SR	121	665	200	377	243	135	472	174	238
RB	96	76	30	173	254	125	95	132	102
ZN	85	55	97	71	57	87	71	71	90
CU	0	97	15	0	0	104	116	158	133
NI	0	0	2	0	0	0	19	4	3
CR	39	45	196	0	0	142	50	52	46

TABLE A.1.2:RHYODACITE,UPPER VOLC.CYCLE

	127	133	168	175	176	181	185	213	258	276
PERCENT										
SIO2	72.62	71.03	75.99	79.66	77.69	71.18	71.23	71.49	75.09	74.56
AL2O3	15.30	16.70	14.41	11.49	12.13	15.61	15.53	14.32	14.96	16.71
FE2O3	0.01	1.36	0.94	0.75	0.85	1.30	1.60	2.34	0.84	0.60
FEO	3.66	0.45	0.32	0.26	0.46	0.01	0.19	0.46	—	—
MGO	0.25	0.35	0.27	0.13	0.32	0.25	0.30	0.50	0.11	0.04
CAO	0.78	0.40	0.25	0.73	1.02	0.13	0.29	0.91	0.64	0.33
NA2O	2.84	2.23	1.28	2.70	2.54	1.70	2.19	2.03	1.25	2.37
K2O	5.87	7.03	6.16	3.94	4.11	9.45	8.26	5.48	6.17	6.74
TIO2	0.30	0.34	0.20	0.22	0.28	0.28	0.31	0.27	0.14	0.21
MNO	0.04	0.02	0.04	0.02	0.03	0.05	0.02	0.04	0.06	0.01
S	0.03	0.02	0.10	0.04	0.04	0.02	0.04	0.05	0.10	0.03
P2O5	0.05	0.02	0.01	0.03	0.04	0.01	0.03	0.03	0.02	0.02
H2O	—	—	—	—	—	—	—	—	—	—
TOTAL	101.75	99.95	99.97	99.97	99.51	99.97	99.99	97.92	99.38	101.62
PPM										
BA	1404	1379	1309	1512	1485	862	1321	601	1210	1106
NB	11	14	9	10	11	13	12	4	6	12
ZR	168	204	90	123	154	157	148	90	92	118
Y	23	23	17	17	17	14	18	19	20	16
SR	101	68	71	110	145	27	48	78	73	43
RB	187	211	212	163	162	266	231	133	183	190
ZN	29	16	5	21	19	14	9	32	10	12
PB	45	42	38	51	35	61	39	—	—	—
CU	0	0	0	0	0	0	0	0	0	0
NI	0	0	0	0	0	0	0	0	0	0
CR	0	0	0	0	0	0	0	0	0	0
MO	0	0	0	0	0	0	0	—	—	—

TABLE A.1.2:RHYODACITE,UPPER VOLC.CYCLE

	277	320	335	336	337	338	349	351	352	359
PERCENT										
SIO2	75.86	67.20	68.31	69.56	68.57	70.63	66.13	67.88	65.96	77.26
AL2O3	13.84	15.42	19.86	15.82	18.49	17.20	17.97	17.28	18.56	14.50
FE2O3	0.96	2.56	1.91	1.55	1.96	1.43	2.58	2.31	2.77	1.47
MGO	0.07	0.46	0.28	0.22	0.25	0.11	0.62	0.56	0.58	0.08
CAO	0.19	2.85	0.42	0.14	0.32	0.33	1.06	1.00	0.50	0.00
NA2O	2.26	1.71	2.40	1.96	1.83	2.20	2.44	2.48	1.79	1.13
K2O	6.04	8.37	7.18	7.39	8.77	7.08	5.78	6.35	6.82	6.04
TIO2	0.19	0.34	0.34	0.29	0.33	0.24	0.45	0.41	0.41	0.26
MNO	0.02	0.04	0.02	0.02	0.02	0.01	0.02	0.02	0.02	0.01
S	0.04	0.12	0.05	0.04	0.04	0.02	0.10	0.08	0.04	0.03
P2O5	0.03	0.05	0.03	0.02	0.03	0.02	0.09	0.09	0.03	0.02
TOTAL	99.50	99.12	100.80	97.01	100.61	99.47	99.24	98.46	97.48	100.80
PPM										
BA	1122	1343	1392	1157	1249	1199	1504	1554	1093	685
NB	11	14	12	10	14	14	11	12	12	7
ZR	108	208	226	190	220	173	215	244	211	152
Y	16	20	21	23	17	22	20	19	8	13
SR	47	335	73	38	50	51	145	187	56	67
RB	187	223	206	215	221	216	156	178	200	136
ZN	23	18	23	15	20	10	136	21	39	11
PB	—	72	43	37	35	37	45	43	58	99
CU	0	0	0	0	0	0	0	0	0	0
NI	0	0	0	0	0	0	0	0	0	0
CR	0	16	0	0	0	0	0	19	20	15
MO	—	0	0	0	0	0	0	0	0	3

TABLE A.1.2:RHYODACITE,UPPER VOLC.CYCLE

375

PERCENT	
SIO2	70.43
AL2O3	19.41
FE2O3	1.59
MGO	0.29
CAO	0.32
NA2O	1.86
K2O	5.41
TIO2	0.32
MNO	0.02
S	0.03
P2O5	0.01
TOTAL	99.50
PPM	
BA	1277
NB	11
ZR	192
Y	13
SR	155
RB	216
ZN	14
PB	47
CU	0
NI	0
CR	0
MO	0

TABLE A.1.2:RHYODACITE,A L T E R E D ,UPPER VOLC.CYCLE

	21	41	128	138	158	159	180	182	186	186A
PERCENT										
SIO2	67.32	66.78	73.95	74.79	75.80	72.66	79.02	76.54	76.11	75.08
AL2O3	18.80	18.40	13.93	13.40	15.74	14.12	11.94	12.82	13.70	15.00
FE2O3	0.82	0.01	0.01	1.13	0.21	0.67	0.85	0.89	0.70	0.61
FEO	1.15	0.01	4.94	0.01	0.33	0.66	0.27	0.12	0.43	—
MGO	0.43	0.39	0.05	0.03	0.61	0.20	0.11	0.37	0.52	0.17
CAO	0.25	0.18	0.66	0.16	0.06	0.12	0.78	2.11	0.16	0.96
NA2O	0.54	1.25	2.49	1.49	0.67	1.41	2.49	1.38	0.78	0.77
K2O	9.17	10.76	5.37	8.17	6.11	9.27	4.23	5.38	7.20	6.88
TIO2	0.24	0.19	0.20	0.18	0.29	0.24	0.19	0.22	0.20	0.19
MNO	0.05	0.03	0.01	0.05	0.03	0.06	0.05	0.02	0.04	0.06
S	0.03	0.02	0.02	0.01	0.09	0.08	0.03	0.14	0.10	0.08
P2O5	0.10	0.08	0.02	0.01	0.02	0.02	0.01	0.03	0.02	0.02
H2O	3.69	2.16	—	—	—	—	—	—	—	—
TOTAL	102.59	100.26	101.65	99.43	99.96	99.91	99.97	100.02	99.96	99.82
PPM										
BA	1030	955	1371	1200	1503	970	1284	1122	1282	1260
NB	9	9	9	6	12	11	7	8	10	11
ZR	163	110	118	109	161	156	116	122	111	113
Y	21	26	14	66	22	19	12	18	18	19
SR	151	47	104	69	168	29	132	316	29	27
RB	113	235	166	175	131	192	163	157	173	183
ZN	42	11	0	0	54	28	22	26	22	10
PB	—	—	63	61	73	52	49	9	40	48
CU	0	0	0	0	0	5	0	0	11	0
NI	0	0	0	0	0	0	0	0	0	0
CR	5	9	0	0	0	1	0	0	0	0
MO	—	—	0	0	0	0	0	0	0	0

TABLE A.1.2: RHYODACITE, A L T E R E D , UPPER VOLC. CYCLE

	189	253	254	261	318	321	322	333	339	340
PERCENT										
SIO2	65.00	74.42	66.30	72.79	66.41	75.31	62.98	66.62	70.24	72.95
AL2O3	19.37	14.64	16.70	13.87	16.28	15.54	19.17	21.05	17.52	15.60
FE2O3	1.52	0.33	3.44	0.78	7.25	0.97	1.70	1.52	1.69	2.00
MGO	0.05	0.01	0.28	0.71	0.28	0.00	0.05	0.28	0.26	0.22
CAO	0.35	0.09	0.53	2.76	0.20	0.15	0.43	0.30	0.37	0.11
NA2O	1.99	1.76	2.16	1.89	0.65	1.44	1.98	1.83	2.09	1.87
K2O	11.06	8.49	9.49	2.29	4.80	5.66	10.80	8.27	7.33	6.40
TIO2	0.46	0.22	0.70	0.10	0.33	0.26	0.47	0.34	0.31	0.28
MNO	0.02	0.01	0.03	0.03	0.09	0.01	0.02	0.03	0.02	0.02
S	0.04	0.02	0.06	0.13	0.14	0.07	0.14	0.05	0.03	0.03
P2O5	0.01	0.02	0.16	0.03	0.10	0.04	0.00	0.01	0.02	0.07
TOTAL	99.87	100.01	99.85	95.38	96.53	99.67	97.74	100.30	99.88	99.55
PPM										
BA	1828	1035	1779	1179	708	896	1705	1135	1273	1379
NB	15	8	9	11	12	10	17	13	11	12
ZR	266	95	176	45	214	194	236	200	191	172
Y	24	13	29	41	24	13	22	14	21	27
SR	93	107	133	223	58	107	99	50	62	62
RB	316	233	301	71	122	186	292	277	219	191
ZN	13	0	59	22	65	7	11	14	19	25
PB	52	—	—	—	—	34	49	38	40	47
CU	0	0	0	0	0	5	0	0	0	0
NI	0	0	0	0	0	0	0	0	0	0
CR	0	2	0	0	2	0	0	0	0	0
MO	0	—	—	—	—	0	0	0	0	0

TABLE A.1.2:RHYOCACITE,A L T E R E D ,UPPER VOLC.CYCLE

	341	348	350	353	354	355	356	357	358	360
PERCENT										
SIO2	67.41	76.81	64.30	64.69	66.68	69.25	69.25	74.80	79.34	68.42
AL2O3	18.39	13.94	19.16	19.99	17.77	16.42	17.86	15.74	13.11	19.40
FE2O3	2.05	1.53	3.19	3.17	3.01	2.41	2.13	1.03	0.54	2.07
MGO	0.26	0.15	0.71	0.37	0.35	0.31	0.19	0.34	0.20	0.36
CAO	0.24	0.00	1.28	0.14	0.33	0.40	0.04	0.46	0.84	0.40
NA2O	1.52	1.06	2.53	1.26	1.50	1.64	1.19	1.31	2.39	1.82
K2O	9.18	6.90	7.08	8.65	8.84	7.76	8.34	6.70	3.85	5.77
TIO2	0.31	0.23	0.46	0.44	0.34	0.30	0.35	0.32	0.28	0.39
MNO	0.05	0.02	0.02	0.02	0.02	0.09	0.02	0.03	0.01	0.02
S	0.08	0.03	0.20	0.07	0.05	0.10	0.04	0.05	0.02	0.04
P2O5	0.02	0.06	0.08	0.08	0.08	0.09	0.03	0.02	0.01	0.07
TOTAL	99.51	100.73	99.01	98.88	98.97	98.77	99.44	100.80	100.59	98.76
PPM										
BA	1320	659	1570	1169	1187	1199	962	1272	1183	1147
NB	16	8	13	12	9	11	11	12	10	10
ZR	240	141	251	226	191	166	189	202	170	222
Y	21	21	19	22	20	22	19	11	17	18
SR	40	152	150	78	67	115	130	91	122	274
RB	245	141	173	216	218	226	211	146	151	191
ZN	22	99	72	14	25	52	85	599	127	61
PB	33	22	48	30	37	41	—	—	115	—
CU	0	0	0	0	0	0	44	87	17	0
NI	0	0	0	0	0	0	4	0	3	0
CR	0	18	10	0	0	0	18	0	0	0
MO	0	0	0	0	0	0	—	—	0	—

TABLE A.1.2:RHYOCACITE,A L T E R E D ,UPPER VOLC.CYCLE

	361	362	363	366	367	368	369	370	371	372
PERCENT										
SIO2	67.81	66.56	69.16	67.76	69.75	71.27	70.22	62.61	68.75	61.84
AL2O3	19.31	18.92	17.71	19.10	18.95	20.01	19.69	24.37	19.59	20.92
FE2O3	2.11	2.47	2.19	1.93	2.09	0.66	1.35	0.04	0.89	1.46
MGO	0.40	0.37	0.41	0.45	0.25	0.01	0.31	0.14	0.24	0.00
CAO	0.65	0.38	0.55	0.51	0.21	0.20	0.27	0.35	0.04	0.23
NA2O	2.35	1.80	2.15	2.39	1.48	2.13	1.81	1.88	1.73	1.43
K2O	5.94	9.38	6.37	6.41	6.30	5.60	5.47	9.84	7.98	9.76
TIO2	0.41	0.32	0.37	0.37	0.34	0.26	0.35	0.44	0.35	0.47
MNO	0.02	0.01	0.02	0.04	0.02	0.00	0.02	0.02	0.02	0.03
S	0.04	0.06	0.05	0.09	0.05	0.05	0.03	0.03	0.04	0.05
P2O5	0.04	0.12	0.03	0.03	0.02	0.02	0.02	0.02	0.01	0.08
TOTAL	99.08	100.39	99.01	99.08	99.46	100.21	99.54	99.74	99.64	96.27
PPM										
BA	1278	1275	1264	1529	883	918	1292	1436	1476	1556
NB	13	11	11	12	14	13	12	16	11	13
ZR	241	218	214	223	235	161	208	261	172	284
Y	13	23	11	19	23	25	9	15	5	31
SR	110	542	79	80	59	54	74	57	77	964
RB	193	178	190	199	197	151	197	311	229	293
ZN	43	87	24	29	16	0	13	12	12	20
PB	—	—	92	48	52	25	44	60	40	128
CU	28	0	0	0	0	0	0	2	0	0
NI	0	0	0	0	0	0	0	0	0	1
CR	0	0	15	0	27	20	0	0	0	23
MO	—	—	0	1	15	0	0	0	0	0

TABLE A.1.2:RHYODACITE,A L T E R E D ,UPPER VOLC.CYCLE

	373	374
PERCENT		
SIO2	65.73	63.93
AL2O3	21.51	22.22
FE2O3	1.34	2.12
MGO	0.26	0.06
CAO	0.23	0.37
NA2O	1.80	1.49
K2O	8.26	9.43
TIO2	0.37	0.36
MNO	0.03	0.06
S	0.04	0.05
P2O5	0.03	0.00
TOTAL	99.08	100.39
PPM		
BA	1418	1126
NB	11	14
ZR	202	273
Y	16	20
SR	65	154
RB	250	255
ZN	30	23
PB	55	157
CU	0	0
NI	0	0
CR	0	0
MO	0	0

TABLE A.1.2:BOREHOLE CORE SAMPLES,HOST ROCK,HARSIT-KOPRUBASI MINE(H)

	HI,18	32	66	100	185	200	HG1,0,5	1,5	4,5	9
PERCENT										
SIO2	73.24	66.79	57.77	67.39	68.78	65.15	52.95	57.95	70.81	86.97
AL2O3	21.14	25.68	26.54	22.87	22.53	27.38	2.91	3.18	4.19	4.71
FE2O3	0.48	0.84	1.05	0.56	0.27	0.80	2.33	5.47	2.19	1.98
MGO	1.09	1.77	2.72	1.60	1.28	1.69	0.04	0.14	0.09	0.26
CAO	0.28	0.77	0.30	0.08	0.24	0.28	0.07	0.07	0.00	0.00
NA2O	0.01	0.09	1.34	0.18	0.16	0.20	0.07	0.04	0.07	0.00
K2O	1.60	3.42	6.42	5.05	4.76	5.93	0.12	0.19	0.58	1.45
TIO2	0.23	0.22	0.29	0.32	0.28	0.39	1.41	0.71	0.22	0.00
MNO	0.08	0.05	0.08	0.04	0.02	0.03	0.02	0.02	0.04	0.02
S	0.30	0.80	0.44	0.53	0.55	0.80	12.88**	13.51**	9.28	2.64
P2O5	0.02	0.04	0.04	0.01	0.02	0.03	0.02	0.01	0.01	0.01
TOTAL	98.47	100.47	96.99	98.63	98.89	102.68	72.82	81.29	87.48	98.04
PPM										
BA	351	385	872	2106	2427	2339	2.20*	1.80*	3868	243
NB	12	13	16	12	11	16	0	0	0	4
ZR	143	178	218	187	175	268	115	126	78	37
Y	22	31	33	24	22	39	28	34	24	5
SR	27	95	85	94	186	287	594	277	128	5
RB	106	121	215	144	126	181	0	0	0	22
ZN	25	8	49	169	33	28	8.70*	5.50*	9.40*	338
SB	20	20	0	72	7	15	1.13	5400	6600	432
CD	0	0	0	0	0	0	534	382	643	0
AG	0	0	0	9	0	0	16	0	11	0
MO	0	0	0	0	0	0	121	78	84	25
PB	219	355	166	450	334	302	6.10*	7.80*	3.70*	1584
CU	0	0	0	108	0	2	2.35*	1.35*	9850	1145
AS	96	151	65	31	136	127	1384	555	543	189

TABLE A.1.2: BOREHOLE CORE SAMPLES, HOST ROCK, HARSIT-KOPRUBASI MINE(H)

	14	HG2,7	13	14	31	35	37	H3,58	62	75
PERCENT										
SIO2	79.92	86.77	48.01	81.03	48.85	22.92	26.79	84.75	86.89	75.42
AL2O3	5.43	8.62	27.01	3.04	2.57	0.50	0.38	6.55	7.55	5.46
FE2O3	1.26	0.17	0.00	0.46	4.33	9.84	25.91	1.33	0.40	4.05
MGO	0.16	0.30	0.00	0.20	0.14	0.14	0.00	0.40	0.10	0.16
CAO	0.06	0.29	0.00	0.00	0.31	0.34	0.00	0.08	0.09	0.06
NA2O	0.06	0.10	0.03	0.03	0.08	0.00	0.06	0.12	0.08	0.10
K2O	0.89	1.39	0.71	1.12	0.20	0.30	0.00	1.88	1.16	0.93
TIO2	0.00	0.77	2.39	0.00	1.40	0.01	0.00	0.00	1.32	0.07
MNO	0.02	0.02	0.05	0.02	0.02	0.03	0.02	0.02	0.02	0.02
S	3.86	1.62	17.82**	2.84	14.21**	25.54**	28.26**	1.76	2.37	5.87
P2O5	0.01	0.02	0.01	0.00	0.01	0.01	0.00	0.00	0.02	0.01
TOTAL	91.67	100.07	96.03	88.74	72.12	59.63	81.42	96.89	100.00	92.15
PPM										
BA	110	4.70*	3.90*	290	3736	175	180	202	925	348
NB	2	3	0	2	0	0	0	4	2	2
ZR	62	68	245	69	122	161	110	48	52	19
Y	22	15	1	22	31	43	31	8	3	3
SR	0	481	4458	19	963	3	0	30	956	87
RB	0	9	0	0	0	0	0	37	30	24
ZN	2.00*	3561	3577	1.28*	1.40*	16.3*	10.4*	149	530	2658
SB	2400	2300	3500	2950	4.85*	4.00*	3700	40	233	1.50*
CD	280	16	0	191	205	1082	634	2	0	88
AG	3	0	0	21	10	52	33	0	0	10
MO	48	24	33	37	466	347	112	4	0	175
PB	2.35*	8450	8600	2.08*	7.00*	12.0*	4.80*	546	424	4100
CU	7050	2481	6100	5450	11.3*	2.40*	4500	45	623	4.80*
AS	476	262	864	591	1714	214	50	43	114	3250

TABLE A.1.2: BOREHOLE CORE SAMPLES, HOST ROCK, HARSIT-KOPRUBASI MINE (H)

	86	88	107	118	121	148	166	182	H4,9	15
PERCENT										
SIO2	44.56	84.62	79.09	59.39	76.44	74.61	33.39	73.97	—	56.26
AL2O3	2.82	6.75	8.56	6.83	15.78	19.37	8.34	13.30	—	25.15
FE2O3	3.25	0.68	0.69	3.58	1.13	0.35	0.06	0.05	—	7.94
MGO	0.03	0.45	0.63	0.25	0.89	1.02	0.54	1.43	—	1.67
CAO	0.05	0.22	0.40	0.24	0.18	0.18	17.65	6.83	—	0.00
NA2O	0.01	0.01	0.06	0.10	0.03	0.12	0.42	0.09	—	0.00
K2O	0.43	2.16	2.59	1.38	3.55	4.08	0.05	1.15	—	0.00
TIO2	0.01	0.55	0.05	0.07	0.17	0.25	0.00	0.06	—	1.48
MNO	0.11	0.02	0.03	0.03	0.02	0.02	0.03	0.08	0.75	0.49
S	15.33**	1.85	1.53	10.06	0.91	0.48	28.12**	3.88	—	6.59
P2O5	0.03	0.01	0.01	0.01	0.02	0.03	0.54	0.13	—	0.32
TOTAL	66.63	97.32	93.64	81.94	99.12	100.51	89.14	100.97	—	99.90
PPM										
BA	25	9509	263	1170	357	504	21	164	2227	1416
NB	2	5	5	0	9	12	6	7	7	6
ZR	87	69	76	107	153	180	47	60	192	213
Y	23	5	14	34	24	30	8	17	31	34
SR	0	671	35	44	38	25	705	80	1684	3782
RB	0	49	44	0	78	95	5	26	0	0
ZN	20.0 **	435	2851	9.60 *	131	28	17	26	127	48
SB	4600	25	24	3020	4	5	0	8	74	70
CD	1522	0	39	784	2	0	0	0	0	0
AG	19	0	0	22	0	0	0	0	0	0
MO	72	0	11	63	10	0	0	0	1	0
PB	4.80 *	206	1568	6.50 *	316	89	14	8	2730	2400
CU	9550	58	167	6700	28	0	0	13	307	504
AS	171	61	27	76	58	39	0	10	1227	2632

TABLE A.1.2:BOREHOLE CORE SAMPLES,HOST ROCK,HARSIT-KOPRUBASI MINE(H)

	18	46	54	78	96	H6,6	10	11	16	41
PERCENT										
SIO2	67.83	66.62	52.17	16.93	74.06	91.10	82.78	35.38	61.05	69.33
AL2O3	17.80	3.06	2.96	1.74	3.32	1.17	5.01	4.53	0.96	1.88
FE2O3	7.15	1.36	1.61	11.31	1.41	2.07	0.64	1.98	14.24	9.31
MGO	0.18	0.26	0.14	0.06	0.35	0.08	0.03	0.14	0.00	0.00
CAO	0.18	0.00	0.24	0.15	0.00	0.00	0.37	0.34	0.00	0.00
NA2O	0.02	0.00	0.00	0.01	0.00	0.00	0.01	0.10	0.24	0.31
K2O	0.07	0.34	0.09	0.17	0.84	0.74	0.73	0.60	0.52	0.10
TIO2	1.27	0.56	0.08	0.01	0.02	0.43	0.21	0.08	0.00	0.01
MNO	0.06	0.02	0.03	0.02	0.03	0.02	0.02	0.02	0.02	0.02
S	3.99	9.07	14.96**	28.20**	6.05	2.55	2.20	23.31**	17.65**	13.09**
P2O5	0.19	0.00	0.02	0.01	0.00	0.44	0.01	0.01	0.00	0.00
TOTAL	98.74	81.29	72.30	58.61	86.08	98.60	92.01	66.49	94.68	94.05
PPM										
BA	1808	9.75*	1542	20	136	6888	2309	20	131	671
NB	7	3	0	0	1	0	0	0	0	0
ZR	128	83	155	221	93	29	128	166	50	95
Y	14	17	44	60	31	5	39	48	19	33
SR	1638	611	21	0	0	156	66	3	0	11
RB	0	0	0	0	0	10	0	0	0	0
ZN	67	3.85*	11.5*	8.60*	4.35*	247	1363	11.2*	9300	8200
SB	42	4000	2250	1800	329	495	8000	3.20*	3550	9800
CD	0	259	1038	780	378	0	190	752	130	99
AG	0	3	28	84	9	0	20	37	11	17
MO	0	47	103	66	149	26	99	317	229	185
PB	2520	2.40*	8.00*	19.0**	3.60*	3121	5.10*	10.9*	1.70*	3.05*
CU	344	5400	1.26*	5.80*	7500	1080	1.39*	7.10*	7400	2.30*
AS	2525	228	680	544	367	353	139	583	579	780

TABLE A.1.2: BOREHOLE CORE SAMPLES, HOST ROCK, HARSIT-KOPRUBASI MINE(H)

	48	57	90	109	H11,9	40	61	75	101	123
PERCENT										
SIO2	77.21	84.03	76.57	84.14	69.13	48.81	41.13	71.74	40.83	75.37
AL2O3	13.04	0.21	17.13	11.68	23.33	2.98	2.21	5.59	2.06	18.56
FE2O3	0.45	3.27	0.31	0.09	2.47	0.62	23.30	0.03	2.59	0.35
MGO	0.79	0.26	1.07	0.49	0.04	0.14	0.14	0.14	0.14	1.28
CAO	0.00	0.00	0.31	0.08	0.28	0.12	0.00	0.36	0.31	0.30
NA2O	0.51	0.26	0.01	0.01	0.01	0.51	0.08	1.22	0.04	0.01
K2O	3.22	0.00	3.50	2.17	0.14	0.28	0.85	0.71	0.17	4.42
TIO2	0.09	0.00	0.20	0.15	1.21	0.01	0.00	1.27	0.02	0.17
MNO	0.02	0.03	0.03	0.02	0.02	0.02	0.02	0.02	0.04	0.03
S	0.40	5.40	0.23	0.11	0.09	19.38 **	27.05 **	7.12	18.41 **	0.59
P2O5	0.01	0.01	0.02	0.11	0.09	0.01	0.00	0.01	0.01	0.06
TOTAL	95.74	93.47	99.38	99.05	96.81	72.88	94.78	88.21	64.62	101.14
PPM										
BA	576	10	504	343	101	25	55	1.20 *	27	560
NB	8	2	13	7	5	1	0	1	0	9
ZR	80	47	155	90	107	108	48	97	123	124
Y	9	15	23	16	11	34	21	28	36	24
SR	44	0	31	45	604	0	0	327	0	25
RB	78	0	83	48	7	0	0	0	0	102
ZN	230	8150	61	30	66	14.8 *	1.22 *	2.55 *	20.0 **	228
SB	80	497	10	17	19	6900	306	6350	442	7
CD	576	92	0	0	0	842	115	274	1793	2
AG	0	1	0	0	0	150	13	65	15	0
MO	12	22	0	0	0	84	20	65	70	0
PB	215	1.48*	97	47	701	6.80 *	2.40*	4.07*	9.00 *	315
CU	23	1.90*	44	7	104	1.20 *	1646	1.32 *	1568	51
AS	48	505	31	13	273	321	117	362	0	27

TABLE A.1.2: BOREHOLE CORE SAMPLES, HOST ROCK, HARSIT-KOPRUBASI MINE(H)

	160	166	H13,2	15	21	35	51	76	88	103
PERCENT										
SIO2	74.66	60.22	67.81	91.76	21.29	81.70	82.25	82.70	81.93	67.56
AL2O3	19.51	26.19	23.98	6.46	27.51	7.42	8.84	11.41	11.96	8.46
FE2O3	0.56	0.89	2.46	0.04	2.47	3.02	2.44	0.96	2.01	0.13
MGO	1.01	1.35	0.05	0.12	0.14	0.12	0.49	0.66	0.61	0.00
CAO	0.34	0.42	0.30	0.36	0.38	0.34	0.00	0.00	0.00	0.00
NA2O	0.06	0.18	0.00	0.20	0.28	0.19	0.00	0.01	0.02	0.42
K2O	3.96	5.47	0.27	0.24	0.32	1.29	2.45	2.65	2.88	0.17
TIO2	0.28	0.38	1.62	1.46	4.53	0.04	0.02	0.04	0.07	4.25
MNO	0.03	0.03	0.04	0.02	0.02	0.02	0.02	0.02	0.02	0.04
S	0.86	1.04	0.09	1.24	16.83**	4.00	2.85	1.21	1.84	8.46
P2O5	0.03	0.04	0.20	0.04	0.02	0.01	0.01	0.00	0.00	0.00
TOTAL	101.30	96.21	96.82	101.94	73.79	98.15	99.37	99.66	101.34	89.49
PPM										
BA	1707	1722	158	6408	3.22*	465	281	216	291	1.11*
NB	11	13	7	3	0	1	5	5	6	0
ZR	177	268	165	76	188	78	47	69	81	132
Y	25	31	19	0	35	24	12	19	17	0
SR	177	300	2733	805	1154	0	5	0	0	2841
RB	138	160	0	0	0	0	37	49	57	0
ZN	105	44	25	1014	9.98*	6300	874	786	221	7400
SB	20	16	3	302	1500	295	90	15	12	376
CD	0	0	0	0	562	69	4	0	3	0
AG	0	0	0	0	0	9	0	0	0	0
MO	0	0	0	0	8	24	2	0	3	0
PB	428	355	775	1237	9.90*	1.35*	621	1861	863	3563
CU	6	4	53	115	3900	1650	297	47	7	943
AS	154	163	309	315	15	123	105	17	72	120

TABLE A.1.2:BOREHOLE CORE SAMPLES,HOST ROCK,HARSIT-KOPRUBASI MINE(H)

	135	155	170	H17,10	17	24	40	H19,6	12	24
PERCENT										
SIO2	70.98	86.31	64.75	52.48	57.02	64.83	84.73	84.92	55.49	21.72
AL2O3	22.58	7.40	3.82	24.18	9.15	12.27	0.94	7.61	0.94	1.38
FE2O3	0.40	0.00	3.87	12.54	0.54	0.66	0.34	3.94	7.05	5.49
MGO	1.30	0.38	0.14	1.38	0.14	0.01	0.14	0.10	0.14	0.14
CAO	0.08	0.00	0.34	0.40	0.07	0.06	0.06	0.38	0.36	0.39
NA2O	0.01	0.00	0.08	0.19	0.01	0.05	0.04	0.19	0.22	0.03
K2O	5.10	1.76	0.30	0.27	0.05	0.88	0.21	1.27	0.12	0.14
TIO2	0.22	0.01	1.03	1.34	4.73	2.97	0.01	0.04	0.00	0.13
MNO	0.02	0.02	0.02	0.56	0.02	0.03	0.02	0.02	0.02	0.02
S	0.25	0.07	11.89	1.29	8.13	5.59	5.68	2.20	17.07 **	28.71 **
P2O5	0.01	0.00	0.01	0.22	0.01	0.08	0.01	0.01	0.01	0.01
TOTAL	100.95	95.95	86.25	94.85	79.87	87.43	92.18	100.68	81.42	58.16
PPM										
BA	645	349	7860	2526	12.6 *	11.8 *	210	265	20	2997
NB	11	5	3	4	2	4	0	5	0	0
ZR	146	54	143	212	99	90	71	97	135	246
Y	23	10	38	29	0	11	24	26	42	65
SR	20	15	685	3125	1057	1088	0	0	57	5
RB	133	43	0	0	3	0	0	0	0	0
ZN	35	65	3.80 *	244	630	5084	3.65 *	1029	5034	11.5 *
SB	1	3	2707	67	44	1450	8600	282	3.03*	2711
CD	0	0	323	0	0	0	546	3	157	265
AG	0	0	4	0	0	26	144	29	384	47
MO	0	0	121	23	0	17	94	15	306	61
PB	55	39	5.40 *	1258	365	8750	4.00 *	2.62 *	9.30*	20.0 **
CU	0	0	2795	247	793	1986	1.22 *	2101	2000	4.10 *
AS	14	19	0	559	172	278	193	0	1354	230

TABLE A.1.2:BOREHOLE CORE SAMPLES,HOST ROCK,HARSIT-KOPRUBASI MINE(H)

	39	49,5	86	105	H 20,5	11	20	22	28	30
PERCENT										
SIO2	56.36	83.65	78.52	79.48	68.33	82.21	70.47	51.45	85.50	63.62
AL2O3	13.44	9.09	18.28	16.73	19.68	11.72	22.12	30.49	2.90	19.32
FE2O3	0.56	0.34	0.14	0.35	6.91	5.34	1.60	9.56	2.44	7.95
MGO	0.14	0.58	0.80	1.10	0.58	0.19	0.18	0.21	0.13	0.27
CAO	0.37	0.00	0.02	0.41	1.54	0.00	0.00	0.25	0.32	0.00
NA2O	0.14	0.01	0.01	0.01	0.00	0.00	0.00	0.01	0.01	0.12
K2O	0.16	2.48	3.38	3.50	0.00	0.27	0.06	0.15	0.00	0.00
TIO2	5.09	0.04	0.11	0.13	0.88	0.36	0.62	0.34	0.00	0.34
MNO	0.02	0.02	0.02	0.04	0.28	0.07	0.31	0.19	0.03	0.04
S	10.09	0.48	0.11	0.22	0.05	0.01	0.17	0.02	2.13	7.97
P2O5	0.01	0.00	0.01	0.03	0.11	0.08	0.00	0.02	0.10	0.01
TOTAL	86.38	96.69	101.40	102.00	98.36	100.25	95.53	92.69	93.56	99.64
PPM										
BA	12.2*	486	500	623	733	176	7315	239	198	38
NB	0	6	9	9	4	6	13	15	1	17
ZR	208	66	111	91	83	149	198	232	20	218
Y	0	9	17	16	9	37	25	32	5	30
SR	4053	9	21	14	602	935	186	70	9	52
RB	0	48	67	93	5	19	5	2	0	3
ZN	1869	125	16	28	53	81	109	75	89	2696
SB	282	20	8	8	6	47	27	110	96	210
CD	0	2	0	0	0	0	0	0	0	0
AG	0	0	0	0	0	0	0	0	0	0
MO	0	0	0	2	0	0	0	0	14	5
PB	1628	159	30	63	216	817	1344	990	3600	4000
CU	916	33	0	4	50	0	188	0	11	0
AS	162	39	12	13	74	229	537	390	2705	2271

TABLE A.1.2:BOREHOLE CORE SAMPLES,HOST ROCK,HARSIT-KOPRUBASI MINE(H)

	84	105	120	185	209	H24,24	36	47	53	60
PERCENT										
SIO2	81.31	76.53	—	55.12	—	89.02	72.18	58.50	76.97	78.79
AL2O3	13.17	16.82	—	9.32	—	6.43	6.52	3.70	11.49	5.14
FE2O3	0.67	1.12	—	1.15	—	0.17	2.18	4.29	3.23	2.63
MGO	1.01	1.28	—	0.64	—	0.38	0.09	0.14	0.66	0.31
CAO	0.01	0.00	—	0.00	—	0.00	0.35	0.35	0.00	0.00
NA2O	0.10	0.14	—	0.00	—	0.06	0.14	0.80	0.00	0.00
K2O	3.20	4.40	—	2.44	—	1.80	1.26	1.46	3.08	1.63
TIO2	0.14	0.17	—	0.10	—	0.00	0.06	0.00	0.06	0.00
MNO	0.03	0.03	0.03	0.05	0.03	0.02	0.02	0.03	0.02	0.02
S	0.58	0.71	—	7.63	—	0.18	6.64	14.42 **	2.68	4.20
P2O5	0.01	0.00	—	0.00	—	0.00	0.01	0.01	0.01	0.00
TOTAL	100.23	101.30	—	76.45	—	98.06	89.45	83.70	98.20	92.72
PPM										
BA	522	632	244	381	437	92	115	20	385	360
NB	9	9	9	2	8	4	1	0	5	3
ZR	100	120	87	158	105	43	167	142	64	115
Y	20	25	20	45	14	4	45	42	9	39
SR	115	23	10	6	11	6	0	0	37	0
RB	71	88	29	0	78	37	0	0	42	0
ZN	78	693	5054	11.8 *	268	102	2.35 *	4.35*	159	491
SB	5	126	1280	305	4	26	2200	4100	62	474
CD	0	3	70	695	2	2	279	855	1	6
AG	0	0	54	15	0	0	11	18	0	6
MO	0	0	15	17	0	0	35	73	8	18
PB	84	570	3958	6.20 *	105	784	7.43 *	6.20 *	1657	6.15*
CU	0	256	1665	1814	10	20	1.75 *	2.20 *	285	5550
AS	29	14	34	0	7	60	848	868	86	237

TABLE A.1.2: BOREHOLE CORE SAMPLES, HOST ROCK, HARSIT-KOPRUBASI MINE(H)

	73	86	134	149	H31,10	13	22	41	116	138
PERCENT										
SIO2	71.34	72.65	34.62	79.29	92.91	55.70	31.98	71.73	66.76	54.10
AL2O3	0.83	19.11	26.59	15.14	3.60	16.77	2.01	8.07	22.40	29.50
FE2O3	7.49	0.69	13.73	0.21	0.00	0.60	0.75	1.13	0.72	1.06
MGO	0.00	1.02	2.98	0.71	0.04	0.00	0.00	0.09	1.45	1.89
CAO	0.00	0.02	12.14	0.09	0.31	0.00	0.07	0.07	0.24	0.06
NA2O	0.00	0.11	0.19	0.02	0.00	0.20	0.02	0.72	0.06	0.19
K2O	0.24	4.50	0.22	3.37	0.00	0.00	0.00	1.15	5.04	6.98
TIO2	0.00	0.13	0.83	0.05	0.17	4.86	0.42	1.73	0.21	0.38
MNO	0.02	0.02	0.27	0.02	0.02	0.04	0.03	0.02	0.06	0.02
S	14.15 **	0.26	0.25	0.16	0.10	9.79	28.11**	8.69	0.94	0.60
P2O5	0.00	0.01	0.62	0.01	0.18	0.02	0.01	0.01	0.05	0.03
TOTAL	94.07	98.52	92.44	99.07	97.33	87.98	63.40	93.41	97.93	94.81
PPM										
BA	10	566	1124	458	379	1209	3126	1.10*	523	1362
NB	1	10	8	6	3	0	1	0	11	19
ZR	118	124	110	54	95	93	150	70	131	298
Y	41	24	23	9	26	0	37	15	26	47
SR	0	48	189	10	2359	1702	57	594	36	31
RB	0	97	4	63	8	0	0	0	119	214
ZN	5461	51	89	37	60	49	17.2*	1.90*	1247	344
SB	2000	0	6	2	22	97	1.98*	4650	17	16
CD	68	0	0	0	0	0	1477	152	8	0
AG	39	0	0	0	0	0	198	24	0	0
MO	48	0	0	0	0	0	207	59	0	0
PB	3.00 *	89	97	39	415	3275	16.0*	1.55 *	204	388
CU	8000	5	0	0	2	138	2.38*	7450	36	38
AS	58	15	18	9	144	569	1406	1365	45	72

TABLE A.1.2:BOREHOLE CORE SAMPLES,HOST ROCK,HARSIT-KOPRUBASI MINE(H)

	H34,6	20	23	27	64	118	127	H38,10	24	31
PERCENT										
SIO2	72.93	58.44	67.80	58.88	66.91	73.66	80.87	81.55	78.02	84.43
AL2O3	16.05	28.89	20.50	34.95	23.52	20.50	13.70	13.52	17.44	13.03
FE2O3	6.62	5.16	2.26	0.46	0.22	0.45	0.03	1.03	3.26	0.82
MGO	0.04	0.09	0.07	0.06	2.19	1.35	0.86	0.22	0.05	0.30
CAO	0.02	0.01	0.01	0.00	0.18	0.01	0.00	0.00	0.00	0.00
NA2O	0.00	0.01	0.01	0.00	0.01	0.01	0.00	0.00	0.61	0.00
K2O	0.04	0.04	0.05	0.23	5.18	4.99	3.65	0.59	0.52	0.55
TIO2	1.01	0.45	1.26	0.49	0.34	0.17	0.09	0.26	0.31	0.46
MNO	0.31	0.17	0.08	0.01	0.02	0.02	0.03	0.03	0.02	0.02
S	0.06	0.11	0.96	0.55	0.73	0.29	0.34	0.07	0.06	1.05
P2O5	0.12	0.02	0.03	0.00	0.01	0.02	0.01	0.05	0.02	0.06
TOTAL	97.20	93.39	93.03	95.63	99.31	101.47	99.58	97.32	100.31	100.72
PPM										
BA	653	1859	20	3150	4409	569	495	90	145	2736
NB	4	16	17	25	15	12	7	9	9	8
ZR	112	250	168	354	176	133	94	133	129	122
Y	10	39	15	9	38	23	23	19	15	12
SR	1236	88	668	127	97	96	39	337	100	540
RB	2	4	9	3	165	106	46	29	129	31
ZN	64	299	165	31	22	855	486	79	52	64
SB	2	73	109	53	6	48	38	8	37	168
CD	0	0	0	0	0	8	6	0	0	0
AG	0	0	0	0	0	0	0	0	0	0
MO	0	0	0	0	0	0	0	0	0	0
PB	410	1132	996	359	340	417	2895	286	567	1066
CU	155	60	46	0	0	52	74	53	0	109
AS	125	415	346	141	161	14	0	51	108	327

TABLE A.1.2:BOREHOLE CORE SAMPLES,HOST ROCK,HARSIT-KOPRUBASI MINE(H)

	37	50	66	96	H41,16	22	49	68	91	131
PERCENT										
SIO2	78.78	67.54	55.85	64.96	65.71	73.20	76.45	76.43	79.03	39.29
AL2O3	16.52	30.66	29.55	25.87	16.99	12.96	17.15	6.09	11.27	32.50
FE2O3	0.35	0.31	0.91	1.08	1.64	2.57	0.85	1.27	0.79	15.93
MGO	0.02	0.04	1.28	1.73	0.93	0.79	0.63	0.39	0.69	1.69
CAO	0.00	0.00	0.41	0.20	0.04	0.20	0.16	0.00	0.01	6.66
NA2O	0.01	0.00	0.08	0.00	0.21	0.10	0.00	0.61	0.12	0.09
K2O	0.00	0.00	5.61	5.46	4.03	3.31	4.12	1.90	2.93	0.00
TIO2	0.54	0.49	1.13	0.47	0.45	0.17	0.14	0.00	0.05	1.53
MNO	0.04	0.01	0.02	0.03	0.03	0.03	0.02	0.03	0.02	0.74
S	0.19	0.43	1.10	0.74	3.51	3.82	0.63	5.75	1.66	0.17
P2O5	0.03	0.03	0.02	0.02	0.00	0.00	0.00	0.00	0.01	0.37
TOTAL	96.48	99.51	95.96	100.56	93.54	97.15	100.15	92.47	96.58	98.97
PPM										
BA	2912	3562	20	2063	4738	1623	229	136	306	541
NB	7	21	19	17	7	7	9	3	5	6
ZR	94	301	359	311	135	92	129	86	73	139
Y	8	13	33	34	34	24	18	28	17	21
SR	316	391	769	245	196	71	18	0	10	1259
RB	20	16	112	130	29	39	77	0	19	0
ZN	133	12	43	385	5024	3210	30	5.50*	5683	589
SB	141	70	17	24	3550	3200	26	730	179	9
CD	0	3	0	4	35	26	0	284	86	0
AG	0	0	0	0	1	21	0	12	0	0
MO	0	0	0	0	44	44	0	18	9	0
PB	1328	836	294	585	1.04 *	5400	180	2.98 *	4750	389
CU	75	0	16	14	2599	2521	3	1256	443	0
AS	298	374	89	179	150	342	26	0	6	19

TABLE A.1.2: BOREHOLE CORE SAMPLES, HOST ROCK, HARSIT-KOPRUBASI MINE(H)

	146	156	H44,12	21.5	49	65	77	101	110	140
PERCENT										
SIO2	55.84	58.28	81.15	32.58	84.65	51.10	83.74	39.23	86.45	72.12
AL2O3	26.99	23.43	7.40	3.07	5.08	2.83	9.29	2.91	5.62	17.80
FE2O3	1.03	1.28	1.19	2.02	1.48	2.51	0.44	6.39	0.46	0.72
MGO	2.50	2.62	0.25	0.14	0.31	0.04	0.50	0.14	0.01	1.30
CAO	2.90	4.10	0.03	0.36	0.00	0.06	0.00	0.37	0.00	0.04
NA2O	0.09	0.11	0.61	0.09	0.02	0.05	0.00	0.15	0.56	0.02
K2O	6.41	5.63	1.27	0.38	1.51	0.29	2.36	0.22	0.64	4.37
TIO2	0.24	0.20	0.57	0.01	0.00	0.01	0.10	0.09	1.33	0.17
MNO	0.14	0.12	0.02	0.03	0.02	0.04	0.02	0.02	0.02	0.02
S	1.02	1.90	3.92	24.73 **	1.89	15.25 **	0.71	24.77**	3.38	0.75
P2O5	0.07	0.08	0.01	0.01	0.00	0.01	0.04	0.01	0.02	0.01
TOTAL	97.23	97.75	96.42	63.42	94.96	72.19	97.20	74.30	98.49	97.32
PPM										
BA	717	593	9312	10	93	10	1512	2676	6915	495
NB	12	10	0	0	2	0	5	0	2	11
ZR	168	148	88	134	37	136	61	227	78	160
Y	31	33	29	41	5	33	9	63	17	27
SR	40	40	260	0	4	0	106	32	1074	44
RB	122	82	0	0	29	0	51	0	0	97
ZN	2099	5569	1.52 *	16.0 *	3211	12.3 *	149	5.74*	1.34 *	111
SB	9	140	1640	1.48 *	17	1.14 *	115	395	119	11
CD	29	93	185	1049	38	1031	1	216	102	0
AG	0	0	0	28	0	46	0	36	0	0
MO	0	4	29	151	4	131	2	25	5	0
PB	2598	3961	2.86 *	15.0 *	551	8.10 *	242	17.0*	1.60 *	279
CU	28	561	4380	3.70 *	70	1.28 *	8	1037	125	7
AS	0	24	171	1437	90	298	33	0	0	55

TABLE A.1.2: BOREHOLE CORE SAMPLES, HOST ROCK, HARSIT-KOPRUBASI MINE(H)

	150	170	H47,12	20	27	58	87	99	102	115
PERCENT										
SIO2	79.11	83.61	77.03	82.31	52.51	59.80	77.19	71.95	43.06	61.29
AL2O3	10.61	7.38	21.20	8.67	36.05	24.53	4.20	4.81	0.92	9.71
FE2O3	1.63	0.93	0.28	1.87	4.81	0.89	1.23	1.02	6.14	9.86
MGO	0.54	0.44	0.10	2.10	0.07	2.71	0.16	0.03	0.00	0.42
CAO	0.08	0.02	0.00	1.02	0.00	0.94	0.00	0.05	0.00	0.00
NA2O	0.06	0.01	0.00	0.18	0.00	0.06	0.08	0.00	0.00	0.39
K2O	2.58	2.10	0.00	0.00	0.00	5.82	1.62	0.52	0.14	2.58
TIO2	0.07	0.10	0.11	0.09	0.42	0.30	0.44	1.22	0.02	0.13
MNO	0.01	0.02	0.02	0.04	0.10	0.12	0.04	0.02	0.07	0.02
S	3.41	1.26	0.46	0.11	0.08	0.74	7.94	7.10	24.93 **	11.06
P2O5	0.01	0.01	0.01	0.04	0.00	0.05	0.00	0.00	0.02	0.00
TOTAL	98.11	95.88	99.21	96.43	94.04	95.96	92.90	86.72	75.30	95.46
PPM										
BA	211	2016	53	1809	1351	948	4758	1.20 *	40	1778
NB	6	6	12	7	21	19	3	0	0	1
ZR	79	54	133	93	293	251	79	92	135	89
Y	11	8	22	24	48	43	23	31	39	25
SR	238	125	23	328	297	94	175	900	0	60
RB	57	38	5	15	0	216	0	0	0	0
ZN	2020	33	104	218	1197	39	3.20 *	3.54 *	12.8 *	1.15 *
SB	54	8	284	34	66	12	4654	7700	1.58 *	2450
CD	312	0	0	0	0	0	372	300	1439	164
AG	0	0	0	0	0	0	9	0	22	2
MO	12	3	0	0	0	0	60	105	169	47
PB	375	196	981	397	1371	208	2.20 *	2.50 *	4.00 *	3.10 *
CU	49	0	39	0	0	0	1.06 *	8300	1.70*	1.20 *
AS	66	31	367	129	597	91	564	215	429	1126

TABLE A.1.2: BOREHOLE CORE SAMPLES, HOST ROCK, HARSIT-KOPRUBASI MINE(H)

	127	H49,13	38	55	80	H55,25	35	39	41	60
PERCENT										
SIO2	78.67	76.23	62.67	66.32	69.51	70.88	71.11	80.72	36.65	58.78
AL2O3	14.48	20.21	24.89	23.94	11.86	17.42	19.02	2.00	5.45	13.69
FE2O3	0.70	0.00	0.98	0.84	0.51	2.19	1.28	2.09	5.71	2.83
MGO	0.68	0.02	2.42	2.00	0.76	0.90	0.90	0.14	0.10	0.38
CAO	0.00	0.00	0.63	0.14	0.33	0.00	0.01	0.00	0.00	0.01
NA2O	0.01	0.00	0.04	0.01	0.07	0.03	0.03	0.01	4.53	1.15
K2O	3.23	0.00	5.20	5.14	2.42	4.50	4.56	0.69	0.93	2.15
TIO2	0.11	0.09	0.22	0.24	0.27	0.21	0.37	0.47	0.41	0.07
MNO	0.02	0.02	0.45	0.40	0.04	0.03	0.02	0.03	0.03	0.03
S	0.72	0.09	0.52	0.49	5.55	1.95	0.80	6.75	18.27 **	7.95
P2O5	0.01	0.01	0.02	0.01	0.01	0.00	0.01	0.00	0.00	0.01
TOTAL	98.63	96.67	98.04	99.53	91.33	98.11	98.11	92.90	72.08	87.05
PPM										
BA	180	136	1348	1425	3668	746	537	7551	5494	10
NB	8	11	16	14	5	12	10	1	0	2
ZR	119	111	179	172	72	186	211	51	139	175
Y	14	18	23	22	23	20	22	15	38	52
SR	12	10	159	63	116	95	62	233	152	40
RB	70	2	184	175	0	99	98	0	0	0
ZN	53	43	43	25	5.55*	193	206	2.40*	13.5 *	2.80*
SB	27	57	21	6	4800	15	5	301	6200	4050
CD	0	0	0	0	630	0	0	201	1401	477
AG	0	0	0	0	7	0	0	0	15	11
MO	7	0	0	0	61	0	0	110	87	63
PB	385	442	355	214	2.00 *	525	310	1.60*	14.0 *	3.80*
CU	34	519	0	0	1.60 *	4	0	2110	1.23 *	2.10*
AS	92	66	150	78	1925	98	122	172	783	869

TABLE A.1.2:BOREHOLE CORE SAMPLES,HOST ROCK,HARSIT-KOPRUBASI MINE(H)

	74	H67,30	36	50	80	H68,7	20	28	29	32
PERCENT										
SIO2	76.32	41.03	74.66	71.12	68.23	45.77	48.43	77.60	79.92	51.79
AL2O3	11.98	14.26	13.87	19.27	22.71	25.02	22.96	12.71	1.20	7.06
FE2O3	1.00	0.14	1.54	1.34	0.34	16.45	13.67	2.44	8.61	1.81
MGO	0.71	0.00	0.50	1.11	1.66	2.23	2.89	0.09	0.01	0.00
CAO	0.00	0.00	0.02	0.02	0.02	0.30	7.75	0.00	0.00	0.00
NA2O	0.23	0.10	1.43	0.01	0.01	0.00	0.06	0.00	0.00	0.02
K2O	3.22	0.00	3.39	4.78	5.84	0.31	0.00	0.22	0.00	0.75
TIO2	0.10	5.35	0.14	0.13	0.21	1.77	1.22	0.74	0.60	2.45
MNO	0.02	0.03	0.02	0.02	0.03	0.60	0.44	0.01	0.02	0.02
S	1.96	9.21	1.50	1.10	0.25	2.92	1.39	1.63	8.39	10.46
P2O5	0.01	0.01	0.01	0.00	0.05	0.04	0.22	0.19	0.03	0.01
TOTAL	95.55	70.13	97.08	98.90	99.35	95.41	99.03	95.63	98.78	74.37
PPM										
BA	379	20.0**	394	844	1296	1343	822	1231	8034	12.4*
NB	6	0	6	10	9	7	3	9	3	2
ZR	100	86	91	133	134	159	98	162	24	114
Y	26	0	32	30	21	29	24	30	9	28
SR	53	1763	16	15	27	977	846	2972	478	794
RB	2	0	71	102	124	0	0	18	11	0
ZN	1.06*	106	248	182	41	77	89	117	61	3.00*
SB	44	78	18	11	12	36	18	84	334	1.12*
CD	85	0	0	0	1	0	0	0	0	243
AG	0	0	0	0	0	0	0	0	0	8
MO	68	0	0	0	0	0	0	0	4	137
PB	1.35*	1341	389	410	41	3086	2088	3000	5051	4.50*
CU	278	146	5	21	0	258	127	64	11	1.40*
AS	0	254	164	77	0	1386	947	3750	1768	639

TABLE A.1.2: BOREHOLE CORE SAMPLES, HOST ROCK, HARSIT-KOPRUBASI MINE(H)

	40	57	62	79	95	110	125	150	162
PERCENT									
SIO2	34.00	34.47	78.92	86.79	75.82	61.88	82.91	74.84	44.03
AL2O3	0.63	1.56	2.40	4.95	9.67	0.00	8.96	18.12	5.25
FE2O3	7.07	14.48	2.26	0.81	0.46	7.77	1.28	0.06	0.61
MGO	0.00	0.00	0.05	0.29	0.25	0.00	0.54	1.14	0.63
CAO	0.00	0.00	0.00	0.00	0.35	0.00	0.14	1.08	15.28
NA2O	0.01	0.09	0.00	0.06	0.01	0.02	0.02	0.01	0.22
K2O	0.08	0.01	0.98	1.45	1.52	0.38	2.30	4.20	1.38
TIO2	0.15	0.02	0.00	0.00	2.65	0.00	0.01	0.15	0.01
MNO	0.02	0.03	0.02	0.02	0.02	0.09	0.02	0.03	0.02
S	23.21**	25.39**	7.16	1.91	4.06	17.61**	2.02	0.83	21.04**
P2O5	0.03	0.01	0.00	0.01	0.02	0.00	0.00	0.10	0.39
TOTAL	95.55	70.13	97.08	98.90	99.35	95.41	99.03	95.63	98.78
PPM									
BA	958	275	10	69	8523	20	169	483	215
NB	0	0	2	3	3	0	4	13	3
ZR	150	137	71	49	95	198	47	140	29
Y	40	45	24	15	2	57	10	24	8
SR	46	0	0	8	2080	0	16	35	340
RB	0	0	0	0	29	0	54	113	26
ZN	11.8*	9.80*	3.20*	3029	276	3.85*	915	44	56
SB	1.95*	1300	1600	1540	0	3250	133	7	6
CD	999	534	295	28	0	447	3	0	0
AG	63	46	9	13	0	38	0	0	0
MO	285	44	74	25	0	64	36	0	3
PB	8.40*	7.20*	3.20*	1.05*	1224	481	1425	92	114
CU	2.45*	3.20*	8700	2511	141	2.95*	5330	18	16
AS	83	997	593	132	66	152	452	10	19

TABLE A.1.2: BOREHOLE CORE SAMPLES, HOST ROCK, HARKKOY MINE (HK)

	HK11,7	14	20	27	43	68	78	94	118	139
PERCENT										
SIO2	67.64	65.81	60.28	82.10	74.51	78.46	81.70	71.41	79.99	71.62
AL2O3	17.51	23.47	5.71	1.11	2.21	10.57	9.51	8.16	11.34	8.97
FE2O3	3.76	4.94	7.09	6.10	5.76	4.75	1.94	6.60	1.56	6.81
MGO	3.09	0.05	6.17	0.04	0.32	0.75	0.62	0.96	0.64	0.41
CAO	2.45	0.25	14.83	0.00	0.00	0.00	0.00	1.43	0.43	0.32
NA2O	1.37	0.22	0.28	0.00	0.28	0.00	0.00	0.00	0.11	0.18
K2O	0.11	0.25	0.03	0.00	0.91	2.22	2.70	2.05	2.94	2.04
TIO2	0.52	0.71	0.15	0.04	0.00	0.10	0.08	0.08	0.07	0.03
MNO	0.12	0.14	0.67	0.02	0.02	0.02	0.02	0.03	0.04	0.01
S	0.09	0.09	0.09	7.60	7.49	3.99	2.41	6.24	1.34	7.09
P2O5	0.06	0.04	0.49	0.04	0.03	0.02	0.03	0.05	0.02	0.00
TOTAL	96.72	95.97	95.79	97.05	91.53	100.88	99.01	97.01	98.48	97.48
PPM										
BA	418	375	978	1352	65	148	196	1343	767	413
NB	6	7	3	2	1	0	3	2	3	0
ZR	154	198	55	22	8	69	70	75	102	48
Y	46	40	42	8	2	18	13	12	19	17
SR	93	238	1123	144	111	47	10	293	101	5
RB	19	1	3	0	14	40	40	25	45	27
ZN	1300	530	1086	60	7600	145	1025	130	26	117
SB	6	3	32	70	28	7	5	0	2	5
CD	0	1	2	0	92	0	13	0	0	0
AG	0	0	0	15	0	0	0	0	0	0
MO	0	0	0	49	95	9	77	9	1	44
PB	61	19	50	1241	1953	1330	973	656	176	284
CU	0	0	15	1060	7000	1.90 *	1502	92	51	45
AS	0	0	423	261	598	442	183	219	43	112

TABLE A.1.2:BOREHOLE CORE SAMPLES,HOST ROCK,HARKKOY MINE(HK)

	153	172	HK12,1	21	35	40	59	77	103	120
PERCENT										
SIO2	45.77	73.36	94.89	71.20	28.24	59.94	56.89	59.08	60.27	52.45
AL2O3	24.55	14.65	1.60	16.80	24.57	24.51	23.09	21.84	22.60	28.07
FE2O3	13.62	1.28	2.63	3.95	7.53	8.05	4.09	7.31	0.94	6.61
MGO	1.99	0.79	0.13	2.34	3.68	0.02	0.58	0.05	1.01	2.37
CAO	3.41	0.02	0.00	1.64	14.84	0.02	3.87	1.97	3.94	0.96
NA2O	0.02	0.08	0.00	0.01	0.24	0.02	0.06	0.07	0.06	0.00
K2O	0.00	3.58	0.11	0.42	0.00	0.20	6.36	4.80	6.93	1.20
TIO2	0.05	0.06	0.01	0.62	0.86	0.42	0.33	0.29	0.30	0.51
MNO	0.23	0.02	0.02	0.03	0.32	0.08	0.12	0.05	0.34	0.04
S	8.34	1.17	0.04	0.10	0.23	0.10	0.04	0.09	0.05	0.06
P2O5	0.08	0.01	0.07	0.07	0.38	0.05	0.11	0.08	0.12	0.03
TOTAL	98.06	95.02	99.50	97.18	80.89	93.41	95.54	95.63	96.56	92.30
PPM										
BA	53	511	64	229	2532	140	361	181	156	40
NB	2	2	1	5	6	6	4	5	5	9
ZR	119	115	39	163	58	122	166	169	164	288
Y	15	23	8	75	23	31	25	22	39	54
SR	175	64	616	126	87	535	123	170	149	17
RB	0	58	21	25	0	0	75	52	82	56
ZN	507	92	45	152	705	259	133	38	51	89
SB	7	0	3	0	0	29	60	74	0	21
CD	1	0	0	0	0	2	0	0	2	0
AG	0	0	0	0	0	0	0	0	0	0
MO	6	7	0	0	0	0	0	0	0	0
PB	182	60	60	35	43	1039	142	62	44	50
CU	542	31	5	0	11	71	0	13	8	11
AS	71	24	11	0	0	340	37	27	14	27

TABLE A.1.2: BOREHOLE CORE SAMPLES, HOST ROCK, HARKKOY MINE(HK)

	133	142	145	151	163	178	192	198	204	220
PERCENT										
SIO2	16.74	54.08	14.70	61.15	64.63	32.41	82.13	60.62	44.65	79.85
AL2O3	0.80	4.80	0.20	5.10	24.89	0.00	10.74	3.76	5.09	10.91
FE2O3	21.84	12.60	27.28	12.60	1.95	23.30	1.33	10.98	14.18	1.60
MGO	0.19	0.29	0.07	0.80	1.22	1.13	1.05	0.73	2.05	1.15
CAO	0.00	0.00	0.00	0.51	0.18	1.72	0.85	0.45	4.08	0.83
NA2O	0.38	0.02	0.20	0.04	0.29	0.82	0.06	0.00	1.10	0.22
K2O	0.49	1.52	0.00	1.48	5.26	0.00	2.76	1.35	1.14	2.98
TIO2	0.01	0.00	0.00	0.00	0.25	0.00	0.02	0.00	0.01	0.04
MNO	0.03	0.02	0.02	0.02	0.02	0.03	0.02	0.02	0.06	0.03
S	21.82**	13.19**	23.26**	12.34	1.30	23.95**	1.55	10.08	12.82	2.06
P2O5	0.02	0.02	0.03	0.00	0.07	0.03	0.04	0.03	0.07	0.02
TOTAL	62.32	86.54	65.76	94.04	100.06	83.39	100.55	88.02	85.25	99.69
PPM										
BA	54	131	11	194	276	22	196	157	156	330
NB	0	0	0	0	6	4	4	1	0	4
ZR	33	35	0	31	248	39	97	32	37	105
Y	15	6	0	6	45	15	24	7	7	19
SR	0	1	0	0	704	13	13	9	72	67
RB	0	11	0	14	108	20	38	16	7	31
ZN	3.86*	930	583	933	274	8400	641	246	2187	3998
SB	98	5	14	0	27	326	6	17	17	26
CD	224	19	21	11	0	66	3	0	74	81
AG	41	34	16	2	0	52	0	6	2	0
MO	185	102	118	174	0	71	81	215	28	37
PB	1.98 *	1764	1579	1656	1086	1.10*	674	1848	1626	3699
CU	20.0**	13.2 *	20.0**	4.60*	141	14.5*	1876	12.0 *	14.4 *	5750
AS	864	229	390	220	430	641	44	323	216	273

TABLE A.1.2: BOREHOLE CORE SAMPLES, HOST ROCK, HARKKOY MINE (HK)

	HK14,8	21	28	33	38	48	66	82	90	98
PERCENT										
SIO2	49.41	74.02	72.72	91.73	40.28	56.58	85.91	51.70	63.86	81.20
AL2O3	25.79	2.87	14.55	5.94	0.44	2.41	10.33	1.61	2.74	8.88
FE2O3	5.60	3.81	1.44	0.02	24.14	5.66	0.00	18.95	13.59	4.37
MGO	2.02	5.40	0.78	0.33	0.14	0.09	0.13	2.93	0.62	0.67
CAO	8.67	12.90	0.12	0.05	0.00	0.00	0.00	5.44	0.45	0.32
NA2O	0.10	0.21	0.07	0.08	0.00	0.02	0.00	0.32	0.08	0.14
K2O	0.00	0.17	1.50	0.80	0.00	0.33	2.47	0.51	0.80	1.55
TIO2	1.05	0.11	2.46	0.03	0.00	0.03	0.03	0.00	0.00	0.02
MNO	0.21	0.51	0.02	0.01	0.02	0.02	0.01	0.10	0.03	0.03
S	0.16	0.13	1.66	0.35	31.43 **	19.94 **	0.08	17.25 **	15.32**	4.61
P2O5	0.19	0.32	0.02	0.02	0.00	0.04	0.04	0.06	0.06	0.01
TOTAL	93.20	100.45	95.34	99.36	96.45	85.12	99.00	98.87	97.55	101.80
PPM										
BA	271	2554	7405	110	22	508	117	83	69	177
NB	9	0	7	3	1	0	3	0	1	3
ZR	277	21	298	43	0	6	102	4	21	67
Y	53	35	49	7	0	1	11	1	4	11
SR	209	555	1161	42	0	65	0	38	253	16
RB	1	1	38	18	0	2	35	7	13	23
ZN	268	235	106	1222	73	1533	143	8300	2747	1013
SB	0	0	4	10	248	3200	4	39	120	0
CD	0	0	0	13	0	88	0	53	19	0
AG	0	0	0	0	12	95	0	2	3	0
MO	0	0	0	0	47	103	0	87	117	298
PB	31	65	2855	786	3131	1.40 *	60	851	920	201
CU	5	15	430	9200	2383	13.0 *	223	784	1925	85
AS	0	0	4030	23	1158	8200	18	247	1808	71

TABLE A.1.2:BOREHOLE CORE SAMPLES,HOST ROCK,HARKKOY MINE(HK)

	107	122	140	159	180	202	208	215	236	245
PERCENT										
SIO2	55.65	57.39	41.78	60.47	41.93	42.12	40.93	39.17	59.16	49.59
AL2O3	10.16	10.35	3.04	6.68	16.10	12.32	4.32	12.94	11.56	22.36
FE2O3	4.30	9.07	13.16	13.58	15.76	18.76	23.51	17.42	10.95	10.79
MGO	4.10	1.47	3.10	1.25	7.33	10.34	3.57	3.40	4.37	7.31
CAO	8.51	2.34	1.87	0.56	2.69	1.97	0.18	1.70	0.51	0.22
NA2O	0.96	0.28	0.68	0.04	0.11	0.23	0.20	0.20	0.19	0.24
K2O	0.23	0.45	0.18	1.79	1.22	2.43	1.15	3.18	1.82	3.39
TIO2	0.07	0.02	1.51	0.02	0.60	0.81	0.06	0.38	0.37	0.93
MNO	0.33	0.08	0.29	0.04	0.27	0.52	0.08	0.10	0.20	0.39
S	5.96	18.53 **	17.45**	15.34 **	11.99	9.54	25.23 **	17.02**	8.91	2.14
P2O5	0.15	0.05	0.04	0.00	0.12	0.12	0.02	0.00	0.05	0.11
TOTAL	90.42	100.03	83.10	99.77	98.12	99.16	99.25	95.51	98.09	97.47
PPM										
BA	1477	110	1720	337	153	240	132	389	187	264
NB	0	1	1	0	0	0	2	0	1	1
ZR	80	44	22	48	34	26	1	24	21	50
Y	23	6	0	10	13	13	3	7	20	27
SR	44	10	482	40	10	39	3	2	4	1
RB	0	7	0	20	14	30	13	37	23	53
ZN	2.30*	4855	2.18*	896	442	2098	111	136	213	367
SB	75	383	3300	107	50	199	3	105	0	0
CD	282	86	351	2	1	28	0	0	0	0
AG	8	2	0	3	1	0	1	13	0	0
MO	49	70	405	55	156	121	36	25	27	0
PB	1.95*	300	1.00*	3348	2388	369	701	2191	517	76
CU	1.50*	9.20*	11.2*	320	94	3.10*	90	6.60*	89	5
AS	1867	4400	6400	1527	1094	138	328	1022	224	18

TABLE,A.1.3: NORMS,LOWER BASIC SERIES,LOWER VOLC.CYCLE

NORMCAL .. R.C.O.GILL

SUMMARY NORM TABLE

	22	23	24	25	26	27	28	29	30	31	32	33
QUARTZ	20.2	27.9	33.2	26.6	24.3	14.7	16.9	17.5	23.0	14.7	26.8	26.2
CORUNDUM	0.0	0.0	0.0	0.0	1.9	0.0	0.0	0.0	0.0	0.0	0.0	0.0
ORTHOCLASE	7.4	13.3	6.1	8.8	19.9	3.7	5.3	10.7	6.4	4.6	16.9	6.1
ALBITE	22.3	20.1	18.4	21.1	17.5	17.6	20.6	15.6	22.8	22.9	25.5	19.6
ANORTHITE	30.3	25.4	30.6	28.4	19.9	35.9	29.8	34.8	25.9	32.3	15.3	33.5
DIOPSIDE	6.2	6.1	2.5	9.1	0.0	8.7	8.5	8.2	7.4	10.0	5.9	5.6
WOLLASTONITE	0.0	0.0	0.0	0.0	0.0	0.0	0.0	0.0	0.0	0.0	4.2	0.0
HYPERSTHENE	7.7	0.8	2.8	0.3	4.6	11.3	8.1	4.3	3.5	6.3	0.0	1.6
MAGNETITE	4.4	4.7	4.8	3.9	5.7	6.2	8.3	6.6	5.4	6.8	3.7	5.3
HEMATITE	0.0	0.0	0.0	0.0	0.0	0.0	0.0	0.1	3.2	0.0	0.0	0.0
ILMENITE	1.0	1.3	1.3	1.3	1.3	1.4	2.0	1.6	1.9	1.9	1.1	1.7
APATITE	0.4	0.4	0.4	0.4	4.9	0.3	0.5	0.4	0.4	0.4	0.5	0.5
PYRITE	0.1	0.1	0.1	0.1	0.0	0.1	0.1	0.1	0.1	0.1	0.1	0.0
DIFF. INDEX	50.0	61.2	57.6	56.5	61.8	36.1	42.8	43.9	52.2	42.2	69.2	51.8
NA/(NA+K)	0.76	0.62	0.76	0.72	0.48	0.64	0.80	0.61	0.79	0.84	0.61	0.77
(NA+K)/AL	0.34	0.41	0.29	0.35	0.44	0.24	0.31	0.28	0.37	0.31	0.59	0.29
F3/(F2+F3)	0.40	0.56	0.55	0.50	0.62	0.39	0.48	0.60	0.74	0.43	0.57	0.55

TABLE,A.1.3: NORMS,LOWER BASIC SERIES,LOWER VOLC.CYCLE

NORMCAL .. R.C.O.GILL

SUMMARY NORM TABLE

	34	35	36	47	49	55	56	130	135	137	179	200
QUARTZ	17.8	14.1	24.0	18.9	15.9	24.5	23.3	22.9	28.6	21.1	14.8	15.2
CORUNDUM	0.0	0.0	0.0	0.0	0.4	0.0	0.0	0.0	13.6	0.0	4.9	0.0
ORTHOCLASE	3.2	3.4	10.5	13.1	10.7	5.2	4.8	7.8	30.5	7.3	33.4	5.1
ALBITE	20.6	25.0	22.9	25.2	23.0	27.9	25.2	20.5	0.0	19.1	0.0	14.0
ANORTHITE	31.4	33.3	26.1	23.7	22.9	24.2	27.5	31.7	1.1	32.8	12.0	34.4
DIOPSIDE	16.5	9.3	5.7	10.9	0.0	5.2	8.2	0.1	0.0	2.2	0.0	9.0
HYPERSTHENE	2.2	8.8	0.9	2.3	18.5	5.6	3.0	12.5	15.9	11.4	21.0	15.6
MAGNETITE	6.3	4.4	6.3	3.9	6.4	5.3	5.9	2.0	1.5	4.5	5.6	4.6
HEMATITE	0.0	0.0	1.7	0.0	0.0	0.0	0.0	0.0	7.4	0.0	7.0	0.0
ILMENITE	1.5	1.4	1.5	1.6	1.8	1.5	1.6	1.7	1.2	1.1	1.3	1.7
APATITE	0.6	0.2	0.4	0.3	0.3	0.5	0.4	0.5	0.0	0.4	0.0	0.3
PYRITE	0.1	0.1	0.1	0.1	0.1	0.1	0.1	0.2	0.1	0.1	0.1	0.2
DIFF. INDEX	41.5	42.5	57.4	57.2	49.6	57.6	53.3	51.2	59.1	47.5	48.2	34.3
NA/(NA+K)	0.87	0.89	0.70	0.67	0.70	0.85	0.85	0.74	0.00	0.73	0.00	0.74
(NA+K)/AL	0.28	0.31	0.40	0.46	0.42	0.42	0.36	0.32	0.28	0.30	0.40	0.22
F3/(F2+F3)	0.53	0.32	0.68	0.44	0.41	0.47	0.54	0.18	0.89	0.42	0.81	0.33

TABLE,A.1.3: NORMS,DACITES,LOWER VOLC.CYCLE

NORMCAL .. R.C.O.GILL

SUMMARY NORM TABLE

	5	6	10	11	15	16	17	18	19	20	37	38
QUARTZ	42.5	26.9	38.1	32.8	25.4	40.3	34.5	28.6	33.7	36.4	31.2	28.3
CORUNDUM	0.7	0.0	11.0	3.1	0.0	7.2	3.9	1.7	0.5	3.4	6.0	2.4
ORTHOCLASE	9.9	20.8	39.0	23.7	28.3	18.5	25.0	21.7	14.9	18.5	30.8	27.8
ALBITE	24.6	19.8	5.4	24.1	21.5	25.6	20.6	29.5	27.5	26.2	17.8	25.9
ANORTHITE	15.2	23.0	1.1	10.9	16.5	4.0	9.4	12.5	17.7	11.2	8.4	10.3
DIOPSIDE	0.0	0.6	0.0	0.0	2.2	0.0	0.0	0.0	0.0	0.0	0.0	0.0
HYPERSTHENE	4.8	5.1	1.2	1.1	3.4	2.4	4.2	3.3	2.9	2.4	2.1	1.4
MAGNETITE	1.3	2.7	2.3	2.2	1.5	0.9	1.5	1.6	1.6	0.9	2.7	2.9
HEMATITE	0.0	0.0	0.8	0.9	0.0	0.0	0.0	0.0	0.0	0.0	0.0	0.0
ILMENITE	0.7	0.8	0.8	0.8	0.7	0.6	0.6	0.8	0.7	0.6	0.6	0.6
APATITE	0.3	0.2	0.2	0.4	0.4	0.2	0.3	0.3	0.3	0.3	0.3	0.3
PYRITE	0.0	0.1	0.1	0.1	0.1	0.1	0.1	0.0	0.1	0.1	0.1	0.1
DIFF. INDEX	76.9	67.6	82.5	80.6	75.3	84.6	80.1	79.8	76.2	81.1	79.8	82.0
NA/(NA+K)	0.73	0.50	0.13	0.52	0.45	0.60	0.47	0.59	0.66	0.60	0.38	0.50
(NA+K)/AL	0.51	0.48	0.42	0.56	0.61	0.49	0.54	0.61	0.54	0.53	0.50	0.62
F3/(F2+F3)	0.28	0.43	0.68	0.67	0.35	0.27	0.30	0.37	0.40	0.31	0.54	0.60

TABLE,A.1.3: NORMS,DACITES,LOWER VOLC.CYCLE

NORMCAL .. R.C.O.GILL

SUMMARY NORM TABLE

	39	40	42	43	44	45	46	48	50	54	57	58
QUARTZ	32.5	31.3	38.2	47.2	33.4	36.6	44.8	14.9	37.9	29.2	49.9	64.7
CORUNDUM	5.6	7.1	8.3	6.7	2.4	4.4	2.8	0.0	3.1	1.4	10.2	15.6
ORTHOCLASE	35.2	42.9	20.1	15.3	26.8	22.3	14.6	16.7	32.3	20.1	20.5	1.5
ALBITE	16.0	10.2	19.5	15.6	23.3	25.7	24.4	17.8	15.2	24.0	12.8	0.0
ANORTHITE	5.5	3.5	8.4	7.6	9.1	4.4	7.6	21.7	3.7	16.4	2.3	4.0
DIOPSIDE	0.0	0.0	0.0	0.0	0.0	0.0	0.0	17.4	0.0	0.0	0.0	0.0
HYPERSTHENE	2.2	1.3	3.8	2.5	3.5	3.2	4.8	2.7	2.5	5.0	1.9	9.8
MAGNETITE	2.2	2.1	0.9	4.0	0.7	1.7	0.0	6.1	4.5	2.7	1.5	3.0
HEMATITE	0.0	0.8	0.0	0.0	0.0	0.0	0.0	0.0	0.0	0.0	0.0	0.4
ILMENITE	0.5	0.7	0.5	0.8	0.5	0.6	0.6	1.9	0.5	0.7	0.6	0.7
APATITE	0.3	0.2	0.2	0.2	0.3	1.1	0.2	0.6	0.3	0.3	0.2	0.2
PYRITE	0.1	0.0	0.1	0.1	0.0	0.0	0.1	0.1	0.1	0.1	0.0	0.0
DIFF. INDEX	83.7	84.4	77.8	78.1	83.5	84.0	83.8	49.5	85.4	73.4	83.2	66.2
NA/(NA+K)	0.33	0.20	0.51	0.52	0.48	0.55	0.64	0.53	0.33	0.56	0.40	0.00
(NA+K)/AL	0.56	0.54	0.40	0.38	0.62	0.60	0.57	0.45	0.67	0.53	0.36	0.02
F3/(F2+F3)	0.50	0.68	0.26	0.59	0.24	0.46	0.00	0.52	0.60	0.45	0.43	0.65

TABLE,A.1.3: NORMS,DACITES,LOWER VOLC.CYCLE

NORMCAL .. R.C.O.GILL

SUMMARY NORM TABLE

	129A	136	139	160	162	163	164	203	212	234	246	247
QUARTZ	43.3	40.2	38.4	60.4	44.3	34.6	37.3	80.4	36.7	45.8	34.7	33.9
CORUNDUM	2.2	6.6	3.1	12.8	0.0	1.1	0.0	11.2	7.7	4.5	5.8	4.7
ORTHOCLASE	13.0	20.0	29.0	8.4	16.6	28.7	13.7	3.7	22.3	20.1	16.9	15.4
ALBITE	23.6	19.6	18.8	3.2	23.7	27.6	27.0	3.2	10.6	20.9	25.1	35.6
ANORTHITE	11.2	9.0	7.2	6.7	10.9	5.2	16.3	0.0	9.8	5.9	9.2	2.7
DIOPSIDE	0.0	0.0	0.0	0.0	0.8	0.0	0.8	0.0	0.0	0.0	0.0	0.0
HYPERSTHENE	6.0	0.5	0.3	6.0	0.9	0.3	1.5	0.0	8.9	0.5	5.3	5.0
MAGNETITE	0.0	-0.1	-0.2	0.1	1.7	0.8	1.3	-0.1	0.2	1.6	1.9	1.8
HEMATITE	0.0	3.1	2.5	1.6	0.1	1.1	1.1	1.4	3.0	0.0	0.0	0.0
ILMENITE	0.5	0.8	0.4	0.6	0.4	0.5	0.5	0.0	0.8	0.6	0.5	0.5
TITANITE	0.0	0.0	0.2	0.0	0.0	0.0	0.0	0.0	0.0	0.0	0.0	0.0
RUTILE	0.0	0.0	0.0	0.0	0.0	0.0	0.0	0.2	0.0	0.0	0.0	0.0
APATITE	0.2	0.2	0.1	0.0	0.4	0.1	0.1	0.1	0.1	0.1	0.1	0.1
PYRITE	0.0	0.1	0.1	0.1	0.2	0.1	0.3	0.1	0.1	0.1	0.4	0.3
CALCITE	0.0	0.0	0.0	0.0	0.0	0.0	0.0	-0.1	0.0	0.0	0.0	0.0
DIFF. INDEX	79.9	0.0	0.0	72.0	84.6	90.6	77.9	0.0	69.5	86.8	76.7	84.9
NA/(NA+K)	0.66	0.00	0.00	0.29	0.60	0.51	0.68	0.00	0.34	0.52	0.61	0.71
(NA+K)/AL	0.52	0.43	0.61	0.12	0.66	0.78	0.56	0.10	0.35	0.54	0.46	0.63
F3/(F2+F3)	0.00	0.88	0.95	0.92	0.60	0.76	0.72	1.00	0.88	0.53	0.57	0.57

TABLE,A.1.3: NORMS,HOST ROCK,LOWER VOLC.CYCLE

NORMCAL .. R.C.O.GILL

SUMMARY NORM TABLE

	12	13	52	53	59	60	100	103	106	107	107A	108
QUARTZ	51.8	47.0	17.5	35.2	50.9	43.3	76.0	80.8	76.1	80.0	64.3	83.1
CORUNDUM	17.5	16.5	1.2	2.4	3.1	6.2	11.0	3.7	9.6	2.0	4.0	3.4
ORTHOCLASE	25.8	27.4	33.1	7.6	19.8	18.7	1.2	5.8	3.8	3.5	6.1	5.6
ALBITE	0.3	0.4	43.9	35.1	14.5	25.8	4.8	3.9	4.4	0.0	4.2	0.0
ANORTHITE	0.0	0.3	0.8	14.1	7.5	0.1	0.2	0.3	0.0	1.8	0.0	0.6
HYPERSTHENE	1.6	7.2	2.2	0.9	3.6	2.1	6.3	5.1	5.7	0.2	0.3	3.4
MAGNETITE	2.0	0.0	0.6	2.0	0.0	1.1	0.0	0.0	0.0	-12.0	6.4	0.4
HEMATITE	0.0	0.0	0.0	0.8	0.0	0.0	0.0	0.0	0.0	8.3	12.9	0.0
ILMENITE	0.9	0.8	0.6	1.4	0.5	0.4	0.4	0.1	0.4	0.6	0.7	0.4
APATITE	0.2	0.2	0.2	0.5	0.2	0.2	0.0	0.0	0.1	0.0	0.0	0.0
PYRITE	0.0	0.4	0.0	0.1	0.1	0.1	0.0	0.4	0.0	15.5	1.1	3.2
CALCITE	-0.0	0.0	0.0	0.0	0.0	0.0	0.0	0.0	-0.0	0.0	0.0	0.0
DIFF. INDEX	0.0	74.7	94.4	77.9	85.1	87.6	82.0	90.4	0.0	0.0	74.6	88.7
NA/(NA+K)	0.00	0.01	0.58	0.83	0.44	0.59	0.81	0.42	0.00	0.00	0.42	0.00
(NA+K)/AL	0.21	0.23	0.91	0.52	0.52	0.51	0.10	0.32	0.14	0.19	0.33	0.22
F3/(F2+F3)	0.53	0.00	0.30	0.62	0.01	0.37	0.00	0.00	0.00	0.00	0.85	0.06

TABLE,A.1.3: NORMS,HOST ROCK,LOWER VOLC.CYCLE

NORMCAL .. R.C.O.GILL

SUMMARY NORM TABLE

	111	113WR	116	120	123	134	140	142	143	145	149	150
QUARTZ	65.5	76.9	82.4	85.7	80.3	69.7	37.2	24.2	49.4	56.5	69.3	63.2
CORUNDUM	8.2	3.3	3.0	1.4	3.4	10.2	4.1	0.0	0.7	8.7	10.3	9.1
ORTHOCLASE	14.0	6.9	4.9	0.9	6.2	3.5	15.5	12.1	0.8	16.2	12.7	15.7
ALBITE	4.0	0.0	3.9	4.0	4.4	2.7	31.6	16.1	47.5	12.7	4.7	4.7
ANORTHITE	0.1	0.9	0.1	0.0	0.3	4.2	6.4	31.2	0.5	1.0	0.4	0.1
DIOPSIDE	0.0	0.0	0.0	0.0	0.0	0.0	0.0	5.4	0.0	0.0	0.0	0.0
HYPERSTHENE	7.1	7.6	5.4	7.7	2.5	8.2	1.4	7.3	0.0	2.9	1.5	1.4
MAGNETITE	0.0	0.0	0.0	0.0	2.5	0.4	0.1	2.9	0.7	0.8	0.5	0.7
HEMATITE	0.0	0.0	0.0	0.0	0.0	0.6	2.9	0.0	0.2	0.0	0.3	0.8
ILMENITE	0.3	0.2	0.2	0.0	0.3	0.4	0.4	0.5	0.1	0.3	0.1	0.2
APATITE	0.0	0.0	0.0	0.0	0.1	0.0	0.1	0.1	0.0	0.0	0.0	0.0
PYRITE	0.8	4.3	0.1	0.2	0.1	0.0	0.1	0.2	0.1	0.8	0.2	0.1
CALCITE	0.0	0.0	0.0	-0.0	0.0	0.0	0.0	0.0	0.0	0.0	0.0	0.0
DIFF. INDEX	83.5	83.8	91.2	0.0	90.9	76.0	84.3	52.4	97.6	85.4	86.6	87.6
NA/(NA+K)	0.23	0.00	0.45	0.00	0.43	0.45	0.68	0.58	0.98	0.46	0.28	0.20
(NA+K)/AL	0.29	0.26	0.35	0.40	0.36	0.09	0.58	0.32	0.91	0.37	0.24	0.33
F3/(F2+F3)	0.00	0.00	0.00	0.00	0.44	0.73	0.92	0.62	0.67	0.29	0.67	0.76

TABLE,A.1.3: NORMS,HOST ROCK,LOWER VOLC.CYCLE

NORMCAL .. R.C.O.GILL

SUMMARY NORM TABLE

	151	153	154	156	169	169A	171	172	183	192A	198	199
QUARTZ	78.2	44.3	72.7	44.5	51.2	62.7	39.7	50.1	60.7	69.4	73.1	42.6
CORUNDUM	7.0	13.1	6.6	12.0	8.5	10.0	1.6	5.7	6.4	28.3	7.5	6.2
ORTHOCLASE	7.8	22.6	14.3	20.3	12.6	3.7	35.2	16.2	11.1	0.2	12.7	11.3
ALBITE	4.7	8.5	4.4	11.3	11.2	4.1	18.2	12.0	3.8	0.0	4.2	0.0
ANORTHITE	0.2	2.2	0.0	2.7	8.1	8.5	3.1	8.8	10.1	0.0	0.0	29.7
HYPERSTHENE	1.2	6.4	1.2	6.6	6.4	8.8	1.4	5.3	6.5	0.0	1.7	8.5
MAGNETITE	0.6	0.8	0.4	1.9	-0.1	0.4	0.3	-0.2	-0.1	-1.1	0.0	0.0
HEMATITE	0.0	1.4	0.0	0.0	1.4	1.1	0.0	1.2	1.0	1.5	0.0	0.0
ILMENITE	0.1	0.2	0.1	0.2	0.6	0.6	0.4	0.6	0.3	0.2	0.3	0.8
TITANITE	0.0	0.0	0.0	0.0	0.0	0.0	0.0	0.0	0.1	0.0	0.0	0.0
RUTILE	0.0	0.0	0.0	0.0	0.0	0.0	0.0	0.0	0.0	0.8	0.0	0.0
APATITE	0.0	0.0	0.0	0.0	0.0	0.0	0.1	0.1	0.0	0.0	0.0	0.2
PYRITE	0.2	0.3	0.3	0.5	0.1	0.1	0.1	0.3	0.1	0.7	0.5	0.8
CALCITE	0.0	0.0	0.0	0.0	0.0	0.0	0.0	0.0	0.0	-0.0	0.0	0.0
DIFF. INDEX	90.8	75.5	91.4	76.1	0.0	70.5	93.1	0.0	0.0	0.0	90.0	53.9
NA/(NA+K)	0.39	0.29	0.25	0.37	0.00	0.54	0.35	0.00	0.00	0.00	0.26	0.00
(NA+K)/AL	0.25	0.29	0.34	0.31	0.28	0.10	0.79	0.37	0.22	0.00	0.29	0.11
F3/(F2+F3)	0.54	0.80	0.36	0.57	0.83	0.90	0.20	0.85	0.89	0.87	0.00	0.00

TABLE,A.1.3: NORMS,UPPER BASIC SERIES,UPPER VOLC.CYCLE

NORMCAL .. R.C.O.GILL

SUMMARY NORM TABLE

	7	8	121	124	132	161	166	178	184	187	188	207
QUARTZ	5.0	C.0	0.8	11.4	9.0	4.9	10.1	13.1	12.4	12.6	9.2	14.6
ORTHOCLASE	34.4	14.9	19.6	12.1	17.5	9.5	19.5	14.8	16.2	28.4	19.6	25.3
ALBITE	18.8	20.1	26.2	24.6	11.4	30.3	12.9	10.8	11.1	25.5	14.4	21.5
ANORTHITE	13.0	26.9	19.5	23.5	30.5	23.4	27.2	31.6	30.8	16.4	26.9	15.6
DICPSIDE	2.0	18.0	15.1	17.5	13.6	2.8	10.7	9.3	10.9	6.4	5.6	5.4
WOLLASTONITE	0.0	0.0	0.0	0.0	0.0	0.0	0.0	0.0	0.0	0.0	0.0	10.7
HYPERSTHENE	15.7	9.5	14.0	6.7	5.8	17.7	10.1	10.0	7.2	3.1	13.6	0.0
OLIVINE	0.0	4.5	0.0	0.0	0.0	0.0	0.0	0.0	0.0	0.0	0.0	0.0
MAGNETITE	2.0	3.8	2.1	1.9	3.1	3.1	6.4	7.7	6.0	4.5	7.7	2.4
HEMATITE	7.1	0.0	0.0	0.0	0.0	0.0	0.0	0.0	2.4	0.0	0.0	2.1
ILMENITE	1.6	1.4	1.8	1.6	2.2	1.9	2.0	1.9	2.0	2.0	2.0	1.4
APATITE	0.2	0.8	0.9	0.6	0.7	0.3	0.7	0.7	0.7	0.9	0.7	0.8
PYRITE	0.1	0.1	0.1	0.1	0.2	0.3	0.3	0.3	0.3	0.2	0.2	0.3
DIFF. INDEX	58.3	35.0	46.7	48.1	38.0	44.7	42.5	38.7	39.6	66.5	43.3	61.3
NA/(NA+K)	0.37	0.59	0.59	0.68	0.41	0.77	0.41	0.44	0.42	0.49	0.44	0.47
(NA+K)/AL	0.68	0.40	0.55	0.45	0.33	0.47	0.38	0.29	0.31	0.63	0.39	0.61
F3/(F2+F3)	0.86	0.25	0.18	0.19	0.55	0.60	0.38	0.58	0.68	0.42	0.54	0.73

TABLE,A.1.3: NORMS,UPPER BASIC SERIES,UPPER VOLC.CYCLE

NORMCAL .. R.C.O.GILL

SUMMARY NORM TABLE

	208	209	210	211	214
QUARTZ	3.0	9.9	7.8	0.0	0.0
ORTHOCLASE	12.9	19.5	22.6	16.4	15.8
ALBITE	21.5	13.8	26.7	26.5	35.1
ANORTHITE	22.5	25.1	17.7	16.6	12.8
NEPHELINE	0.0	0.0	0.0	0.0	2.2
DIOPSIDE	14.7	5.4	11.7	12.4	14.4
HYPERSTHENE	16.3	14.6	5.0	15.1	0.0
OLIVINE	0.0	0.0	0.0	1.0	8.4
MAGNETITE	6.7	0.5	5.7	3.5	8.7
HEMATITE	0.0	8.8	0.0	6.4	0.0
ILMENITE	1.5	1.6	1.7	1.5	1.7
APATITE	0.7	0.6	0.7	0.5	0.6
PYRITE	0.2	0.1	0.2	0.1	0.3
DIFF. INDEX	37.4	43.2	57.1	42.9	53.1
NA/(NA+K)	0.64	0.43	0.56	0.63	0.72
(NA+K)/AL	0.44	0.41	0.59	0.57	0.69
F3/(F2+F3)	0.47	0.91	0.54	0.82	0.60

TABLE,A.1.3: NORMS,RHYOLACITE,UPPER VOLC.CYCLE

NORMCAL .. R.C.O.GILL

SUMMARY NORM TABLE

	21	41	127	128	133	138	158	159	168	175	176	180
QUARTZ	28.0	18.0	28.4	29.2	29.8	34.8	47.6	28.7	44.1	47.2	44.9	46.6
CORUNDUM	7.9	4.8	2.9	1.7	4.7	2.0	8.0	1.6	5.2	1.5	1.8	1.9
ORTHOCLASE	54.8	64.8	34.1	35.6	41.6	48.6	36.1	54.8	36.4	23.3	24.4	25.0
ALBITE	4.6	10.8	23.6	19.9	18.9	12.7	5.7	11.9	10.8	22.9	21.6	21.1
ANORTHITE	0.6	0.0	3.5	3.0	1.9	0.3	0.2	0.5	1.2	3.4	4.8	3.8
HYPERSTHENE	2.2	1.0	6.8	10.1	0.9	0.1	1.5	0.6	0.7	0.3	0.8	0.3
MAGNETITE	1.2	-0.1	0.0	0.0	0.5	-0.0	0.1	1.3	0.3	0.2	0.7	0.4
HEMATITE	0.0	0.0	0.0	0.0	1.0	1.2	0.2	0.0	0.7	0.6	0.4	0.6
ILMENITE	0.5	0.1	0.6	0.4	0.6	0.1	0.6	0.5	0.4	0.4	0.5	0.4
TITANITE	0.0	0.4	0.0	0.0	0.0	0.3	0.0	0.0	0.0	0.0	0.0	0.0
APATITE	0.2	0.2	0.1	0.0	0.0	0.0	0.0	0.0	0.0	0.1	0.1	0.0
PYRITE	0.1	0.0	0.1	0.0	0.0	0.0	0.2	0.1	0.2	0.1	0.1	0.1
CALCITE	0.0	-0.0	0.0	0.0	0.0	0.0	0.0	0.0	0.0	0.0	0.0	0.0
DIFF. INDEX	87.4	0.0	86.1	84.8	90.3	0.0	89.3	95.4	91.3	93.4	90.9	92.6
NA/(NA+K)	0.08	0.00	0.42	0.37	0.33	0.00	0.14	0.19	0.24	0.51	0.48	0.47
(NA+K)/AL	0.58	0.74	0.72	0.79	0.68	0.64	0.49	0.87	0.61	0.76	0.71	0.73
F3/(F2+F3)	0.39	0.47	0.00	0.00	0.73	1.00	0.36	0.54	0.73	0.72	0.62	0.74

TABLE,A.1.3: NORMS,RHYOLACITE,UPPER VOLC.CYCLE

NORMCAL .. R.C.O.GILL

SUMMARY NORM TABLE

	181	182	185	186	186A	189	213
QUARTZ	24.6	43.0	26.0	43.0	41.9	10.4	37.1
CORUNDUM	2.6	1.0	2.6	4.4	4.6	3.7	4.5
ORTHOCLASE	55.9	31.8	48.8	42.6	40.7	65.4	32.4
ALBITE	14.4	11.7	18.5	6.6	6.5	16.6	17.2
ANORTHITE	0.0	10.0	1.0	0.7	4.6	1.2	4.3
HYPERSTHENE	0.6	0.9	0.7	1.3	0.8	0.1	1.2
MAGNETITE	-0.1	-0.4	-0.1	0.7	0.3	-0.1	0.7
HEMATITE	1.3	1.2	1.7	0.2	0.0	1.5	1.9
ILMENITE	0.1	0.3	0.4	0.4	0.4	0.6	0.5
TITANITE	0.5	0.2	0.2	0.0	0.0	0.4	0.0
RUTILE	0.0	0.0	0.0	0.0	0.0	0.0	0.0
APATITE	0.0	0.1	0.1	0.0	0.0	0.0	0.1
PYRITE	0.0	0.3	0.1	0.2	0.1	0.1	0.1
CALCITE	-0.0	0.0	0.0	0.0	0.0	0.0	0.0
DIFF. INDEX	0.0	0.0	0.0	92.1	89.1	0.0	86.7
NA/(NA+K)	0.00	0.00	0.00	0.14	0.15	0.00	0.36
(NA+K)/AL	0.83	0.63	0.81	0.66	0.58	0.79	0.61
F3/(F2+F3)	0.99	0.87	0.88	0.59	0.29	0.85	0.82

APPENDIX TWO

MINERAL ANALYSES

A.2.1 Electron probe microanalysis

The instrument employed during this study was a Cambridge Instrument Company, "Geoscan Mark II" electron microprobe, with a take-off angle 75°. The polished ore-specimens were prepared by Mr. G. Randall of this departmen and the material to be analysed was chosen on the basis of minerology and texture.

The instrument was operated under a high vacuum, at an accelerating voltage of 20kV, and a specimen current of 0.04μA. The electron beam was kept focussed throughout, giving a spot analysis of diameter 2-5μM.

Efforts were made to standardize operating conditions, in order to avoid undue bias, and all the phases were analysed for the same elements under similar conditions. Analytical runs were made by counting for 5 (or more often 10) seconds counts on each standard and unknown peak and backgrounds. This counting technique was applied to all unknowns as long as there was no interfering pulses on low ($2\theta-2^{\circ}$) or high ($2\theta+2^{\circ}$) 2θ side of peak positions. In the presence of interfering element background counts were taken only on one side of the peak.

Data from the "Geoscan" was corrected for the effects of atomic number, mass absoprtion and fluorescence. This correction procedure was made using an on-line Varian 620-100 mini computer and the program (Tim 3) was devised by Dr. A. Peckett of this department.

The general analysing conditions for each element are shown in Table A.2.1. Detection limits for the trace elements in Table A.2.1 are in the order of 200-300 ppm, calculated from the given formula:

$$LLD(\%) = \frac{3}{M}\sqrt{Rb/_{Tb}}$$

LLD lower limit of detection

M = mean peak counts/sec.

Rb = Mean background counts/sec.

Tb = counting time on the background.

Atomic number (z)	Element	Line	Crystal	Counter	2θ Peak	2θ Background	Standard
16	S	$K\alpha_1$	P.E.T.	Flow	$75^{\circ}32'$	$\pm 2^{\circ}$	FeS_2
24	Cr	"	LiF	"	$69^{\circ}16'$	$\pm 2^{\circ}$	Cr_2O_3
25	Mn	"	"	"	$62^{\circ}52'$	$\pm 1^{\circ}30'$	Mn
26	Fe	"	"	"	$57^{\circ}23'$	$\pm 2^{\circ}$	Fe, FeS_2
27	Co	"	"	"	$52^{\circ}41$	$\pm 2^{\circ}$	Co
28	Ni	"	"	"	$48^{\circ}30'$	$\pm 2^{\circ}$	Ni
29	Cu	"	"	"	$44^{\circ}51'$	$\pm 2^{\circ}$	Cu
30	Zn	"	"	"	$41^{\circ}33'$	-2°	Zns
33	As	"	"	"	$33^{\circ}44'$	$\pm 3^{\circ}$	As
33	As	$L\alpha_1$	K.A.P.	"	$42^{\circ}37'$	$\pm 2^{\circ}$	As
34	Se	"	LiF	"	$31^{\circ}49'5"$	$\pm 2^{\circ}$	CdSe
47	Ag	"	P.E.T.	"	$56^{\circ}22'$	$+2^{\circ}$	Ag
48	Cd	"	"	"	$53^{\circ}25'$	$\pm 1^{\circ}30'$	CdSe
51	Sb	"	LiF	"	$117^{\circ}16'$	$\pm 2^{\circ}$	Sb_2S_3
52	Te	"	"	"	$109^{\circ}29'5"$	$\pm 2^{\circ}$	Te
82	Pb	$K\alpha_1$	"	"	$33^{\circ}55'$	$\pm 2^{\circ}$	PbS
82	Pb	$M\alpha_1$	P.E.T.	"	$70^{\circ}38'$	$\pm 2^{\circ}$	PbS
83	Bi	$L\alpha_1$	LiF	"	$33^{\circ}00'$	$\pm 2^{\circ}$	Bi

TABLE A.2.1: Optimum analysing conditions and standards used for electron microprobe analysis

Overall accuracy for the major constituents is estimated to be $\pm$ 2%. Electron probe microanalysis for various sulphides were presented in Chapter 6.

A.2.2 X-ray diffraction studies

Hydrothermal alteration products as well as some ore and gangue minerals were determined by X-ray diffraction analysis, using a Phillips PW 1130 generator and PW1050/25 high angle goniometer - diffraction assemblage, X-ray diffractometer. The samples were ground to -250 mesh and packed either in aluminium metal holders (cavity mount) or smeared onto a glass slide (smear mount).

Prior to analysis, preliminary runs were made to obtain optimum conditions of scanning speed, pulse height analysis and slit widths. The samples were scanned from 3-4 degrees to 70-80 degrees. The obtained diffraction peaks were then converted to d-spacings by means of conversion tables.

In order to determine the dioctohedral or trioctohedral nature of the clay minerals the 060 reflections were accurately measured by using internal standards.

The optimum analysing conditions for the X-ray diffractometer are shown in Table A.2.2, below.

Radiation:	Co Kα, Cu Kα and Cr Kα.
Slits :	2^{o}, 0.2^{o}, 2^{o}.
Scanning rate:	1^{o} - 2^{o}/min.
Counter :	Sealed proportional with pulse height analysis.
Operation:	Ratemeter.
Time constant:	4 sec.
Multiplications factor:	2×10^{2}, 4×10^{2}, 1×10^{3} cps.